Vol. 58 MARCH, 1954 No. 3

THE JOURNAL OF PHYSICAL CHEMISTRY

(Registered in U. S. Patent Office)

THE JOURNAL OF PHYSICAL CHEMISTRY will appear monthly in 1954
After January 1, 1954, Notes and Communications to the Editor
will be accepted for publication.

THE JOURNAL OF PHYSICAL CHEMISTRY

(Registered in U. S. Patent Office)

Published monthly by the American Chemical Society at 20th and Northampton Sts., Easton, Pa.

Entered as second-class matter at the Post Office at Easton, Pennsylvania.

The *Journal of Physical Chemistry* is devoted to the publication of selected symposia in the broad field of physical chemistry and to other contributed papers.

Manuscripts originating in the British Isles, Europe and Africa should be sent to F. C. Tompkins, The Faraday Society, 6 Gray's Inn Square, London W. C. 1, England.

Manuscripts originating elsewhere should be sent to W. Albert Noyes, Jr., Department of Chemistry, University of Rochester, Rochester 3, N. Y.

Correspondence regarding accepted copy, proofs and reprints should be directed to Assistant Editor, Allen D. Bliss, Department of Chemistry, Simmons College, 300 The Fenway, Boston 15, Mass.

Business Office: American Chemical Society, 1155 Sixteenth St. N. W., Washington 6, D. C.

Advertising Office: American Chemical Society, 332 West 42nd St., New York 36, N. Y.

Articles must be submitted in duplicate, typed and double spaced. They should have at the beginning a brief Abstract, in no case exceeding 300 words. Original drawings should accompany the manuscript. Lettering at the sides of graphs (black on white or blue) may be pencilled in, and will be typeset. Figures and tables should be held to a minimum consistent with adequate presentation of information. Photographs will not be printed on glossy paper except by special arrangement. All footnotes and references to the literature should be numbered consecutively and placed on the manuscript at the proper places. Initials of authors referred to in citations should be given. Nomenclature should conform to that used in *Chemical Abstracts*, mathematical characters marked for italic, Greek letters carefully made or annotated, and subscripts and superscripts clearly shown. Articles should be written as briefly as possible consistent with clarity and should avoid historical background unnecessary for specialists.

Symposium papers should be sent in all cases to Secretaries of Divisions sponsoring the symposium, who will be responsible for their transmittal to the Editor. The Secretary of the Division by agreement with the Editor will specify a time after which symposium papers cannot be accepted. The Editor reserves the right to refuse to publish symposium articles, for valid scientific reasons. Each symposium paper may not exceed four printed pages (about sixteen double spaced typewritten pages) in length except by prior arrangement with the Editor.

Remittances and orders for subscriptions and for single copies, notices of changes of address and new professional connections, and claims for missing numbers should be sent to the American Chemical Society, 1155 Sixteenth St., N. W., Washington 6, D. C. Changes of address for the *Journal of Physical Chemistry* must be received on or before the 30th of the preceding month.

Claims for missing numbers will not be allowed (1) if received more than sixty days from date of issue (because of delivery hazards, no claims can be honored from subscribers in Central Europe, Asia, or Pacific Islands other than Hawaii), (2) if loss was due to failure of notice of change of address to be received before the date specified in the preceding paragraph, or (3) if the reason for the claim is "missing from files."

Subscription Rates: to members of the American Chemical Society, $8.00 for 1 year, $15.00 for 2 years, $22.00 for 3 years; to nonmembers, $10.00 for 1 year, $18.00 for 2 years, $26.00 for 3 years. Postage free to countries in the Pan American Union; Canada, $0.40; all other countries, $1.20. Single copies, $1.25; foreign postage, $0.15; Canadian postage $0.05.

THE JOURNAL OF
PHYSICAL CHEMISTRY

(Registered in U. S. Patent Office) (Copyright, 1954, by the American Chemical Society)

VOLUME 58 MARCH 24, 1954 NUMBER 3

A NEW METHOD FOR DETERMINATION OF ACTIVITIES OF BINARY SOLUTIONS OF VOLATILE LIQUIDS

BY ROBERT S. HANSEN AND FREDERICK A. MILLER

Contribution No. 292 from the Institute for Atomic Research and the Department of Chemistry, Iowa State College, Ames, Iowa[1]

Received October 1, 1952

A new method for the determination of activities of both components in binary mixtures of volatile solvents is described. The method involves the transfer of vapor from a generator flask through an intermittent bleeder valve to a reservoir flask, measurement of total pressure in the reservoir flask, condensation and analysis of vapors in the flask. The intermittent bleeder valve appears essential to the transfer of vapor of equilibrium concentration to the reservoir in a reasonable period of time. Activities of both components at 25° in water–ethanol and water–propanol-1 systems determined by this method are given and compared with best literature values. It is concluded that the method described is comparable in accuracy to the gas saturation method, and is approximately eight times as rapid.

The activities of components in binary solution have fundamental thermodynamic importance. Several methods for evaluating these quantities are in fairly common use. Of these, the most important types of method suitable for non-electrolytes are as follows.

1. Direct measurement of the activity of one component and inference of the activity of the other component by use of the Gibbs–Duhem equation. Methods involving measurement of the freezing point depression to evaluate the activity of the component freezing out are the most accurate of this type, and Jones and Bury[2] have published what appears to be excellent work on activities of components of aqueous fatty acid solutions obtained in this manner. The freezing point depression method suffers from the disadvantage that the activities are determined directly at the freezing temperature, and in order to obtain activities at arbitrary temperatures the partial molal enthalpies of the components must be known as functions of temperature between the freezing point and the temperature of interest.

2. Measurement of partial pressures of both components in the vapor in equilibrium with the solution of interest, establishing the activity of a component at the ratio of partial pressure to saturated vapor pressure (strictly speaking the corresponding fugacity ratio should be used; the error involved in using pressure ratios is negligible for the systems studied in this work). Such methods have an important advantage over those of the first type in that activities of both components are obtained independently, and the Gibbs–Duhem equation permits data to be checked for self-consistency.

A common method of this type is one in which the equilibrium vapor is transferred from the vicinity of the generating liquid by an inert gas, and subsequently trapped out, weighed and analyzed. Butler, Thomson and MacLennan[3] have used this method extensively with aqueous–aliphatic alcohol systems, and a countercurrent flow apparatus on this principle has been described by Randall and Weber.[4] A practical disadvantage exists in that a period of approximately eight hours is required for each experimental point. As in the parallel determination of vapor pressure of a single component, considerable care must be taken to ensure equilibration between inert gas and solution, and, in our experience, to avoid mechanical transport of spray.

The method herein presented is of the second general type, involving measurement of partial pressures of both components of the binary solution. Total pressure is measured directly; the vapor phase is then condensed and analyzed. No third component is introduced. Although the principles of measurement are obvious, important

---

[1] Work performed in the Ames Laboratory of the Atomic Energy Commission.

[2] E. R. Jones and C. R. Bury, *Phil. Mag.*, [7] **4**, 481 (1927).

[3] J. A. V. Butler, D. W. Thomson and W. H. MacLennan, *J. Chem. Soc.*, 674 (1933).

[4] M. Randall and H. Weber, THIS JOURNAL, **44**, 917 (1940).

precautions must be taken in apparatus design to secure equilibration and hence to obtain accurate results. A period of about one hour is required for complete determination of activities of both components at a given solution concentration.

Apparatus.—The apparatus designed and used in this work is illustrated by Fig. 1 (front view) and Fig. 2 (a portion of the apparatus from side view). In these illustrations, A is a 1-liter Pyrex flask with ₮ 29/42 top joint. Flask A contains a Teflon covered magnet H activated by a magnetic stirrer H′, and is immersed in a water-bath B thermostated to 25.00 ± 0.02°. D is a 20-liter Pyrex flask with ₮ 71/60 joint, connected to the generator flask A directly through stopcock S2 (10-mm. bore) and also through the intermittent bleeder C and stopcock S6 (2-mm. bore). Flask D is also connected to a mercury manometer E and through stopcock S4 to a liquid nitrogen cooled trap (F,G). Stopcock S1 provides connection to the atmosphere and stopcocks S3 and S5 (three way) provide connection to atmosphere and vacuum line.

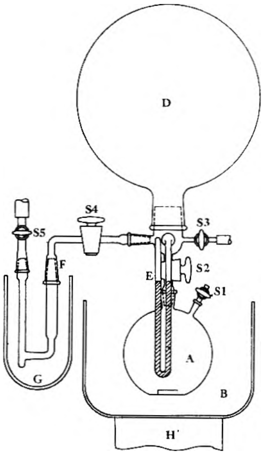

Fig. 1.—Apparatus for determination of activities of components of volatile binary solutions (front view).

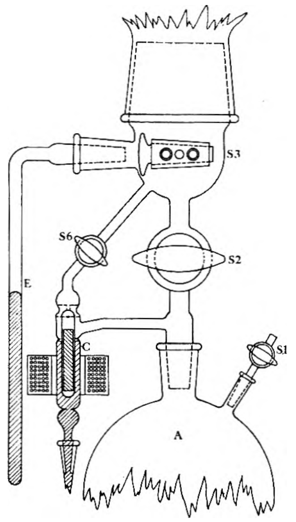

Fig. 2.—Portion of apparatus for determination of activities of components of volatile binary solutions (side view).

The intermittent bleeder, C, consists of a solenoid-operated valve in the form of a glass cartridge containing an iron core floating in a mercury pool. The solenoid was operated through an Eagle Signal Corp. Flexopulse timer in a $^1/_2$ second on, 15 second off cycle. When the solenoid was off, the mercury floated the cartridge into its female joint (male and female joints were approximately hemispherical and were lapped into each other with carborundum grinding powder prior to inclusion in the apparatus). When the solenoid was on, the cartridge was pulled from its joint and the connection thus opened.

Under operating conditions, the initial pressure increment in the reservoir flask per opening was about 1.0 mm. in the case of ethanol (vapor pressure = 58.7 mm.) and 0.5 mm. in the case of water.

The whole apparatus was enclosed in an air-bath thermostated to 27.0 ± 0.1° to prevent condensation in the reservoir flask D.

Procedure.—Approximately 300 ml. of the binary solution of interest is introduced into the generator flask A through S1. S1, S2, S4 and S6 are closed and the reservoir flask D evacuated through S3. S3 is now closed and S2 opened slightly (to avoid spray transport) while the solution is vigorously stirred by the magnetic stirrer H′. S2 is closed and the reservoir flask D evacuated through S3. In our experience, one such degassing operation, with the solution boiling under reduced pressure, sufficed to outgas the generator flask and the solution therein. Trap F is evacuated through S5.

All stopcocks are now closed except S6; the intermittent bleeder C is turned on until the change in pressure per opening of the shut-off valve is small (0.1 mm. or less, usually about 20 minutes). S2 is now opened for 10 minutes to permit final equilibration. The total pressure is read from the manometer by means of a cathetometer (in our case, a Gaertner M-901 cathetometer permitting reading of total pressure to 0.05 mm.).

S2 and S6 are now closed and S4 opened, the vapors condensing in trap F (this process is accelerated without loss of material by opening S5 to the vacuum line very slightly). A period of about 3 minutes is required for this operation and the total pressure in the reservoir flask D drops to zero on its completion. Closing S4, dry, CO_2-free air is admitted through S5, trap F allowed to warm to room temperature, removed, agitated mildly to ensure homogeneity of the condensate, and an aliquot of the condensate removed and analyzed.

Knowing the mole fraction of each component in the condensate and the total pressure of the gas phase prior to condensation, the partial pressure of each component is calculated and the activity of each component obtained as the ratio of its partial pressure to the vapor pressure of the pure component. The corresponding solution concentration is obtained by analysis prior to the degassing operation and on completion of the experiment. The measured activity corresponds in good approximation to the average of the solution concentrations preceding and on completion of the vapor collection run.

The crucial feature of this apparatus and procedure is the intermittent bleeder valve. Even if the tube connecting the generator A and reservoir D has 1 cm.^{2} cross-section at its smallest part, times of the order of magnitude of 10 days would be required to attain diffusional equilibrium across it if the vapors initially transported to the reservoir flask are not equilibrium vapors. Pressure equalization, on the other hand, is almost immediate. It is therefore essential that vapor enter flask D in equilibrium concentration, *i.e.*, that the vapor in flask A be in equilibrium at all times during collection, and that there be no effusional fractionation between A and D. While in principle a small bore stopcock might be expected to perform the function of the intermittent bleeder, in practice we failed to obtain equilibrium vapor concentrations by its use in reasonable periods of time (high partial pressures were always obtained for water as compared to best literature values probably reflecting effusional fractionation). It is, of course, obvious that any connection will lead to equilibrium concentrations in flask D eventually; it is also obvious that the time required for attainment of such equilibrium concentration will be a criterion of practicality of the method.

Experimental.—Activities of all components of water–ethanol and water–propanol-1 solutions were determined at 25.00° using the procedures and apparatus given. Water was redistilled from alkaline permanganate solution. One thousand five hundred ml. of Commercial Solvents Corp. absolute ethanol, 15 g. of silver nitrate and 5 g. of sodium hydroxide were refluxed overnight to remove impurities such as aldehydes, and filtered. The ethanol was then further purified by the method of Lund and Bjerrum.[5] Fisher Scientific Co. C.P. propanol-1 was treated with bromine to persistence of bromine coloration to aid in the removal of allyl alcohol. The excess bromine was reduced by a slight excess of sodium sulfite, and the propanol further purified by the method of Lund and Bjerrum. Both alcohols were finally distilled through a 30-plate Oldershaw distilling column at a 10/1 reflux ratio. Boiling ranges of the central fractions collected, corrected to 760 mm., were 78.50–78.52° for ethanol and 97.43–97.51° for propanol-1.

Analyses were made by means of a Hilger liquid interferometer using Teflon cell covers sealed with mercury.

Treatment of Data.—A reasonable treatment of binary solution activity data obtained by methods of the present type is represented by the treatment of the butanol-1–water system followed by Randall and Weber.[4] In this treatment, activity–concentration curves are established by raw activity data, and slopes of the curves of the two components compared with those predicted by the Gibbs–Duhem equation. The deviations permit an estimate of the reliability of the data.

---

[5] H. Lund and J. Bjerrum, *Ber.*, **64**, 210 (1931).

A treatment which is preferred by the authors is one in which each activity–concentration curve reflects not only raw activity data for the particular component, but also raw data for the second component in the binary solution as required by the Gibbs–Duhem equation. The deviation of experimental points from the activity–concentration curves permit an estimate of the reliability of the data, but the curves themselves are the best representation of activity data consistent with all experimental and theoretical information available for the system of interest. The treatment used in the present work is based on the following argument.

The logarithm of the activity coefficient for a given component in binary solution can be expanded in power series in mole fraction of the second component; if the activity coefficient is based on pure liquid component as standard state the leading term in this expansion will be the square term.[6] The coefficients in the corresponding expansion of the activity coefficient of the second component are then established by the Gibbs–Duhem equation.

Let $\Phi(x) = \ln \gamma_A/(1 - x)^2$, $f(x) = \ln \gamma_w/x^2$, in which x is the mole fraction of component A. The Gibbs–Duhem equation requires

$$x \frac{d \ln \gamma_A}{dx} = -(1 - x) \frac{d \ln \gamma_w}{dx} \qquad (1)$$

Applying equation 2 to equation 1 there is obtained

$$\frac{d}{dx}(x^2 f) = 2x\Phi - x(1 - x)\frac{d\Phi}{dx} \qquad (2)$$

If Φ can be represented by a polynomial

$$\Phi_1 = \sum_{i=0}^{n} A_i x^i$$

then by substitution of this polynomial in equation 2, integrating, and requiring that f(0) be finite there results

$$f_1(x) = \sum_{i=0}^{n-1}\left(A_i - \frac{i+1}{i+2}A_{i+1}\right)x^i + A_n x^n \qquad (3)$$

It is, of course, not necessary to limit functions chosen to polynomial form. By proceeding as in the polynomial case it is readily shown that

$$\Phi_2(x) = \alpha e^{-\beta x} \text{ implies } f_2(x) = \alpha e^{-\beta x} + \frac{\alpha}{\beta x^2}[1 - e^{-\beta x}\ (1 + \beta x)]$$

and

$$\Phi_3(x) = \gamma x e^{-\delta x} \text{ implies } f_3(x) = \gamma x e^{-\delta x} + \frac{\gamma}{(\delta x)^2}[1 - e^{-x}\{1 + \delta x + (\delta x)^2\}]$$

A function $\Phi(x)$ obtained by addition of several of the functions $\Phi_i(x)$ listed above leads to a function $f(x)$ which is the sum of the corresponding functions $f_i(x)$. It is desirable, but not essential, to represent $\Phi(x)$ using a function with comparatively few terms and constants.

Figure 3 illustrates this treatment for the ethanol–water system; curves are the self-consistent functions $\Phi(x)$ and $f(x)$ used to compute activities, and points are experimental points with hatchings corresponding to 1% uncertainty (note that a small relative error in γ_A leads to a large absolute error in $\Phi(x)$ as x approaches 1, and $f(x)$ behaves similarly as x approaches 0).

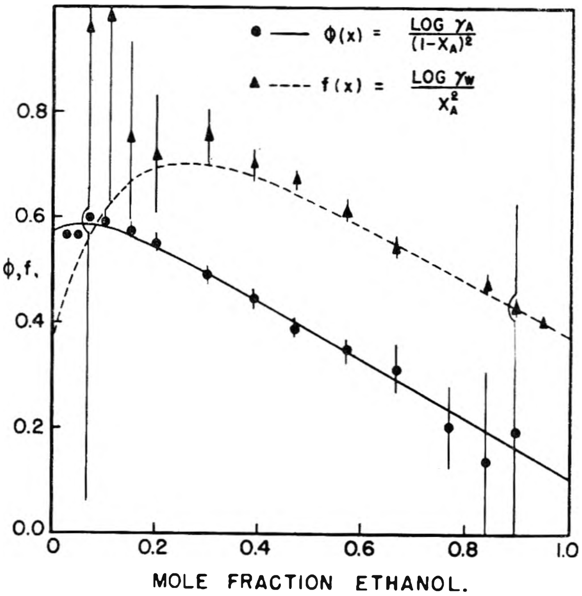

Fig. 3.—Method of establishing self-consistent activity–concentration diagrams, system ethanol–water at 25°.

Results.—Results are shown graphically in Fig. 4 in which our data are compared with best available literature data for these systems. Comparison data are from Butler, Thomson and MacLennan[3] for water–propanol-1, and from Dobson[7] for water–ethanol. Tabular experimental data will be furnished by one of us (R.S.H.) on request. Where x is the mole fraction of the alcohol, γ_A and γ_w the activity coefficients of alcohol and water, respectively, the following self-consistent functions were found to represent the data with indicated average absolute deviations.

System ethanol–water:

$$\log \gamma_A = (1 - x)^2\{0.665 - 0.560x - 0.090e^{-11x}\} \pm 0.0055$$

$$\log \gamma_w = x^2\left\{0.945 - 0.560x - 0.090e^{-11x} - \frac{0.00818}{x^2}[1 - e^{-11x}(1 + 11x)]\right\} \pm 0.0040$$

System propanol-1–water:

$$\text{og}\ \gamma_A = (1 - x)^2\{1.105e^{-2.20x} + 0.26x + 4.5xe^{-24x}\} \pm 0.0055$$

$$\log \gamma_w = x^2\left\{1.105e^{-2.20x} + 0.26x + 4.5xe^{-24x} - 0.13 + \frac{0.503}{x^2}[1 - e^{-2.20x}(1 + 2.20x)] + \frac{0.00945}{x^2}[1 - e^{-24x}(476x^2 + 24x + 1)]\right\} \pm 0.0059$$

Logarithms are to the base 10; and uncertainty of 0.0043 in the logarithm corresponds to a 1% uncertainty in the activity coefficient.

Discussion.—Activity data obtained by the method described are in good agreement with best literature values for all systems investigated. Deviations of experimental points from self-consistent activity curves established by use of the

---

[6] J. H. Hildebrand and R. L. Scott, "The Solubility of Nonelectrolytes," 3rd Ed., Reinhold Publ. Corp., New York, N. Y., 1950, pp. 34–35.

[7] H. J. E. Dobson, *J. Chem. Soc.*, **127**, 2866 (1925).

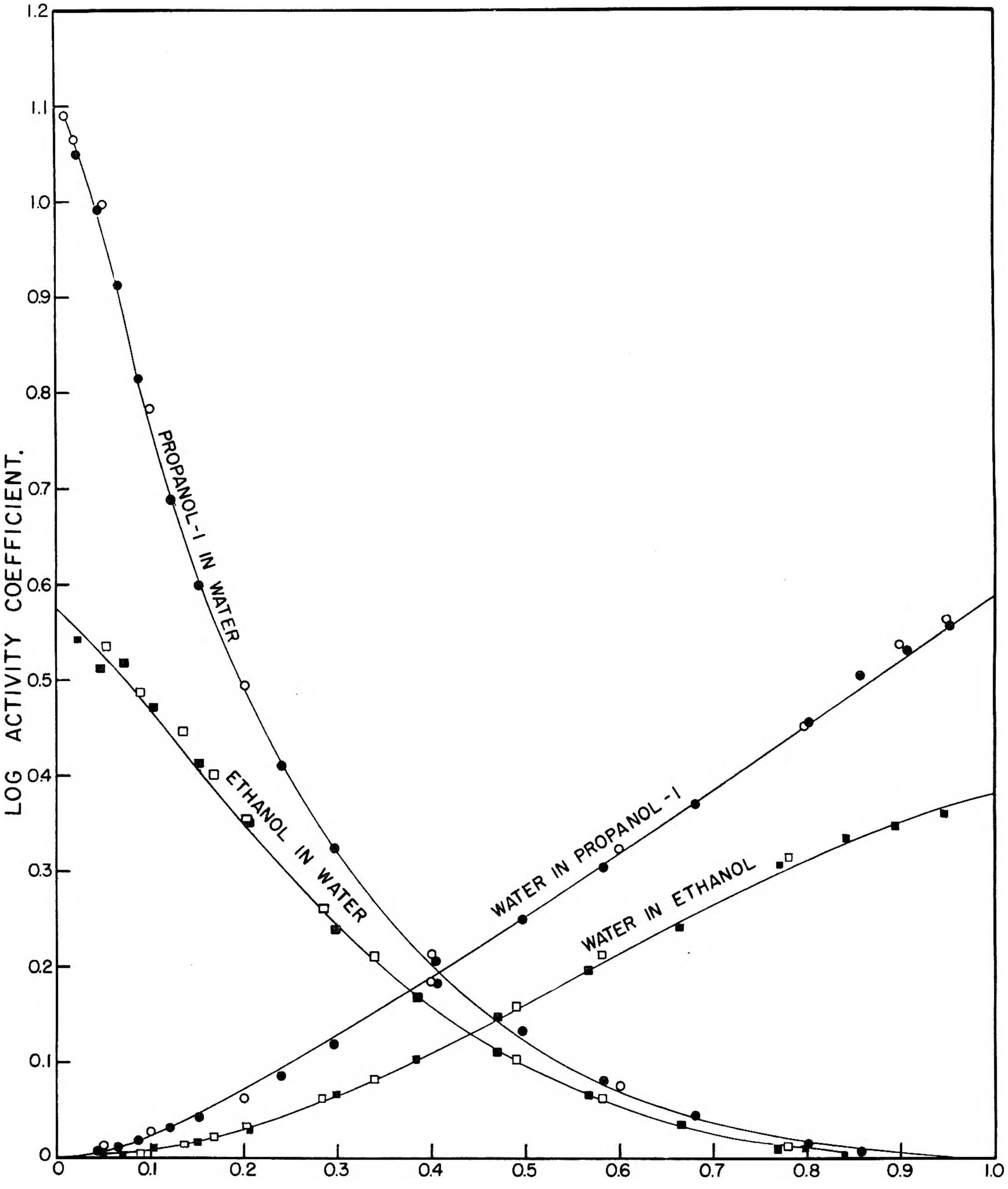

Fig. 4.—Self-consistent activity–concentration diagrams, systems water–ethanol and water–propanol at 25°. ●, ■, present work; □, Dobson; ○, Butler, Thomson and Maclennan.

Gibbs–Duhem equation are low, reflecting excellent self-consistency of data.

On the basis of these results, we believe the method described is a rapid and accurate method for the determination of activities of both components in binary mixtures of volatile solutes.

KINETICS OF THE PRE-STEADY STATE SYSTEM OF CATALASE WITH HYDROGEN PEROXIDE

BY ROLAND F. BEERS, JR.[1]

Division of Physical Biochemistry, Naval Medical Research Institute, Bethesda 14, Maryland

Received June 11, 1953

The transient phase of the kinetics of the catalase–hydrogen peroxide system has been examined analytically. For the simple case, where the two consecutive reactions between catalase and the substrate are assumed to be irreversible and no hydrogen donor other than hydrogen peroxide reacts with the primary complex, an analytical solution of the differential equation for the rate of formation of the primary complex, p, has been found. This was accomplished by substituting into the differential equation for the variable s (substrate concentration) a function correlating s with p. From arguments developed for two limiting cases, this equation reduces to the empirical equation of Chance, *et al.*[2] The empirical correction factor of Chance's equation has been found from comparison of the two equations to vary directly with p, s_0/e and $1/R_k$ (s_0 is initial substrate concentration; R_k is the ratio of the two consecutive specific reaction rates of catalase with hydrogen peroxide: k_4/k_1). The k_1 values calculated from the differential analyzer data of Chance, *et al.*,[4] by this equation and the k_1 values put into the differential analyzer are found to agree within 3.2% with a standard deviation of ±2.1%.

Introduction.—Solutions of the kinetics of the catalase–hydrogen peroxide system have been derived for the special case in which the concentration of the enzyme–substrate complex is constant and independent of the substrate concentration or time.[2,3] In an earlier paper[3] Beers and Sizer mention some of the difficulties encountered in attempting to solve the kinetics for the case when the enzyme–substrate is not constant but increases with time. They suggested that a rigorous solution would not be possible unless one had simultaneous rate curves for both the formation of the intermediate complex and for the decomposition of the substrate, hydrogen peroxide. Recently, Chance, *et al.*,[2] derived an equation describing the rate of formation of the intermediate complex. By making the approximation that the substrate was constant during the time the intermediate complex was increasing, and taking advantage of the steady state solution and the empirical approximations provided from analog computation studies,[4] they arrived at an integrated expression which described quite satisfactorily the kinetics of this system.

A further development of the mathematical analysis of this system would be justified, therefore, only if one could by more rigorous methods arrive at a solution which could at least duplicate the accuracy of Chance's equation. In particular, one would like to find a method for solving simultaneously the rate of formation of the enzyme–substrate complex and the rate of decomposition of the substrate. With this objective in mind, we have attempted to solve the transient state solution for the reacting system

$$\overset{e\,-\,p}{\mathrm{E}} + \overset{s}{\mathrm{S}} \xrightarrow{k_1} \overset{p}{\mathrm{ES}} \tag{1}$$

$$\overset{p}{\mathrm{ES}} + \overset{s}{\mathrm{S}} \xrightarrow{k_4} \overset{e\,-\,p}{\mathrm{E}} + \text{products} \tag{2}$$

where e is the total enzyme concentration (moles of active centers per liter) and s and p are the instantaneous concentrations of the substrate and primary complex, respectively. On the basis of schemes 1 and 2, an irreversible pair of consecutive reactions in which the only donor species is hydrogen peroxide, one can obtain a differential equation, $f(p', p, t) = 0$, in which by means of one well defined approximation, whose error can be ascertained from theory, one may separate the variables. When the integral of this equation is solved for k_1et, the right-hand member consists of two terms. Under specific limiting conditions one or the other of these terms vanishes. The resulting equations are found to have close similarities to that of Chance, *et al.*[2]

Theory.—The rate expressions for the schemes 1 and 2 are

$$\mathrm{d}p/\mathrm{d}t = (k_1e/p_\mathrm{M})[s_0 - (x + p)](p_\mathrm{M} - p) \tag{3}$$

$$\mathrm{d}s/\mathrm{d}t = -[s_0 - (x + p)][k_1e - p(k_1 - k_4)] \tag{4}$$

where

$$p_\mathrm{M} \equiv k_1e/(k_1 + k_4)$$

and x is the total amount of substrate decomposed (in the k_4-step) up to time t. In an earlier paper[3] p_M (Chance's terminology[2]) was introduced as the value which p obtains whenever the time decay of s is first order, and it was shown incidentally that under these conditions p was in the steady state, *i.e.*, $\mathrm{d}p/\mathrm{d}t = 0$. From this one may infer that p_M is some sort of a maximum. The precise nature of this maximum is readily discovered. Dividing (3) by (4) and integrating we obtain (*cf.* ref. 2)

$$s = s_0 - [p_\mathrm{M}/(k_1 + k_4)][(k_1 - k_4)p/p_\mathrm{M} - 2k_4 \ln(1 - p/p_\mathrm{M})] \tag{6}$$

Physical requirements stipulate that the initial value of p be 0, and that s never be negative or complex. From these restrictions and (6) it follows that the absolutely maximum value attainable by p is p_M and that $p = p_\mathrm{M}$ is reached only under the special conditions that $s_0 = \infty$ (for practical purposes, s_0 need only be a few times greater than e) in which case $s = 0$. Because of (4), $s = s_0 - (x + p) = 0$ means that $\mathrm{d}p/\mathrm{d}t = 0$. In other words, under these several conditions, p is at a true *absolute* maximum. It has its greatest physically attainable value, and its time derivative vanishes. Under other conditions (s_0 of the order of e or less), p can also reach values at which $\mathrm{d}p/\mathrm{d}t = 0$; *i.e.*, maxima; however, these are

---

(1) The opinions expressed in this article are the private ones of the author, and do not necessarily reflect the opinions of the Navy Department or the Naval Service at large.

(2) B. Chance, D. S. Greenstein and F. J. W. Roughton, *Arch. Biochem. Biophys.*, **37**, 301 (1952).

(3) R. F. Beers, Jr., and I. W. Sizer, THIS JOURNAL, **57**, 290 (1953).

(4) B. Chance, D. S. Greenstein, J. Higgins and C. C. Yang, *Arch. Biochem. Biophys.*, **37**, 322 (1952).

always less than p_M, and to emphasize the distinction Chance, *et al.*,[2] have denoted these by p_m. Referring again to (3) we see that for p to reach one of these "lesser" maxima, *i.e.*, $dp/dt = 0$ but $p_m < p_M$, it is, as in the case of the absolute maximum, still required that $s = 0$.[5]

In order to faciliate the search for a solution of the transient phase kinetics of the catalase–hydrogen peroxide system it is desirable to find a relation which will correlate the change of s with p. In particular, we wish to find p as a function of t only. Consider

$$B(p) \equiv \frac{xe}{p(x+p)} = R_k + f(p) \qquad (7)$$

where R_k is k_4/k_1 and $f(p)$ is to be found. Substituting x and $x + p$ from (6) into (7) it can be shown analytically (appendix i) that

$$\lim_{p\to 0} B = R_k,\ i.e.,\ f(p) = 0 \qquad (8)$$

$$\lim_{p\to p_M} B = R_k + 1,\ i.e.,\ f(p) = 1 \qquad (9)$$

For the approximation $B(p) \cong R_k$, the per cent. error is $100 \times f(p)/R_k$ and depends on the value of p/p_M (Fig. 1). For all known catalases the error is 5% or less when $0 < p/p_M < 0.5$. It should be noted that the condition $p/p_M = 0.5$ does not (except in the case $p_m = p_M$) define the experimental "half-time." The latter is always shorter than the time required to reach $p/p_M = 0.5$, and consequently the error at the "half-time" will be considerably less than 5%.

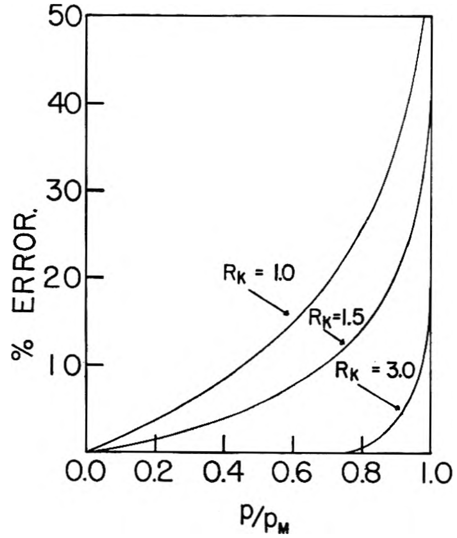

Fig. 1.—Per cent. error of the equation: $xe/p(x + p) = R_k$, as a function of p/p_M for three values of k_4/k_1 (see text for details).

Rearranging (7) and solving for $x + p$, we obtain

$$x + p = \frac{ep}{e - (R_k + f(p))p} \qquad (10)$$

Substituting (10) into (3)

$$dp/dt = k_1e(1 - p/p_M)\left(s_0 - \frac{ep}{e - (R_k + f(p))p}\right) \qquad (11)$$

Treating f(p) as small and rearranging (11) we may evaluate the error in (11) made in assuming that f(p) is zero.

$$dp/dt = k_1e(1 - p/p_M)\left(s_0 - \frac{ep}{e - R_kp}\left[1 - \frac{f(p)p}{e - R_kp}\right]\right) \qquad (11a)$$

We observe that the error is the term: $f(p)p/(e - R_kp)$ and is always less the f(p), inasmuch as the term $p/(e - R_kp)$ is always less than unity (except when $p = p_m$) and, in fact, decreases to zero for very small p. With this limitation of error in mind we will make the approximation that f(p) is zero. Integration of (11) between the limits of t and collection of terms yields (see appendix ii)

$$k_1et = \frac{\left(\frac{e}{e + R_ks_0}\right)\ln\left(1 - \frac{e + R_ks_0}{s_0e}p\right) - \frac{p_M}{e}\ln(1 - p/p_M)}{\frac{s_0}{e} - 1} \qquad (12)$$

where R_k may be determined experimentally from the rearrangement of (5).

$$R_k \equiv (e - p_M)/p_M \qquad (5a)$$

Equation 12, a general solution of (3), contains only one approximation, *viz.*, f(p) = 0, which is significant as a source of error only when p/R_kp_M is large. With the exception of this limiting case, (12) should describe the kinetics of the rate of formation of p on the basis of scheme 1 and 2 for all values of s_0 and p. Let us first consider two limiting cases.

Case I. Large s_0/e.—The first term of the right hand side of (12) vanishes

$$k_1et = (p_M/s_0)\ln p_M/(p_M - p) \qquad (13)$$

Equation 13 is formally identical with a reversible first-order equation. Chance, *et al.*,[2] derived this equation directly from (3) by assuming that s is constant. However, they found this assumption did not always hold true. This is so because (13) assumes that f(p) is zero and also because, as was shown above, when p approaches p_M or p_m s approaches zero (see, however, footnote 5).

Case II. Small s_0/e.—With decreasing values of p the second term of the right hand side of (12) vanishes before the first, and we obtain

$$k_1et = \frac{e}{(e/s_0) + R_k}\ln\left(1 - \left[\frac{e + R_ks_0}{s_0e}\right]p\right) \qquad (14)$$

or, on rearranging

$$p = \frac{e}{(e/s_0) + R_k}\left(1 - \epsilon^{-k_1(e + R_ks_0)t}\right) \qquad (14a)$$

From (14a) it is clear that p reaches a maximum value which is less than p_M, since by hypothesis, $e > s_0$; in other words, p reaches what we have called a "lesser" maximum, a plateau value since according to (14a) p does not decrease with time once it has attained p_m

$$p_m = \frac{e}{(e/s_0) + R_k} \qquad (15)$$

Accordingly, we may rewrite (14) as

$$k_1et = (p_m/s_0)\ln p_m/(p_m - p) \qquad (16)$$

---

(5) This, of course, does not hold for the case where any competing reaction is taking place, since under these conditions p can reach a maximum before $s = 0$. *Cf.* Chance, *et al.*[2]

Compare this equation with the empirical equation of Chance, *et al.*[2]

$$k_1et = (1.1p_m/s_0)\ln p_m/(p_m - p) \qquad (17)$$

The arguments leading to eq. 16 provide a theoretical basis for the empirical substitution of p_m for p_M in eq. 13. Equations 13 and 16 represent the limiting conditions under which but for the correction factor of 1.1 Chance's equation 17 is identical with 12. The value of p_m given by 15 has been obtained under the approximation $e/s_0 < 1$; however, the exact value of p is given implicitly by (6) on setting $s = 0$ (it will be recalled that $s = 0$ implies that dp/dt is zero for the scheme 1 and 2.[6]

Discussion.—This reasonably rigorous solution of the simple system represented by scheme 1 and 2 now permits us to make some direct comparisons with the solutions published for the complete system[2] in which are found also the reverse reaction, k_2p, and the competing reaction, $k_4^*a_0$, or the reaction of p with a donor other than hydrogen peroxide. In this manner we will ascertain whether the proposed analytical solution makes any significant contribution to the general theory of catalase kinetics.

A comparison of (12) and (17) over a wide range of s_0/e values and under the assumption that the correction factor, 1.1, is a variable, Z, will show graphically that Z varies directly with p, $1/s_0$, and $1/R_k$. Of particular interest, however, is the variation of Z with s_0/e at the "half-time" of the reaction, *i.e.*, at $p_m/2$. Figure 2 illustrates the rise and fall of Z with a maximum at approximately $s_0/e = 1$. It is smaller for larger R_k. The actual maxima and per cent. errors are 1.08 (−9.95%) and 1.077 (−7.5%) for $R_k = 1$ and 3, respectively. These values are to be compared with the empirical value calculated by Chance, *et al.*,[4] from their differential analyzer data: 1.1 (−10%) for the case when $R_k = 1$. Included in the figure are four empirical values of Z calculated from the differential analyzer data.

From the differential analyzer data we may also compute k_1 values by means of eq. 12. The values put into the machine are k_1, k_4, s_0, e and $k_4^*a_0$; from the resulting differentiation are obtained $p(t_4)$ and p_m values. Table I contains the data published by Chance, *et al.*, in the first four columns. The average value of k_1 calculated by means of (12) is 2.9 × 10^7 mole^{-1} sec.$^{-1}$ (theory 3.0 × 10^7) or a per cent. error of −3.2% and a standard deviation of ±2.1%. Because of the potentially large error in (12) with large p, the calculated values of k_1 at $p = 0.49$ and 0.497 have been omitted from the averages. The average value of k_1 determined by Chance's equation on the basis of a correction factor of 1.11 is 3.0 × 10^7 mole^{-1} sec.$^{-1}$ with a standard deviation of ±3.85%. The larger standard deviation probably reflects the variation of Z previously noted.

Because of the close agreement given by eq. 12 it is useful to estimate what the approximation, $f(p) = 0$, contributes to the error. For the $p(t)$ values quoted in the first 14 rows the average value of $f(p)$ is 0.07 or smaller than R_k by one order of magnitude. Therefore, we may use the approximation of eq. (11a) for an estimation of the error. The average error is approximately 1.5%. It is also of interest to note that the p_m values computed by the differential analyzer agree with those predicted by eq. 6 (based on scheme 1 and 2) to within 1%.

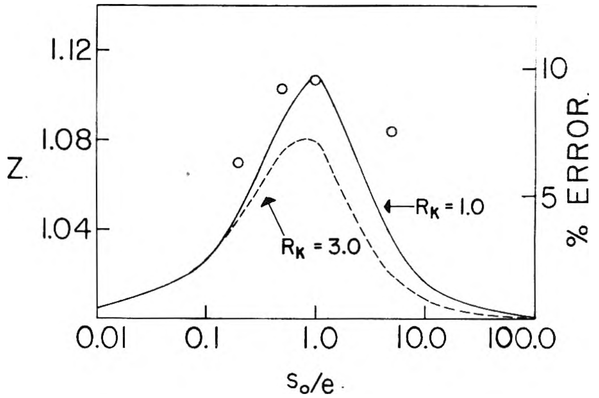

Fig. 2.—Variation of the correction factor, Z, of Chance's equation at $p_m/2$ with s_0/e (see text for details).

From these observations we may conclude that although eq. 12 is based on a simple scheme it is an excellent approximation of the solution representing the complete scheme of Chance, *et al.* This suggests that possibly the parameters, k_2p and $k_4^*a_0$, are making no significant contribution to the transient phase kinetics prior to the time p reaches p_m. Of course, once the substrate is exhausted or very small, then these parameters become important. This has been observed experimentally and with differential analyzer studies.[4]

Acknowledgment.—The author wishes to acknowledge his indebtedness to Dr. M. F. Morales for his continued interest and help in the preparation of this paper and in several of the analytical solutions.

Appendix i

From eq. 6 is obtained

$$x = -(2k_4p_M^2/k_1e)(r + \ln(1 - r))$$

where $r = p/p_M$. Let $2R_k \equiv a$ and $2R_kp_M/e \equiv b$. Then

$$xe/p(x + p) = \frac{-(a/r)(r + \ln(1 - r))}{r - b(r + \ln(1 - r))}$$

Expanding yields

$$xe/p(x + p) = \frac{a(r/2 + r^2/3 + \ldots)}{r + b(r^2/2 + r^3/3 + \ldots.)}$$

The limits of this equation are

$$\lim_{r\to 0} xe/p(x + p) = ar/2r = R_k$$

$$\lim_{r\to 1} xe/p(x + p) = \frac{a(1/2 + 1/3 + \ldots\ldots)}{b(1/2 + 1/3 + \ldots\ldots)} = R_k + 1$$

Appendix ii

From eq. 11 is obtained

$$-(1/k_1e)\,dp/dt = (1 - r)\frac{(s_0/p_M) - (1 + R_ks_0)r}{(1/p_M) - (R_kr/e)}$$

---

(6) A third limiting condition of interest is Case III: $s_0/e = 1$. After simplification, integration of (3) yields (see appendix ii)

$$k_1et = \frac{p_M{}^2p}{e^2(p_M - p)} - R_k\ln\frac{p_M}{p_M - p} \qquad (18)$$

TABLE I

DETERMINATION OF k_1 BY MEANS OF EQUATIONS 12 AND 17 ($Z = 1$) FROM COMPUTATION DATA OF DIFFERENTIAL ANALYZER[4]

Initial conditions: $e = 10^{-4}\ M$, $k_1 = k_4 = 3 \times 10^4$ mole^{-1} sec.$^{-1}$, $k^*a_0 = 0.02$ sec.$^{-1}$.

s_0/e	p_m[a]	p	Time, sec.	$k \times 10^{-7}$ (eq. 17)[b]	Error, %	$k_1 \times 10^{-7}$ (eq. 12)	Error, %	Z[c]
0.2	0.164	0.0175	3.33	2.769	7.70	2.796	6.80	1.083
.2	.164	.073	16.7	2.892	3.60	2.914	2.87	1.037
.2	.164	.082[d]	20.3	2.800	6.67	2.925	2.50	1.071
.2	.164	.093	25.0	2.745	8.47	2.940	2.00	1.092
.5	.314	.0425	3.33	2.716	9.47	2.787	7.00	1.104
.5	.314	.157[d]	16.0	2.721	9.30	2.948	1.73	1.103
.5	.314	.160	16.7	2.680	10.67	2.924	2.60	1.119
.5	.314	.203	25.0	2.612	12.93	2.922	2.60	1.149
1.0	.430	.0825	3.33	2.680	10.67	2.850[e]	5.00	1.119
1.0	.430	.215[d]	11.0	2.71	9.67	2.991[e]	0.30	1.107
1.0	.430	.272	16.7	2.578	14.07	3.001[e]	0.00	1.164
1.0	.430	.325	25.0	2.424	19.20	2.906[e]	3.13	1.238
5.0	.499	.250[d]	2.5	2.767	7.77	2.872	4.21	1.084
5.0	.499	.300	3.33	2.756	8.13	2.882	3.93	1.089
5.0	.499	.490[f]	16.7	2.400	20.00	2.707	9.77	1.250
5.0	.499	.497[f]	25.0	2.117	29.43	2.331	22.30	1.417
Av.[f]				2.704	− 9.9%	2.904	− 3.2	1.111
Standard deviations				±3.85%		±2.07%		

[a] The corresponding p_m values from eq. 6 are 0.1645, 0.316, 0.4325 and 0.49998. [b] Recalculated by the author from the data of Chance, first four columns. [c] Based on the theoretical value of k_1: 3×10^7. [d] Half time of the reaction: $p/p_m = 0.5$. [e] Calculated by eq. 18. [f] Data omitted from the averages for reasons given in the text.

where r is p/p_M. Let s_0/p_M be α and $1 + R_k s_0/e$ be β. Since $e/p_M = R_k + 1$, then

$$-[1/(R+1)k_1]\ \mathrm{d}r/\mathrm{d}t = \frac{(1-r)(\alpha - \beta r)}{(1/p_M) - (R_k r/e)}$$

Separating fractions, we have

$$k_1 e \mathrm{d}t = \frac{\mathrm{d}r}{p_M(1-r)(\alpha - \beta r)} - \frac{R_k r \mathrm{d}r}{e(1-r)(\alpha - \beta r)}$$

or

$$k_1 e\ \mathrm{d}t = \frac{\mathrm{d}r}{p_M(1-r)(\alpha - \beta r)} - \frac{R_k}{(1+R_k)} \frac{r \mathrm{d}r}{(1-r)(\alpha - \beta r)}$$

If $s_0 \neq e$, then $\alpha \neq \beta$ and integration yields

$$(\alpha - \beta)k_1 e t = 1 - \left(\frac{R_k}{1+R_k}\right) \ln(1 - \beta r/\alpha) - \left(1 - \frac{R_k}{1+R_k}\right) \ln(1-r)$$

With appropriate substitutions this equation becomes (12).

If $s_0 = e$, then $\alpha = \beta$ and

$$\alpha k_1 e\ \mathrm{d}t = \frac{\mathrm{d}r}{(1-r)^2} - \left(\frac{R_k}{1+R_k}\right) \frac{r\ \mathrm{d}r}{(1-r)^2}$$

Integration yields

$$\alpha k_1 e t = \frac{r}{1-r} - \left(\frac{R_k}{1+R_k}\right) \frac{r}{1-r} - \left(\frac{R_k}{1+R_k}\right) \ln(1-r)$$

With appropriate substitutions this equation becomes eq. 18.

THE PHYSICAL-CHEMICAL BEHAVIOR OF OIL-DISPERSIBLE SOAP SOLUTIONS. I. SODIUM PHENYL STEARATE IN BENZENE[1a]

BY J. G. HONIG AND C. R. SINGLETERRY

Surface Chemistry Branch, Chemistry Division, Naval Research Laboratory, Washington 25, D. C.

Received August 12, 1953

The rheological behavior of dilute solutions of sodium phenyl stearate in benzene is profoundly affected by the addition of small amounts of certain polar additives. The anhydrous system has a viscosity too high for convenient measurement in a capillary viscometer; this viscosity is reduced to a value only slightly above that of the solvent by the addition of water. organic acids, alcohols or phenols to the extent of 0.1 to approximately 1.0 mole per mole of soap. Further additions of water or of glycol lead to very high but non-Newtonian viscosities and pronounced elastic properties. The viscosity effects resulting from additions of water, alcohols and phenol are reversed on heating to 70°; the effect produced by addition of phenylstearic acid is virtually irreversible. The rheological phenomena are believed to indicate that the dispersed soap is organized into three types of structure: (1) long polymeric chains of anhydrous soap held together by ionic forces, (2) a small and relatively compact micelle which exists in the presence of a fraction of a mole of additive per mole of soap, and (3), for water and glycol additions, an extensive but loosely bonded structure formed through a bridging between small micelles by the excess of bifunctional additive present. Additives containing an acidic hydroxyl-group are believed to break down the original polymer chain by the direct introduction of slightly ionic carboxyl groups or by the production of such groups *in situ* through hydrolysis.

Introduction.—A previous communication[1b] has reported the high viscosity of dilute anhydrous solutions of calcium xenyl stearate in benzene and the extraordinary sensitivity of these systems to traces of water. The phenomenon is general for oil-soluble carboxylate soaps of a wide range of metal ions and provides an important approach to the study of states of aggregation of the solute in these systems. It throws light also on the forces responsible for micelle formation and on the extent of interaction between the soap micelle and polar substances which are molecularly soluble in the solvent. These systems furnish, in addition, models for the study of rheological phenomena hitherto familiar only for the aluminum soaps, and permit such study in the presence of a better controlled and wider range of variables than was before possible.

Experimental Procedure

Materials Used.—The sodium phenyl stearate used was prepared from phenylstearic acid and was dried and stored as previously described.[2] It contained about 10% of a lower molecular weight acid. Sodium soap prepared later from molecularly distilled phenylstearic acid gave results essentially similar to those obtained with soaps prepared from the original acid stock.

The alkaline sample of sodium phenyl stearate used contained 0.1 mole excess sodium hydroxide per mole of soap. It dispersed in dry benzene to give an optically clear system.

Benzene (A.C.S. specification) was percolated through silica gel and stored over metallic sodium until used. Phenylstearic acid was dried at elevated temperatures *in vacuo* over phosphorus pentoxide. Absolute ethanol was dried with sodium metal and diethyl phthalate.[3,4]

n-Amylamine (The Mathieson Co.) was stored over fused sodium hydroxide. Di-*n*-amyl ketone (Eastman Kodak Co.) was percolated through alumina and silica gel in a dry atmosphere before use. Phenol (Baker's Analyzed) was dried at elevated temperatures at reduced pressure and recrystallized.

Ethylene glycol was redistilled and then percolated through silica gel and charcoal. Pinic acid, prepared at this Laboratory,[5] was dried over phosphorus pentoxide and used as a solid.

All non-aqueous reagents were stored and handled in a dry atmosphere.

Methods Used.—The viscometers used in this study were of the capillary type with three measuring bulbs placed one above the other to permit detection of non-Newtonian flow.[6] Viscosities could be measured at three average hydrostatic pressures in the ratio 4:2:1. Determinations could be repeated at will, and gave reproducible results for a given system. The viscometers were calibrated with National Bureau of Standards viscosity standards No. D-8 and I-9 and with benzene. All viscosities were determined at 25.0° (unless otherwise specified) in a constant temperature bath controlled to ±0.003°.

The data obtained from a non-Newtonian liquid with such a viscometer are conveniently discussed in terms of the exponential viscosity equation. In logarithmic form this is

$$\log \gamma_w = \left[\log \frac{1}{\zeta}\right] + n \log \tau \qquad (1)$$

where γ_w is the actual shearing rate at the capillary wall, τ is the corresponding shearing stress and ζ is the viscosity counterpart[7] specifying the viscosity of the non-Newtonian system at unit shearing stress. The exponent, n, is the index of departure from Newtonian flow. Procedures for the graphic or analytical derivation of the constants ζ and n from rheological data are described elsewhere.[6] The experimental results in this paper are expressed as relative nominal viscosities, obtained by treating each bulb as a separate viscometer. The nominal viscosity is the viscosity of a Newtonian liquid which has the same flow-time under the same shearing stress as the solution measured.

All non-aqueous additions were made in a dry-box in which dried air under positive pressure was recirculated through a column of anhydrous calcium chloride by a turbine-type blower. The glass-stoppered viscometers were kept sealed with fused wax for additional protection. The highly viscous solutions approached equilibrium extremely slowly (up to 20 days). The system was assumed to be at equilibrium if no change in flow time was recorded over a 24-hour period. The rate of equilibration was roughly proportional to the viscosity of the solution.

Experimental Results

The Effect of Added Water.—To two soap solutions, c = 1.76 g./100 ml. of solution and c = 0.68 g. soap/100 ml. solution, small portions of distilled water were added. The changes in relative nominal viscosity, $(\eta_{\text{nom}}/\eta_0)$, are summarized in Fig. 1. The concentrated soap was redried at the end of the run and the determinations were repeated with essentially the same results as before. A small

---

[1a] Presented at the 124th Meeting of the American Chemical Society, Chicago, Ill., September 6-11, 1953.

[1b] Lorraine S. Arkin and C. R. Singleterry, *J. Coll. Sci.*, **4**, 537 (1949).

[2] C. R. Singleterry and Lorraine A. Weinberger, *J. Am. Chem. Soc.*, **73**, 4574 (1951).

[3] R. H. Manske, *ibid.*, **53**, 1106 (1931).

[4] E. L. Smith, *J. Chem. Soc.*, 1288 (1927).

[5] C. M. Murphy, J. G. O'Rear and W. A. Zisman, *Ind. Eng. Chem.*, **45**, 119 (1953).

[6] J. G. Honig and C. R. Singleterry, NRL Report No. 4133, April, 1953.

[7] J. G. Krieble and J. C. Whitwell, *Textile Research J.*, **19**, 253 (1949).

amount of water reduces the relative viscosity of the system to a minimum while further additions of water produce a highly non-Newtonian viscous-elastic system. Observation of the birefringence of these latter systems shows relaxation times of the order of several minutes for the highly elastic systems. Precipitation occurred after 3.6 sru[8] of water had been added to the more concentrated solution and 5.0 sru to the more dilute solution.

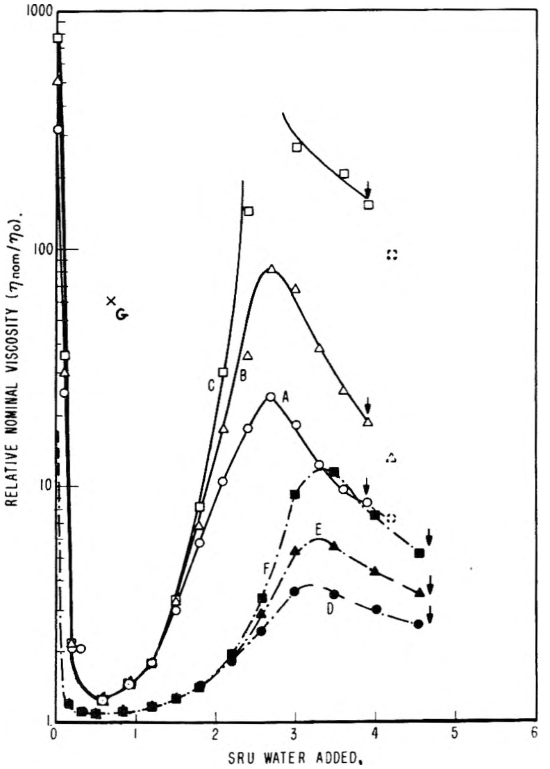

Fig. 1.—Effect of adding water to two soap solutions of different concentrations: curves A, B and C are for c = 1.76 at high medium and low shearing stresses; D, E and F are the corresponding curves for c = 0.68.

With an alkaline soap solution (c = 2.22; 0.1 mole of excess sodium hydroxide per mole of soap) the effect of added water was almost negligible The variation of viscosity with water content followed a pattern similar to that for the neutral soap, but the minimum relative viscosity (G of Fig. 1) was 59.6; all other compositions were too viscous for accurate measurement. The soap precipitated after the addition of 3.8 sru of water.

Sodium xenyl stearate solutions in benzene yielded results similar to those for sodium phenyl stearate although more water was required to produce equivalent effects.

When 0.6 sru of water was added to a sodium phenyl stearate solution (c = 1.52) its relative viscosity was 1.67. This solution was examined by the fluorescence depolarization method[2] to determine the volume of a sphere hydrodynamically equivalent to the micelle. The volume of a gram-micelle so found was 168,000 cc.

The Effect of Added Acid.—Successive portions of dried phenylstearic acid were added to a soap solution (c = 1.59). The resulting relative nominal viscosities are shown in Fig. 2. The effects of adding water to sodium phenyl stearate solutions containing 0.15 and 1.0 sru of phenylstearic acid, respectively, are shown in Fig. 3, curves IV to VII. The thickening usually produced in neutral soap solutions by water contents in excess of 1 sru was almost completely suppressed by the acid. Fluorescence depolarization measurements were made on a solution containing 0.2 sru of acid and no water. The volume of a gram micelle was found to be 105,000 cc.

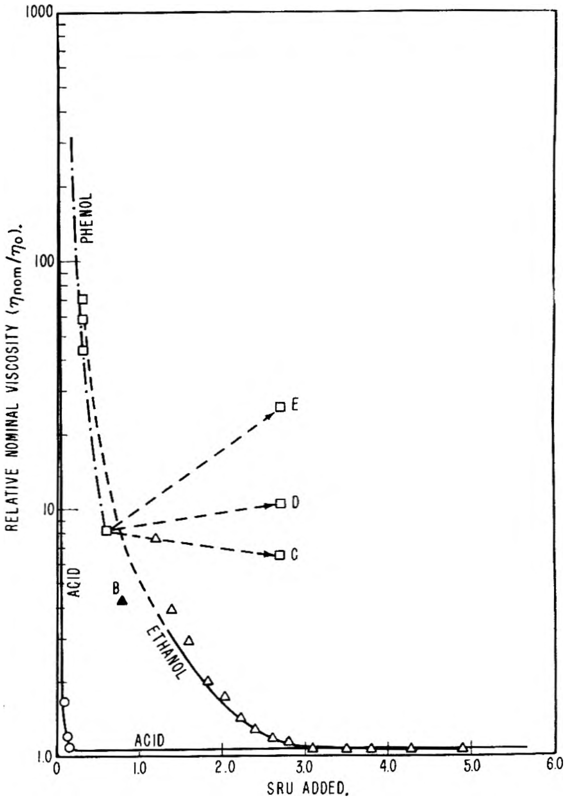

Fig. 2.—Effect of adding phenylstearic acid (○), alcohol (△) or phenol (□) to soap solutions.

An attempt to treat a soap solution (c = 1.48) with the benzene-soluble dibasic pinic acid was unsuccessful because a metathesis occurred to give an insoluble pinate soap.[9]

The Effect of Added Alcohol, Phenol and Glycol.—The monotonic decrease in viscosity produced by the addition of dried ethanol to a soap solution (c = 2.04) is recorded in Fig. 2. The effects of two additions of phenol to a soap solution (c = 1.92) are also shown in Fig. 2. The dotted arrows indicate the viscosities resulting from the addition of 2.5 sru of water to the phenol-containing solution. The viscosity rise and the increase in non-Newtonian behavior were much more pronounced than when water was added to the acid-containing soap systems of Fig. 3.

The very different effect produced by adding an excess of the bifunctional glycol instead of ethanol to a soap solution is shown in Fig. 3. In this case

---

[8] sru = solute ratio units = moles of solute added per equivalent dissolved soap.

[9] (a) G. H. Smith, L. B. Rogers and K. J. Mysels, *J. Am. Oil Chem. Soc.*, **26**, 135 (1949); (b) V. D. Tughan and R. C. Pink, *J. Chem. Soc.*, 1804 (1951).

0.8 sru of ethanol was first added to a soap solution (c = 1.84) to produce a low viscosity (point B of Figs. 2 and 3), after which glycol additions were made which carried the viscosity through a maximum qualitatively similar to that produced by water. This system did not precipitate a separate soap phase, but after the addition of sufficient glycol separated into two clear liquid phases. (The moderate increase in viscosity just before phase separation has been noted in other mixtures of a polar and a non-polar liquid.[10])

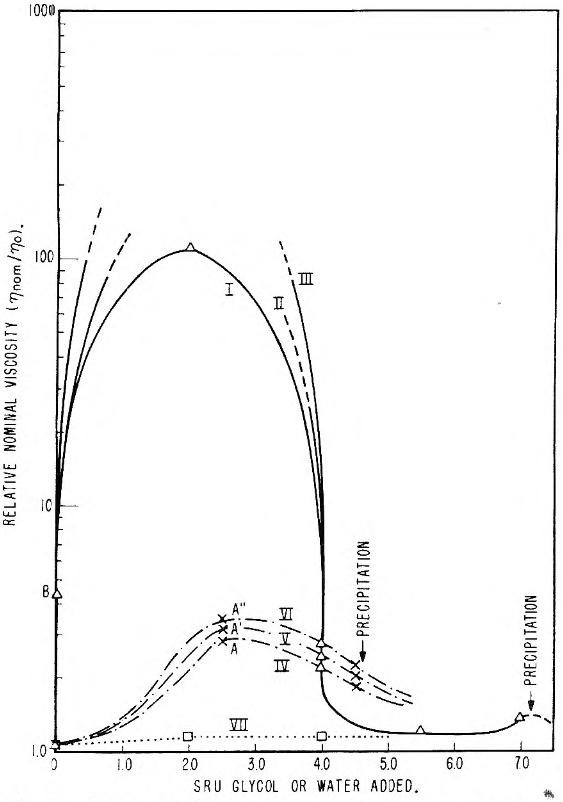

Fig. 3.—Effect of adding ethylene glycol to a soap solution containing 0.8 sru of ethanol (I, II, III); of adding water to a soap solution containing 0.15 sru of phenylstearic acid (IV, V, VI); and of adding water to a soap solution containing 1.0 sru of phenylstearic acid (VII).

The Effect of Added Amine or Ketone.—Neither dry n-amylamine nor dry di-n-amyl ketone produced detectable changes in the viscosity of dry soap solutions (c = 2.10 and 2.17, respectively) when added in the ratio of 4.8 moles of reagent per mole of soap. The amine did not prevent a subsequent addition of 0.1 sru of phenylstearic acid from exerting its full effect; this amount of acid, even in the presence of a 48-fold excess of amine, reduced the relative viscosity to 1.24.

The Effect of Temperature.—The effect of an increase in temperature depends strongly on the kind and amount of additive present (Fig. 4). The relative nominal viscosities of solutions containing a moderate amount of water (1.05 sru) or of ethanol (0.8 sru) increased sharply toward values characteristic of the original dry soap solution. The viscous system containing a large excess (4.0 sru) of water retraced only a part of the path followed during the addition of water, becoming thin and losing its non-Newtonian behavior with increasing temperature. Solutions containing even a small amount of acid, as well as those containing a large excess of ethanol (4.9 sru), increased in relative viscosity only slightly on heating.

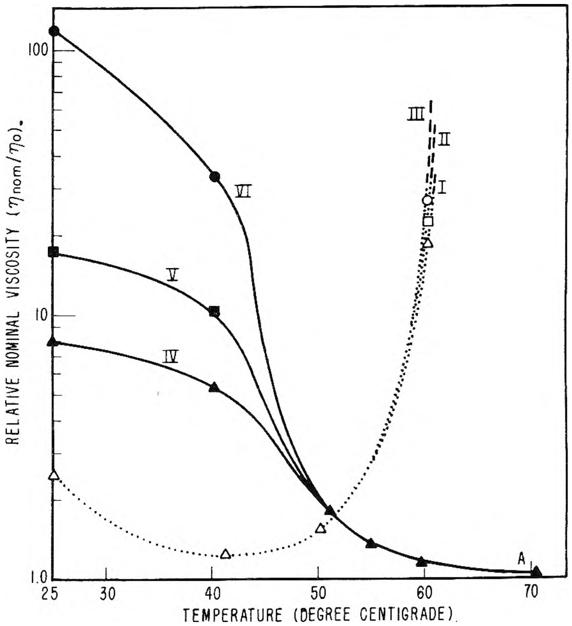

Fig. 4a.—Effect of temperature on soap solutions containing 1.05 sru of water (I, II, III) and 4.0 sru of water (IV, V, VI).

Discussion

The rheological properties of these systems are more easily discussed if the curves of Figs. 1 to 3 are considered to extend through three regions A, B and C in which characteristically different phenomena appear.

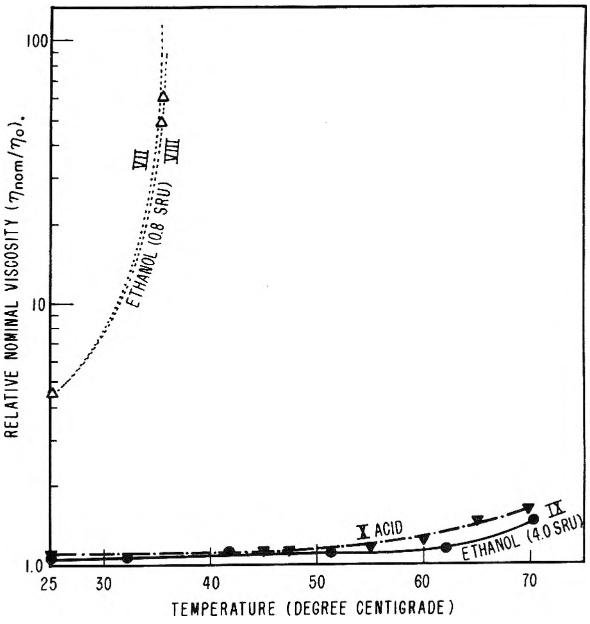

Fig. 4b.—Effect of temperature on soap solutions containing 0.8 sru of ethanol (VII, VIII), 4.9 sru of ethanol (IX) and 0.15 sru of phenylstearic acid (X).

---

(10) V. K. Semenchenko and E. L. Zorina, *Doklady Akad. Nauk. S.S.S.R.* **80**, 903 (1951).

Region A.—Region A is characterized by a rapid decrease in relative viscosity with increase in the amount of polar additive present. The index, n, of non-Newtonian behavior is approximately 1.6 and decreases rapidly as the relative viscosity falls. Such relatively small departure of n from unity (Newtonian flow) is characteristic of dilute solutions of very large linear macromolecules such as cuprammonium cellulose[11] and polystyrene.[12] The non-Newtonian character of the flow arises chiefly as a result of orientation and deformation of the very long polymer molecules under shear. Highly viscous soap systems in region A also exhibit strong birefringence. Taken together, this evidence indicates that in the initial anhydrous system the soap is present in polymer-like chains of very great length. The chain is conceived to consist of soap molecules whose polar ends are joined and whose hydrocarbon portions extend radially from the long axis (Fig. 5a). The polar ends are held together in part by charge effects and possibly in part by weak coördination bonds between the sodium ion and the two carboxylate ion oxygens. The two oxygens, as Duval, *et al.*,[13] have pointed out on the basis of infrared spectra of solid soaps, should be equivalent in charge and in coördinating power because of the resonance of the carboxylate ion. Such a chain, if fully extended, would have a backbone length of the order of 7 Å. per monomer unit. In this extended configuration the hydrocarbon tails of the acid are unlikely to furnish complete shielding of the polar backbone from interaction with the solvent or with the exposed backbone of other micelles. The soap molecules in such a structure would occupy only one-fifth of the volume of a cylinder of radius equal to the length of the fully extended 18 carbon chain of the phenyl stearate molecule. It is to be expected that in stable systems a more effective shielding will be achieved either by parallel alignment of two or more backbones, as indicated in Fig. 5b, or by a short range kinking or coiling of the backbone in such a way as to give an analogous electrical interaction between adjacent turns of the helix. At the same time the over-all length per soap monomer unit will be decreased to a point where the core is shielded from interaction with the polar portion of other polymer units. The coiled arrangement seems more probable. Halsey,[14] considering primarily aqueous systems, has discussed the theory of linear aggregation in soap micelles which are free to grow indefinitely in one direction only.

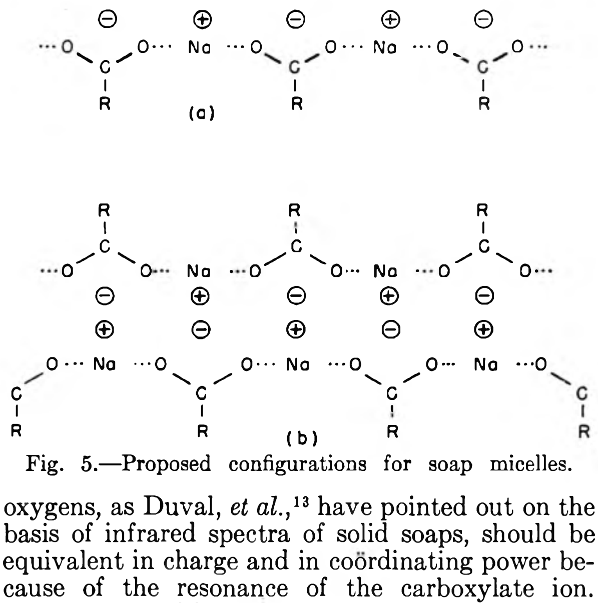

Fig. 5.—Proposed configurations for soap micelles.

A carboxylic acid is several times as effective, mole for mole, as water, alcohol or phenol in reducing the viscosity of the dry soap solution. The acid must act as a chain stopper which, by association with a soap molecule of the chain, saturates the forces that would otherwise hold the units of the chain together. The less effective viscosity reduction by water may be understood if it is assumed that acid is essential to the process, and that water is effective only to the extent that it hydrolyzes the soap to give weakly ionic carboxylic acid groups at intervals along the chain. The reversion of the water-containing systems to higher viscosities on warming could result from a displacement of the hydrolytic equilibrium as the water shifts from the soap micelles toward solution in benzene. Such a shift would be promoted both by the weakening of the hydrogen bonding between the soap and water and by the increased solubility of water in benzene at higher temperatures. In accord with the experimental results the presence of a large excess of water would favor hydrolysis and minimize the viscosity increase upon warming. The part played by hydrolysis is further confirmed by the inability of water to produce the usual decrease in viscosity when it was added to a soap system containing 0.1 sru of excess sodium hydroxide (Fig. 1, point G). The reductions in viscosity produced by additions of ethanol and of phenol are attributed to a similar mechanism. The effects of ethanol or phenol are temperature reversible for the same reasons as in the case of water. Polar molecules, such as n-amylamine and di-n-amyl ketone, which cannot hydrolyze the soap, have no detectable effect on the viscosity of the original system, even after 30 days of contact.

Region B.—The flow in region B is strictly Newtonian, but the minimum viscosities reached are larger than the values calculated from the Einstein or Guth–Simha equations for suspended spheres. The discrepancy suggests that the micelles are still strongly anisometric or that an appreciable amount of solvent is associated with them in the flow process. Consider a typical acid–soap solution (c = 1.73; phenylstearic acid = 0.2 sru; dry solute volume fraction ϕ = 0.08; relative viscosity = 1.08). The application of the Guth–Simha equation ($\eta_{sp}/\phi_{solvated} = 2.5 + 14.1\ \phi_{solvated}$) leads to an estimated solvation amounting to 36.7% of the dry solute volume. Applying the Kuhn equation ($\eta_{sp}/\phi = 2.5 + J^2/16$), which attributes all excess viscosity effects to dissymmetry, one gets an axial ratio, J, of 4.8 for a prolate ellipsoid hydrodynamically equivalent to the micelle. Fluorescence depolarization measurements indicate that the volume of a sphere hydrodynamically equivalent to the

---

[11] C. M. Conrad, *Ind. Eng. Chem., Anal. Ed.*, **13**, 526 (1941).

[12] L. J. Sharman, R. H. Sones and L. H. Cragg, *J. Appl. Phys.*, **24**, 703 (1953).

[13] C. L. Duval, J. Lecomte and E. Douvillé, *Ann. phys.*, **17**, 5 (1942).

[14] G. D. Halsey, Jr., THIS JOURNAL, **57**, 87 (1953).

micelle is 105,000 cc. per gram micelle. Assuming 36.7% solvation, this volume would correspond to a micelle containing approximately 200 monomer units. For a structure of this size, either solvation or dissymmetry furnishes a physically possible explanation of the departure of the viscosity from simple Einstein behavior. Assuming 200 monomer units per micelle it will be seen that 0.2 sru of acid corresponds to a possible 40 molecules of acid per micelle. This is an order of magnitude greater than the anticipated acid requirement for a simple chain-stoppering mechanism to give micelles consisting of single continuous chains, or of four or fewer of such chains in parallel orientation with their polar backbones in close association. It is not clear from the data available whether the major portion of the acid is associated with the micelle, but not effective for chain-breaking, or whether there is a substantial fraction of the acid present in true molecular solution in the benzene phase.

The minimum relative viscosities of solutions containing alcohol or phenol are similar to those of the acid systems. The water system, however, fails to reach this minimum value because another aggregative process sets in which leads to the unusual consistency phenomena found in region C. The solution containing 1.5153 g. of soap per 100 ml. solution and 0.6 sru of water showed a relative viscosity of 1.67 and fluoresence depolarization data showed the volume of a gram-micelle to be 168,000 cc. (assuming spherical symmetry). The viscosity excess in this solution is relatively large and it is not convincing to interpret the effect as caused entirely by solvation (the Guth–Simha equation would require 9.6 volumes of solvent per solute volume). Dissymmetry ($J = 19.2$ from the Kuhn equation) is more acceptable as an explanation of the departure from the simple Einstein viscosity. On heating a solution containing an excess (4.0 sru) of water the region C phenomena are reversed while the large excess of water prevents further reversion to the high viscosities of region A. A minimum value (point A, Fig. 4a) is thereby reached which indicates that in the absence of reaggregation processes water-bearing micelles can exist which are rheologically similar to those found in acid-, alcohol- and phenol-containing systems.

Region C.—In region C the behavior of a solution to which water or glycol is added diverges sharply from that characteristic of phenylstearic acid–, ethanol– and phenol–soap systems. Figure 6 summarizes, for a typical system, the effects of water on the relative viscosity at unit shearing stress (ζ/η_0), and on the index, n, of departure from Newtonian flow. The high values of n in this region are correlated with pronounced viscoelastic behavior, and with a strong flow birefringence having a relaxation time of several minutes, as compared with several seconds for the viscous solutions in region A.

It is concluded that in this region the micelles present in region B are joined into an extensive structure through some bridging action of the water molecules, which at this stage outnumber the soap monomer units in the micelles. The interaction is not a coagulation or precipitation, since the solutions remain brilliantly clear, indicating that the diameter of the linear element of the structure is of the same small magnitude as that of the micelles or polymer chains of regions A or B. The elastic effects suggest that the structure is somewhat branched, and the rapid reduction in nominal viscosity as the shearing stress is increased (a much larger effect than would be expected as a result of orientation and deformation alone) implies that the bonds holding the structure together are broken by the forces applied during shear, so that the units present during rapid shear are smaller than those in the stationary liquid.

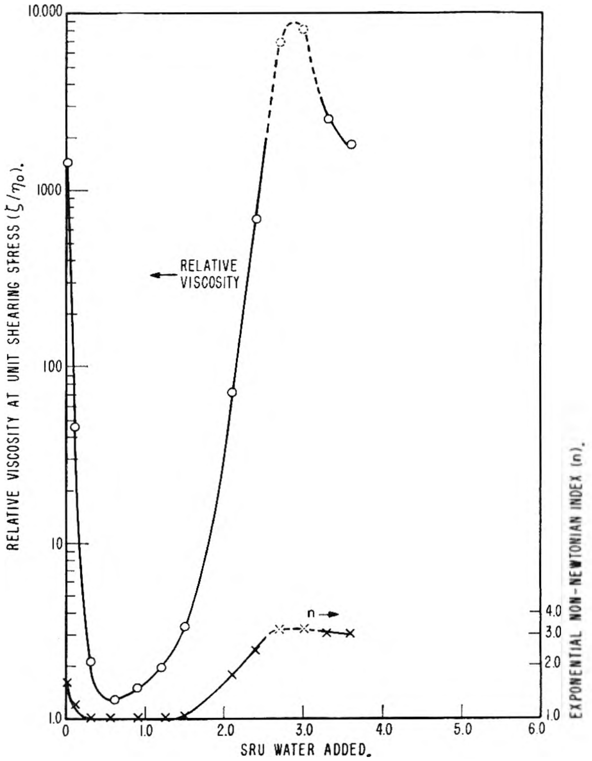

Fig. 6.—Effect of water additions on the relative viscosity at unit shearing stress (ζ/η_0) and the index, n, of deviation from Newtonian flow of a soap solution $c = 1.76$. (Dotted lines indicate a much greater degree of experimental uncertainty than in the region of solid lines.)

Water differs from acid, ethanol and phenol in having two potentially active hydrogens, and in having no hydrocarbon portion which might offer steric interference to bridging action. Ethylene glycol, with similar characteristics, was at least as effective as water in raising the viscosity of a soap solution containing ethanol. If one accepts the more or less coiled configuration suggested for the anhydrous soap chains, the adsorption of water or glycol by the polar backbone of the chain would be expected to increase the distance between adjacent turns of the coil. This would decrease the screening effectiveness of the hydrocarbon portion of the soap; at the same time the polar backbone would be loaded with molecules capable of hydrogen-bridging to exposed polar areas of other chains. Alcohol or phenol, on the other hand, although they might expand the turns in the polymer coil, would themselves shield the backbone with their own hydrocarbon portions so that intermicellar interactions would be no more probable than before.

It is of interest that the characteristic region C thickening has been observed only when sodium hydroxide was postulated to be present as a result of hydrolysis, or had been deliberately added. The powerfully basic hydroxyl ion may well be the point of anchorage of the water or glycol molecules responsible for the bridging between micelles. No evidence of extensive micellar interaction was obtained when water was added to the acid–soap system, in which hydrolysis to form hydroxyl ions would be suppressed by the free acid.

Despite some general resemblance between the behavior of dilute solutions of sodium phenyl stearate and of aluminum dilaurate in hydrocarbon solvents,[15–18] it should be noted that the systems differ in important aspects. No phenomenon corresponding to the thickening effect of water in region C has been reported for aluminum dilaurate, and the order of effectiveness of amines, alcohols, phenols and acids in reducing the viscosity is exactly opposite in the two cases. It appears that acidic hydrogen is an important factor in the interaction of additives with sodium phenyl stearate; on the other hand Alexander and Gray,[1] McRoberts and Schulman[11] and Scheffer[14] correlate peptization of aluminum soaps with the tendency of the additive to be coördinately bound by aluminum.

Acknowledgment.—The authors wish to express their appreciation to Mr. Samuel Kaufman for making the fluorescence depolarization determinations used in this investigation.

---

(15) A. E. Alexander and V. R. Gray, THIS JOURNAL, **53**, 9 (1949); *Proc. Roy. Soc.* (*London*), **A200**, 162 (1950).

(16) J. McBain and E. Working, THIS JOURNAL, **51**, 974 (1947).

(17) T. S. McRoberts and J. H. Schulman, *Proc. Roy. Soc.* (*London*), **A200**, 136 (1950).

(18) H. Scheffer, *Can. J. Research*, **26B**, 481 (1948).

THE INFRARED ABSORPTION SPECTRA OF SOME AMINO ACIDS IN ANTIMONY TRICHLORIDE SOLUTION[1]

BY JOHN R. LACHER, V. D. CROY, A. KIANPOUR AND J. D. PARK

Department of Chemistry, University of Colorado, Boulder, Colorado

Received August 17, 1953

It is shown that liquid antimony trichloride is an infrared transmitting solvent for amino acids. A method of purification of the solvent is described. The spectra of phenol, benzoic acid and acetamide when measured as solution in antimony trichloride demonstrate that the solvent produces very little to no shifts in the position of the O–H, N–H and C–H fundamental vibration. The spectra of DL-alanine, L(–)-leucine, DL-isoleucine, DL-valine and DL-threonine are shown for the LiF and NaCl regions.

The infrared absorption spectra of amino acids have been the subject of a large number of investigations.[2–13] One of the difficulties with these studies has been the lack of a suitable solvent for the amino acids. Some measurements have been carried out in heavy water, but most samples were prepared as Nujol pastes or as a thin film on a salt plate. The spectra are characteristic of the solid state in which the molecules are strongly hydrogen bonded. Recently[14] we showed that molten antimony trichloride is a good solvent for pyrimidines. This solvent is also suitable for the simple amino acids. The present paper describes the results obtained using solutions of DL-alanine, L(–)leucine, DL-isoleucine, DL-valine and DL-threonine.

Experimental Details

A Perkin-Elmer model 12B spectrometer was used. Two monochromators were employed. One was fitted with a lithium fluoride prism for use in the region 1–4 μ and the other a sodium chloride prism which was used out to 12 μ. The instruments were calibrated in the usual way.

The antimony trichloride was purified by vacuum sublimation. A 500-ml. distilling flask was used to hold the crude material and several 250-ml. flasks as receivers. The procedure consisted in melting the material under a pressure of 10–15 mm. Then the heat was reduced and the vacuum increased while the entire train was flamed. The material could then be sublimed into the several traps by chilling them in an ice-bath. After they were filled, the heat was turned off and dry air was admitted slowly through drying towers. The receivers were then sealed from the system leaving a side arm on each which could later be used in transferring the antimony trichloride to an absorption cell. All transfers were carried out in a dry-box. If care is used in the preparation and handling of the fused salt, material can be produced which is transparent in the region 1 to 4 μ when measured in a 1-cm. quartz cell. Ordinarily, if a 5-cm. cell with silver chloride windows is used, one obtains some absorption at 2.75 and about 6 μ.[15] This is apparently due to traces of water and hydrolysis products.[16] Wide absorption bands occur at about 10 and 13 μ with the latter being considerably more intense. These are thought to be the first and second overtones of some of the fundamental frequencies

---

(1) This research was supported by the Atomic Energy Commission Contract No. AT(29)-787, Program A.

(2) E. Heintz, *Compt. rend.*, **201**, 1478 (1935).

(3) N. Wright, *J. Biol. Chem.*, **127**, 137 (1939).

(4) H. Lenormant, *Compt. rend.*, **222**, 1432 (1946); **234**, 1959 (1952).

(5) H. M. Randall, *et al.*, "Infrared Determination of Organic Structures," D. Van Nostrand Co., Inc., New York, N. Y., 1949.

(6) I. M. Klotz and D. M. Gruen, THIS JOURNAL, **52**, 961 (1948).

(7) S. E. Darmon, G. B. B. M. Sutherland and G. R. Tristam, *Biochem. J.*, **42**, 508 (1948).

(8) H. W. Thompson, D. L. Nicholson and L. M. Short, *Faraday Soc. Disc.*, **9**, 222 (1951).

(9) K. Kuratani, *J. Chem. Soc. Japan, Pure Chem. Sect.*, **70**, 453 (1949).

(10) M. L. Josien and M. Fuson, *Compt. rend.*, **232**, 2016 (1951).

(11) U. Scheidt and H. Reinwein, *Z. Naturforsch.*, **7b**, 270 (1952).

(12) T. Gaumann and H. Gunthard, *Helv. Chim. Acta*, **35**, 53 (1952).

(13) L. Larsson, *Acta Chem. Scand.*, **4**, 27 (1950).

(14) J. R. Lacher, D. E. Campion and J. D. Park, *Science*, **110**, 300 (1949).

(15) D. Emery, Master's Thesis, University of Colorado, 1952.

(16) J. Lecomte and C. Duval, *Bull. soc. chim.*, **12**, 91 (1945).

of antimony trichloride.[17] As a result of this the practical long wave length limit of this solvent is 12.5 μ. For the region 1 to 3.5 μ commercial quartz absorption cells were used. They were furnished with ground stoppers and had a diameter of 3.4 cm. Cells of 1 and 5 cm. length were used. For use at longer wave lengths metal cells having silver chloride windows were used. Teflon gaskets were placed on both sides of the windows in order to make a tight seal and to prevent contact between the silver chloride and the metal portions of the cell. If this is not done, the silver chloride will be reduced to metallic silver. It is desirable, particularly if brass is used as material of construction, to coat the inside of the cell with Teflon suspension. Cells of 1 and 5 cm. length were used. The greatest difficulty encountered in the use of the silver chloride cell was the loss in transmission of infrared radiation due, we believe, to the crystallization of the silver chloride. The opaqueness was not caused by the continual contact between the silver chloride and the molten antimony trichloride, but to a partial solidification on the surface during a run or while cleaning the cell. If care is taken, a set of windows can be used for several runs. Since antimony trichloride melts at about 73°, the cells were heated to 85°. This was accomplished using removable jackets constructed of sheet copper; the jackets were heated electrically.

The compounds were thoroughly dried either in an oven or a vacuum desiccator before using. DL-valine and DL-threonine were obtained from the General Biochemicals Inc., DL-alanine and DL-isoleucine were from Eastman Kodak, Co., while L(−) leucine was obtained from Merck, Inc.

Results

The spectra obtained in the region from 1.0 to 4.0 μ are illustrated in Fig. 1 and the region from 2.0 to 12.0 μ in Fig. 2. Tables I and II give the wave length of the absorption bands. It is apparent that, if the amino acids are dissolved in liquid antimony trichloride, the resulting solution will give a spectrum showing a considerable amount of structure. In order to determine the effect of the solvent on some fundamental hydrogen stretching vibrations, the spectra of pure phenol, benzoic acid and acetamide were run in the lithium fluoride region. The results are given in Fig. 3. The absorption at 3.28 μ for phenol and 3.26 μ for benzoic acid is close to the value of 3.27 μ reported for the aromatic C–H stretching frequency.[18] The CH_3 group in acetamide shows absorption at 3.25, 3.38 and 3.42 μ which is close to the reported[18] values of 3.38 and 3.48 μ for this group. All the amino acids studied show an aliphatic C–H stretching vibration at 3.36 to 3.39 μ and a first overtone at 1.66 to 1.77 μ.

TABLE I

OBSERVED FREQUENCIES AND ASSIGNMENTS 1 TO 4 MICRONS

Alanine	Leucine	Isoleucine	Valine	Threonine	Assignment
	1.16				
1.26					
	1.48	1.48		1.44	
1.58	1.60	1.59	1.57	1.61	N–H first overtone
1.66		1.70	1.63		
1.71	1.70	1.72	1.74		C–H first overtone
			1.77		
				1.96	
2.08	2.10	2.10	2.11	2.11	
2.12	2.14	2.14	2.15	2.20	
2.24	2.30	2.26		2.28	
2.27	2.35	2.30		2.34	
2.37		2.34	2.36		
2.43	2.42	2.44	2.44	2.46	
				2.80	O–H fundamental
2.92	2.92	2.92	2.92	2.92	C=O first overtone
3.08	3.12	3.11	3.14	3.15	N–H fundamental
				3.33	
3.39	3.38	3.36	3.38	3.38	C–H fundamental
	3.48	3.41			
	3.65	3.48			
	3.72				
3.76	3.81	3.81			
3.89	3.98	3.92			

TABLE II

OBSERVED FREQUENCIES AND ASSIGNMENTS 4 to 12 MICRONS

Alanine	Leucine	Isoleucine	Valine	Threonine	Assignment
5.75	5.70	5.78	5.97	5.75	C=O fundamental
6.05	6.05	6.05	6.08	6.00	N—H bending
6.50	6.50	6.37		6.37	
6.80	6.90	6.91	6.90	6.87	C—H bending
				7.10	
7.27	7.22				
7.60	7.74	7.84	7.75	7.87	
7.94	7.90				
	8.15		8.05	8.22	
8.60	8.68	8.60	8.70	8.60	
	8.90				
9.15	9.05	8.97	9.20	9.22	
	9.55		9.65	9.57	
	9.80	10.00	9.95	9.90	
10.35	10.40		10.05		
11.00	10.79		10.80		
11.18	11.16	11.02	11.40	11.25	
11.40					
11.90		11.24	11.75		
		11.58			

The O–H bond having more ionic character than the C–H bond might be expected to interact more with the antimony trichloride. Benzoic acid shows a strong absorption at 2.86 μ due to the O–H fundamental when 0.001 M in antimony trichloride. Davies and Sutherland[19] report that this acid absorbs at 2.835 μ when dissolved in carbon tetrachloride to give a 0.0167 molar solution at 71°. The absorption shifts 0.025 μ to longer wave length when the antimony trichloride is used as a solvent. In case of phenol a similar situation obtains. In antimony trichloride it absorbs at 2.80 μ whereas in carbon tetrachloride, it absorbs at 2.769 μ.[19] This represents a shift of 0.031 μ again to longer wave length. According to Mecke[20] the frequency of the OH band in phenol depends on the solvent used. Solvents having a strong proton attracting power will produce a shift to longer wave length. Also the band tends to become broad and decreases in intensity. Using the second overtone in phenol as an example, Mecke shows that changing the solvent from cyclohexane to benzene causes a shift of 0.0157 μ. Acetone produces one of 0.075 μ. We infer that in antimony trichloride, this effect is rela-

---

(17) G. Herzberg, "Infrared and Raman Spectra of Polyatomic Molecules," D. Van Nostrand Co., Inc., New York, N. Y., 1945.

(18) J. J. Fox and A. E. Martin, *Proc. Roy. Soc. (London)*, **176A**, 208 (1941).

(19) M. M. Davies and G. B. B. M. Sutherland, *J. Gen. Phys.*, **6**, 755 (1938).

(20) R. Mecke, *Faraday Soc., Disc.*, **9**, 161 (1951).

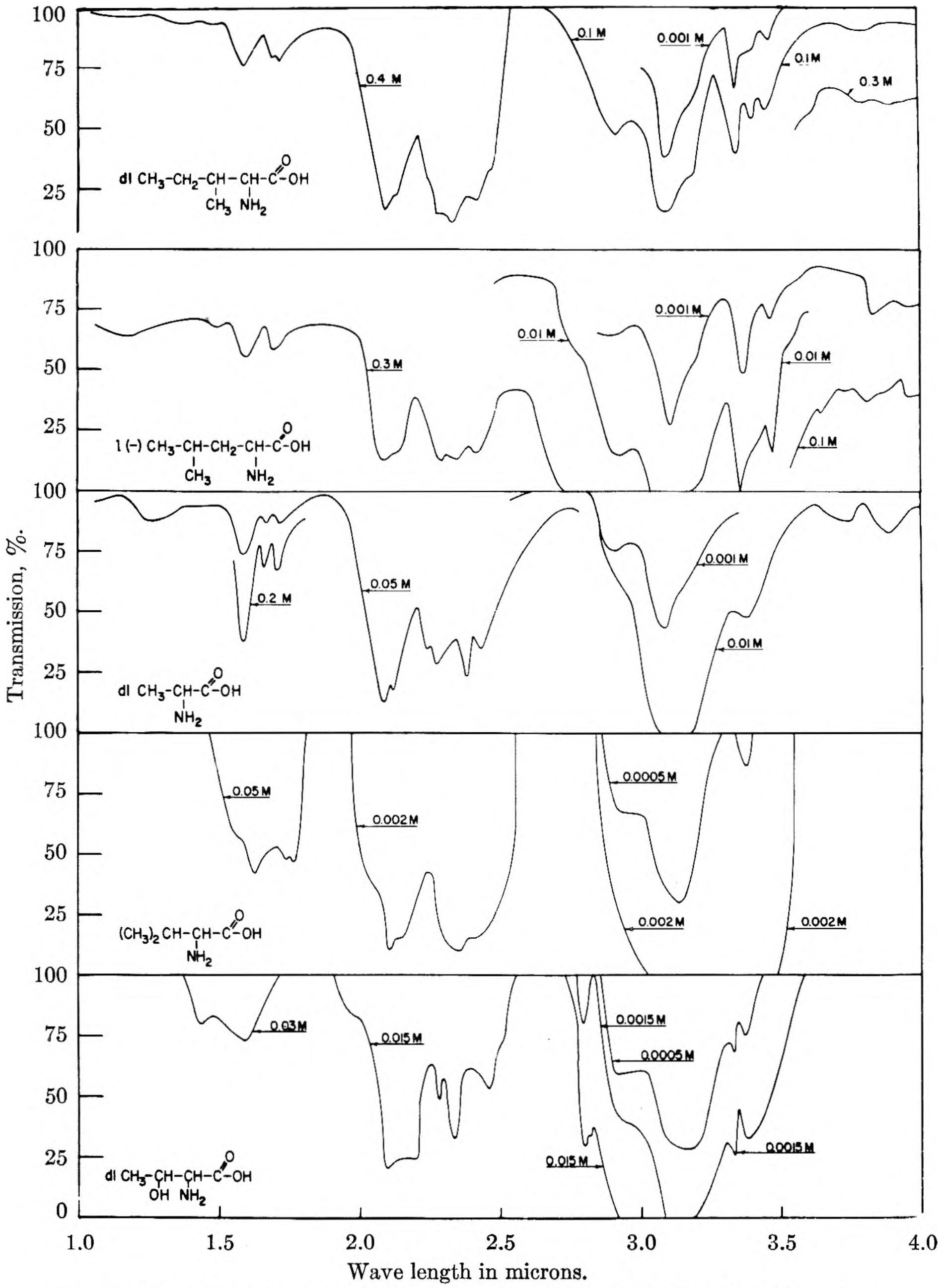

Fig. 1.—The absorption spectra of some amino acids in the lithium fluoride region.

tively small. In dilute solutions, about 0.001 *M*, intermolecular hydrogen bonding is also small and we should be able to locate the position of the O–H fundamental and its overtones. None of the amino acids studied, except threonine, show absorption due to the O–H stretching vibration. In case of threonine, there is present an OH group in the β-position, and absorption occurs at 2.80 μ. The lack of absorption by the unsubstituted amino acids in this region indicates either that they exist mainly in the zwitterion form in antimony trichloride solution or that the intensity of the O–H fundamental in the un-ionized carboxyl group is weak.

Since the N–H bond has less ionic character than the O–H, we expect the antimony trichloride to have very little effect on the position of the N–H fundamental band. In case of acetamide one obtains very intense absorption at about 3 μ. The band has three peaks located at 2.94, 3.03 and 3.08 μ. The amino acids all show sharp peaks which are single and fall in the range of 3.08 to 3.15 μ. This absorption we ascribe to the N–H stretching fundamental. The first overtone occurs at 1.57 to 1.61 μ. According to Cohn and Edsall[21] un-ionized primary amines show two intense Raman lines in the region of the N–H stretching fundamental. When the amino group becomes ionized and is studied in aqueous solution, these lines are replaced by broad weaker bands of longer wave length. Thompson,[22] *et al.*, report N–H stretching frequencies ly-

---

(21) E. J. Cohn and J. T. Edsall, "Proteins, Amino Acids and Peptides," Reinhold Publ. Corp., New York, N. Y., 1943.

(22) H. W. Thompson, D. L. Michalson and L. M. Short, *Faraday Soc. Disc.*, **9**, 22 (1951).

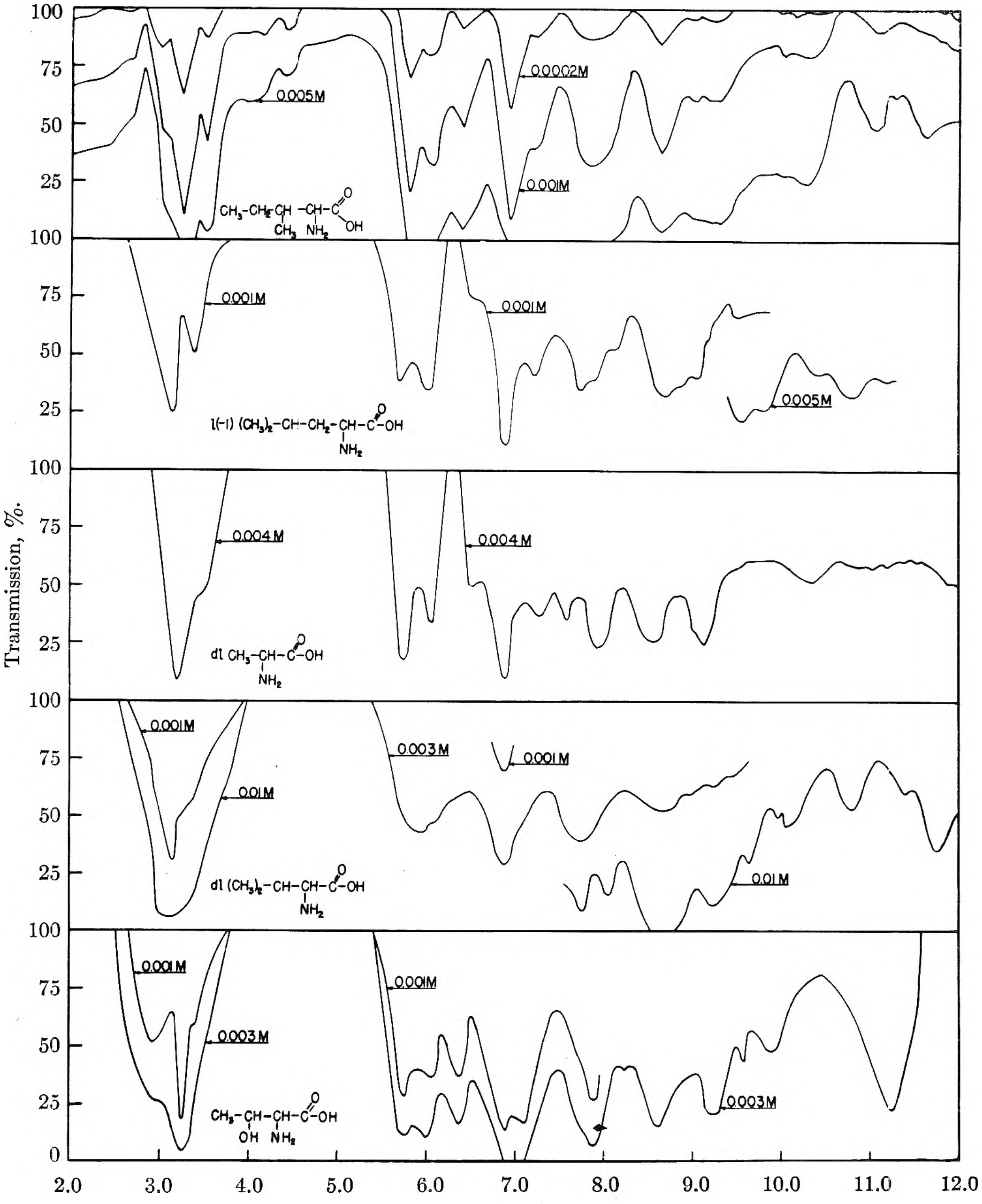

Fig. 2.—The absorption spectra of some amino acids in the rock salt region.

ing between 3.125 and 3.33 μ for some amino acids. Apparently solid samples were used for their studies.

The spectra obtained in the region from 5 to 12 μ are not directly comparable with those obtained by other investigations. The reason is that the present studies refer to molecules in a dilute solution with a solvent that interacts very little with the amino acids. The spectra run on solid samples will be characteristic of highly hydrogen bonded materials with resulting shifts in fundamental group vibrations. Also combination bands may appear involving frequencies characteristic of the lattice vibrations of the solid.[23]

All the compounds studied show strong absorption in the region 5.75–5.97 μ. This is apparently the C=O fundamental of the un-ionized carboxyl group.[21,24,25] The first overtone occurs at 2.92 μ, Table I. The absorption near 6.90 μ could be due to the ionized carboxyl[21] or to a C–H bending vibration.[21,6] The absorption at 6.00 to 6.08 may be due to an N–H bending vibration[26] and common absorption band near 8.60 is not assigned. The present studies do not permit one to say whether the amino acids exist in antimony trichloride as the zwitterion or as the un-ionized form. The absence

---

[23] E. L. Wagner and D. F. Hornig, *J. Chem. Phys.*, **18**, 296 (1950).

[24] R. C. Herman and R. H. Hofstadter, *ibid.*, **6**, 534 (1938).

[25] J. W. Ellis, *J. Am. Chem. Soc.*, **51**, 1384 (1929).

[26] H. M. Randall, R. G. Fowler and N. Fuson, "Infrared Determination of Organic Structures," D. Van Nostrand Co., Inc., New York, N. Y., 1949.

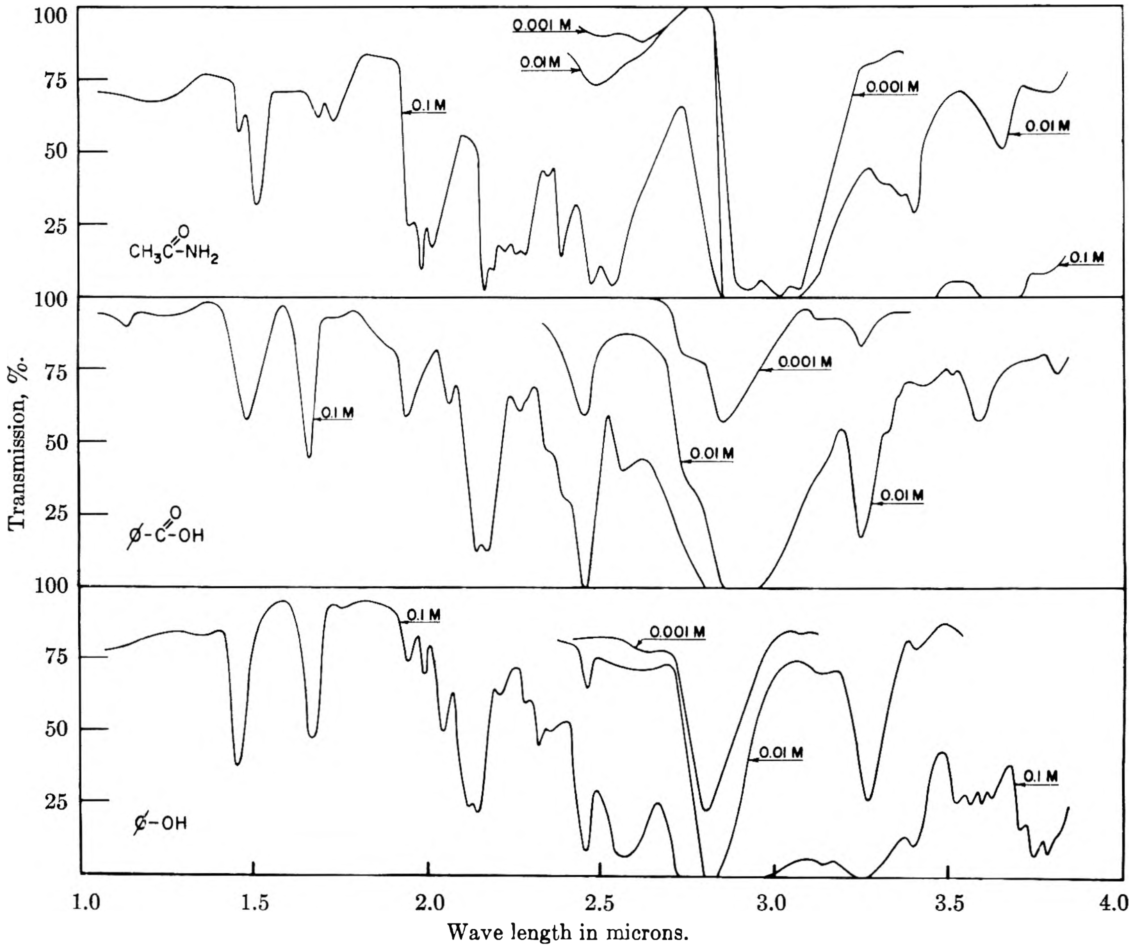

Fig. 3.—The absorption spectra of acetamide, benzoic acid and phenol in the lithium fluoride region.

of OH absorption in the LiF region could be due to a weak intensity relative to the other groups which absorb in this region. The strong absorption at 5.75 and 6.90 μ suggests that appreciable amounts of each form may be present in an equilibrium mixture. We are studying this problem further.

THE ADSORPTION OF ALIPHATIC ALCOHOLS AND ACIDS FROM AQUEOUS SOLUTIONS BY NON-POROUS CARBONS[2,3]

BY ROBERT S. HANSEN AND ROY P. CRAIG[4]

Contribution No. 283 from the Institute for Atomic Research and Department of Chemistry, Iowa State College, Ames, Iowa[1]

Received August 21, 1953

Isotherms have been determined for the adsorption at 25° of the homologous primary normal aliphatic alcohols from ethanol to heptanol-1 and the homologous normal aliphatic acids from acetic acid to heptanoic acid from aqueous solution by the three non-porous carbons Spheron-6, Graphon and Acheson Graphite DAG-1. The marked progression of amounts adsorbed at a given concentration on ascending a homologous series becomes almost non-existent if amounts adsorbed are compared at given absolute activity of the organic solute, and at low absolute activities (less than 0.1) of solute the amounts adsorbed at a given solute activity appear to be independent of position in the homologous series. With non-porous adsorbents, relative adsorption of members in a homologous series is therefore determined primarily by solute activity; this principle furnishes not only a rational basis for Traube's rule but also for inversion of Traube's rule.

Introduction

The regular increase in adsorption of aliphatic acids, at given concentration, on ascending the homologous series, has long been known, both as regards adsorption at solution–air[5] and solution–solid[6] interfaces. More recently, Hansen, Fu and Bartell,[7] investigating the adsorption of slightly soluble organic compounds from their binary aqueous solutions by a carbon black and several graphites, found that the adsorptions of valeric and caproic acids were congruent functions of reduced concentration of acid (concentration divided by saturation concentration) on each of the above adsorbents. Adsorptions of *n*-butyl and *n*-amyl alcohols were nearly congruent functions of reduced concentrations on the same adsorbents. Adsorptions of aniline and phenol were congruent functions of reduced concentration on the carbon black, but differed markedly only the graphites. Hansen, Fu and Bartell pointed out that the work required to remove solute from a solution as pure solute depended only on the absolute activity of the solute, and that, if the adsorbent acted on the same functional group, congruency of adsorption isotherms in a homologous series when plotted as functions of reduced concentration (closely paralleling absolute activities) was not surprising.

The purpose of the present work was to investigate the dependence of adsorption on activity over more extensive homologous series ranges, including both completely and slightly miscible liquid pairs. Adsorbents were limited to non-porous carbons so that results would not be affected by steric factors.

Experimental

The adsorbents Spheron-6, Graphon and DAG-1 were selected for use. Spheron-6 is a pellatized medium-processing channel carbon black, produced by Godfrey L. Cabot, Inc. Graphon is made by partially graphitizing Spheron-6 in an induction furnace at 3200°. These two adsorbents have been described by Beebe, Biscoe, Smith and Wendell and surface oxygen complexes on Spheron-6 have been discussed very recently in papers by Anderson and Emmett.[9] DAG-1 is a deflocculated artificial graphite produced by the Acheson Colloids Company. All adsorbents were heated in a vacuum (10^{-5} mm.) for 24 hours at 1000° to eliminate volatile impurities; the adsorbents were then stored in Mason jars until used, so that the probability of surface oxide formation[9] must be acknowledged. Surface areas of the adsorbents were determined by the Brunauer–Emmett–Teller technique to be 114.0 meters^2/g. for Spheron-6, 78.7 meters^2/g. for Graphon, and 102.4 meters^2/g. for DAG-1.

All water was redistilled from alkaline permanganate solution. All alcohols and acids used were central fractions from distillation through a 30-plate vacuum jacketed Oldershaw column at reflux ratio 10:1, except for heptanol-1, caproic acid and heptylic acid where a reflux ratio of 20:1 was used. Except for butanol-1 (commercial grade), hexanol-1 and caproic acid (Eastman Kodak Co. practical grade), all starting materials were reagent grade. Prior to distillation the ethanol was purified by the method of Lund and Bjerrum[10] and a water insoluble impurity of the butanol-1 was removed tediously by dissolving the butanol in water, heating to separate a butanol-rich phase, and drying this phase with anhydrous magnesium sulfate. Boiling ranges of fractions used did not exceed 0.02° for ethanol, butanol-1 and pentanol-1. Other boiling ranges were: propanol-1, hexanol-1, heptanol-1 and propionic acid, 0.1°; acetic and *n*-butyric acids, 0.3°; *n*-valeric and *n*-heptylic acids, 0.5°; *n*-caproic acid, 2°.

Adsorption isotherms were determined according to the techniques described by Hansen, Fu and Bartell[7] with minor modifications as described by Hansen, Hansen and Craig.[11]

Experimental mole fractions of organic solute in completely miscible systems were converted to absolute activities using activity data obtained in this Laboratory[12]; the activity data for the systems ethanol–water and propanol–water were in substantial agreement with data published by Dobson[13] and Butler, Thomson and MacLennan,[14] respectively.

Results

Results are presented graphically in Figs. 1–6, in which the quantity $V\Delta C/m$ (V is the number of ml. of solution added to m grams of adsorbent, ΔC is the solute concentration decrease due to adsorption in mmoles/ml.; the quantity $V\Delta C/m$ is equivalent

---

[1] Work was performed in the Ames Laboratory of the Atomic Energy Commission.

[2] Based in part on a dissertation submitted by Roy Phillip Craig in partial fulfillment of the requirements for the degree of Doctor of Philosophy, Iowa State College, Ames, Iowa, December, 1952.

[3] Presented at the 123rd National Meeting of the American Chemical Society, Los Angeles, California, March 18, 1953.

[4] Dow Chemical Company, Rocky Flats Plant, Boulder, Colorado.

[5] J. Traube, *Ann.*, **265**, 27 (1891).

[6] H. Freundlich, *Z. physik. Chem.*, **57**, 385 (1907).

[7] R. S. Hansen, Y. Fu and F. E. Bartell, THIS JOURNAL, **53**, 769 (1949).

[8] R. A. Beebe, J. Biscoe, W. R. Smith and C. B. Wendell, *J. Am. Chem. Soc.*, **69**, 95 (1947).

[9] R. B. Anderson and P. H. Emmett, THIS JOURNAL, **56**, 753, 756 (1952).

[10] H. Lund and J. Bjerrum, *Ber.*, **64B**, 210 (1931).

[11] R. S. Hansen, R. D. Hansen and R. P. Craig, THIS JOURNAL, **57**, 215 (1953).

[12] R. S. Hansen and F. A. Miller, to be submitted for publication.

[13] H. J. E. Dobson, *J. Chem. Soc.*, **127**, 2871 (1925).

[14] J. A. V. Butler, D. W. Thomson and W. H. MacLennan, *ibid.*, 674 (1933).

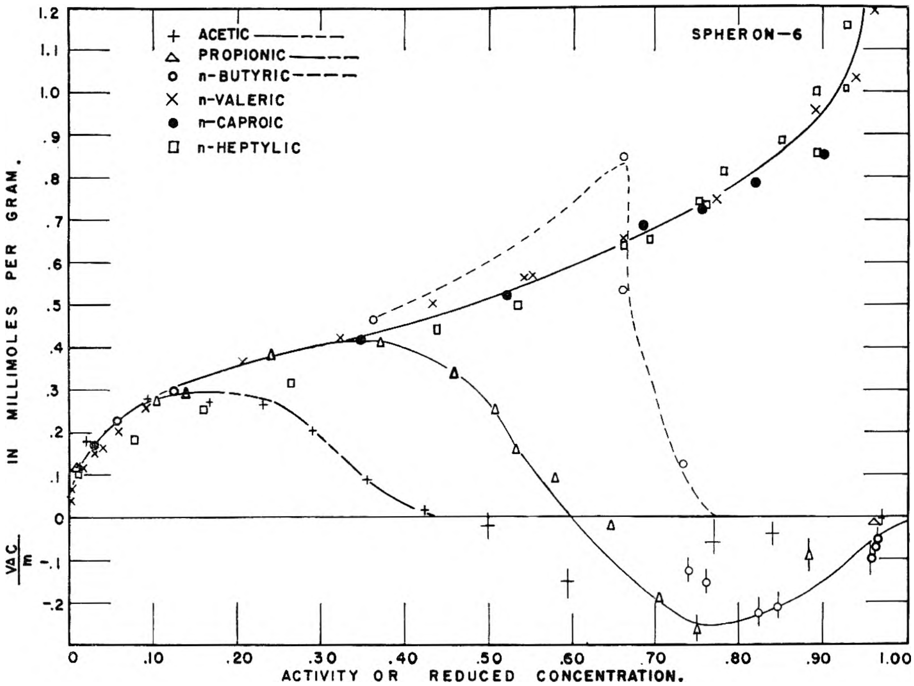

Fig. 1.—Adsorption of fatty acids from aqueous solution on Spheron-6.

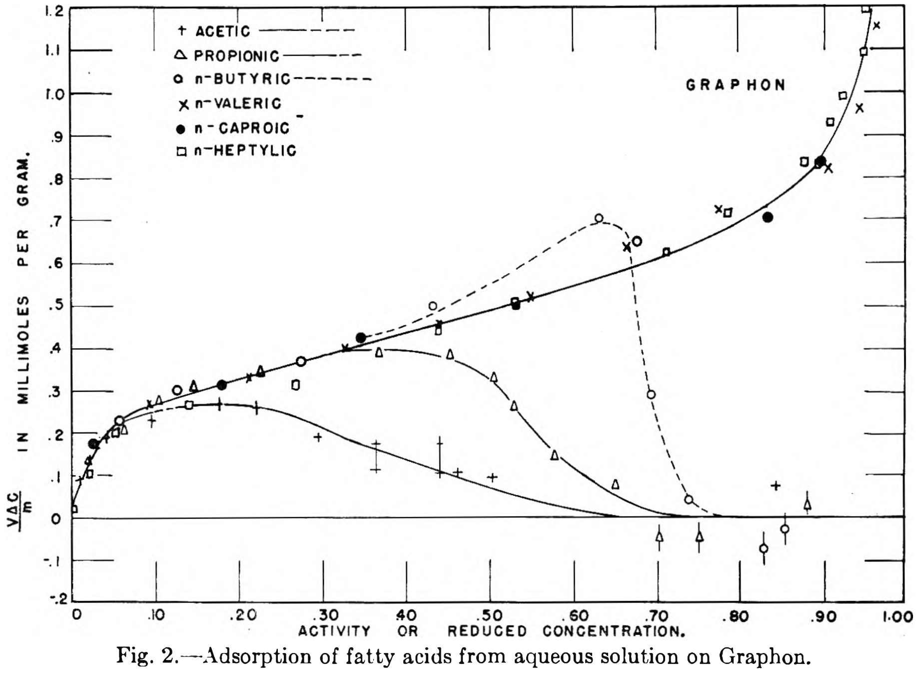

Fig. 2.—Adsorption of fatty acids from aqueous solution on Graphon.

to the product of the specific surface area and the surface excess of solute in the Guggenheim and Adam (*V*) convention[15,16]) is plotted against absolute solute activity, in the case of completely soluble solutes, or reduced concentration (concentration divided by saturation concentration) in the case of slightly soluble solutes. Tabular experimental data can be obtained from one of us (RSH) on request. Except as otherwise indicated by elongated symbols the experimental reproducibility was from 0.01 to 0.02 mmole/g.

Discussion

The similarity of adsorption isotherms in the homologous series when considered as functions of absolute solute activity is marked, especially at low activities. This similarity is emphasized further in Fig. 7, in which the adsorptions of aliphatic acids on Spheron-6 are compared at low concentrations (7A) and at low activities (7B); the latter figure indicates that congruency of adsorption isotherms for members in a homologous series (expressed as functions of activity) is at least a limiting law at low activities. A similar conclusion can be reached for adsorption at the water–air interface, and hence for

[15] E. A. Guggenheim and N. K. Adam, *Proc. Roy. Soc. (London)*, **A139**, 218 (1933).

[16] R. S. Hansen, THIS JOURNAL, **55**, 1195 (1951).

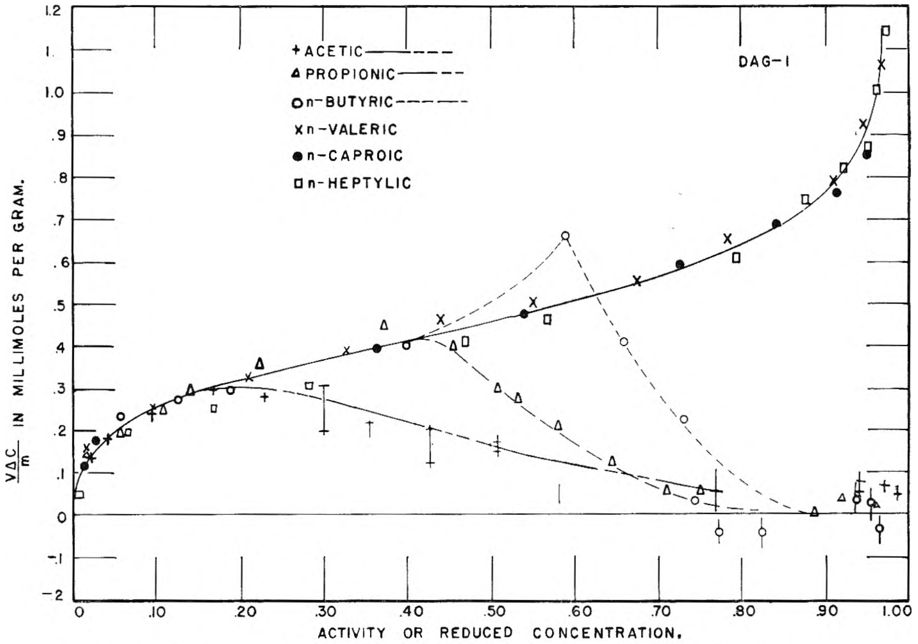

Fig. 3.—Adsorption of fatty acids from aqueous solution on DAG-1.

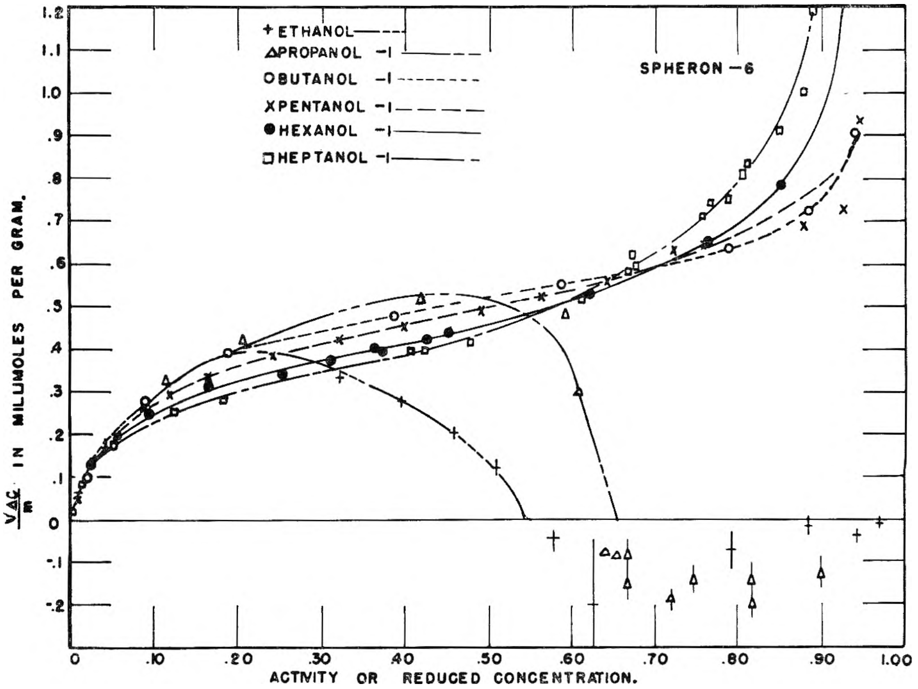

Fig. 4.—Adsorption of normal alcohols from aqueous solution on Spheron-6.

surface tensions of aqueous solutions of aliphatic alcohols and acids; this has been strongly implied by Ward.[17]

Inversions of Traube's rule in aqueous solution may well occur with porous adsorbents; this probability has been demonstrated with especial clarity by Kiselev and co-workers[18] who found that the maximum adsorption *volume* was nearly constant over the homologous series of fatty acids and aliphatic alcohols in their adsorption from CCl_4 solution by porous alumina-silica gel. Even in these cases, the initial slopes would be expected to be substantially constant when adsorption isotherms are plotted as functions of activity.

There appears to be no definitive work on adsorption of aliphatic alcohols and acids from hydrocarbon solutions by non-porous adsorbents, but an inversion of Traube's rule would clearly be expected in such cases, for the absolute activity coefficient at low solute concentrations would decrease monotonically on ascending the homologous series.

[17] A. Ward, *Trans. Faraday Soc.*, **42**, 399 (1946).

[18] A. Kiselev, *Zhur. Fiz. Khim.*, **23**, 452 (1949). Translation by E. Rabkin available as TT-237, National Research Council of Canada, Ottawa, 1951.

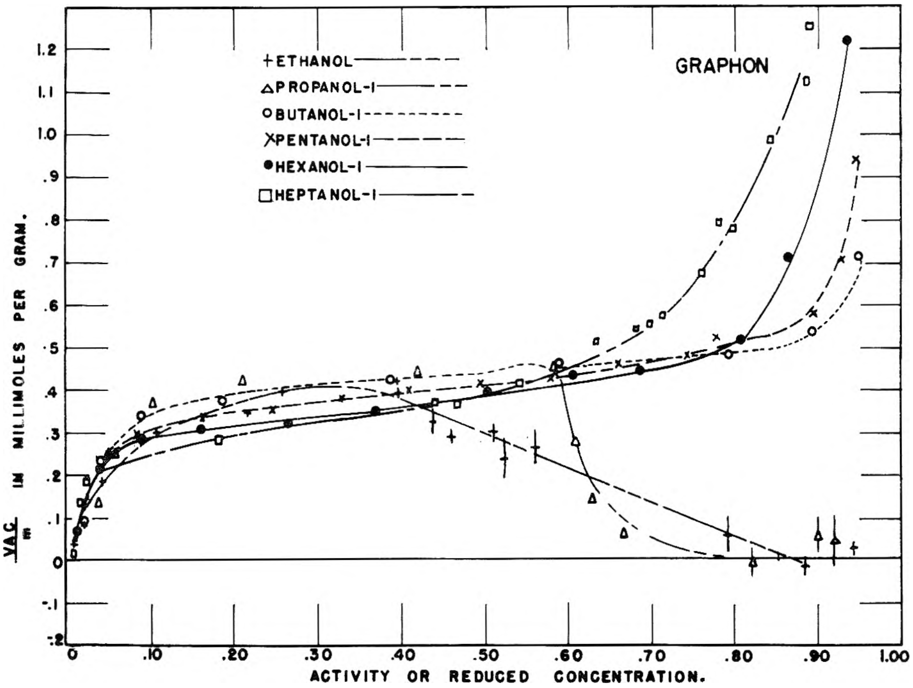

Fig. 5.—Adsorption of normal alcohols from aqueous solution on Graphon.

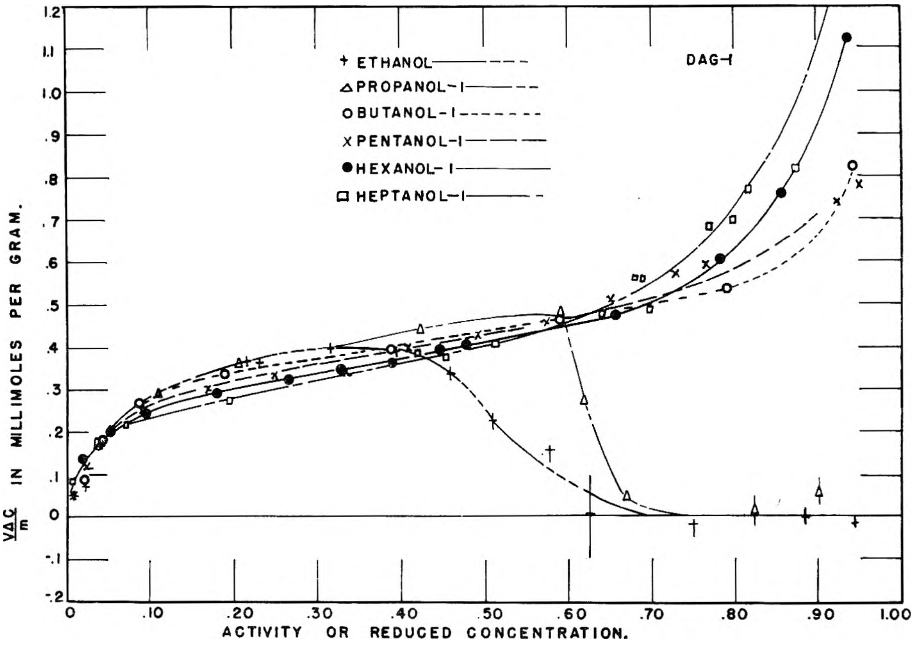

Fig. 6.—Adsorption of normal alcohols from aqueous solution on DAG-1.

The quantity $V\Delta C/m$ is a surface excess and not the total quantity of adsorbed solute in the adsorption region (this latter region being admittedly a rather ill-defined but none the less suggestive concept). Even if the concentration of solute as a function of distance from surface depended only on activity for all members in the series, isotherms for completely miscible homologs would necessarily deviate negatively from those of the slightly soluble homologs at higher activities, and indeed would be expected to do so in a marked way at activities which were lower the lower the position of the solute in the series. The general behavior of both alcohol and acid adsorption isotherms is in accord with this observation.

The rather marked deviation of the butyric acid adsorption isotherm from the other fatty acid adsorption isotherms should be noted; it presumably arises from an inconsistency in plotting which is difficult to remedy quantitatively but which is readily explained qualitatively. The higher fatty acids are of limited solubility; the abscissa in these cases is the reduced concentration, and $-RT \ln c/c_0$ is very nearly the free energy required to concentrate the solute to saturation, hence also to solute saturated with water, rather than to pure liquid solute. The concentrations of organic solute in the two cases would be quite similar (this is because the organic component generally has a much larger molar volume than water) but the organic solute saturated with water is thermodynamically more easily obtained, and can therefore be obtained at greater distance from the surface and by weaker adsorptive forces. In the completely miscible systems, especially such systems as butyric acid–water in which the next member of the series is incompletely miscible, the activity–concentration diagram shows an initial rapid rise in activity with concentration (Henry's law), reaches a plateau in which activity changes little with concentration, and finally increases again with concentration approaching Raoult's law as a limit. It is most probable that substances such as butyric acid are concentrated by adsorption to a part of the plateau region of the activity–concentration diagrams, rather than to pure acid. Since the upsweep of activity with concentration is not sharp it is difficult to select this part unambiguously; a value of 0.73 for the plateau point would cause the butyric acid adsorption values to agree well with the other fatty acids up to a reduced activity of 0.90 and would not be inconsistent with the activity–concentration diagram. Similar comments apply to propanol, and, to a lesser extent (because plateau regions in the activity–concentration diagram are less pronounced) to propionic acid, acetic acid and ethanol.

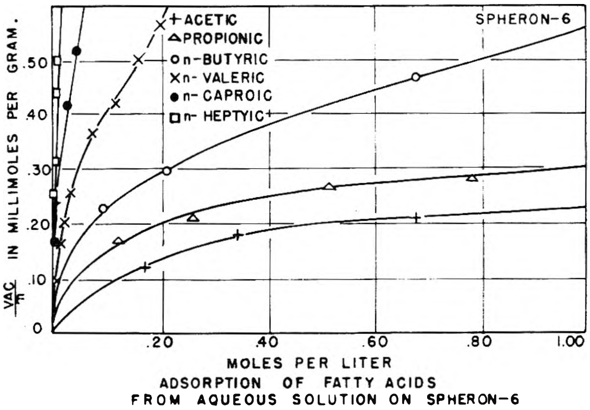

Fig. 7a.—Adsorption of fatty acids from aqueous solution on Spheron-6.

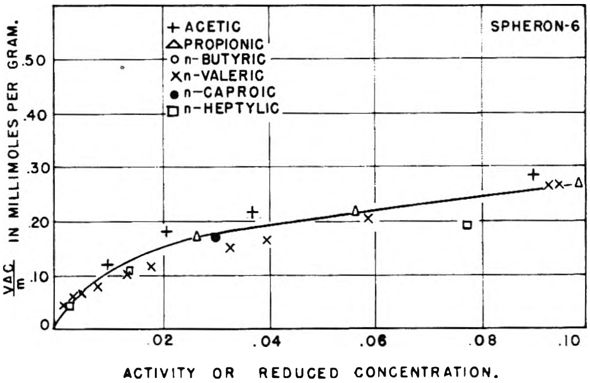

Fig. 7b.—Activity or reduced concentration.

PYROLYSIS OF GRAPHITIC ACID

By Eitaro Matuyama

Faculty of Engineering, Yamaguchi University, Ube, Japan

Received August 26, 1953

Thermal decomposition of graphitic acid (prepared by the mixture of graphite with sulfuric acid, nitric acid and potassium chlorate) was studied with a thermo-balance and by the X-ray powder method. Observation of weight decrease with a constant rate of heating, revealed several rather sharp changes in the decomposition rate, which correspond to the rapid decrease of inter-layer spacing observed with X-rays. Under condition of constant temperature, the decomposition proceeded without any discontinuity, proportionally to the log of time. A series of microphotometer curves of the diffraction patterns at various stages of decomposition up to 1800° are shown. These figures illustrate the process of graphitization of the lamellar compound, *i.e.*, the decrease of inter-layer spacings and the reorientation of mutual layer planes. With a specially designed Debye–Scherrer camera which permits direct comparison of the compound with Ceylon graphite, slight expansions or contractions of the layer planes of the order of 0.5% were observed; these changes are due to variation in the length of carbon–carbon bond and to the displacement of carbon atoms from the layer planes in the formation of the lamellar compound and in the intermediate stages of the decomposition. Results obtained with other lamellar compounds are described briefly.

Introduction

Considerable work has been done on the carbonization of carbon compounds and the graphitization of carbons such as carbon blacks, charcoals and cokes. All these carbons are in intermediate stages between the so-called amorphous state and the perfect graphite crystal. Some carbons are in a state which is readily transformed to graphite at elevated temperatures, while others do not easily undergo this change to a regular crystalline form. The structure of carbons and the different rates of crystal growth have been studied by Hofmann,[1] Riley,[2] Warren,[3] Bacon,[4] Franklin[5] and others; however, all their starting materials were in rather complicated states to begin with. On the other hand, a series of compounds, the graphitic acids or oxides, is known in which carbon atoms are linked aromatically in planes as in graphite, and between them atoms or molecules

[1] U. Hofmann and D. Wilm, *Z. Elektrochem.*, **42**, 504 (1936).

[2] H. F. Blayden, H. L. Riley and A. Taylor, *J. Am. Chem. Soc.*, **62**, 180 (1940).

[3] J. Biscoe and B. E. Warren, *J. Appl. Phys.*, **13**, 364 (1942).

[4] G. E. Bacon, *Acta Cryst.*, **3**, 137 (1950).

[5] R. E. Franklin, *ibid.*, **4**, 253 (1951).

are interleaved forming lamellar compounds. Most of these compounds are unstable in water or in moist air, decomposing gradually to the original graphite structure. On heating they decompose explosively with a small flash of light into soot which exhibits the X-ray diffraction pattern of ordinary carbon black; or on slower heating they gradually regain the graphite structure by loosing step by step the interleaved molecules. A somewhat detailed study of the thermal decomposition of Brodie's compound was made by Kohlschütter and Haenni[6]; more recently the stepwise thermal decomposition of graphite–potassium compound was observed by Hérold.[7] In some respects these decompositions seem to represent the simplest case of carbonization and graphitization of carbon compounds. The objectives of this paper were a more detailed study of the decomposition process by using a thermo-balance and the X-ray powder camera designed especially for this purpose, and a further examination of the small changes of covalent carbon–carbon bond length which occur in the formation of lamellar compounds and in the intermediate stages of pyrolysis. Only recently Beckett and Croft[8] reported a slight expansion of the layer planes (based on observations with the electron microscope) to occur in the oxides prepared with Staudenmaier's and Brodie's reagents.

Experimental

A. **Graphite**.—Ceylon graphite grains mixed with a small quantity of rock salt were crushed in an agate mortar, washed with boiling water and dried. As the grain size decreased the action of the oxidation agents was accelerated, but the effect on pyrolysis and on the X-ray patterns was small. Also graphites from cast iron were used which have a crystal structure slightly inferior to that of the natural graphite.

B. **Oxidation Treatments**.—Relatively few compounds were suitable for both X-ray and pyrolysis investigation, but results have been obtained with samples prepared by the following procedures.

(1) **Green and Brown Graphitic Acids**.—As described by Hofmann and König,[9] 110 g. of potassium chlorate was added slowly to a mixture of 175 cc. of concentrated sulfuric acid, 90 cc. of 63% nitric acid and 10 g. of graphite. After two days the mixture turned green. It was difficult to separate by centrifuging at 4000 r.p.m. and was therefore filtered through sintered Pyrex glass. The greenish paste obtained was transferred promptly to a glass specimen tube. When water was added, the paste turned black indicating decomposition to graphite. When graphite which had been treated with a two- or threefold excess of potassium chlorate was poured into water, a brown precipitate formed which settled less and less readily upon repeated washing. The gelatinous brown precipitate was centrifuged and dried at 80°. Then the compound was peeled off the evaporating dish as a brown semi-transparent film—0.1–0.01 mm. thick—which was very stable; no noticeable changes were observed even after a year's exposure to air at room temperature.

(2) **Blue Graphitic Acid**.[10]—Graphite treated with a 2:1 mixture of concentrated sulfuric acid and 66% nitric acid showed a bluish color after one day; the treatment was continued for 14 days. After it had been filtered through sintered Pyrex glass, the bluish paste was rapidly transferred to a glass specimen tube which was then sealed. The compound was unstable in air and turned black beginning at the surface due to absorption of moisture. When it was dried at 190°, black powder resulted.

(3) **Ferric Chloride Compound**.[11]—When graphite and anhydrous ferric chloride were heated in a sealed glass tube for three days at 200–205°, the ferric chloride was slowly absorbed (presumably from the vapor state), by the graphite powder, giving a hygroscopic powder with a greenish luster; it was stored in a sealed tube.

C. **Pyrolysis**.—The sample was placed in a fused-silica crucible which was suspended from one arm of the balance into a tubular furnace and balanced by the tension of a helical spring attached to the other arm and by weights added to the pan. The deflection was about 1 mm. per 1 mg. weight. The balance was installed in a constant temperature room controlled within 0.5°. A heating rate of 42° per hour was used throughout, because this is the maximum rate of heating by which brown graphitic acid is decomposed without explosion. The scale readings were taken at intervals of five minutes; the temperature was measured by a thermocouple placed just under the sample holder. The gases evolved were not analyzed chemically, since this had been done by Hofmann and his collaborators[10] and by others. The highest temperature attained in the thermo-balance experiment was about 400°. At temperatures higher than this, the rate of decomposition was low and oxidation of the residual graphite by air began. Up to 1000°, samples for X-ray examination were prepared by heating in an evacuated fused-silica tube; from 1000 to 1800°, a vacuum carbon resistance furnace was used. The carbon tube, 8 mm. in diameter and 2 mm. bore with water-cooled electrodes, was supported vertically in a water-cooled iron tube of 9 cm. bore. It was evacuated with an oil diffusion pump, but a very good vacuum was not attained because of the given off gases by the carbon. Prior to use, the carbon tube was heated for several hours at 1800°.

D. **Debye–Scherrer Camera**.—A specially designed Debye–Scherrer camera 200 mm. in diameter was used which was equipped to photograph on the same film diffraction patterns of Ceylon graphite and of the treated samples. The surface of the film is covered by a concentric cylinder provided with a slit 5 mm. in width. When a shaft attached at the center of the cylinder is pushed, the slit is shifted by 5 mm.; therefore, two diffraction patterns may be photographed on one film side by side. The specimen tube holder is attached to the shaft bearing the conical cylinder; thus it is possible to exchange the specimen and reset the specimen tube exactly at the center of the camera with an error of less than $^3/_{100}$ mm. With this device it was possible to detect small line shifts by direct comparison. CuKα radiation was used unless otherwise stated.

Results

A detailed study was made largely with brown films, prepared by Staudenmaier's method, which was found to be most suitable for our purpose. Typical pyrolysis curves are shown in Fig. 1. To examine the effect of grain size, crystal imperfections, time of treatment, extent of washing and heating rate, ten series of measurements were made with different samples, and the curves obtained showed nearly the same trends. The curve B was obtained by raising the temperature at a constant rate of 42°/hr. At first the weight decrease was rapid, but it became slower as the temperature approached 100°; below this temperature the greater part of the absorbed water was expelled. Another period of rapid decrease in weight began around 150°; this discontinuity was quite sharp in some samples as in curve B, but more gradual in others as in curve A. At about 190°, at the mid-point of the second ascending portion of the curve, the decomposition was further accelerated. With a greater rate of heating it has been found that explosion occurs at this temperature. Even with a heating rate of 42°/hr., when 450 mg. was used instead of the usual 300-mg. sample (which

---

[6] V. Kohlschütter and P. Haenni, *Z. anorg. Chem.*, **105**, 121 (1919).

[7] A. Hérold, *Compt. rend.*, **232**, 1484 (1951).

[8] R. J. Beckett and R. C. Croft, THIS JOURNAL, **56**, 929 (1952).

[9] U. Hofmann and E. König, *Z. anorg. Chem.*, **234**, 311 (1937).

[10] U. Hofmann and A. Frenzel, *Ber.*, **63**, 1262 (1930).

[11] W. Rüdorff and H. Schulz, *Z. anorg. allgem. Chem.*, **245**, 121 (1940).

had been prepared from flake graphite from gray cast iron), explosion occurred at this temperature presumably because of accumulation of heat of decomposition. At 220° the rate of decomposition slowed down again, and at 280° the decomposition was nearly complete, as is shown by the flattening out of the curve; however, the weight continued to decrease very slowly beyond this temperature. That the discontinuities in decomposition rate are not true transformation points as stated by previous authors,[6] is apparent from curve A. In this case the temperature was raised at the rate of 42°/hr. to 156°, at which the second period of rapid weight loss began, and from then on maintained constant; this experiment is represented by the broken line. As may be seen, the decomposition proceeded without discontinuity. Readings were continued for 36 hours. It was found that this portion of the curve follows the empirical formula very closely; weight loss was proportional to the logarithm of the time.

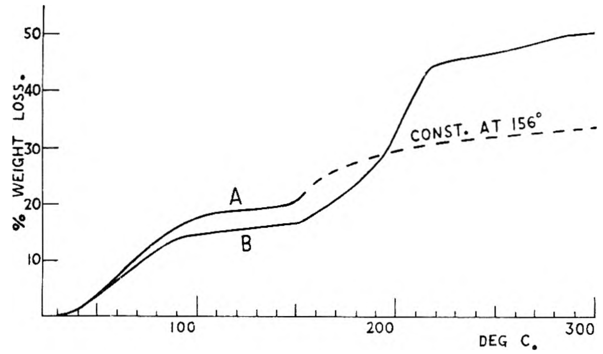

Fig. 1.—Pyrolysis curve: Curve B represents the thermal decomposition of the lamellar compound of graphite (prepared by the treatment of graphite with a mixture of sulfuric acid, nitric acid and potassium chlorate), at a heating rate of 42°/hr. The broken line (curve A) is the decomposition which occurred when temperature was maintained at 156°.

A pronounced feature of this compound, as revealed by X-rays, is the appearance of very few diffraction lines, *viz.*, 0002, $10\bar{1}0$ and $11\bar{2}0$, which appear as long as the carbon atoms are arranged in planes as in graphite and these planes are stacked parallel to each other with some disorientation of mutual layer planes. The 0002 line is shifted markedly toward smaller angles by the interleaved molecules, while the other two lines remain almost unaffected.

The microphotometer curves of the diffraction patterns obtained with the samples at various stages of pyrolysis are shown in Fig. 2 in which peaks corresponding to the 0002, $10\bar{1}0$ and $11\bar{2}0$ lines of graphite are shown with their respective heights; the four vertical lines give the position of the lines of natural graphite as indicated at the top. To prepare the X-ray specimens, narrow pieces of cut brown film were lightly pressed into glass specimen tubes (8 mm. length and 0.6 mm. bore). A bundle of the tubes and a thermocouple were placed in a furnace, and the temperature was raised at the same rate as in the pyrolysis experiments. Tubes were removed at intervals of 30 minutes, sealed as rapid as possible with a vacuum wax of low melting point to avoid excess heating, and stored in a desiccator. Samples heated *in vacuo* at 600, 1400 and 1800° were transferred to specimen tubes after heating. At the lowest stage of thermal decomposition (bottom of Fig. 2), a peak pertaining to the 0002 line appears in the left corner and shifts gradually to right as the temperature rises, until a jump to the right occurs between 215 and 235°; then the line broadens markedly as seen in the curve for 235°, owing to the non-uniformity of the inter-layer space after partial decomposition. The appearance of the two peaks in the curves for 235 and 275° suggests that two intermediate states occur simultaneously in the inter-layer space; however, with some other samples the second peak did not appear so clearly. As the temperature continues to increase, the peak gradually approaches the 0002 line for normal graphite, but even for the sample heated at 1400° for 10 minutes, the peak still appears slightly to the left of the normal line. Finally, the samples heated at 1800° for 10 minutes show nearly perfect recovery to the normal graphite structure; this is also indicated by the double peak of the 0002 line which is usually observed in well-crystallized graphite powder and results from the preferential orientation of crystals in the specimen tube. Consequently the line produced in this way is rather broad and its apparent slight displacement to the left seems doubtful. As many workers have observed, 1800° is the temperature at which the graphitization of carbons is accelerated. The second peak, which appears at about 10° at the bottom of Fig. 2, soon disappears at about 110° without much shift to the right; comparison with the pyrolysis curve in Fig. 1 indicates that it is due to absorbed water.

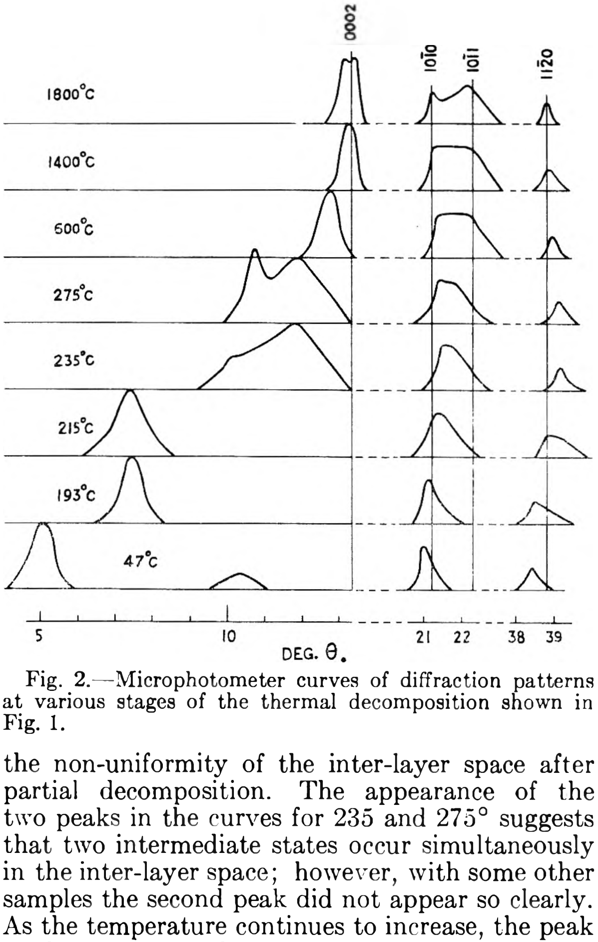

Fig. 2.—Microphotometer curves of diffraction patterns at various stages of the thermal decomposition shown in Fig. 1.

In Fig. 2 at the earlier stages of pyrolysis, the $10\bar{1}0$ and $11\bar{2}0$ lines appear to the left of the corresponding graphite lines. In the stages between 193 and 215° an abrupt shift to the opposite side takes place which ceases at the next stage (235°), but the peaks persist to the right of the graphite lines over a wide range of temperature. Accompanying this discontinuous change is an abrupt decrease of the inter-layer spacings. At the same time the breadth of the $10\bar{1}0$ line increases, due to the appearance of the overlapping $10\bar{1}1$ line; this indicates that an orderly rearrangement of the orientation of the successive layers occurs at this stage. The line continues to broaden as the temperature increases, and finally at 1800° it separates into two distinct peaks, the left one coinciding exactly with the $10\bar{1}0$ line while the right one is slightly to the left of the $10\bar{1}1$ line. Curves having nearly the same form were obtained with graphite from black-heart malleable cast iron.[12] The successive changes of the $11\bar{2}0$ line are simple, since there is no overlapping line; the shift parallels that of the $10\bar{1}0$ line as would be expected.

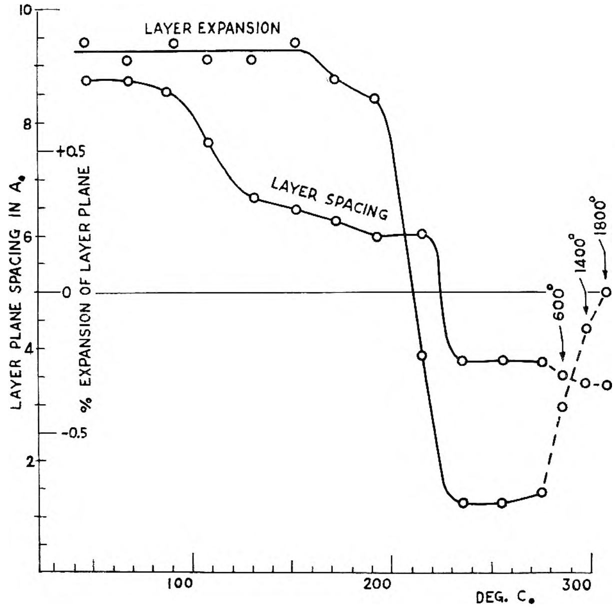

Fig. 3.—Inter-layer spacing and expansion or contraction of the layer planes calculated from the diffraction patterns shown in Fig. 2.

The relationships between the inter-layer spacing and the percentage expansion of the layer plane are shown more clearly in Fig. 3. The values for the percentage expansion calculated from the $10\bar{1}0$ and $11\bar{2}0$ lines agree within the experimental error. The values calculated from the latter line were plotted because this line is always sharp and the shift is twice as large as that of the former. A comparison of Fig. 3 with Fig. 1 reveals that the first and the second rapid decrease of inter-layer spacing occur, respectively, at the temperatures at which the first and the second stages of decomposition are completed; the inter-layer spacing finally reaches 3.35 Å., the value for perfect graphite. The expansion of the layer plane changes abruptly to contraction by nearly the same amount at a comparatively low temperature, and this contraction persists at higher temperatures. Consideration of these facts has led to the assumption that the expansion is closely related to the interleaved molecules, but the contraction is due to other causes; wavy or uneven planes of the layers were formed as a result of the removal of the molecules between them at a temperature too low to allow regular rearrangement. In the case of expansion, the carbon–carbon bond length (1.42 Å.), which is 2/3 and $2/\sqrt{3}$ of the spacing of the $10\bar{1}0$ and $11\bar{2}0$ reflection, respectively, should also be expanded; but in the case of contraction we cannot state the effect on the carbon–carbon bond length with certainty, if we assume that the carbon atoms are displaced from the layer planes.

No results were obtained with a sample of green acid prepared by the same oxidizing agent.

With the blue graphitic acid as with the brown film, the characteristic lines of the lamellar compound were observed. In this case all the lines were as sharp as those of the original graphite. Two sharp lines corresponding to 0002 appeared which were displaced by 1° 47′ and 2° 22′, respectively, to the left, *i.e.*, toward smaller angles, of the graphite line. On the basis of these values, the inter-layer spacing was estimated to be 3.86 Å. for the stronger line and 4.07 Å. for the other. The $10\bar{1}0$ and $11\bar{2}0$ lines were both slightly displaced toward greater angles. The contraction of the layer plane calculated from the shift of either line was 0.26% and the variation was in the opposite direction to that of the brown film. The $10\bar{1}1$ line appeared somewhat broadened and displaced by 17′ toward shorter angles. The displacement may be explained by the enlargement of inter-layer spacing. The shift, calculated from the value 3.86 Å., agreed exactly with the observed value. When the sulfuric and nitric acids were evaporated at 190°, the residual graphite exhibited a diffraction pattern which was identical to the original graphite in intensity, in sharpness and in scattering angles. Residual graphite was also obtained by washing with water. In this case the lines coincided with those of the original graphite, but they were less sharp and their intensity was generally modified.

In Fig. 4 the pyrolysis curve of the ferric chloride

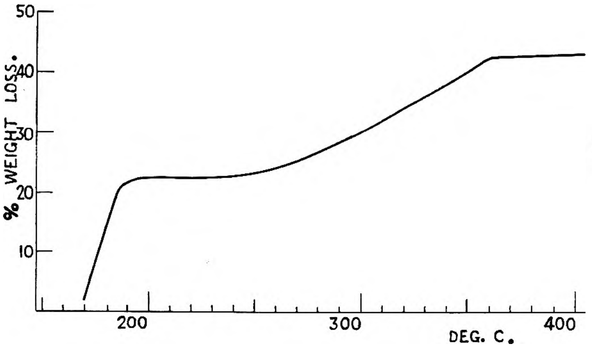

Fig. 4.—Pyrolysis curve: thermal decomposition of ferric chloride–graphite compound at a heating rate of 42°/hr.

---

(12) E. Matuyama, *Nature*, **170**, 1123 (1952).

compound is shown. In order to reduce the absorption of moisture, the temperature was raised to 170° in the first hour and from then on at the usual rate. When the usual rate was used from the beginning, the over-all aspect of the curve was similar, but the transformation was less sharp. The bends in the curve at 200 and at 470° correspond, respectively, to the first and the third stage of Rüdorff and Schulz's[11] curve, which was obtained by weighing samples which had been kept in the saturated vapor for a long time at various temperatures. No X-ray data are available.

ELECTRON MICROGRAPHIC STUDIES IN THE SYSTEM $BeO-In_2O_3$[1]

By C. R. ADAMS AND W. O. MILLIGAN

The Rice Institute, Houston, Texas

Received August 26, 1953

Comprehensive electron microscopic studies have been made on a series of eleven heat-treated (500° for 2-hour periods) gels selected at every 10 mole per cent. in the system $BeO-In_2O_3$. The samples, dispersed in dilute HCl at a *p*H value of 6.0, were deposited on a collodion membrane and examined at a magnification of approximately 16,000 diameters, using 100 kv. electrons. Particle size and pore size distributions were made from photographic prints at a final magnification of about 200,000 diameters, counting 700–1000 particles or pores. The most frequent particle radii for pure BeO and pure In_2O_3 were 60 and 84 Å., respectively. The most frequent particle radii for the dual gel series are a linear function of composition within the precision of the data. From the particle radii distributions, calculated "surface areas" have been obtained, which are approximately linear with composition. This result demonstrates that the dual composition zones of mutual protection, known to exist in this system from X-ray diffraction studies and water vapor adsorption data, do not result from variations in secondary particle size as viewed in the electron microscope. "Roughness factors," defined here as the ratio of "water surface area" to the electron microscope "surface area," show two pronounced maxima when plotted against composition. The "roughness factor" maxima correspond to the previously observed dual zones of mutual protection. The most frequent pore radii for pure BeO and pure In_2O_3 were 25 and 125 Å., respectively. As the BeO content is increased the pore radii decrease in size uniformly, the largest changes occurring at 10 and 90 mole per cent. BeO. The electron microscope pore size distributions are in close quantitative agreement with Kelvin pore size distributions previously reported.

Introduction

In previous reports from this Laboratory systematic X-ray diffraction[2] and sorption–desorption[3] studies of the dual hydrous oxide system $BeO-In_2O_3$ demonstrated the existence of two composition zones of mutual protection[4] against crystallization, and confirmed an earlier prediction[5] that such zones of protection may correspond to regions of maximum surface, and which, therefore, may exhibit enhanced adsorptive properties. In the two composition zones of mutual protection in the system $BeO-In_2O_3$, the gels exhibit enhanced surface areas, and higher integral and differential heats of adsorption.[3] The Kelvin pore radii distributions computed from the desorption branches of the water isotherms exhibit most frequent pore radii varying from about 125 Å. for pure indium trioxide to about 25 Å. for pure beryllium oxide. It is the purpose of this paper to present the results of an extensive electron micrographic study of the pore and secondary particle sizes in this system.

Experimental

The dual hydrous oxide gels employed in these studies were the identical samples used in the previous adsorption studies.[3] Briefly, measured amounts of ammonium hydroxide were added rapidly to solutions of indium nitrate and beryllium nitrate and the resulting gels were washed free of nitrate ion. These gels, after drying in air, were then heated at 500° for a period of 2 hours. Dilute suspensions of the samples dispersed in hydrochloric acid at a *p*H value of 6.0 were allowed to dry on thin collodion films mounted on metal grids. It is not considered likely that the use of such a dilute peptizing agent will result in significant modification of the oxide gels. Most of the photographs were taken on Process Ortho film with an exposure time of 4 seconds or less, using 100 kv. electrons, and a calibrated magnification of about 16,000 diameters. Optical enlargements of 13 diameters were made from the center portion of the negative, where the rotational distortion was less than 2%. Statistical counts and measurements were made directly on the positive prints, approximately 700–1000 pores or particles being counted for each sample.

Results and Conclusions

In Fig. 1 are shown portions of electron micrographs (200,000 diameters) of the gels in the system $BeO-In_2O_3$, heat-treated at 500° for two-hour periods. The gels consist of small, spheroidal particles packed in a random, non-close-packing manner. Occasional cubic pseudomorphs were found in the gel formed from heating the pure indium hydroxide, known to crystallize in the cubic systems,[6] but no pseudomorphs were found in the heat-treated products of the other gels which are essentially amorphous to X-rays.[2] The absence of many mono-disperse particles indicates strong cohesion between the secondary particles. The strength of the aggregates is shown by the fact that the degree of dispersion of the secondary particles varies but little upon suspension in water and subsequent evaporation to dryness, as shown below by a comparison of pore sizes measured in the electron microscope with those measured by adsorption methods.

In Fig. 2 are plotted the area distributions of the secondary particles found in this system, assuming the particles to be smooth spheres. The most fre-

---

[1] Presented before the Division of Colloid Chemistry at the 124th Meeting of the American Chemical Society, Chicago, Ill., September 6–11, 1953.

[2] L. M. Watt and W. O. Milligan, THIS JOURNAL, **57**, 883 (1953).

[3] W. O. Milligan and C. R. Adams, *ibid.*, **57**, 885 (1953).

[4] W. O. Milligan and J. Holmes, *J. Am. Chem. Soc.*, **63**, 149 (1941).

[5] H. B. Weiser, W. O. Milligan and G. A. Mills, THIS JOURNAL **52**, 942 (1948).

[6] W. O. Milligan and H. B. Weiser, *J. Am. Chem. Soc.*, **59**, 1670 (1937).

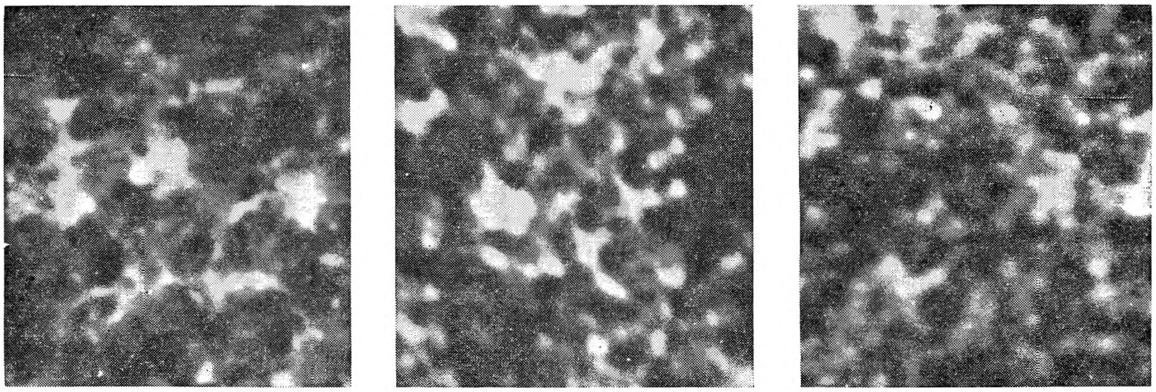

0 mole % BeO. 10 mole % BeO. 20 mole % BeO.

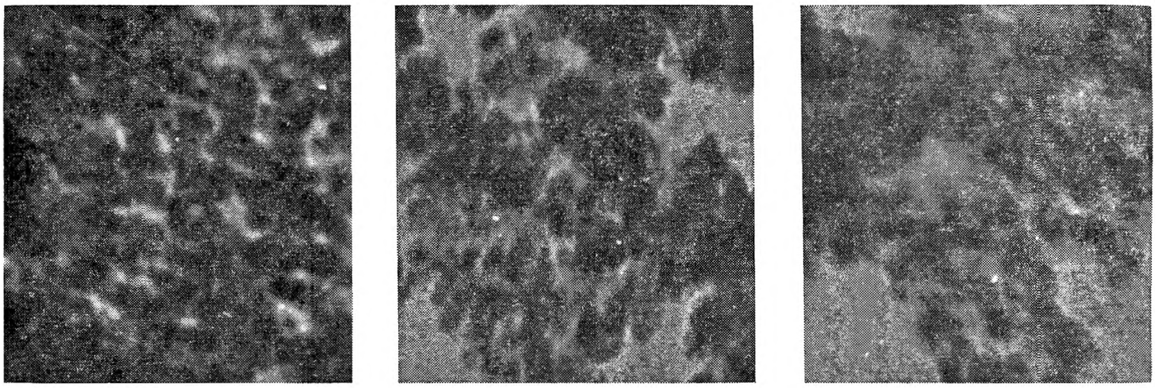

30 mole % BeO. 40 mole % BeO. 50 mole % BeO.

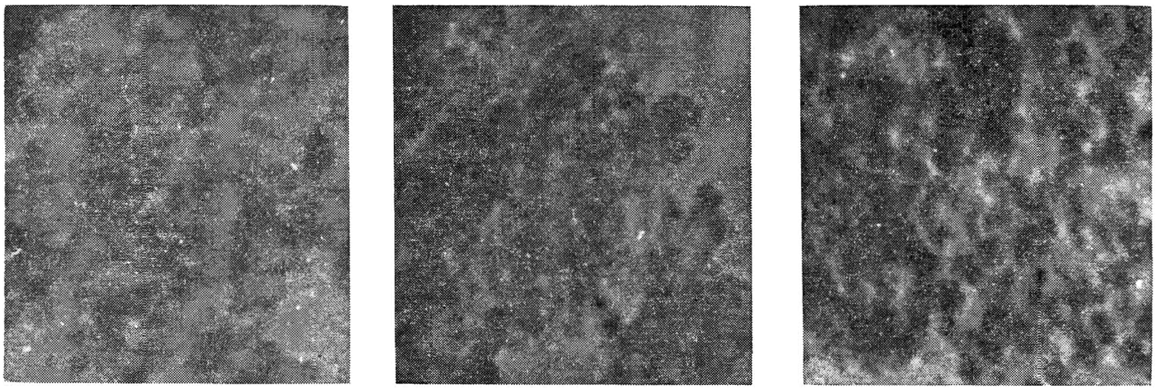

60 mole % BeO. 70 mole % BeO. 80 mole % BeO.

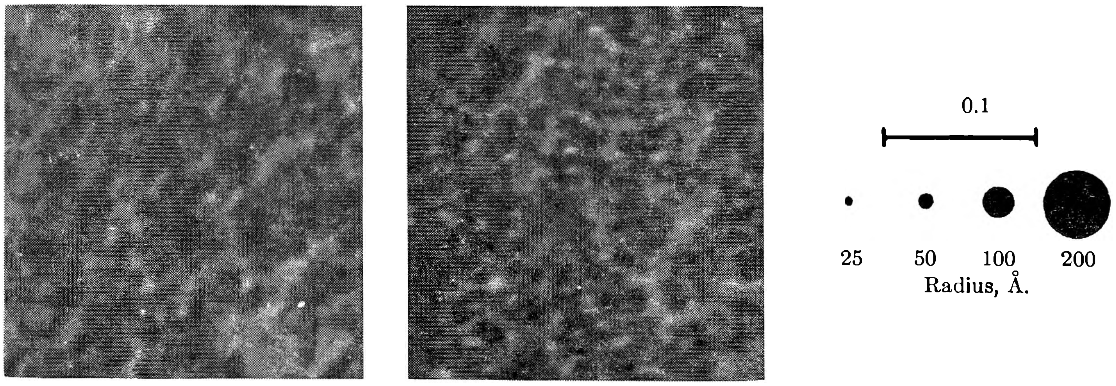

90 mole % BeO. 100 mole % BeO.

Fig. 1.—Electron micrographs of heat-treated gels in the system $BeO-In_2O_3$ (200,000 diameters).

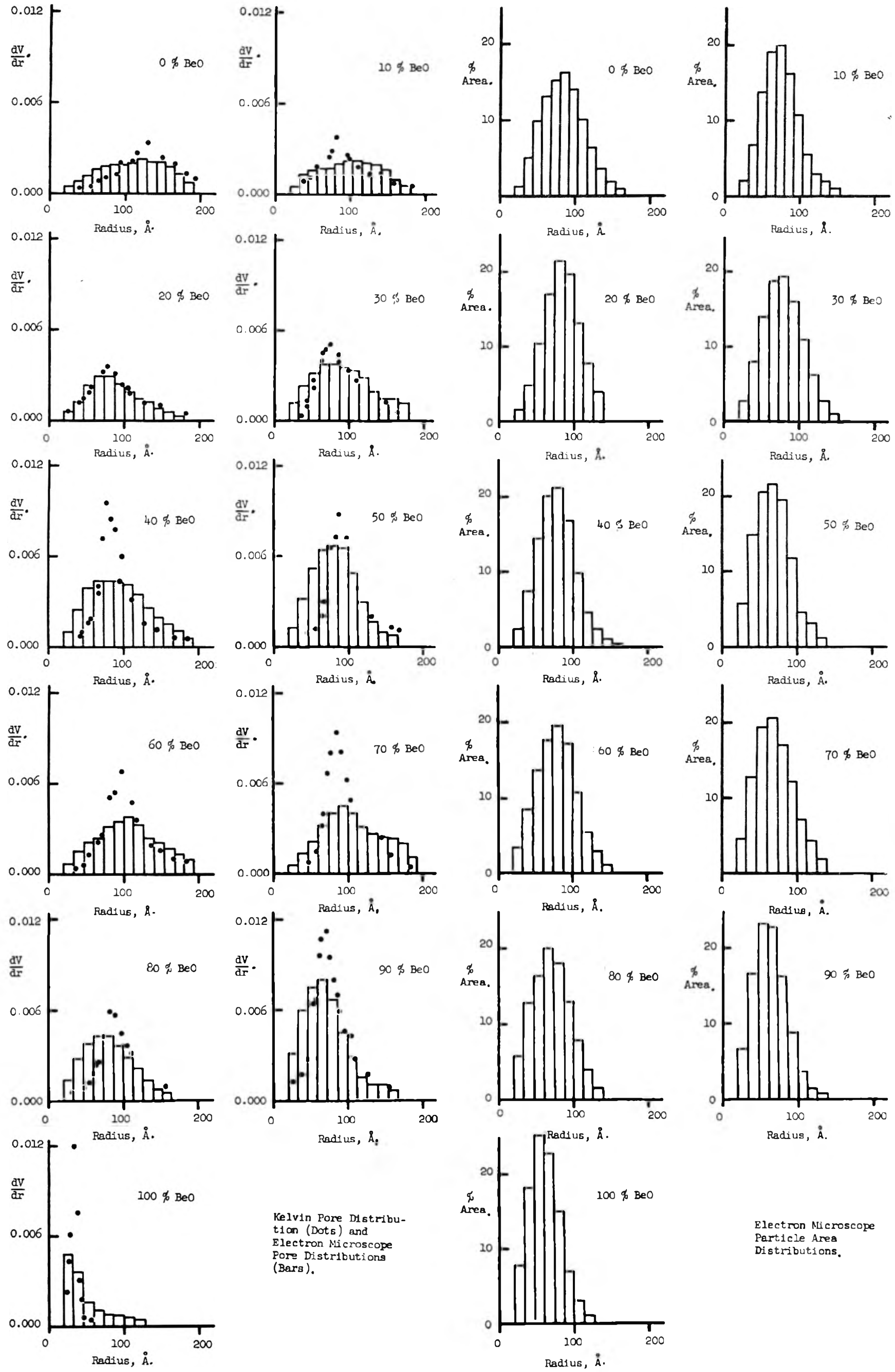

Fig. 2.—Pore volume and particle area distributions of heat-treated gels in the system BeO–In$_2$O$_3$.

quent particle radii for pure BeO and pure In$_2$O$_3$ were 60 and 84 Å., respectively. The most frequent particle radii for the dual gel series are a linear function of composition within the precision

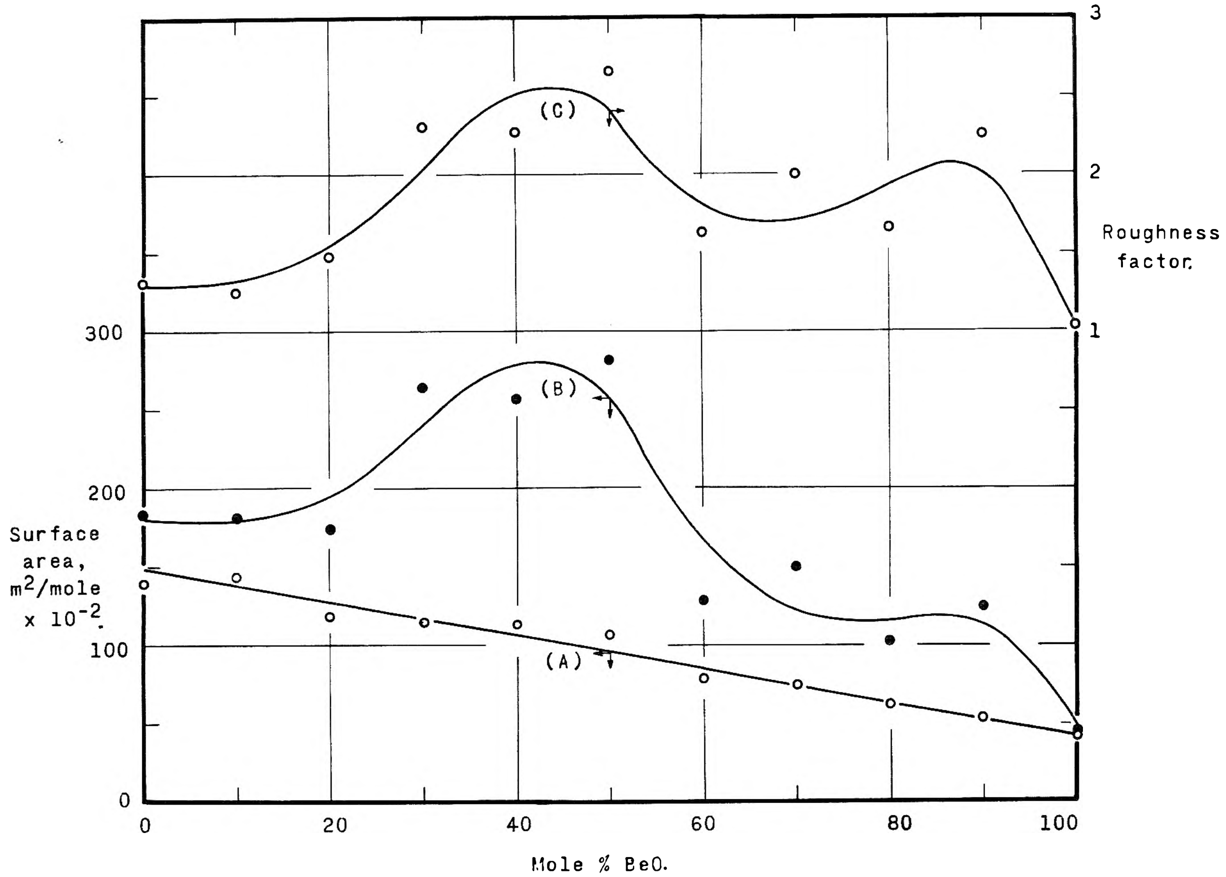

Fig. 3.—Electron microscopic (A) and water adsorption (B) surface areas, and roughness factors (C) of heat-treated gels in the system $BeO-In_2O_3$.

of the data. In Fig. 3 is given the electron microscope "surface area" per mole and BET water adsorption "area" per mole as a function of composition. The microscope surface area is a linear function of composition, indicating the absence of interaction as the secondary particle size increases. Also in Fig. 3 is plotted a "roughness factor," here defined as the ratio of the BET water "surface area" to the electron microscope "surface area," as a function of composition. Two pronounced maxima exist at the same compositions which had previously shown protection against crystallization,[2] enhanced surface area,[3] and enhanced integral and differential heats of adsorption.[3] Noting the magnitude of the "roughness factor maxima," it is apparent that the aggregates as viewed in the electron microscope must be composed of still smaller particles whose area is in part accessible to water molecules. It is hoped that studies of crystallite size by means of X-ray and electron diffraction, and of inhomogeneities by small angle X-ray scattering will yield more information about the structure of the smaller units composing these secondary particles.

In Fig. 2 are also given the pore volume size distributions calculated from the desorption isotherms by means of the Kelvin equation (points) and from electron microscopic count (bars). The desorption radii have been corrected for two monolayers of adsorbed water. The total pore volume obtained from electron microscopic measurements has been equated to the pore volume obtained from the desorption branch of the water vapor isotherm, thereby placing both pore distributions on the same quantitative basis. The volume of the pores was calculated assuming right circular cylinders of height proportional to the radius.

The most frequent pore radii for pure BeO and pure In_2O_3 are found to be 25 and 125 Å., respectively. As the BeO content is increased the pore radii decrease in size uniformly, the largest changes occurring at compositions of 10 and 90 mole per cent. BeO. Excellent quantitative agreement is obtained between the two completely independent measurements. This is taken to be a strong justification of the Kelvin equation for calculating pore radii from desorption isotherms of this type. Foster[7] has shown that the Kelvin equation gives correctly the relative dependence upon the physical properties of the condensed liquid. The adsorption work[3] has shown the temperature coefficient to be correct. Finally, the present electron microscopic studies have shown the absolute magnitude of the radii of the pores as given by the Kelvin equation to be satisfactory. In view of these data it is difficult to question the validity of the Kelvin equation when it is applied to pores in the size range studied here.

---

[7] A. G. Foster, *Disc. Faraday Soc.*, No. 3, 41, 106 (1948).

THE VAPOR PRESSURE OF BERYLLIUM FLUORIDE[1]

BY K. A. SENSE, M. J. SNYDER AND J. W. CLEGG

Battelle Memorial Institute,
Columbus, Ohio

Received August 31, 1953

Vapor pressures of BeF_2 were measured over the temperature range of 746–968° by use of the transpiration method. The extrapolated boiling point is shown to be 1159°. The melting point is about 803°.

Introduction

Since no experimental data on the vapor pressure of beryllium fluoride are available in non-classified literature, it is considered of interest to report our findings. Because the pressure range was approximately 0.5–50 mm., the so-called "difficult" range, the streaming (or transpiration) method of measuring vapor density was employed.[2–4]

Outline of the Method.—An inert gas is passed over the salt to be investigated, becomes saturated with it (or nearly so), passes through a condenser where the salt is deposited, and finally passes into a gas-measuring device. Assuming that the ideal gas laws hold, and that Dalton's law of partial pressure is applicable, the following relation holds

$$p = \frac{m_1 - m_2}{M + m_1 - m_2} P \qquad (1)$$

where

p = vapor pressure of salt
P = total pressure of salt and carrier gas
m_1 = total moles salt collected in condenser
m_2 = moles salt collected in condenser due to diffusion
M = moles carrier gas collected

Salt is deposited in the condenser as the result of two effects, transpiration and diffusion. From equation 1, it is evident that neglect of the diffusion factor would lead to erroneous results, for then, $p \rightarrow P$ as $M \rightarrow 0$. Hence, the amount deposited in the condenser due to diffusion must be subtracted from the total amount. A mathematical analysis of this problem has been made.[5]

Description of Apparatus.—The carrier gas used in these runs was highly purified nitrogen which was passed for further purification over heated copper oxide for hydrogen removal, Ascarite[6] for carbon dioxide, magnesium perchlorate for water and heated metallic copper for oxygen removal. This highly purified nitrogen was then passed into a McDanel[7] tube, which, because of the corrosive properties of BeF_2, contained a nickel liner, within which was placed a nickel boat. The condensers were nickel, about 18 inches long with a $^1/_8$-inch i.d. The condenser and the nickel thermocouple shield were inserted the same distance from opposite ends of the McDanel tube, each being $^3/_{16}$ inch from the exact center. Figure 1 shows the details.

After passing through the condenser, which collected the salt, the nitrogen passed through a drying tube (to prevent water vapor from diffusing into the McDanel tube) into a Mariotte flask, where the nitrogen was collected over water.

The hottest region of the furnace turned out to be exactly in the center. At 866°, the temperature was found to be $^1/_4$° lower $^3/_8$ inch from the exact center. Only calibrated Chromel–Alumel thermocouples were used. The temperature gradients across the nickel shield or a quartz shield were established over the temperature range by inserting into the hot zone a couple without a shield and one with a shield. The voltages generated by the thermocouples were measured by a potentiometer. Temperature was controlled by the use of a Brown Electronic controller–recorder in conjunction with a resistance coil which cut the power to 90% of its full value with the recorder relay in the off position. Temperature stabilization was further aided by the use of a Temcometer.[8] The result was that the temperature fluctuated by ±1.4° or less about a mean temperature.

The quantity of BeF_2 deposited in the condenser was determined by difference weighings on an analytical balance, and by chemical analysis.

The rate of diffusion of the salt into the condenser at various temperatures was determined by simply clamping off the exit end of the condenser while in the McDanel tube for a given length of time. For each run, then, the amount of BeF_2 deposited by diffusion alone could be determined and subtracted from the total deposited.

Material.—The BeF_2 used was supplied by the Brush Beryllium Company and reportedly had the following composition: a minimum of 99.0% BeF_2, with about 0.02% iron, 0.02% aluminum and 0.01% magnesium. The remainder was made up primarily of BeO and moisture.

Experimental Procedure.—After a charge of about 20 g. of BeF_2 was placed in the boat and the apparatus was assembled, the system was purged by passing a rapid stream of nitrogen through the system. Then the temperature was raised to about 200° for approximately 4 hours while nitrogen was passed through fairly rapidly. This served to drive moisture out of the BeF_2, which is hygroscopic. Then, using a moderate nitrogen flow rate, the temperature was raised for several hours to that at which the run was to be made. This served to purify the charge further by driving off any low boiling components which might be present. During this procedure, a "dummy" condenser with the exit end sealed off from the atmosphere by dibutyl phthalate, was inserted into the McDanel tube. When the run was started, the dummy condenser was removed and the regular condenser inserted. Immediately upon insertion of the condenser, the clamped-off rubber tubing leading to the Mariotte flask was attached. This procedure permitted the air in the condenser to be flushed out. Generally, about 10 minutes were allowed to let the condenser get up to temperature. Then, the clamp on the rubber tubing to the Mariotte flask was released, and the run was started. Readings were taken at regular intervals throughout the runs to ensure proper control. At the end of the runs, the regular condenser was removed and replaced by a dummy condenser. From the regular condenser, the amount of BeF_2 deposited was determined.

Results

The stability of BeF_2 was established by Brewer,[9] who calculated, from Herzberg's[10] data, that with a total pressure of 2×10^{-6} atm., BeF_2 is not 50%

---

[1] Work performed under A.E.C. Contract W-7405-eng-92.

[2] H. Von Wartenberg, *Z. Elektrochem.*, **19**, 485 (1913).

[3] E. Thiele, *Ann. Physik*, **14**, 937 (1932).

[4] K. Jellinek and G. A. Rosner, *Z. physik. Chem.*, **A143**, 51 (1929).

[5] J. V. Lepore and J. R. Van Wazer, "A Discussion of the Transpiration Method for Determining Vapor Pressure," MDDC-1188, U. S. Atomic Energy Commission.

[6] An absorbent of asbestos impregnated with sodium hydroxide manufactured by the A. H. Thomas Company.

[7] An unglazed, vitreous refractory porcelain tube manufactured by the McDanel Refractory Porcelain Company.

[8] A voltage regulator manufactured by the Thermo Electric Mfg. Co., Dubuque, Iowa.

[9] L. L. Quill, "The Chemistry and Metallurgy of Miscellaneous Materials. Thermodynamics," McGraw-Hill Book Co., Inc., New York, N. Y., 1950, p. 215.

[10] G. Herzberg, "Molecular Spectra and Molecular Structure," Prentice-Hall, Inc., New York, N. Y., 1939.

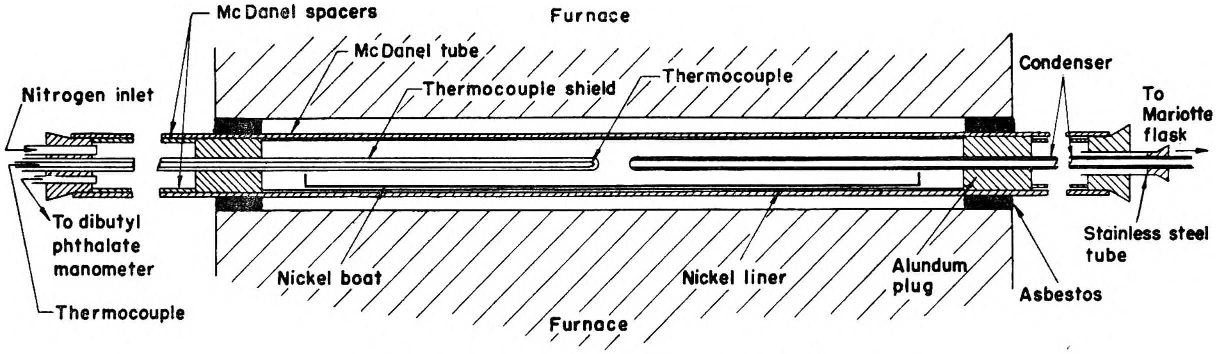

Fig. 1.—Cross section of vapor pressure apparatus.

dissociated until about 3000°K. Since BeF_2 does not dissociate appreciably at the temperatures studied, the vapor pressure of BeF_2 can be calculated directly from the data obtained in the runs. Data on the results of runs conducted in this work are given in Table I.

Table I

Temp., °C.	Vapor pressure, mm. Obsd.	Calcd.	Flow rate of nitrogen, cm.³/min.
745.9	0.484	0.467	4.89
745.9	.493	.467	2.84
746.4	.519	.473	7.64
746.5	.453	.474	8.75
762.9	.656	.740	2.84
762.9	.704	.740	8.46
763.1	.698	.743	4.62
776.4	1.04	1.05	4.41
777.2	1.12	1.08	2.84
778.9	1.28	1.12	7.12
781.1	1.15	1.19	7.24
781.4	1.12	1.20	2.82
781.6	1.25	1.20	4.55
820.5	2.96	3.01	8.38
820.5	3.11	3.01	2.83
820.6	2.87	3.02	4.62
833.5	4.38	3.97	2.58
833.7	4.46	3.98	7.55
834.0	3.80	4.01	4.04
879.2	10.46	9.93	4.39
879.2	10.60	9.93	2.26
879.7	10.12	10.01	2.85
880.6	11.37	10.21	8.17
916.8	20.0	20.0	2.26
917.0	20.1	20.1	4.60
917.0	17.4	20.1	7.13
940.5	30.7	30.6	7.12
941.1	34.3	30.8	7.27
941.4	30.9	31.0	2.80
941.7	32.4	31.2	4.07
967.4	50.1	48.3	2.73
968.1	48.2	48.9	7.13
968.1	48.4	48.9	4.09

Within the limits of experimental error, it is apparent from these data that extrapolation to zero flow rate is unnecessary, since saturation of the carrier gas was achieved at the fastest flow rate. Hence, the data were plotted without regard to the flow rate. The following relations were derived.

From 740–803°

$$\log p\ (\text{mm.}) = 11.822 - 12385/T,\ ^\circ\text{K.} \qquad (2)$$

$$\Delta H_{\text{sublimation}} = 56.64\ \text{kcal./mole} \qquad (3)$$

From 803–968°

$$\log p\ (\text{mm.}) = 10.651 - 11125/T,\ ^\circ\text{K.} \qquad (4)$$

$$\Delta H_{\text{vaporization}} = 50.88\ \text{kcal./mole} \qquad (5)$$

$$\text{Extrapolated boiling point} = 1159^\circ \qquad (6)$$

Equation 2 was obtained by application of the least squares method. From 2 and 4, the melting point is found to be 803°.

In a recent paper,[11] the melting point of BeF_2 was determined to be 543°. However, visible evidence from our work indicates that BeF_2 is still in the solid state at a temperature of 754°. Moreover, Novoselova, *et al.*,[12] determined the melting point of BeF_2 to be close to 800°.

The reliability of this vapor pressure apparatus was checked by making runs with KCl. The only change in the apparatus when KCl determinations were made was the use of quartz instead of nickel. The results indicated good agreement with current literature.

---

[11] D. Roy, R. Roy and E. F. Osborn, *J. Am. Ceram. Soc.*, **33**, 85 (1950).

[12] A. V. Novoselova, M. E. Levina, Y. P. Simanov and A. G. Zhasmin, *J. Gen. Chem.* (*U.S.S.R.*), **14**, 385 (1944).

BINARY FREEZING-POINT STUDIES FOR BORON BROMIDE WITH INORGANIC HALIDES[1]

By Robert F. Adamsky and Charles M. Wheeler, Jr.

Department of Chemistry, University of New Hampshire, Durham, N. H.

Received September 2, 1953

Freezing point and solubility data are presented for the binary systems boron bromide–aluminum bromide, boron bromide–arsenic bromide, boron bromide–stannic bromide and boron bromide–stannic iodide. All systems had simple eutectic points and there was no evidence of compound formation. Comparisons of ideal and experimental solubilities have been made and are interpreted with the aid of the internal pressure concept.

The number of molecular coördination compounds with boron bromide is far less than that reported for boron fluoride and boron chloride. Martin[2] has reported compounds with BBr_3 in which the donor atoms belong to Group V (nitrogen, arsenic, phosphorus), Group VI (oxygen and sulfur) and Group VII (chlorine and bromine). No element of Groups I, II, III or IV has been found to act as a donor to boron bromide.

This paper reports the results of cryoscopic and solubility studies of systems of boron bromide with some halides of Group III (aluminum bromide), Group IV (stannic bromide and stannic iodide) and Group V (arsenic bromide).

Experimental

Materials.—Boron bromide was prepared by metathesis of boron fluoride and anhydrous aluminum bromide.[3] The boron bromide was shaken with mercury, distilled and stored in all glass containers. The boron bromide was redistilled immediately prior to its use, b.p. 90.6–91°.

The aluminum bromide (Matheson, Coleman and Bell) was twice distilled yielding a pure white crystalline product which froze at 97.0°.

Stannic bromide was synthesized from the elements and purified by two successive distillations, freezing point 30.2°.

Stannic iodide was prepared by reaction of granular tin with iodine dissolved in carbon disulfide, the solvent being evaporated after the reaction. The compound was purified by crystallization from benzene, freezing point 143.5 to 144.0°.

Arsenic bromide was prepared from the elements and purified by distillation, freezing point 30.8°.

Procedure.—The freezing points of the stannic iodide–boron bromide systems, at stannic iodide concentrations of 30 mole per cent. or greater, were obtained by the sealed tube (static) method of Collett and Johnston.[4] Stannic iodide solutions less than 30 mole per cent. and all other systems were studied by the freezing point method. The freezing points were determined by means of cooling curves using a copper–constantan thermocouple to determine temperatures. The thermocouple was calibrated against an electronic resistance thermometer.

The freezing point cell was 20 cm. long × 2 cm. diameter fitted with a 24/40 joint. The cell cap carried a thermocouple well, a mercury seal with a glass coil vertical motion stirrer and a glass stoppered addition tube. All determinations were made with 10 to 15 cc. of solution. All additions were made in a "dry" box. The cooling curves were obtained over the entire composition range for each system studied with the exception of the part of the stannic iodide system noted above.

Results and Discussion

The freezing point–composition diagrams for the four systems reported in this paper are given in Figs. 1, 2, 3 and 4. The solubilities of aluminum bromide, stannic bromide, stannic iodide and arsenic bromide in boron bromide are shown in Figs. 5–8 inclusive, plotted as the logarithm of the mole fraction of the halide *vs.* the reciprocal of the absolute temperature. These plots were made to

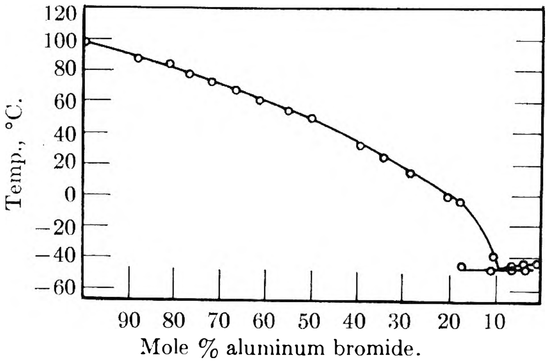

Fig. 1.—The aluminum bromide–boron bromide system.

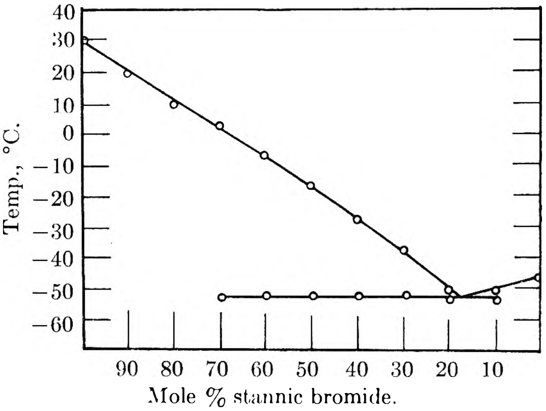

Fig. 2.—The stannic bromide–boron bromide system.

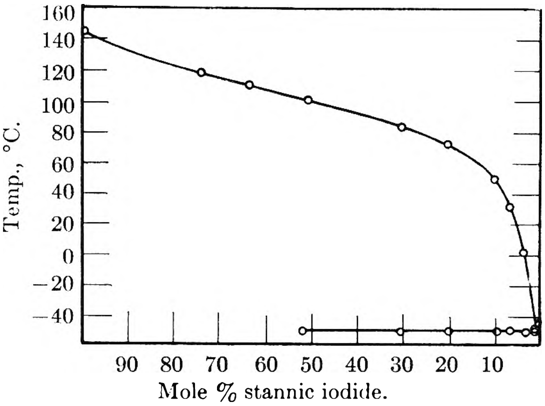

Fig. 3.—The stannic iodide–boron bromide system.

---

[1] Taken in part from the M.S. thesis of Robert F. Adamsky.

[2] D. R. Martin, *Chem. Revs.*, **42**, 581 (1948).

[3] L. F. Audrieth, ed., "Inorganic Syntheses," Vol. III, McGraw-Hill Book Co., Inc., New York, N. Y., 1950, p. 27.

[4] A. R. Collett and J. Johnston, This Journal, **30**, 70 (1926).

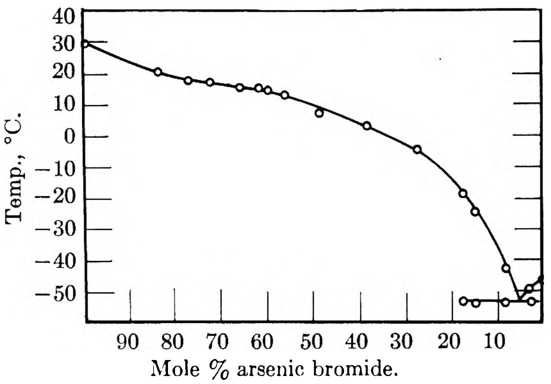

Fig. 4.—The arsenic bromide–boron bromide system.

determine the deviation from ideal solubility after the method used by Hildebrand.[5] The ideal solubilities were calculated from the heats of fusion and heat capacities, where available, of the solutes.

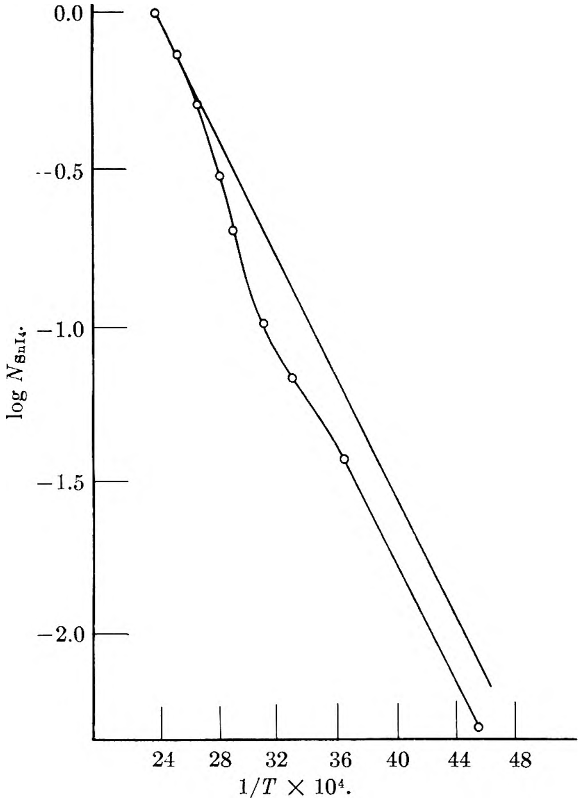

Fig. 5.—The solubility of stannic iodide in boron bromide: ——, ideal; ○—○, experimental.

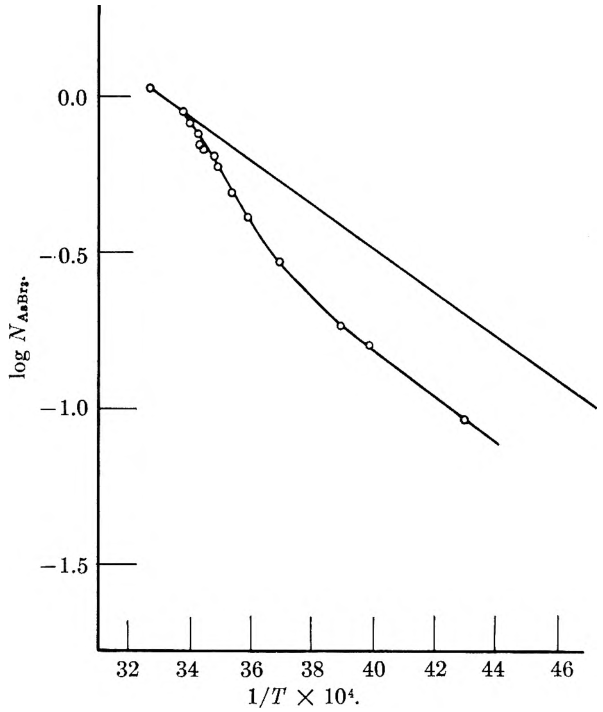

Fig. 6.—The solubility of arsenic bromide in boron bromide: ——, ideal; ○—○, experimental.

The aluminum bromide–boron bromide system has a eutectic at −46.1 ± 0.5° and 5.24 mole per cent. aluminum bromide as Al_2Br_6, with no evidence of compound formation. Aluminum bromide has been considered to be Al_2Br_6 throughout this present work in view of the knowledge of its molecular state when no chemical reaction has occurred. The cooling curves of pure aluminum bromide showed no phase transformation down to room temperatures. This observation is in accord with and supports the reports of Burbage and Garrett[6] and others[7] whose conclusions were not in agreement with Kendall, Crittenden and Miller.[8] The latter workers reported a phase transformation near 70° for solid aluminum bromide.

The stannic bromide–boron bromide system has a eutectic at −52.5 ± 0.5° and 18.3 mole per cent. stannic bromide. There is no compound formed in this system.

The stannic iodide–boron bromide system forms no compound and has a eutectic at −51.1 ± 0.5° and 0.94 mole per cent. stannic iodide.

The system arsenic bromide–boron bromide has a eutectic at 5.8 mole per cent. arsenic bromide, freezing at −54.1 ± 0.5°. There was no evidence of compound formation in this system. In a previous study of boron bromide reactions, Tarible[9] observed that arsenic bromide was soluble in boron bromide, but that no reaction occurred at 18°. Our findings are consistent with those of Tarible, and his observation may thus be extended to the entire concentration range.

It is apparent from the present phase studies that bromine in aluminum, stannic and arsenic bromides and iodine in stannic iodide show no tendency to coördinate with boron in boron bromide. Only one instance is reported in which bromine is considered the donor atom, in the case of the compound $PBr_5 \cdot BBr_3$.[10] In contrast, Cueilleron,[11] in a study of the system Br_2–BBr_3, found that no maximum occurred, the system having a simple eutectic at 80 mole per cent. BBr_3 and −60.4. His work indicated that free bromine apparently

---

[5] J. H. Hildebrand and R. L. Scott, "The Solubility of Non-Electrolytes," 3rd ed., Reinhold Publ. Corp., New York, N. Y., 1950, Chap. XVII.

[6] J. J. Burbage and A. B. Garrett, THIS JOURNAL, **56**, 730 (1952).

[7] J. D. Heldman and C. D. Thurmond, *J. Am. Chem. Soc.*, **66**, 427 (1944).

[8] J. Kendall, E. D. Crittenden and H. K. Miller, *ibid.*, **45**, 963 (1923).

[9] J. Tarible, *Compt. rend.*, **132**, 204 (1901).

[10] J. Tarible, *ibid.*, **116**, 1521 (1893).

[11] J. Cueilleron, *ibid.*, **217**, 112 (1943).

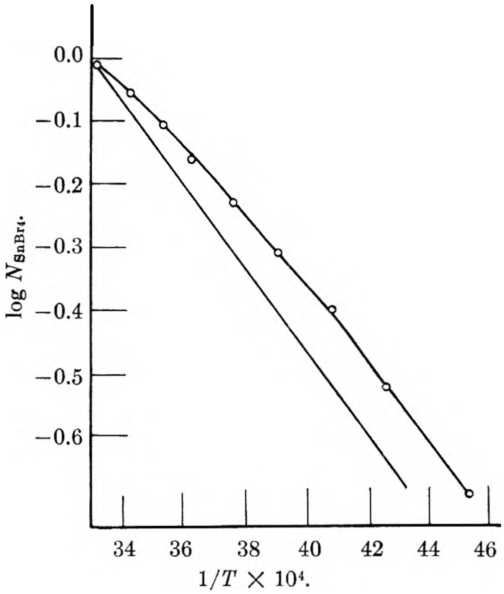

Fig. 7.—The solubility of stannic bromide in boron bromide: ——, ideal; ○—○, experimental.

has no tendency to donate electrons to boron bromide to form a molecular compound. The data obtained in the present research indicates the same conclusion with respect to bromine as bromide.

Of the three metal components used in this research, only arsenic has previously been considered to be a donor atom with boron in boron bromide. An investigation[12] of the system boron bromide-arsine gave evidence of a 1:1 complex between arsine and boron bromide. In the complex which was formed arsenic was considered to be the donor atom. In contrast, no tendency for coördination was shown by arsenic in arsenic bromide in this research.

Hildebrand[5] has shown that in non-polar systems the relative values of the internal pressures of the two components are important factors in determining the solubilities (or freezing point depressions) in the systems. Therefore a comparison of the deviation from ideal solubility shown in Figs. 5–8 and the internal pressures of the added halides seemed desirable.

Stannic iodide and arsenic bromide exhibited positive deviations from ideal solubility. Their calculated internal pressure values are 135.8 and 120.5 cal./cc., respectively, compared to 80.5 cal./cc. for boron bromide. This positive deviation is consistent with Hildebrand's observation that large differences in internal pressures, between solute and solvent, are generally reflected in decreased solubilities. The plot of the experimental data for these two solutes in Figs. 5 and 6 forms an S shaped curve, typical of solutions which have been classified as regular by Hildebrand. Sufficient data are not available to allow calculations over a wide temperature range to test this classification.

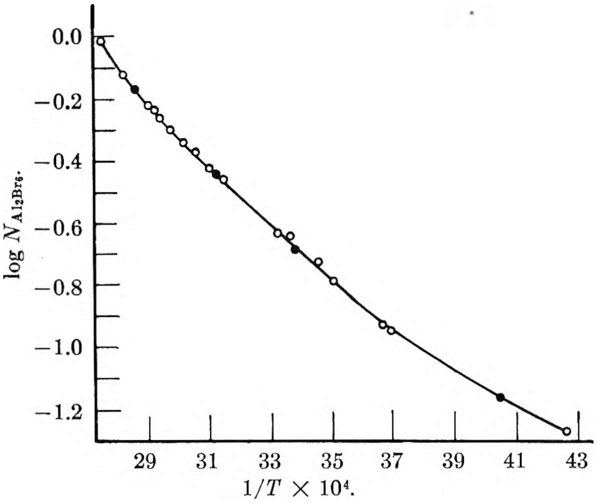

Fig. 8.—The solubility of aluminum bromide in boron bromide: ●, ideal; ○, experimental.

A comparison of the experimentally determined solubility with the calculated ideal solubility for stannic bromide shows a negative deviation. The internal pressure was calculated to be 77.5 cal./cc., somewhat lower than the similar quantity for boron bromide.

The experimental data for aluminum bromide corresponded closely to the calculated ideal solubility curve. The latter curve was plotted by calculating the heat of fusion for aluminum bromide at a number of different temperatures using available heat capacity data. The internal pressure value for aluminum bromide was found to be 78.6 cal./cc.

From the above comparisons, large differences in internal pressures appear to be significant in determining solubility relationships in these systems. However, additional thermodynamic data, such as heat capacity of liquid boron bromide, are needed for a more rigorous treatment of the solubility curves.

---

[12] A. Stock, *Ber.*, **34**, 949 (1901).

STUDIES ON IONIZED SURFACE LAYERS USING α-RECOIL ATOMS. THE COADSORPTION OF Bi-212 IONS AT SODIUM DODECYLSULFATE SURFACE LAYERS

BY NAFTALI H. STEIGER[1] AND GUNNAR ANIANSSON

Division of Physical Chemistry, Royal Institute of Technology, Stockholm 70, Sweden

Received September 4, 1953

A new radioactive method for measuring the adsorption of solutes at the surface of a solution has been developed. Utilizing the α-recoil mechanism the coadsorption of Bi-212 ions at the surface layer of aqueous solutions containing nitric acid (10^{-1}–10^{-4} M) and sodium dodecylsulfate in various concentrations has been studied. Upon the α-decay of Bi-212 the beta and gamma active Tl-208 atoms recoiled from the surface of the solutions and were collected on a negatively charged metal plate placed over the solutions. When the activity of the recoil atoms on the plate had reached saturation the plate was removed and its activity followed with a GM-counter thus giving a relative measure of the coadsorption of the Bi ions. The range of the recoiling Tl-208 atoms in water is about 1000 Å. and should thus be of suitable magnitude for the investigation of surface layers. The surface tension of the solutions as well as the amounts of radiocolloidal Bi-212 and Pb-212 in the solutions were determined. Optimum conditions for the above mentioned method are obtained in solutions containing 0.1–0.5 mmole of sodium dodecylsulfate/l. and 10^{-2}–10^{-3} mole of HNO_3/l. In these concentration intervals relatively high recoil activities, resulting in good precision, are obtained and further the amount of radiocolloids is not important. The ratio of polyvalent ions such as Pb-212, Pb-208, Bi-212, etc., to dodecylsulfate ions in the surface layer was estimated to be less than 1:100. The coadsorption of polyvalent ions should thus not change the general character of the surface layer to any important extent.

1. **Introduction.**—Many different methods have been developed for the measurement of the adsorption of solutes at the surface of solutions. Recently radioactive methods have been introduced by Hutchinson[2] Dixon, Weith, Argyle and Salley[3-7] and Aniansson and Lamm.[8-11] In these methods the amount of coadsorbed radioactive ions or radioactively tagged soap molecules in the surface layer was measured with a GM-tube. None of the methods permitted a direct measurement of the thickness of or the concentration gradient in the surface layer of the soap solution.

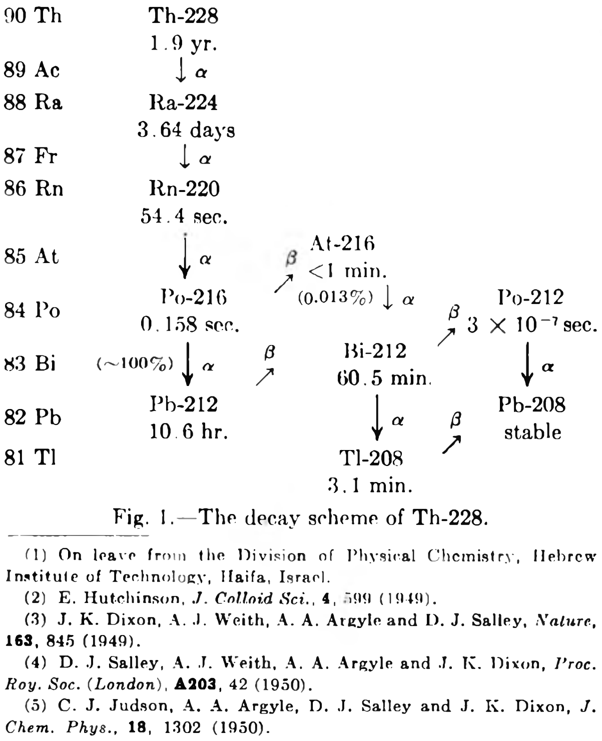

Fig. 1.—The decay scheme of Th-228.

Such direct measurements, however, may be possible using the α-recoil mechanism.[9,10,12] A preliminary report on experiments based on these ideas has been published recently.[13] It seems plausible to suppose that the layer thickness as far as it is possible to define the lower bounding surface is between some ten and some hundred Å.[14-16] The range of the Tl-208 (ThC″) atoms resulting from the α-decay of Bi-212 (ThC) is about 1000 Å. in water and should thus be of a suitable magnitude for such measurements. The measurements reported here were undertaken to find suitable conditions for a detailed investigation of the surface layer. The surface active substance chosen was sodium dodecylsulfate in the following abbreviated to SDS.

Various factors have been investigated, *e.g.*, the total amount of coadsorbed Bi ions with varying SDS concentration, the influence of the concentration of nitric acid necessary to suppress the hydrolysis of Bi ions and the formation of radiocolloids, the amount of these radiocolloids and finally the solubility of lead and bismuth ions in the solutions.

2. **The Principles of the Measurements and the Recoil Atom Mechanism.**—All measurements were made on nitric acid solutions, of differing pH values, which had been activated with Pb-212/Bi-212 (ThB/ThC) from a platinum wire. These isotopes, decay products from Rn-220 (Tn), were collected in an electrical field on the wire in the Rn-220 containing air above a Th-228 (RdTh) source (see Fig. 1). After removal of the wire the activated solution was allowed to stand overnight.

---

[1] On leave from the Division of Physical Chemistry, Hebrew Institute of Technology, Haifa, Israel.

[2] E. Hutchinson, *J. Colloid Sci.*, **4**, 599 (1949).

[3] J. K. Dixon, A. J. Weith, A. A. Argyle and D. J. Salley, *Nature*, **163**, 845 (1949).

[4] D. J. Salley, A. J. Weith, A. A. Argyle and J. K. Dixon, *Proc. Roy. Soc. (London)*, **A203**, 42 (1950).

[5] C. J. Judson, A. A. Argyle, D. J. Salley and J. K. Dixon, *J. Chem. Phys.*, **18**, 1302 (1950).

[6] C. M. Judson, A. A. Argyle, J. K. Dixon and D. J. Salley, *ibid.*, **19**, 378 (1951).

[7] C. M. Judson, A. A. Lerew, J. K. Dixon and D. J. Salley *ibid.*, **20**, 519 (1952).

[8] G. Aniansson, *Arkiv Fysik*, **2**, No. 22, **229** (1949).

[9] G. Aniansson and O. Lamm, *Nature*, **165**, 357 (1950).

[10] G. Aniansson, THIS JOURNAL, **55**, 1286 (1951).

[11] G. Nilsson and O. Lamm, *Acta Chem. Scand.*, **6**, 1175 (1952).

[12] G. Aniansson, to be published.

[13] G. Aniansson and N. H. Steiger, *J. Chem. Phys.*, **21**, 1299 (1953).

[14] E. Hutchinson, *Trans. N. Y. Acad. Sci.*, **11**, 266 (1949).

[15] J. C. Henniker, *Revs. Mod. Phys.*, **21**, 322 (1949).

[16] C. Bacon, Thesis, Stanford University (1933).

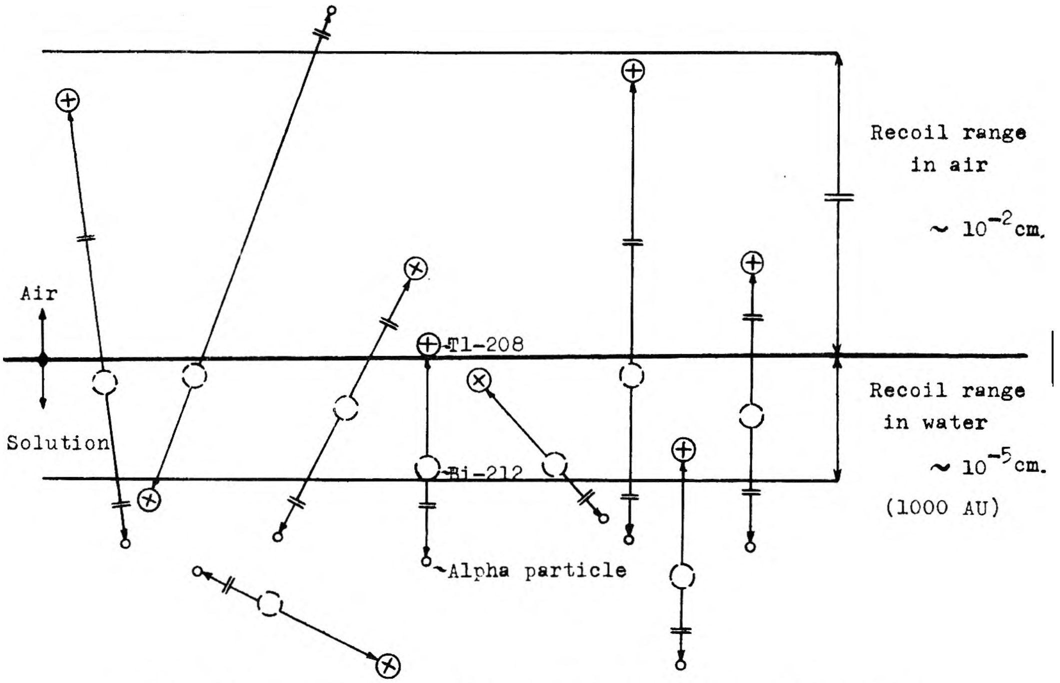

Fig. 2.—Schematic picture illustrating the recoil action in the liquid surface layer.

The transient equilibrium between the mother substance, in this case Pb-212 ($T_{1/2}$ = 10.6 hr.), and its decay products, Bi-212 ($T_{1/2}$ = 60.5 min.), Po-212 ($T_{1/2} = 3.10^{-7}$ sec.) and Tl-208 ($T_{1/2}$ = 3.1 min.), is practically reached in a few hours. When the solution was used the next day it therefore had an apparent half life of 10.6 hours.

One can assume that a large part of the polyvalent metal ions in these nitric acid and SDS solutions are coadsorbed at the surface together with the soap ions. They presumably replace an equivalent number of normal gegenions, in this case sodium and hydrogen ions. The polyvalent metal ions are the radioactive elements, Pb-212 and Bi-212, and the stable decay product, Pb-208.

The recoil atom mechanism used in the measurements of these adsorptions will now be examined. Figure 2 gives a schematic picture of the surface layer of the radioactive solution. Every α-particle emitted leaves a recoiling nucleus, in this case Tl-208, which may recoil down into the solution or leave the surface layer depending on the direction of the corresponding α-particle.

In the β-decay of Pb-212 the resulting Bi-212 atom is also given a certain recoil energy. The maximum recoil energy of these Bi ions is however only about 3 ev. This energy will most probably not be enough to take the Bi-212 atom out of the solution. Although no measurements seem to have been made on the penetrating power of atoms in this energy interval, experiments[17,18] with recoil atoms from β- and γ-decays indicate that even a monoatomic layer would be sufficient to stop atoms of this energy. According to the common concept of the surface of soap solutions, the coadsorbed Pb-212 ions should have several "atom layers" between their position and the air space. It therefore seems most unlikely that any recoiling Bi-212 ion should reach the air over the solution and be collected on the plate. In addition the results do not indicate any influence due to a 60-minutes half life (Bi-212).

The energy of most of the α-particles emitted due to the decay of Bi-212 can with good approximation be put equal to 6.1 mev. According to Chang and Coor[19] the energies of the lines α_4 and α_5 were found to be 6.07 and 6.113 mev., respectively, and both lines together constitute approximately 100% of the emitted α-particles. With this value the energy, for the recoiling Tl-208 atom. E_M = 0.117 mev., is obtained. For the following investigations it is of interest to know the range of the recoil atoms in the solutions. Except for the surface layer, the concentration of nitric acid and SDS is so small that it is possible to put this range equal to that in pure water. Direct measurements of the range of α-recoil atoms in water have not been made but it is possible to estimate this range from the measured ranges of Tl-208 in H_2 (0.54 mm.)[20] and of Po-215 (127 kev.)[21] and Pb-212 (112 kev.)[22] in air (0.092 and 0.099 mm., respectively). The range of Tl-208 in air can be interpolated from the last two measurements; the result 0.095 mm., can be assumed to be practically equal to the range in O_2.

Using the Bragg law concerning the additivity of atomic stopping powers, the range in water has been computed, resulting in the value 1050 Å.

The number of recoil atoms dN which reach the surface of a solution and leave it, is (neglecting the "straggling")

$$dN = \frac{nA\,dx(R - x)}{2R} \qquad (1)$$

---

(17) C. W. Sherwin, *Phys. Rev.*, **75**, 1799 (1949).

(18) H. Frauenfelder, *Helv. Phys. Acta*, **23**, 347 (1949).

(19) W. Y. Chang and T. Coor, *Phys. Rev.*, **74**, 1196 (1948).

(20) W. Kolhörster, *Z. Physik*, **2**, 257 (1920).

(21) L. W. McKeehan, *Phys. Rev.*, **10**, 473 (1917).

(22) L. Werthenstein, *Ann. Physik*, [9] **1**, 347 (1914).

where A = the surface area, n = the number of Bi-212 decays per unit volume, x = the depth under the surface. If n does not change with the depth, 1 can be integrated giving

$$N = nAR/4 \qquad (2)$$

Thus $^1/_4$ of the recoil atoms emitted within a depth R reach the surface in a homogeneous surface layer.

When the stopping process in the air space is completed the recoil atom carries a positive charge. A negatively charged brass plate was placed above the surface of the liquid in order to collect the positively charged recoil atoms. Depending on the stopping medium, the recoil atom can also be negatively charged.[23] By reversing the polarity on the collecting plate to positive, so as to collect negative ions, the collected activity decreased to less than 0.2% (experimental sensitivity). This shows that under the present conditions negatively charged recoil atoms are practically non-existent. It has also been reported[23] that a collecting efficiency of 100% can only be achieved in vacuum and that it is probably somewhat smaller in air. It may safely be assumed however that the collecting efficiency is independent of the composition of the solution and thus without importance in relative measurements.

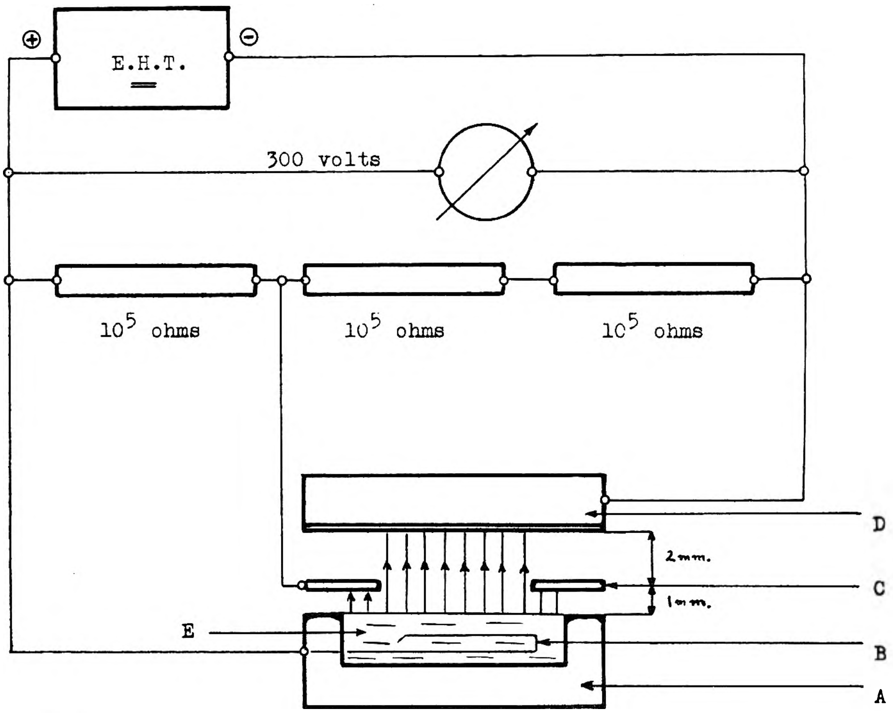

Fig. 4.—Experimental arrangement: A, Lucite cell; B, circular platinum wire; C, brass ring; D, brass plate; E, solution.

As is shown in Fig. 1, the Tl-208 atoms which are collected on the plate are beta and gamma active and can thus in the conventional way be measured using a GM-tube.

3. **The Purity of the Solutions.**—A commercial sample of SDS was dissolved in ethyl alcohol, filtered, three times recrystallized and finally extracted with diethyl ether in a Soxhlet apparatus. The surface tension of an aqueous solution of SDS was measured as a function of the concentration with a du Noüy tensiometer at three occasions, before the purification (Fig. 3, curve A), after 24 hours extraction with ether (curve B) and after 8 hours further extraction (curve C). These curves show the same tendency as those reported by Miles and Shedlovsky.[24] Although the minimum was not removed by this purification, it is most probable that higher homologs and not lauryl alcohol are the cause of the remaining minimum.

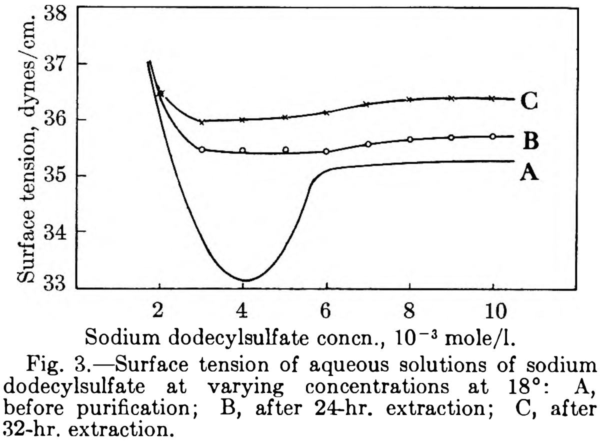

Fig. 3.—Surface tension of aqueous solutions of sodium dodecylsulfate at varying concentrations at 18°: A, before purification; B, after 24-hr. extraction; C, after 32-hr. extraction.

The nitric acid used was prepared from very pure concentrated HNO_3 diluted with conductivity water. The conductivity water was made from ordinary distilled water which was passed through a column of mixed cation and anion exchangers (Amberlite IR-120 and IRA-400, resp.).[25] The specific conductivity of this water was 8×10^{-7} ohm^{-1} cm.$^{-1}$.[26]

The diluted nitric acid was always activated with Pb-212/Bi-212 for one hour on the afternoon before the day of the measurements.

4. **The Experimental Arrangement.**—Figure 4 shows the experimental arrangement. A is a 5-mm. deep Lucite cell on the bottom of which is a circular platinum wire B with a connection to the outside of the cell. B is connected to the positive pole of a d.c. voltage source. One mm. above the liquid surface and the top of the cell, a brass ring C is placed to which a negative potential of 100 v. is applied. In this way edge effects could be neglected and a precise definition of the surface area obtained. Thus only those recoil atoms which leave the surface within the inner edge of the brass ring reach the brass plate D. This consisted of a thin brass sheet fixed to a thick Lucite plate. D is connected to the negative pole of the 300-v., d.c. supply. The whole arrangement was placed in a so-called "gloved box" where all experiments were performed. The use of the gloved box involved several advantages; dust could be fairly well excluded, the temperature held at a desired value and the relative humidity kept high thus minimizing surface evaporation. The evaporation was furthermore kept low by the relatively small gas space over the surface in the apparatus (about 2.4 cm.^{3}). The temperature of the box was 24.0 ± 0.5°.

---

[23] Rutherford, Chadwick and Ellis, "Radiations from Radioactive Substances," Cambridge University Press, New York, N. Y., 1930.

[24] G. D. Miles and L. Shedlovsky, This Journal, **48**, 57 (1944).

[25] R. Kunin and R. J. Myers, "Ion Exchange Resins," John Wiley & Sons, Inc., New York, N. Y., 1950, p. 109.

[26] This measurement was made by Mr. G. Nilsson in this Institute.

5. Preparatory Measurements.—To determine when the efficiency in collecting the recoil atoms had reached its full value, the recoil activity was measured over an interval of 400 v. Figure 5 shows that a maximum in the collecting efficiency is obtained even at relatively low voltages, *i.e.*, about 50 v. All the following measurements were made at a voltage of 300 v.

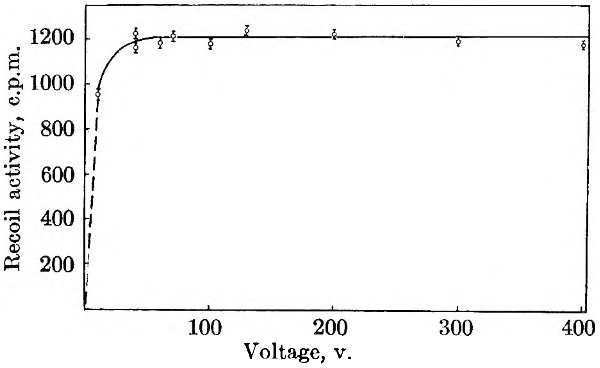

Fig. 5.—Recoil activity as a function of collecting voltage.

The transient equilibrium between Pb-212 and Bi-212, obtained by the activation of the platinum wire over the emanating source, is destroyed during the activation of the nitric acid solutions in that bismuth is dissolved to a lower degree than lead. Even if no Bi-212 were dissolved from the platinum wire, equilibrium should be reached to within 0.03% if the solutions have been standing overnight (15 hr.).

In the first preliminary measurements with this method it was found that a component with long half life became slowly enriched on the plate during repeated activations and measurements. Its half life proved to be about 10.6 hr. and is therefore thought to have been Pb-212. As the Pb-212/Bi-212 proved to contain small amounts of Ra-224 (ThX) it is most probable that the Pb-212 obtained on the plate originated from Rn-220 (radioactive daughter of Ra-224) which had diffused into the air over the solution. Approximate computations showed also that the amount of Ra-224 present was sufficient for this explanation.

The Th-228 source with which these results were obtained was replaced by a new one which emitted much less Ra-224. The component of long life could then no longer be detected on the plate.

Curious variations in the surface tension with time have been reviewed by Sutherland and it was shown that the results of different research workers were very contradictory.[27] Diffusion of the surface active agent cannot alone explain many of the results and thus it is necessary to assume hindering effects on the penetration of the surface layer or the presence of small amounts of surface active impurities. Such changes in the surface layer would result in a changing coadsorption of Bi-212 ions. However still stronger influences on the variation of the recoil activity with time may result from a slow transport of Bi-212 ions to the surface layer. In the extreme case that all Bi-212 and Pb-212 ions are adsorbed at the surface layer after equilibration, it is possible to compute how fast these ions diffuse to the surface layer during the initial unequilibrated state.[28] The total fraction, f, adsorbed is

$$f = 1 - 0.8e^{-t/\tau} \qquad (3)$$

where t = time and $\tau \sim 5.6$ hr. If diffusion alone determined the rate of adsorption of the polyvalent ions the recoil activity would certainly vary greatly for several hours even though at most only 15% of the Bi-212 ions is coadsorbed at the surface layer. However turbulence must result when the solutions are poured into the cell from a pipet. This will probably continue for an appreciable time after the rapidly occurring formation of the surface layer of dodecylsulfate ions and thus greatly enhance the transport of the Bi-212 ions to this layer. When turbulence has stopped thermal convection currents will act in the same direction. Experimental measurements on the change of recoil activity cannot be expected to be very reproducible because of these factors. Measurements were made on four 10^{-3} *M* HNO_3 solutions containing SDS in the concentrations (mole/l.), 0.5×10^{-3}, 1.0×10^{-3}, 1.5×10^{-3} and 3.0×10^{-3}, and Pb-212/Bi-212 in transient equilibrium were poured into the measuring cells from a pipet and their recoil activities were followed for several hours after the formation of the liquid surface (compare section 6). The results corrected for the radioactive decay using the 10.6 hr. value for the half life of Pb-212, are given in Fig. 6. In three of the measurements equilibrium is reached within the 20 minutes used for reaching saturation in recoil activity but in the fourth equilibrium is reached only after several hours. Curves A, B and D show that the slow diffusion is mostly sufficiently enhanced by turbulence or similar influences to give a rapid attainment of equilibrium. The greatly different appearance of curve C is naturally explainable in terms of the slow diffusion in a non-turbulent solution but the difference between this curve and the other ones is so large that some other, accidental influence is probably responsible.

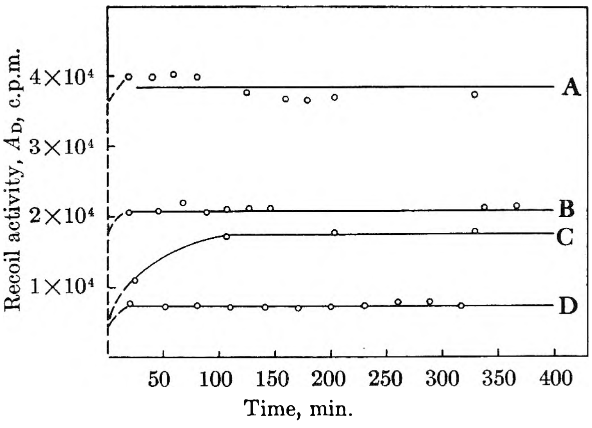

Fig. 6.—The recoil activity of the solution as a function of the time elapsing since the formation of the surface (cor. for the 10.6-hr. decay); all the solutions are 10^{-3} *M* with respect to HNO_3: A, 0.5×10^{-3} mole/l. sodium dodecylsulfate; B, 1.0×10^{-3}; C, 1.5×10^{-5}; D, 3.0×10^{-3}.

---

(27) K. L. Sutherland, *Revs. Pure and Appl. Chem.* (*Australia*), **1**, 35 (1951).

(28) W. Jost, "Diffusion in Solids, Liquids, Gases," Academic Press, Inc., New York, N. Y., 1952, p. 35.

The curve C was obtained during some auxiliary experiments made after the measurements reported in section 7 and thus in this section, no precautions were taken against the appearance of such slow attainments of equilibrium as in curve C.

6. Computations.—Each series of measurements usually lasted one day and was made using SDS dissolved at various concentrations in a nitric acid solution of specified *p*H value and containing Pb-212, Bi-212, etc., in transient radioactive equilibrium. To correct for the 10.6-hr. decay in the activity of the solution, a reference time was chosen for every series. This was usually chosen to be the time when the plate was first removed from the field over the solution, τ_1. The time of removal of the plate was for all the following measurements determined with a stop-watch. These points are called τ_n. To correct for the variation in activity of the solution from one series of measurements to another the activity of 2 ml. of the solution was measured and the corresponding value for the time τ_1 calculated. From this a correction factor, f_2, was computed with which all the results were multiplied.

Since the half life of Tl-208 is very short (3.1 min.), the integrated activity of the plate A_T was measured over a well defined interval, $t_2 - t_1$, (usually 10 min.) from which the activity at the time of removal from the liquid (τ) was calculated (see Fig. 7).

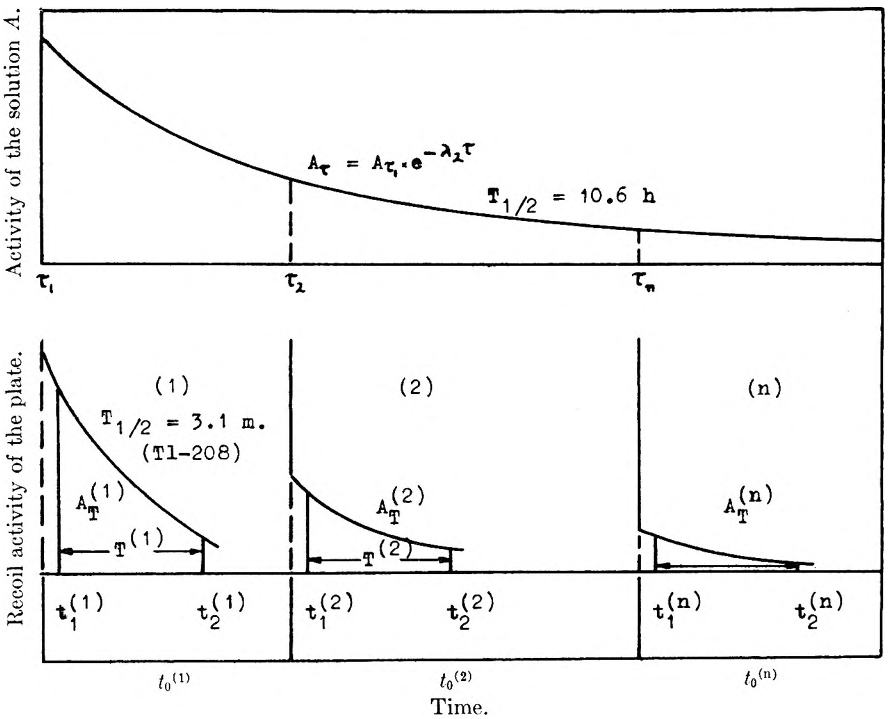

Fig. 7.—Illustration of the method of calculation of the recoil activity, A_D.

Collecting all these factors into the one formula 4, the recoil activity A_D in c.p.m., which is a direct measure of the adsorption of the Bi-212 ions at the surface layer, is obtained.

$$A_D = (A_T - TN)f_1 \frac{\lambda_1}{e^{-\lambda_1 t_1} - e^{-\lambda_1 t_2}} \times e^{-\lambda_2 \tau} \times f_2 \times f_3 \tag{4}$$

where

$$f_1 = \frac{[1 + (A_T - TN)\lambda_1 \delta]}{2} \frac{[e^{-\lambda_1 t_1} + e^{-\lambda_1 t_2}]}{[e^{-\lambda_1 t_1} - e^{-\lambda_1 t_2}]} \tag{5}$$

and symbols

A_T = total activity (background included) of the plate measured over the interval, $T = (t_2 - t_1)$
N = background in c.p.m.
T = interval, $t_2 - t_1$, min.
f_1 = correction for coincidence losses
δ = dead time of the counting circuit, min.
f_2 = factor correcting for the variation in total activity (total amount of Pb-212, Bi-212, etc.) between different series of measurements
f_3 = factor correcting for the variation in counting efficiency of tube and scaler
τ = time difference, $\tau_n - \tau_1$, between the zero time for the 10.6-hr. decay of the solutions and the time, τ_n, of the recoil measurement (*i.e.*, the moment when the plate is removed from the solution—corresponding to $t_0{}^n$)
λ_1 = decay constant of Tl-208, min.$^{-1}$
λ_2 = decay constant of Pb-212, min.$^{-1}$

7. Results of the Recoil Activity Measurements.—The recoil measurements were made on Pb-212, Bi-212, etc., active solutions of nitric acid in the concentrations, 10^{-1}, 10^{-2}, 10^{-3} and 10^{-4} mole/l., using a series of SDS concentrations from 0 to 15×10^{-3} and the recoil activity values defined by formula 4 calculated. Altogether 15 series of measurements were made each comprising 10 different concentrations of SDS. Figure 8 gives a mean value representation of part of these measurements, *i.e.*, those which were made under the most favorable conditions which were only reached after a series of introductory measurements. Good reproducibility required a thorough exclusion of dust and other impurities, thermostating, reduction of evaporation and constancy in the general experimental conditions. At low SDS concentrations, *i.e.*, below 1×10^{-3} mole/l., good reproducibility was especially difficult to achieve, but could after practice be obtained rather well even in that range. It should be mentioned, however, that the general tendency in the results was completely clear and reproducible even in the first preliminary measurements.

With all concentrations of nitric acid, the maximum is located between 0.1 and 0.05×10^{-3} mole SDS/l.

The expected standard deviation in the radioactivity measurements lies between ±0.5% for the highest activities and *ca.* ±2.5% for the lowest activities.

Two series of measurements were made with the addition of 5 mg. of sodium hexametaphosphate/ml. As could be expected from the complex forming ability of the phosphate, the adsorption of

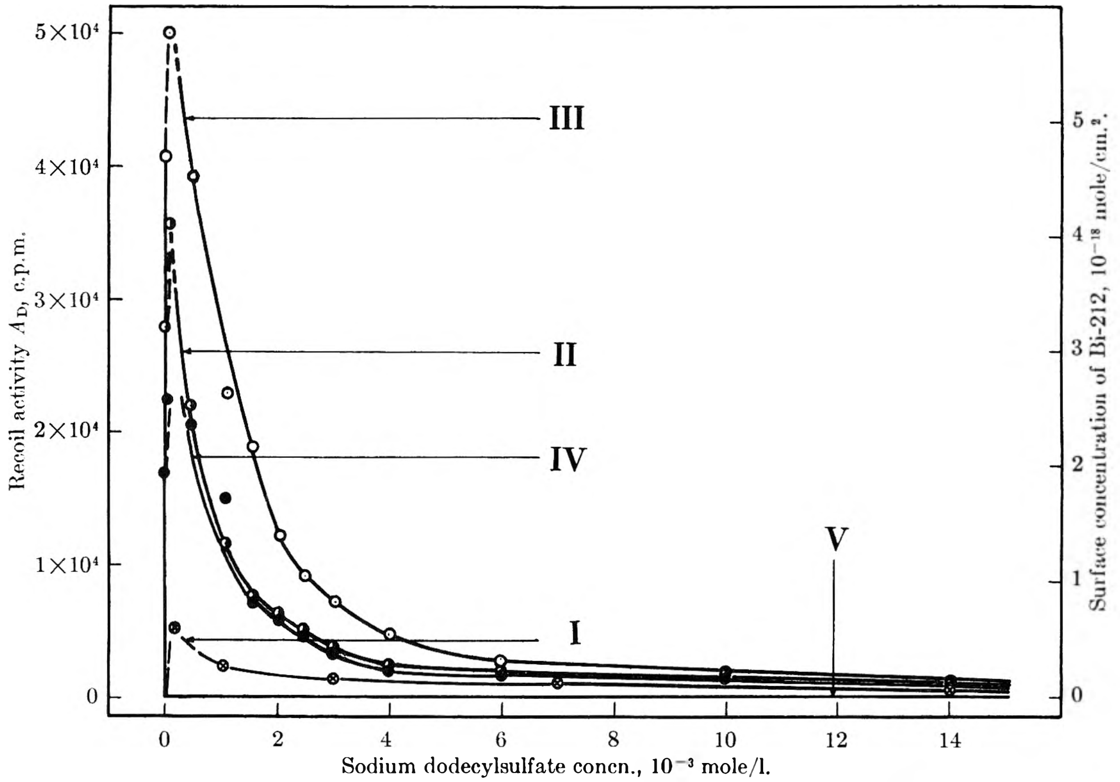

Fig. 8.—The recoil activity of the solutions A_D as function of the sodium dodecylsulfate concentration at 24°: I, in 10^{-1} *M* HNO_3; II, in 10^{-2} *M;* III, in 10^{-3} *M;* IV, in 10^{-4} *M;* V, in 10^{-2} *M* plus sodium hexametaphosphate to a concentration of 5 g./l.

Bi-212 was suppressed. The result is represented by the curve V in Fig. 8. The recoil activity is almost constant between 0 and 10 c.p.m. over all the concentrations of SDS. The ordinate on the right-hand side in Fig. 8 gives in the first approximation the surface concentration of Bi-212 which was estimated in the following way

$$\Gamma_{\text{Bi-212}} = \frac{A_D}{F\eta_m \frac{1}{2} N^0 \lambda_{\text{Bi-212}} \frac{1}{3} f_4} \qquad (6)$$

in which

A_D = recoil activity according to 4 and Fig. 8, c.p.m.
F = area of the liquid in the cell A, *i.e.*, the area of the opening in the brass ring C (Fig. 4), cm.²
η_m = fraction of the Tl-208 disintegrations which are registered by the GM-tube in the standard measuring position ~ 0.20
N^0 = Avogadro's number
$\lambda_{\text{Bi-212}}$ = decay constant for Bi-212, min.$^{-1}$

The factor, $^1/_2$, is placed in the denominator because only 50% of the recoil atoms are directed upwards (all of which are supposed to reach the air space). The factor $^1/_3$ which also appears in the denominator is introduced because only $^1/_3$ of the Bi-212 disintegrations involve the emission of an α-particle (see Fig. 1).

f_4 = fraction of recoil atoms emitted within the measuring area that are collected on the plate, the value chosen being 0.9

Figure 9 shows the variation of the recoil activity with the *p*H value of the solution at a low SDS concentration (0.1 mole/l.).

8. Supplementary Measurements. a. Surface Tension.—The surface tensions of the solutions were measured as a function of the SDS concentration with a du Noüy tensiometer at 22 ± 1°. Figure 10 shows the resulting curves for the concentrations, 10^{-2} and 10^{-3} mole HNO_3/l., for both radioactive and non-radioactive solutions. The higher ionic strength in these solutions compared with solutions of pure SDS results in a marked movement of the critical concentration to lower values.

b. Radiocolloids.—It is a well-known fact that Pb-212 and Bi-212 tend to form radiocolloids in neutral or weakly acid solutions.[29] It was necessary to determine to what extent such radiocolloid formation occurred in these experiments since radiocolloids must be supposed to behave quite differently to simple polyvalent ions in the electrical double layer which is formed in the surface of the solution.

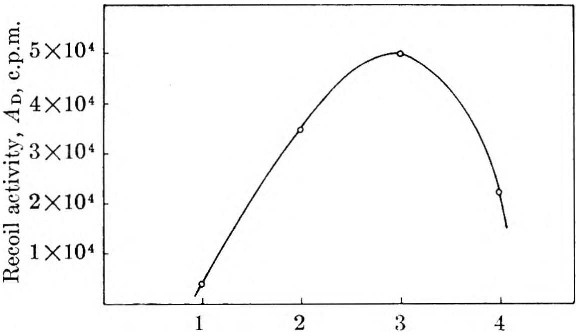

Fig. 9.—The dependence of the recoil activity A_D on the *p*H value of the solutions for a sodium dodecylsulfate concentration of 0.1 × 10^{-3} mole/l.

---

(29) F. Paneth, *Kolloid. Z.*, **13**, 297 (1913).

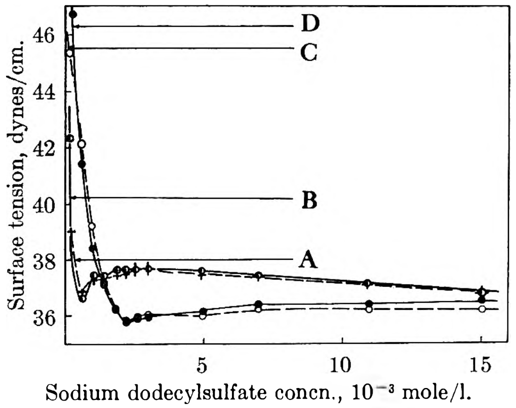

Fig. 10.—The surface tension of the solution as a function of the sodium dodecylsulfate concentration at 22°: A, inactive solution, 10^{-2} M HNO_3; B, active solution, 10^{-2} M HNO_3; C, inactive solution, 10^{-3} M HNO_3; D, active solution, 10^{-3} M HNO_3.

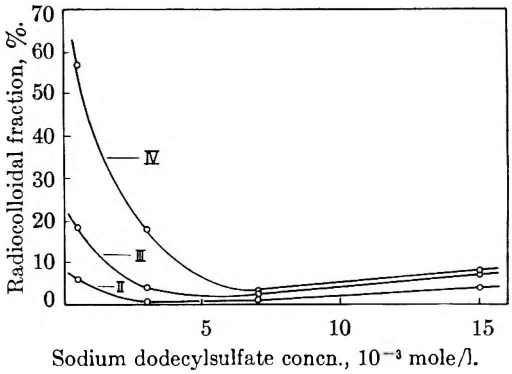

Fig. 11.—The radiocolloidal fraction of the solution as a function of the sodium dodecylsulfate concentration: II, in 10^{-2} M HNO_3; III, in 10^{-3} M HNO_3; IV, in 10^{-4} M HNO_3.

For this purpose a series of centrifugation experiments were carried out which were similar to those made by Werner,[30] Haissinsky[31] and Chamié and Haissinsky.[32]

The mean values of duplicate centrifugations at 5000 r.p.m. and a radius of 7.0 cm. and lasting 70 min. are given in Fig. 11. The sensitivity of the measurements was not sufficient to reveal any difference between lead and bismuth in the colloidal formation tendency.

c. Solubility of Lead and Bismuth in the Solutions.—In order to make sure that precipitation of insoluble compounds of lead and bismuth did not occur the solubilities of lead and bismuth in dodecylsulfate were determined. The radioactive method introduced by Hevesy and Paneth[33] was used from which the solubility of lead and bismuth ions in the presence of 10^{-3} M SDS and 10^{-2} M nitric acid was obtained

$$\text{for lead } 2.8 \times 10^{-6} \text{ mole/l.}$$
$$\text{and for bismuth } 8 \times 10^{-6} \text{ mole/l.}$$

Assuming that the precipitates formed are of the types PbD_2 and BiD_3, the corresponding solubility products could be computed

$$S_{PbD_2} = 2.8 \times 10^{-11}$$
$$S_{BiD_3} = 8 \times 10^{-16}$$

The highest concentration of SDS used was 1.5 × 10^{-2} mole/l. Even without considering that at this concentration of SDS the concentration of single dodecylsulfate ions is much smaller, one obtains solubilities for lead ions

$$C_{Pb(max)} = 1.3 \times 10^{-7} \text{ mole/l.}$$

and bismuth ions

$$C_{Bi(max)} = 0.36 \times 10^{-7} \text{ mole/l.}$$

which, as will be shown, are much larger than the concentrations of lead and bismuth actually used.

The total amount of lead (Pb-212 and Pb-208) and bismuth (Bi-212) introduced into the solution was computed from the activities and Pb-208 content of the wire before activation allowing for the fraction of lead and bismuth dissolved from the wire.

The concentrations of bismuth ions 0.8 × 10^{-11} mole/l., and lead ions 4 × 10^{-10} mole/l., thus obtained are far below the limits of solubility. In addition the solubility measurements were made at 18° while all of the recoil measurements were made at 24°.

Finally the concentrations of the other two decay products of Bi-212 are given for the maximal Pb-212 activity of 25 mc./l. used in the solutions.

$$C_{Tl\text{-}208} = 1.5 \times 10^{-13} \text{ mole/l. and,}$$
$$C_{Po\text{-}212} = 0.5 \times 10^{-21} \text{ mole/l. } (ca.\ 10 \text{ atoms/l.!})$$

These concentrations are far too low to be of chemical importance.

9. Electrolysis and Radiation–Chemical Effects.—It is necessary to make clear to what extent interfering reactions could be important. An estimation of the ionization current appearing in the air space between the liquid surface and the collecting plate D gave about 10^{-10} ampere. For a usual experiment (about 6 hr.) 10^{-11} equivalent of electrolyzed substance should result. An oxidation or reduction of the SDS of this magnitude should not noticeably interfere with the results.

The primary chemical effect of the radiation is presumably the disintegration of water into H and OH. This effect of the α- and β-rays over a total period of 6 hr. was estimated according to Allen[34] to be 10^{-10} mole water/ml.

No decomposition yield for aqueous solutions containing HNO_3 and dodecylsulfate have been found, but it is possible that the presence of HNO_3 would somewhat increase the decomposition yield.

Thus, in the extreme case of interaction between all the disintegration products with dodecylsulfate, the radiochemical action could possibly lead to some changes in the character of the surface.

But it should be safe to assume that such an extreme case does not actually exist and that in most cases recombination results and only in the few remaining ones may a reduction or oxidation of SDS occur.

Therefore it should be possible to assume that this influence should not interfere with the investigations.

(30) O. Werner, *Z. physik. Chem.*, **A156**, 89 (1931).

(31) M. Haissinsky, *Compt. rend.*, **198**, 580 (1934).

(32) C. Chamié and M. Haissinsky, *ibid.*, **198**, 1229 (1934).

(33) G. Hevesy and F. Paneth, *Z. anorg. Chem.*, **82**, 322 (1913).

(34) A. O. Allen, THIS JOURNAL, **52**, 479 (1948).

10. The Relative Amounts of Bi-212 and Sodium Dodecylsulfate in the Surface Layer.—It is of primary importance to know to what extent the surface layer is changed by the coadsorption of Bi-212 and the other polyvalent ions. The total amount of polyvalent ions in the bulk of the cell (3.5 ml.) is according to section 8: 1.4×10^{-12} mole. Even if all of the polyvalent ions were coadsorbed at the surface layer the total concentration on the surface (6.6 cm.^{2}) would have been 2×10^{-13} mole/cm.^{2}.

An accurate determination of the surface concentration of SDS is, however, only obtainable from a large series of exact surface tension measurements or with the radioactive method.[3,9,10] Since the primary object here is to set an upper limit for the concentrations of polyvalent ions and dodecylsulfate in the surface, it is possible to use the values given by Hutchinson.[35] These values, measured for pure SDS solutions are no doubt lower than those in which nitric acid was added to the solution. For an SDS concentration of 0.1×10^{-3} mole/l., Hutchinson gives

$$\Gamma_{SDS} = 2 \times 10^{-11} \text{ mole/cm.}^2$$

An upper limit to the ratio of $\Gamma_{P.I.}$ (P.I. = polyvalent ions) to Γ_{SDS} should thus be

$$\Gamma_{P.I.}/\Gamma_{SDS} \sim 10^{-2}$$

This calculated limit is probably much larger than the actual one and shows that the character of the surface layer cannot be appreciably changed by the polyvalent ions.

It would seem reasonable to suppose that the adsorption of SDS on the Lucite walls of the cell is of the same magnitude as that on the free surface. (Compare preliminary measurements by Aniansson on polystyrene.[10]) If it is further assumed that the coadsorption of polyvalent ions on the walls occurs according to the same mechanism and thus is equal to the coadsorption at the free surface, the total lowering of the bulk concentration in the extreme case (10^{-3} M HNO_3 and C_{SDS} = 0.1×10^{-3} mole/l.) would be about 35%.

11. Results and Discussion.—For further closer investigations on the extent of the diffuse double layer and of the concentration gradients in the layer of inhomogeneity between the gas phase and the bulk of the solution, a high recoil activity will be very desirable.

Figure 8 shows that the highest values for the recoil activity A_D are obtained at concentrations of SDS between 0.1×10^{-3} and 0.5×10^{-3} M and for nitric acid concentrations between 10^{-2} and 10^{-3} M.

The general appearance of the adsorption isotherms in Fig. 8 is principally the same as that obtained by Aniansson for calcium with the radioactive method.[10] That the polyvalent ions disappear from the surface in the concentration range where the soap begins to form micelles is explainable if one assumes that the micelles form an inner surface of the same general kind as the surface layer. As this inner surface increases with concentration, a decreasing number of polyvalent ions will be left for adsorption at the free surface. In the investigations on calcium it was shown, however, that the decrease began at markedly lower concentrations than the CMC (critical micelle concentration). A kind of pre-micelle in extremely small amounts initiated by the polyvalent ions or some other kind of soluble complex could explain this phenomenon. That the maximum in coadsorption of bismuth ions occurs at a still lower concentration than that for calcium is in any case partly explainable by the fact that the higher ionic strength caused by the presence of nitric acid should depress the CMC considerably. The higher charge of the bismuth ion compared with that of the calcium ion might also have some influence although this question cannot be decided without a precise determination of the CMC in the nitric acid solutions used.

The precision of the investigations was, however, not sufficient to permit a precise determination of the SDS concentration at which the maximum of the recoil activity for different pH values occurred. The reason for this is that at such low concentrations of the surface active substance it is hardly possible to obtain sufficiently reproducible results to define the activity maximum. It is therefore useless to try to find a relation between the SDS concentration at which maximum recoil activity is obtained and the pH values of the solutions.

As mentioned above, the strong colloid formation tendency of the radioactive bismuth ions could greatly change the mechanism of coadsorption. From Fig. 11 one can infer that in this respect it is better to work with nitric acid concentrations around 10^{-2} M because in this case the radiocolloid formation is small.

In section 10 it was shown that the character of the surface layer could not be changed appreciably by the coadsorption of lead and bismuth ions. This was also confirmed by the agreement between the surface tension curves for inactive and active SDS solutions (Fig. 10).

Acknowledgments.—The authors wish to thank the head of the division, Professor Ole Lamm, for his stimulating interest in and support of these investigations.

The nucleonic equipment used in the radioactivity measurements was put at our disposal from the Nuclear Chemistry section which is financially supported by the Swedish Atomic Committee.

---

[35] E. Hutchinson, *J. Colloid Sci.*, **3**, 413 (1948).

PROPERTIES OF FILMS OF ADSORBED FLUORINATED ACIDS[1]

BY E. F. HARE, E. G. SHAFRIN AND W. A. ZISMAN

Naval Research Laboratory, Washington 25, D. C.

Received September 4, 1953

Monomolecular films of perfluorinated butyric, valeric, caproic, caprylic, capric and lauric acids were prepared by physical adsorption on platinum from their solutions in organic solvents. Their wetting properties for a number of selected liquids were then characterized by contact angle measurements. Regular but small increments in the contact angles were observed with increasing acid chain length. Thus, although perfluorolauric acid monolayers provided the lowest energy surface yet reported, films of even the very short acids were significantly more non-wettable than other types of surfaces, including the fluorinated polymers studied earlier. For the shorter chain acids, monolayer formation was rapid; the two longest chain acids, however, required progressively longer periods of contact between the adsorbing surface and the acid solution for completion of a monolayer exhibiting maximum contact angle. The remarkable liquid-repellency of the perfluoroacid monolayers is caused by the presence of an exposed plane rich in perfluoromethyl groups. Electron diffraction examination of the longer chain acids reveals a molecular orientation consistent with this explanation. Included are surface tension data for several new API hydrocarbons of exceptional purity.

In a recent report we described the remarkably large contact angles of nearly all liquids on the surface formed by a close-packed adsorbed monolayer of perfluorodecanoic acid.[2] The recent availability of perfluorolauric acid and four lower homologs made possible the investigation of the effect of acid chain length on these liquid-repellent properties. A higher member of this series of acids should adsorb as a more closely packed monolayer and hence exhibit greater liquid repellency (or larger contact angles). Since the lower members are more available, however, it was interesting to learn how much loss of liquid repellency would result from their use. In addition, electron diffraction examination of films of perfluorolauric acid was expected to provide supplementary information on the structure and orientation of the adsorbed molecules.

Experimental Methods.—The various perfluorinated acids (hereafter designated as ϕ-acids) were made available through the coöperation of the Minnesota Mining and Manufacturing Company. The ϕ-butyric and ϕ-valeric acids were water-white liquids with reported boiling points of 120° (at 735 mm.) and 139° (at 749 mm.), respectively. The ϕ-caproic, ϕ-caprylic, ϕ-capric and ϕ-lauric acids had melting points of 14.2–16.5°, 43.3–44.4°, 79–85° and 101–106°, respectively, as received; in addition, each compound showed a tendency to change from a white, crystalline powder to a translucent "wet" material over a several degree range of temperature about 10 to 20° below the true melting points. Successive recrystallizations from carbon tetrachloride and toluene eliminated these changes and resulted in melting points of 11.2–13.4°, 54.9–55.6°, 87.4–88.2° and 112.6–114.7°, respectively, for these four acids.

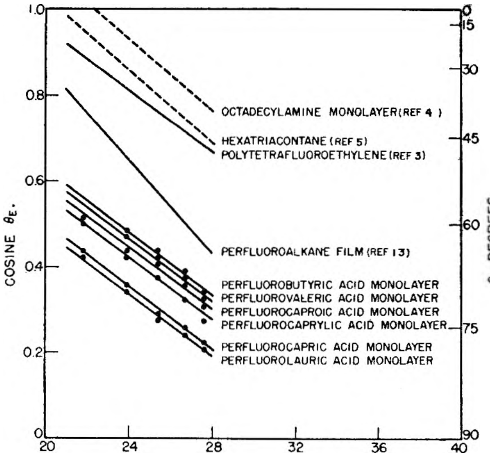

Fig. 1.—Comparison of $\gamma_{LV°}$ *vs.* cos θ_E relationships for a series of *n*-alkanes on several different low-energy surfaces.

Oleophobic films of the acids were prepared in the usual manner[2,3] by immersing freshly-flamed rolled platinum foil in 10^{-3} to 10^{-6} mole per cent. solutions of the ϕ-acids in decane. After a suitable period of contact, the dipper surfaces emerged unwetted by the generating solution. The use of a standard immersion period of 60 minutes ensured the formation of films exhibiting the greatest liquid repellency obtained.

The source, purity and surface tension of many of the test liquids have been reported previously.[4] In addition, several hydrocarbons prepared for the American Petroleum Institute Project 42 (designated as PSC compounds) were received in a highly purified state from Prof. R. Schiessler of Pennsylvania State College. Surface tension measurements were made at this Laboratory using the ring method for all the PSC compounds listed, as well as for the 1,3-dicyclopentylcyclopentane received from the Sun Oil Co.

The equilibrium contact angle data (θ_E) reported here are the results of goniometric measurements of the slowly advancing contact angles measured on at least three separately prepared surface films. The reproducibility was ±2°. When solvent attack of the monolayer was observed, measurements were made using a sessile drop of the liquid which had first been saturated with the appropriate ϕ-acid.

Experimental Wettability Results.—Striking regularities in contact angles resulted from the effects of homology in either the adsorbed acid monolayers or in the liquids wetting them. Individual plots of surface tension ($\gamma_{LV°}$) against the cosine of the contact angle (θ_E) for the *n*-alkanes on each of the acid monolayers (Fig. 1) emphasize these regularities for homologous liquids on a given substrate. As anticipated from previous studies[2,4a,5] straight-line relationships were obtained in each case. In addition, the several lines for the family of ϕ-acids were parallel and arranged in a regular sequence corresponding to the number of carbon atoms (N) in the acid molecule. Extrapolation of the γ *vs.* cos θ lines for the *n*-alkane series to the $\theta = 0°$ axis leads to extremely low values of the intercepts or "critical surface tensions"[4a]; these decrease in the order of 9.2, 9.0,

---

(1) Presented at the Symposium on Fluorine Chemistry under the auspices of the Division of Industrial and Engineering Chemistry, American Chemical Society, at the Fall Meeting in Chicago, Illinois, September 6–11, 1953.

(2) F. Schulman and W. A. Zisman, *J. Colloid Sci.*, **7**, 465 (1952).

(3) W. C. Bigelow, D. L. Pickett and W. A. Zisman, *ibid.*, **1**, 513 (1946).

(4) (a) H. W. Fox and W. A. Zisman, *ibid.*, **5**, 514 (1950); (b) E. G. Shafrin and W. A. Zisman, *ibid.*, **7**, 166 (1952).

(5) H. W. Fox and W. A. Zisman, *ibid.*, **7**, 428 (1952).

8.6, 7.9, 6.1, and 5.6 dynes/cm. as the length of the fluorocarbon chain increases through 4, 5, 6, 8, 10 and 12 carbon atoms. Comparable values for bulk polytetrafluoroethylene[4a] and for adsorbed octadecylamine monolayers[4b] are 18.4 and 22 dynes/cm., respectively.

The effects of homology in the acid monolayer are even more evident in Fig. 2 where cosine θ_E for each of the n-alkanes has been plotted as a function of the number of carbon atoms in the molecule of the adsorbed film. These data fall along parallel straight lines whose displacements are roughly proportional to the differences in the surface tensions of the alkanes. Similar data (Fig. 3) for the miscellaneous liquids fall on a series of curves. Greater curvature is noted for the lower surface tension liquids on the shorter-chain acid films where solubility effects become more significant.

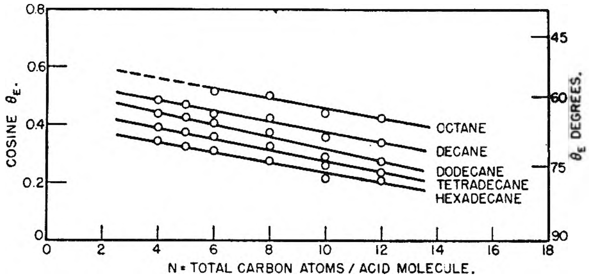

Fig. 2.—The effect of homology in the fluorinated acid monolayers on the contact angles observed for the n-alkane liquids.

Attempts to determine the contact angle for water on these films were relatively unsuccessful as erratic results were obtained, particularly on films of the acids shorter than ϕ-capric. Extreme solvent attack of the monolayers could not be forestalled by the use of acid-saturated water drops since the shorter chain acids are miscible with water in all proportions and even the intermediate acids show appreciable solubility.[6]

Data for the adsorbed monolayers of the ϕ-acids prior to recrystallization were, for the most part, comparable to those reported here. The important exceptions occurred in the case of the two longest chain acids. Whereas the acids as received had adsorbed from solution instantly, the recrystallized ϕ-capric and especially the ϕ-lauric acids now required up to 60 minutes in contact with the solutions to form the most liquid-repellent films. A slight increase in maximum contact angle was also noted for the films from the recrystallized acids. Thus, the n-alkane data described lines slightly shifted from their positions in Fig. 1, but still showing approximately the same slope. The immersion time dependency of these long chain acids is shown by the fact that θ_E for cetane on ϕ-lauric acid ranged from 65–70° for a one-minute immersion to a highly reproducible 78° for immersion times of 60 minutes or longer at the concentrations used.

Experiments on the adsorption of ϕ-lauric acid from decane and hexadecane solutions of comparable concentrations indicated that the critical induction period is a function of the solute concentration and is roughly proportional to the viscosity of the solvent. No evidence was obtained to indicate that the acid molecules underwent any rearrangement phenomena, subsequent to the initial adsorption. For the shorter chain acids, neither time of immersion effects nor changes in θ_E were noted as a result of recrystallization.

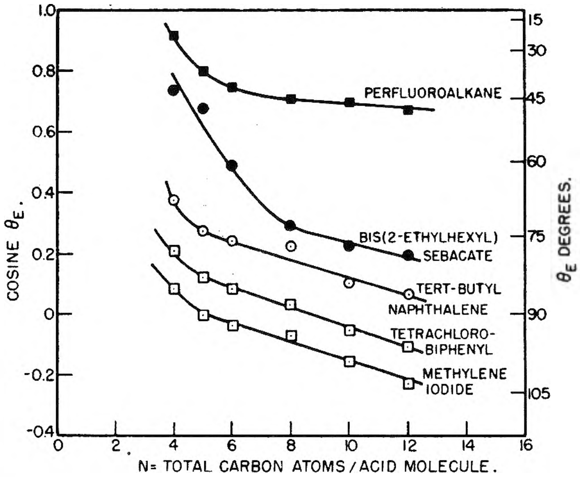

Fig. 3.—The effect of homology in the fluorinated acid monolayers on the contact angles observed for some miscellaneous fluids.

Since the ϕ-lauric acid monolayers on platinum provided the lowest energy surfaces ever reported, a more extensive survey of their wettability properties was undertaken. The results of measurements on a variety of liquids are listed in Table I along with values of the final spreading coefficient (S_{LV°/SV°) calculated on the assumption that $f_{SV^\circ} = 0$ for these highly repellent surfaces. A plot of the γ vs. cos θ_E data for all of the liquids indicates that the same general relationships found in previous studies[2,4a,4b] obtain in the present instance: linear relations hold for individual series of homologous liquids; the higher surface tension liquids exhibit larger contact angles; and, those liquids which are good solvents for the films or which are capable of hydrogen-bonding[7] with the surface exhibit lower contact angles than would be predicted from surface tension considerations alone. The latter liquids, therefore, show the greatest deviation from the extrapolated line for the n-alkane data, which represents a case of normal behavior.

Electron Diffraction Results.—An electron diffraction examination was made of some of the fluorinated acids using a General Electric unit (Type G-2) at 30,000 volts accelerating potential and 50 cm. specimen-to-plate distance. Only the two longest chain acids proved capable of withstanding exposure to the high vacuum (10^{-5} mm.) and the electron beam.

Perfluorolauric acid was handled most successfully since crystals of the bulk acid remained virtually intact throughout the experiment; ϕ-capric acid crystals, however, diminished rapidly in size during examination. Both acids gave diffraction patterns characteristic of highly crystalline material.

---

(6) E. A. Kauck and A. R. Diesslin, *Ind. Eng. Chem.*, **43**, 2332 (1951).

(7) A. H. Ellison, H. W. Fox and W. A. Zisman, THIS JOURNAL, **57**, 622 (1953).

TABLE I

SURFACE ENERGY DATA FOR SOME LIQUIDS ON AN ADSORBED MONOLAYER OF PERFLUOROLAURIC ACID AT 20°[a]

Liquid	Surface tension, $\gamma_{LV°}$, dyne/cm.	Contact angle, θ_E	$S_{LV°/SV°}$, erg/cm.^{2}
n-Alkanes			
Hexadecane	27.6	78	−21.9
Tetradecane	26.7	76	−20.2
Dodecane	25.4	74	−18.4
Decane	23.9	70[b]	−15.7
Octane	21.8	65[b]	−12.6
Miscellaneous Hydrocarbons			
1,1-Di-(α-decalyl)-hendecane PSC 122	35.1	88	−33.9
1,3-Dicyclopentylcyclopentane	34.6	85	−31.5
1,7-Dicyclopentyl-4-(3-cyclopentylpropyl)-heptane PSC 113	34.6	86	−32.1
9-*n*-Dodecylperhydrophenanthrene PSC 141	34.2	86	−31.8
1-α-Decalylhendecane PSC 544	32.7	84	−29.2
1-Cyclohexyl-2-(cyclohexylmethyl)-pentadecane PSC 65	32.7	84	−29.2
4-Cyclohexyleicosane PSC 104	31.6	83	−27.8
9-(α-(*cis*-0,3,3-Bicycloöctyl)-methyl)-heptadecane PSC 178	31.2	84	−27.9
Polyethylene SS903	30.4	81	−25.7
Polyethylene V-120	27.8	78	−22.0
t-Butylnaphthalene	33.7	86	−31.3
n-Decylbenzene	31.2	83	−27.4
8-*p*-Tolylnonadecane PSC 161	30.7	83	−27.0
Benzene	28.9	75[c]	−21.4
Esters			
Tricresyl phosphate	40.9	83	−35.9
Benzylphenyl hendecanoate	37.7	92	−39.0
Bis-(2-ethylhexyl) phthalate	31.2	78	−24.7
Bis-(2-ethylhexyl) sebacate	31.1	79	−25.2
Pentaerythritol tetracaproate	30.4	80	−25.1
1,6-Hexamethylene glycol bis-2-ethylhexanoate	30.2	77	−23.4
Fluorine-containing Liquids			
$CFCl_2-CF_2-CCl_3$	27.8	66	−16.5
$H(CF_2)_2CH_2OH$	27.6	68	−17.2
p-Difluorobenzene	27.0	66[d]	−16.0
$H(CF_2)_4CH_2OH$	24.5	65	−14.1
$H(CF_2)_6CH_2OH$	23.8	62	−12.6
$CF_2Cl-CCl_2-CF_2Cl$	22.8	49	−16.5
Perfluoroalkane (FCD-330)	20.2	48	− 6.7
Non-fluoro Halocarbons			
Methylene iodide	50.8	103	−62.2
Trichlorobiphenyl (Araclor 1242)	45.3	94	−48.5
α-Bromonaphthalene	44.6	92	−46.2
Tetrachlorobiphenyl (Araclor 1248)	44.2	96	−48.8
Hexachloropropylene	38.1	81	−34.1
Hexachlorobutadiene	36.0	81	−30.4
Carbon tetrachloride	26.7	69[c]	−17.1
Miscellaneous Liquids			
Water	72.8	105 (erratic)	−91.7
Glycerol	63.4	102	−76.6
n-Caprylic acid	29.2	69	−18.7
Di-(*n*-decyl) ether	28.4	79	−23.0
n-Capryl alcohol	27.6	70	−18.2
Di-(*n*-amyl) ether	24.9	68	−15.6
Linear polymethylsiloxane (pentamer)	18.1	60	− 9.1

[a] Films adsorbed on platinum foil during 60-minute immersion. [b] Liquid saturated with perfluorolauric acid. [c] Volatile. [d] Liquid attacks film.

Monolayers of φ-lauric acid adsorbed on platinum foil surfaces gave patterns similar to those obtained from films of considerably longer chain hydrocarbon derivatives adsorbed as oleophobic monolayers.[8] A study of them showed some two to four diffuse bands indicating a repeated interatomic distance oriented within 15° of normal to the surface as a whole, *i.e.*, the carbon skeleton of the molecule is extended away from the adsorbing surface at angles

---

(8) L. O. Brockway and J. Karle, *J. Colloid Sci.*, **2**, 277 (1947).

ranging from 75 to 90°. The position of the diffraction bands indicates a chain repeat distance of 2.6–2.7 Å., somewhat larger than that found for the hydrocarbons. This compares with a reported chain repeat distance of 2.62 Å. for polytetrafluoroethylene[9] as against 2.54 Å. for the alternate carbon-to-carbon distance in hydrocarbons and polyethylenes.[10]

Continued exposures of the acid monolayers to the camera vacuum resulted in photographs with considerably more diffuse features, but still indicative of the presence of some adsorbed material. This decrease in film population was reflected in wettability measurements, for the cetane contact angles dropped slightly to 65–70° after an exposure of some 20-minutes duration and to 45° after repeated exposures totalling some 60 minutes of evacuation.

Discussion

Perfluorinated acid monolayers are noteworthy for their pronounced non-wettability as reflected by the extremely large contact angles observed for all members of the series. While the longest chain acid available (ϕ-lauric acid) provided a surface with the lowest free surface energy yet reported, the effect of each perfluoromethylene increment was relatively small. For example, increasing the chain length from ϕ-butyric to ϕ-lauric acid increased the cetane contact angle but 8° (from 70 to 78°). This is in contrast with the results reported for hydrocarbon-type monolayers, in which the wettability is strongly influenced by chain length.[11,12] Although directly comparable data for the hydrocarbon acids are not available, cetane contact angles of 0 and 21° have been reported[12] for butylamine and laurylamine monolayers, respectively. The disparity in the contact angle increases is due to the differences in the contribution of the van der Waals forces to each system, the lateral attractive forces being considerably weaker in the case of the fluorocarbons than in the analogous hydrocarbons.

The large contact angles observed for the fluorinated acid monolayers further attest to the inherent inertness of the fluorine-containing surfaces. Wettability studies on even the shortest chain homolog (ϕ-butyric acid) indicate a free surface energy considerably below that reported for a surface composed essentially of $—CF_2—$ groups (polytetrafluoroethylene).[4a] The remarkable non-wettability of the ϕ-acid monolayers is caused by the presence of the extremely inert $—CF_3$ groups in the surface. Confirmation of this is obtained from the electron diffraction results reported here for ϕ-lauric acid monolayers in which the adsorbed molecules are shown to be oriented so as to expose a surface composed primarily of $—CF_3$ groups.

Further illumination is afforded by a comparison of the free surface energies of the fluorinated acid monolayers with those of the other low-energy fluorine-containing surfaces. It has been established that the degree to which a surface can be wetted is determined by the constitution and configuration of the atomic groups comprising the surface. Thus, in the case of hydrocarbon surfaces, the surface energy decreases in the order: $—CH_2—$ (bulk polyethylene)[5]; a mixture of $—CH_2—$ and $—CH_3$ groups (thin films of hexadecane)[13]; $—CH_3$ groups in a monolayer (octadecylamine monolayer)[4b]; $—CH_3$ groups in a crystal plane (hexatriacontane cleavage surface).[5] A similar ordering is observed (see Fig. 1) for fluorocarbon surfaces in that the surface energy decreases in proceeding from bulk polytetrafluoroethylene ($—CF_2—$ groups),[4a] to a thin film of perfluoroalkane (a mixture of $—CF_2—$ and $—CF_3$ groups),[13] and finally to perfluoroalkanoic acid monolayers. This would indicate at least a very high ratio of $—CF_3$ groups to exposed $—CF_2—$ groups. On this same basis it would appear that a plane of $—CF_3$ groups in crystalline array (as in a surface of a crystal of *n*-perfluoroalkane) should result in a surface of even lower energy.

As noted previously, a standard time of immersion of 60 minutes was employed for all of the acids for the sake of internal consistency, although only the ϕ-capric and ϕ-lauric acids required extended contact betwen dipper and solution to complete monolayer formation. The ϕ-capric acid required some 20 minutes and the ϕ-lauric acid roughly 60 minutes in the concentrations used. The absence of any immersion-time effect prior to recrystallization of the acids is accounted for by the presence of lower-chain acid contaminants. Since it was shown experimentally that the time effect is related to the ability of the acid molecules to diffuse through the solution, the shorter chain components would be expected to adsorb most rapidly. Further confirmation lies in the fact that purification, while increasing t_{imm} for ϕ-capric and ϕ-lauric acids, does result in a slightly larger θ_{max} toward a given liquid. Further, an extension of the time of immersion beyond the critical induction period characteristic of an acid caused no further increase in θ_{max}. The quantitative differences between the results of this study and the previous investigation of ϕ-capric acid[2] are due to these considerations and do not significantly alter the earlier conclusions.

The extreme non-wettability of films of adsorbed perfluorinated acids is significant for the many applications in which it is desirable to impart liquid-repellent characteristics without appreciably increasing the bulk of the system. The present study indicates that for many such purposes the shorter chain acids, which are cheaper and more readily available, may be just as serviceable as the rarer long-chain acids. This could not have been predicted from previous knowledge which was necessarily based on considerations of hydrocarbon type materials. Extremely short chain perfluorinated acids, although providing remarkable nonwetting behavior, may prove unsatisfactory because of solubility problems, particularly in systems involving the presence of water. Further, the high volatility of the shortest members of the acid series increases the possibility of danger from compounds of high corrosivity and unknown toxicity.

---

[9] H. A. Rigby and C. W. Bunn, *Nature*, **164**, 583 (1949).

[10] C. W. Bunn, *Trans. Faraday Soc.*, **35**, 482 (1939).

[11] H. R. Baker, E. G. Shafrin and W. A. Zisman, THIS JOURNAL, **56**, 405 (1952).

[12] E. G. Shafrin and W. A. Zisman, *J. Colloid Sci.*, **4**, 571 (1949).

[13] H. W. Fox, E. F. Hare and W. A. Zisman, *ibid.*, **8**, 194 (1953).

PHOTOSENSITIVE AND PHOTOTROPIC PRODUCTS OF SOLID STATE REACTION BETWEEN SILVER SULFIDE AND MERCURIC IODIDE

BY LAWRENCE SUCHOW AND GEORGE R. POND

Signal Corps Engineering Laboratories, Fort Monmouth, New Jersey

Received September 8, 1953

Solid state reactions have been carried out between silver sulfide and mercuric iodide in various proportions, and the products studied for structure and optical properties. Several different phases have been found at different compositional ratios. X-Ray diffraction work has led to the identification of phases with zinc blende and wurtzite structures having cationic vacancies, as well as a phase with a body-centered cubic lattice which is probably structurally related to α-Ag_2S and α-AgI. All products have colors directly related to those of the parent compounds, except for the golden-yellow product of formula Ag_2HgI_2S, which appears to be a new compound. The diffuse reflectance spectra are given. All products, except those which are black, darken rapidly when exposed to ultraviolet or visible light at wave lengths up to the respective reflectance edges. Those with 30 mole % Ag_2S or less are phototropic at room temperature. Rapid reversal at room temperature appears to be associated with the modified zinc blende structure.

Introduction.—Exploratory experiments indicated the likelihood that the system Ag_2S–HgI_2 would be quite fruitful in its yield of interesting and useful products exhibiting phototropic and "print-out" characteristics. It was therefore decided to make a more comprehensive investigation of the system by carrying out solid state reactions between silver sulfide and mercuric iodide in various proportions over the composition range, and by characterizing the products with respect to their structures and optical properties. This paper reports the results of the investigation.

Preparation.—All preparations were made by thoroughly grinding together weighed quantities of Ag_2S and HgI_2, and then heating the mixtures for 16 hours at 200° in sealed evacuated tubes. The reactions were comparatively rapid at this temperature, so that the 16-hour period was considerably more than sufficient to achieve complete reaction. Materials prepared were those containing molar percentages of Ag_2S at 10% intervals starting at 10%, as well as those with 2, 3, 4 and 5 mole % Ag_2S.

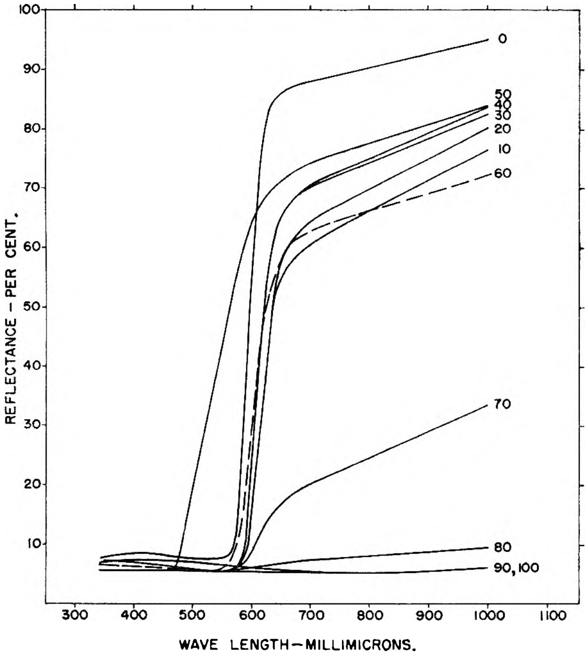

Fig. 1.—Diffuse reflectance spectra: numbers at right indicate mole % Ag_2S; 60% curve plotted as dotted line only to avoid confusion.

Color and Spectral Reflectance.—With the exception of the preparation containing 50 mole % Ag_2S, the colors of the products appeared to be close to averages of the colors of the black and red parent compounds. The 50% preparation, whose composition is Ag_2HgI_2S, is golden-yellow. The reflectance spectra of all the 10% interval preparations as well as of Ag_2S and HgI_2 were determined with a Beckman DU spectrophotometer, using the diffuse reflectance attachment. Sample surfaces of photosensitive materials were renewed when necessary. The results of measurements made over the range 3500–10,000 Å. are plotted in Fig. 1. It will be seen that addition of 10 mole % Ag_2S to HgI_2 shifts the reflectance edge to a higher wave length, and that this reflectance edge is fairly constant throughout the series except for the 50% product and those which are too black to reflect at all. The reflectance spectra of the 2–5 mole % preparations were not determined, but these products were also red.

Photosensitivity.—All the products which reflect in the visible have been found to darken very rapidly upon exposure to light. This includes the preparations with 2–5 mole % Ag_2S, which are very much more sensitive than HgI_2, though not as much so as other preparations containing 10% or more Ag_2S. The most sensitive are those containing 60 and 70 mole % Ag_2S, exposure to sunlight for less than one second being sufficient to blacken them. To get approximately equal darkening of the other preparations, an exposure period of about 3–5 seconds is required. Of the two most sensitive preparations, the 60% material yields the greater contrast since it is fairly bright red prior to exposure whereas the 70% product is quite dark red-purple.

The darkening brought about by light may be reversed very rapidly by heating at 200°. In addition, those preparations containing 30 mole % Ag_2S or less are phototropic at room temperature. Those containing 20% or less will revert after only about 8 hours of storage in the dark, while the 30% preparation requires about 30 hours for reversal.

In general, the products have been found to be sensitive to ultraviolet light as well as to visible light up to the respective reflectance edges. The limits of sensitivity were determined by exposing samples for ten-minute periods to monochromatic

TABLE I

RESULTS OF X-RAY INVESTIGATIONS

Mole % Ag_2S	Phases observed	Symmetry	Structure type	Lattice parameters, Å.
2	Red HgI_2	Tetragonal	......	Usual values
3, 4, 5	Red HgI_2	Tetragonal	......	Usual values
	+ Small amount of phase I	Face-centered cubic	Zinc blende with cationic vacancies	3%, a = 6.30 4%, a = 6.29 5%, a = 6.28
10, 20	Phase I	Face-centered cubic	Zinc blende with cationic vacancies	10%, a = 6.23 20%, a = 6.24
30, 40	Phase II	Hexagonal	Wurtzite with cationic vacancies	30%, c = 7.20, a = 4.44, c/a = 1.62. 40%, c = 7.30, a = 4.46, c/a = 1.64.
50	Phase III—complex pattern, not indexed. See Table II	......	......	......
60	Phase IV	Body-centered cubic	Probably related to α-Ag_2S and α-AgI	a = 4.95
	+ small amount of phase V	......	......	......
70	Phase V—complex pattern, not indexed. See Table III	......	......	......
80, 90	Phase V	......	......	......
	+ Monoclinic Ag_2S (small amount in 80%; larger amount in 90%)	......	......	Usual values

radiation emanating from a Beckman DU spectrophotometer at intervals of 25 mμ. The Beckman tungsten lamp in its housing (which includes a focusing mirror) was used as the source in the visible, and a 125-watt Hanovia mercury vapor lamp (Type 16200) as the source in the ultraviolet.

X-Ray Diffraction Investigations.—Since all the reaction products were powders, the X-ray diffraction work was of course carried out by the powder method. A North American Philips powder camera of 57.3 mm. radius and Cu Kα radiation were employed. None of the patterns displayed back reflections so that methods for precision determination of lattice constants could not be applied. However, the values were calculated as accurately as possible.

Various structures were observed to occur at different compositions. Some patterns could be indexed with Hull–Davey charts or by comparison with patterns of compounds with known structures, but others were more complex and could not be thus interpreted from the powder data. Table I summarizes the results of these X-ray investigations. The various phases observed, whether their patterns were indexed or not, are referred to in this table as phases I–V. Tables II and III are listings of the interplanar spacings of the preparations whose patterns could not be indexed.

X-Ray diffraction patterns of the darkened materials also were obtained. In each case, conversion of a sufficient quantity of sample was accomplished by long, gentle grinding in sunlight. New lines were observed in the preparations containing 10–40 and also 60 mole % Ag_2S. The additional lines in the 10 and 20% products are due to red HgI_2, but the light-induced phases in the others are all different and have not been identified.

Discussion.—The X-ray diffraction investigations indicate that the cubic and hexagonal phases formed in the system at 40 mole % Ag_2S or less are built up from a combined sulfide–iodide anion lattice with the cations in tetrahedral holes. Variations in the lattice constants of these phases with composition indicate solid solution formation. The unique color and X-ray pattern of the 50% preparation appear to establish it as a new compound, Ag_2HgI_2S. This compound is very similar in appearance and somewhat similar in photochemical behavior to the phototropic compound, $Hg_3S_2I_2$, and also may be prepared by solid state

TABLE II

X-RAY DIFFRACTION POWDER PATTERN OF Ag_2HgI_2S (PHASE III)

S, strong; M, medium strength; W, weak; V, very.

d, Å.	d, Å.	d, Å.	d, Å.
6.55 (M)	2.54 (M)	1.894 (VVW)	1.494 (VW)
4.81 (VW)	2.49 (M)	1.870 (M+)	1.471 (VVW)
3.93 (S)	2.46 (M−)	1.810 (VVW)	1.460 (VW)
3.73 (W)	2.42 (VVW)	1.779 (VVW)	1.442 (VVW)
3.56 (M)	2.31 (S−)	1.754 (VVW)	1.425 (VW)
3.44 (M)	2.24 (VW)	1.721 (M+)	1.412 (VVW)
3.29 (M+)	2.20 (VW)	1.688 (VW)	1.340 (VW)
3.14 (S−, broad)	2.10 (M)	1.647 (VVW)	1.302 (VVW)
2.98 (VVW−)	2.03 (M)	1.615 (VW, broad)	1.292 (VW)
2.82 (VVW−)	2.00 (VVW)	1.565 (VVW)	1.274 (VVW)
2.64 (VW)	1.967 (VW)	1.553 (VW)	1.243 (VVW)
2.58 (S−)	1.940 (VW)	1.514 (VW)	1.233 (VW)

TABLE III

X-RAY DIFFRACTION POWDER PATTERN OF PHASE V

S, strong; M, medium strength; W, weak; V, very.

d, Å.	d, Å.	d, Å.	d, Å.
7.10 (W)	2.59 (VVW)	1.906 (VVW)	1.553 (VVW)
3.90 (M)	2.43 (M−)	1.879 (VW)	1.522 (VVW)
3.37 (VVW)	2.38 (VW)	1.784 (VW)	1.472 (VW)
3.30 (W)	2.34 (W)	1.746 (VVW)	1.420 (VW)
3.10 (VW)	2.07 (VW)	1.688 (VW)	1.365 (VVW)
2.83 (S)	2.00 (VVW−)	1.666 (VVW)	1.293 (VVW)
2.62 (W)	1.955 (VVW−)	1.602 (VVW)	

reaction between silver iodide and mercuric sulfide in a 2:1 molar ratio. The primary phase in the 60 mole % preparation must be taken to be body-centered cubic, for a smaller primitive unit cell is ruled out by the presence of a plane with $h^2 + k^2 + l^2 = 7$. The proximity of the lattice constant of the phase with pattern thus indexed to those of the body-centered cubic phases, α-Ag_2S and α-AgI, suggests that the product has a structure similar to those found in these compounds.

The phototropic behavior at room temperature appears to be associated primarily with the modified zinc blende structure. The observed formation of HgI_2 upon exposure to light of products containing this face-centered cubic phase indicates that the ultimate effect of light is to decompose the phase. The darkening may be due either to Ag_2S itself or to metallic silver produced upon photoreduction of Ag^+ and simultaneous oxidation of equivalent amounts of sulfide or iodide.

ADSORPTION STUDIES ON METALS. III. THE SORPTION OF WATER VAPOR ON NICKEL, STEEL AND MOLYBDENUM

By A. C. Zettlemoyer and J. J. Chessick

Contribution from the Surface Chemistry Laboratory,
Lehigh University, Bethlehem, Penna.

Received September 11, 1953

A study of the oxide films present on the surface of nickel, steel and molybdenum was made using both gas adsorption and calorimetric techniques. Nickel and steel powders degassed at 25° were found to exhibit only physical adsorption of water vapor, and the heat of emersion in water was about 550 ergs/cm.^{2} for both. Water diffused through the polymolecular film present on molybdenum degassed at 25°; the heat of emersion was 9,500 ergs/cm.^{2}. Degassing the nickel powder at 300° removed a strongly bound layer of water and raised the heat of emersion to 950 ergs/cm.^{2}. After activation of steel at 400°, the equivalent of 10–13 layers of water could be adsorbed indicating the presence of a polymolecular hydrous oxide film. Activation of molybdenum at 400° caused a surprising decrease in the amount of water sorbed per unit area, due probably to the transformation of the porous oxide film to a chemically different, non-porous oxide. Extraction of molybdenum powder with ethyl alcohol removed most of the polymolecular film of oxide from the surface; a hydrous oxide layer, apparently monomolecular, remained.

Introduction

The importance of oxide films on metals in such fields as corrosion, lubrication and adhesion has long been recognized. For this reason, a detailed knowledge of the physical and chemical properties of such films is important. To this end, the techniques of adsorption and calorimetric measurements were utilized to provide information concerning the hydrous nature, molecular thickness, porosity and stability of oxide films on a variety of metals.

Experimental

Materials.—The molybdenum powder[1] was prepared by the Westinghouse Electric Company, Bloomfield, New Jersey, by high temperature reduction of the oxide. The purity of the freshly prepared sample was reported to be greater than 99.9%. The nickel powder was prepared by the International Nickel Company, Inc., New York, by high temperature reduction of the carbonyl and was of very high purity. The SAE 1020 steel powders were furnished by the Exomet Corp., Conneaut, Ohio. The steel had been atomized at a maximum temperature of 1620° and annealed at a temperature of about 1000° under hydrogen cover with a small amount of propane present to prevent carbonization. Since the droplets formed during atomization were molten the resultant particles had a relatively smooth surface and the metal in this form should possess properties characteristic of some practical steel surfaces. The steel had the following per cent. composition: C, 0.25; Si, 0.15; Mn, 0.34; S, 0.007; and P, 0.012.

High purity tank argon and helium were used in the adsorption measurements. The argon was further purified by passage through fine copper gauze heated to 500° and dried with anhydrous calcium sulfate. The helium used in dead space determinations was purified by passing it slowly through a charcoal trap immersed in liquid nitrogen. Distilled water was evacuated for long periods of time before use to remove dissolved gases.

Pretreatment of Surfaces.—Adsorption and heat of wetting measurements were determined on all the unreduced samples. These powders had been subjected to no treatment after manufacture except storage under normal atmospheric conditions long enough for an oxide film to have developed on their surfaces. Before use these samples were degreased with benzene and degassed under high vacuum either at 25° for 24.0 hours or at 400° for 3.0 hours.

Since the molybdenum metal was known[2] to possess a polymolecular surface film of the complex oxide molybdenum blue, $MoO_2 \cdot 4MoO_3 \cdot xH_2O$, additional samples of this metal were further pretreated by extracting with ethyl alcohol in a Soxhlet apparatus. The oxide is soluble in alcohol and the treatment was continued until no further blue coloration was imparted to the liquid. The molybdenum powder was then transferred to a suitable bulb while still wet and evacuated at 400° to remove adsorbed alcohol. This treatment removes most of the oxide film from the metal—probably all except the monomolecular film in contact with surface metal atoms. Molybdenum samples treated in this manner were used in the adsorption and heat of wetting measurements in addition to molybdenum which had only been degreased with benzene.

The difficulties generally encountered in the preparation of metal powders with large surface areas are well known. Therefore, it is interesting to note that alternate soxhleting of molybdenum powder with alcohol and reoxidation with moist oxygen can be utilized as a method for the preparation of high area samples of molybdenum.

Apparatus and Procedure.—The adsorption measurements were determined in an apparatus described by Orr.[3] However, in this work absolute pressures were measured rather than differential pressures. An oil manometer allowed adsorption pressures in the range 0.10 to 50.0 mm. of mercury to be measured. Apiezon "B" was used in the manometer. This oil has a very low vapor pressure and did not dissolve any of the gases used. Blank determinations showed that the volume of water vapor adsorbed on the walls of the glass sample system at 25° was negligible in comparison to that volume absorbed by the sample in the relative pressure region from zero to 0.4.

---

[1] All samples were furnished by Dr. Norman Hackerman of the University of Texas.

[2] F. H. Healey, J. J. Chessick and A. C. Zettlemoyer, This Journal, **57**, 178 (1953).

[3] W. J. C. Orr, *Proc. Roy. Soc.* (*London*), **173A**, 349 (1939).

Argon was adsorbed on the samples at −195°; water vapor at 20°. Specific areas of the samples were calculated using the usual BET method.

The calorimeter used in the heats of wetting measurements has been fully described.[4] A thermistor was used to measure temperature changes.

Results and Discussion

The results of the adsorption and heat of wetting measurements on the unreduced metal powders are summarized in Table I. The specific surface areas in column four were obtained from argon adsorption data. To illustrate the differences in the water vapor sorption by the various powders activated at different temperatures the V_m values which generally represent the STP volumes of gas required to cover the surface of one gram of powder with one layer, were obtained from water adsorption data by the BET method.[5] These calculated V_m values, however, may include not only this monomolecular volume of gas, but also water sorbed into the porous oxide layer, and/or water irreversibly sorbed on the surface, *i.e.*, water which cannot be removed by evacuation at 20°, the temperature of the adsorption run. These V_m values were arbitrarily converted for the purpose of comparison into an amount equivalent to the number of layers of water molecules which could be accommodated on the external surface of the powders as measured by the argon adsorption data.[6] A typical set of isotherms for the adsorption of argon and water vapor on an unreduced metal powder is shown in Fig. 1.

TABLE I

THE ADSORPTION AND HEAT OF EMERSION OF WATER ON UNREDUCED METAL POWDERS

Powder	Activation		Surface area, m.^{2}/g.	Calcd. no. of water layers	Heat of emersion, ergs/cm.^{2}
	Time, hr.	Temp., °C.			
Nickel	24.0	25	0.68	1.1	590
	3.0	300	0.74	1.9	953
Steel	24.0	25	0.16	0.9	500
	3.0	400	0.08	10 to 13	
Molybdenum	24.0	25	0.55	7.9	9,510
	3.0	400	0.91	0.9	
Molybdenum[a]	24.0	25	0.38	5.1	4,750
(sintered)	3.0	400	0.69	1.0	
Samples Soxhleted with Alcohol					
Molybdenum	3.0	400	0.97	4.4	5,502
Molybdenum[a]	3.0	400	0.49	4.1	5,050

[a] Sintered samples had been reduced repeatedly at elevated temperatures. They were then stored for long periods of time (in the presence of air) before use at 25°.

The area occupied by a single adsorbate molecule was calculated on the basis of hexagonal close packing. The cross-sectional areas used were 13.9 and 10.8 Å^2 for argon and water, respectively.

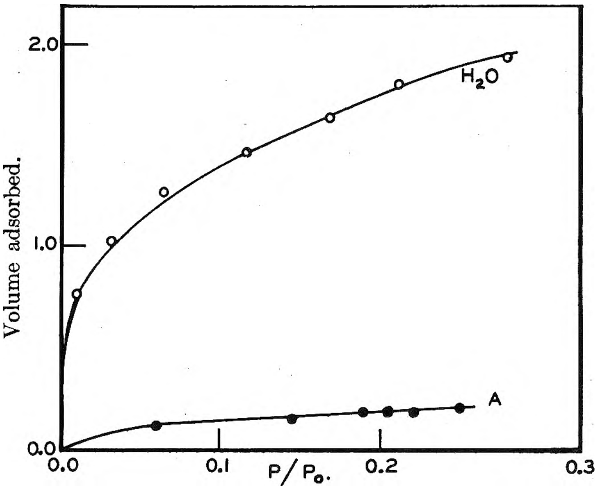

Fig. 1.—Adsorption of water and argon on molybdenum.

Studies on Metal Powders Activated at Room Temperature.—It is evident from Table I that the adsorption of water vapor by nickel and steel powders degassed at 25° differs markedly from that by molybdenum studied under similar conditions. Good agreement was found between areas calculated from both argon and water vapor adsorption data for the first two powders; water vapor was only physically adsorbed on their external surfaces. On the other hand the original molybdenum sorbed about eight times more water than could be accounted for on the basis of external area alone. Diffusion of water molecules through the polymolecular, porous-oxide film of molybdenum blue present on the surface of the powder accounts for the high sorption of water. Evidently this water of hydration forms a weak enough bond with oxide molecules so that it can be readily removed by evacuation at room temperature.

The heat of emersion of nickel degassed at 25° was determined to be 590 ergs/cm.^{2}; this is a reasonable value for the wetting of a non-porous oxide which physically adsorbs water on its surface.[7] The heat of emersion value determined for steel degassed at 25°, about 500 ergs/cm.^{2}, was the same order of magnitude as that for nickel.[8] For the original sample of molybdenum, however, the heat value was found to be 9,510 ergs/cm.^{2}, or about 1,200 ergs/cm.^{2} per water layer. This high value suggests that water diffuses into the surface oxide layer on molybdenum and forms a hydrogen bond with an oxide molecule.

The amount of complex oxide removed from the surface of molybdenum powder by extraction with alcohol amounted to 1.03% of the total weight of powder. If it is assumed that one layer of water is physically adsorbed on the surface of the oxide, and further that the stoichiometric formula of the oxide is given by $MoO_2 \cdot 4MoO_3 \cdot 4H_2O$, then the ratio of the moles of water of hydration per mole oxide amounts to 4.2. The average heat of hydration has been calculated to be 19,800 calories per mole of water.

Metal Powders Activated at 400°.—After activation at 400°, the calculated number of water layers

---

[4] A. C. Zettlemoyer, G. J. Young, J. J. Chessick and F. H. Healey, THIS JOURNAL, **57**, 649 (1953).

[5] S. Brunauer, P. H. Emmett and E. Teller, *J. Am. Chem. Soc.*, **60**, 309 (1938).

[6] The V'_m values for both argon and water vapor were converted into specific areas by use of the proper factors. The equivalent number of water layers was then obtained by dividing the water surface area by the argon surface area.

[7] W. D. Harkins, "The Physical Chemistry of Surface Films," Reinhold Publ. Corp., New York, N. Y., 1952, p. 264.

[8] Unfortunately, the surface area of steel powder activated at room temperature was too small to allow the accurate determination of heat of emersion values with the present calorimeter.

sorbed on a nickel surface was found to be approximately two, an amount almost double that for a sample of nickel activated at 25°. The heat of emersion increased from 590 to 953 ergs/cm.². These results support the statement of Tingle[9] that the surface of nickel is covered with a tough, compact film of oxide impervious to water. This film, however, adsorbs a monomolecular film of water strongly enough so that it resists removal by room temperature evacuation at 10^{-5} mm.

The steel samples activated at 400° sorbed large quantities of water vapor, an amount equivalent to 10–12 surface layers of water. Evidently, these powders also have a polymolecular, hydrous oxide on their surface. However, unlike molybdenum, the water sorbed into the interior of the oxide layer is bound strongly enough to the metal oxide sites to resist removal by evacuation at low temperatures.

Because of the polymolecular, hydrous oxide film on the surface of molybdenum, it was presumed that high temperature activation of these powders would lead to an increased sorption of water vapor. Surprisingly, the uptake of water was found to decrease with increasing activation temperature. It is evident from an inspection of Table II that the specific area of the powder, as calculated from argon adsorption data, about doubled as the activation temperature increased from 25 to 400°, whereas the calculated number of water layers decreased eightfold. Further, good agreement was found between areas calculated from both argon and water adsorption data after the 400° activation. Apparently water was only physically adsorbed on the exposed surface of the molybdenum. There is no doubt that high temperature activation of molybdenum causes profound changes in the oxide structure present on its surface. Transformation of the complex oxide "molybdenum blue" initially present into a more dense, non-porous but rougher oxide layer would account for the increase in specific area as well as the decrease in water uptake.

TABLE II

EFFECT OF ACTIVATION TEMPERATURE ON THE SORPTION OF WATER VAPOR BY MOLYBDENUM POWDER (ORIGINAL SAMPLE)

Argon area, mg.²/g.	Water area, m.²/g.	Calcd. no. water layers	Activation Time, hr.	Activation Temp., °C.
0.55	4.35	7.9	24	25
.68	1.33	2.0	1.0	350
.91	0.87	0.9	3.0	400

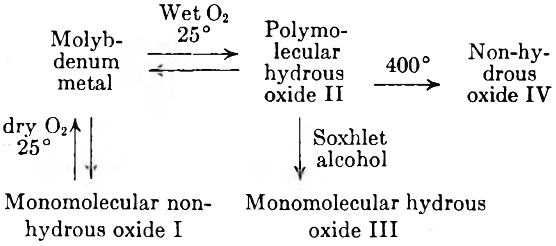

Fig. 2.—Oxide films on molybdenum.

To check the belief that the surface oxide was changed chemically by activation at elevated temperature, a pure sample of the complex oxide "molybdenum blue," which had been dissolved from a large sample of molybdenum powder by soxhleting with ethyl alcohol, was heated to 350°. The blue oxide changed to a more dense, grayish mass which no longer dissolved in water or alcohol. The composition of the new oxide was not determined.

The results for the adsorption of water on two samples of molybdenum, which were soxhleted with alcohol before use, are tabulated in the last two rows of Table I. Though the samples differed appreciably in area, both sorbed the equivalent of four layers of water with an average heat of wetting of 1,300 ergs/cm.² per layer of water. These values seem high since, presumably, the bulk of the surface oxide film was removed. The weight loss of a sample of the larger area material after soxhleting to remove the oxide layer was determined to be 1.03% of the total weight of powder used. The calculated weight loss due to the removal of oxygen and water from this oxide film by reduction was calculated to be 0.64% assuming the oxide formula to be $MoO_2 \cdot 4MoO_3 \cdot 4H_2O$. The weight loss found experimentally after reduction of a second sample of this material amounted to 0.62%. This direct evidence supports the contention that most of the oxide film was removed by soxhleting. However, the reduced sample only physically adsorbed water on its surface, whereas the soxhleted powder sorbed the equivalent of four layers of water, and so strongly that it could only be removed by high temperature activation. It appears, then, that all the surface oxide on molybdenum is removed by treatment with alcohol with the exception of a thin, perhaps monomolecular, hydrous oxide film. The average heat of hydration per mole of water sorbed on this film was found to be 24,900 calories.

Oxide Films on Molybdenum.—The data concerning oxide films on molybdenum reported here and in previous publications[2,10] are shown diagrammatically in Fig. 2.

The oxidation of molybdenum metal with dry oxygen at 25° produces a non-hydrous, monomolecular oxide film I with the probable formula MoO_2.[10]

The oxidation of molybdenum metal with moist oxygen at 25° yields a polymolecular, hydrous oxide film II of molybdenum blue $MoO_2 \cdot 4MoO_3 \cdot 4H_2O$. This film forms naturally on molybdenum powders stored at room temperatures in the presence of moist air.

Extraction with alcohol of molybdenum containing a surface film of "molybdenum blue" removes all the oxide except the hydrous layer adjacent to surface molybdenum atoms.

A "molybdenum blue" film is transformed into a non-porous, chemically different oxide by high temperature activation. The composition of this oxide is not as yet known.

---

(9) E. T. Tingle, *Trans. Faraday Soc.*. **46**, 43 (1950).

(10) A. C. Zettlemoyer, J. J. Chessick and F. H. Healey, "Heterogeneity of Surfaces, Adsorption of Gases on Metals," Technical Report No. 4, Office of Naval Research, June 1952. On file at the Library of Congress, Washington, D. C.

Acknowledgment.—This work was carried out under contract N8onr-74300 with the Office of Naval Research whose support is gratefully acknowledged. The authors wish to thank Miss Yung-fang Yu for assistance in obtaining some of the adsorption data.

HARTREE–FOCK–SLATER SELF-CONSISTENT FIELD AND THE CALCULATION OF SOME PROPERTIES OF THE Cu^+ ION[1]

BY J. C. MORROW

Contribution from the Department of Chemistry, University of North Carolina, Chapel Hill, N. C.

Received September 18, 1953

Recent modification of the Hartree–Fock self-consistent field method by J. C. Slater has simplified the problem of obtaining approximate wave functions corrected for exchange effects. The utility of Slater's approximation is demonstrated by calculation of diamagnetic susceptibility, polarizability and refractivity, Lamb diamagnetic shielding at the nucleus, and structure factors for X-ray and fast electron scattering. The calculations are carried out for the Cu^+ ion, for which Hartree–Fock, Hartree, and Hartree–Fock–Slater wave functions are available. The results show that the Slater modification is an excellent approximation to the Hartree–Fock method in the calculation of atomic properties; this conclusion is of special moment in investigations of heavy systems for which the Slater method offers great reduction in labor of obtaining wave functions.

Introduction.—Slater recently has developed[2] a modification of the Hartree–Fock self-consistent field method, the importance of which lies in the fact that it is a good approximation and that numerical solution is much easier than in either the Hartree–Fock or Hartree method. Slater's free electron approximation for the exchange potential, with the assumption of spherical symmetry for the distribution of charge in an atom or ion, results in the following radial Schrödinger equation

$$\mathrm{d}^2P_{\mathrm{nl}}/\mathrm{d}r^2 + [E_{\mathrm{nl}} + 2Z_{\mathrm{p}}/r - l(l+1)/r^2 + 6r^{-1}(3\pi^2/32r)^{1/3}(\mathrm{d}^2Z_{\mathrm{p}}/\mathrm{d}r^2)^{1/3}]P_{\mathrm{nl}} = 0$$

This equation has recently been solved[3] numerically by Pratt, the atomic system chosen being the Cu^+ ion.

The direct result of such calculations is a comparison of the Hartree, Hartree–Fock, and Hartree–Fock–Slater wave functions and energy parameters. Comparison of other properties of the Cu^+ ion is very important in that it shows the error to be expected when one uses a scheme simpler than the Hartree–Fock method. Such knowledge is important because the coupling of accuracy and simplicity which characterizes the Slater procedure makes it a most likely tool to be used in obtaining the much needed exchange corrected self-consistent field wave functions of heavy atoms and ions.

Diamagnetic Susceptibility and Polarizability.—By far the largest part of the difference between the Hartree–Fock and Slater wave functions arises from the improper behavior of the free-electron exchange potential energy approximation at large r. In the evaluation of average quantities by means of the expression

$$\bar{Q} = \int \psi^*Q\psi\mathrm{d}\tau / \int \psi^*\mathrm{d}\tau$$

the relative magnitudes of $\psi^*Q\psi$ at large and at small values of r will control the error. An interesting property to use for testing the Slater functions is the diamagnetic susceptibility, since dependence on r is such that the effects at large r are considerably magnified.

It is well known that the diamagnetic susceptibility per gram atomic weight is related to electron position through the expression[4]

$$\chi_{\mathrm{A}} = -(Ne^2/6mc^2)\sum_i \overline{r_i^2}$$

where N is Avogadro's number, e is the electronic charge, m is the electronic mass, c is the velocity of light and r_i is the electron–nucleus separation for the ith electron. The average of r_i^2 is summed over all electrons in the system. Using Hartree atomic units for r and expressing the above average in terms of the radial wave functions of the atom, one has

$$\chi_{\mathrm{A}} = -0.7923(10^{-6})\int_0^\infty \sum_i P_i^2r^2\mathrm{d}r \bigg/ \int_0^\infty \sum_i P_i^2\mathrm{d}r$$

For the Cu^+ ion, the susceptibility is

$$\chi_{\mathrm{A}} = -0.7923(10^{-6})\int_0^\infty \sum_{nl} 2(2l+1)P_{nl}^2r^2\mathrm{d}r \quad (1)$$

if the functions $P_{\mathrm{nl}}(r)$ are the normalized radial wave functions. The factor r^2 increases the relative importance of terms at large r. Since the various electron groups have different extensions, it is of interest to compare their individual contributions to the susceptibility. The terms in the integrand of equation 1 have been computed from the Hartree[5] and Hartree–Fock–Slater[3] wave functions by numerical integration. They are compared in Table I with the values obtained by Hartree and Hartree from the Hartree–Fock solutions[6] of the one-electron wave equations for Cu^+.

The close agreement of the Hartree–Fock and Hartree–Fock–Slater results is clearly shown in Table I and in Table II which compares properties calculated from the wave functions.

Error introduced by the free electron exchange term is seen to be small compared with the improvement gained by including exchange effects. The

---

(1) Presented before the 124th Meeting of the American Chemical Society, Chicago, Illinois, September, 1953.

(2) J. C. Slater, *Phys. Rev.*, **81**, 385 (1951).

(3) G. W. Pratt, Jr., *ibid.*, **88**, 1217 (1952).

(4) J. H. Van Vleck, *ibid.*, **31**, 599 (1928).

(5) D. Hartree, *Proc. Roy. Soc.* (*London*), **A141**, 282 (1933).

(6) D. Hartree and W. Hartree, *ibid.*, **A157**, 490 (1936).

Table I

Values of $2(2l + 1)r^2$ in Atomic Units

Group	Hartree	Hartree–Fock	Slater
1s	0.01	0.01	0.01
2s	.14	.13	.13
2p	.32	.32	.32
3s	1.25	1.21	1.23
3p	4.23	4.07	3.93
3d	17.55	12.85	10.96

Table II

Properties Obtained from Different Sets of Wave Functions

Property	Hartree	Hartree–Fock	Slater
$\sum_i \overline{r_i^2}$	23.47	18.58	16.58
$-\chi_A(10^{+6})$	18.59	14.72	13.14
$-\alpha$, Å.^{3}	1.296	0.8119	0.6468
$-(4/3)\pi N\alpha$, cm.^{3}	3.268	2.048	1.632
$-3mc^2H'(0)/eH$	133.5[a]	135.1[a]	136.5

[a] W. C. Dickinson, *Phys. Rev.*, 80, 563 (1950).

largest part of the error comes from the ten 3d electrons, the extension of which is greater than that of any other group. Pratt has shown[3] that, even though this extension is relatively large, 92% of the time the value of r for these 3d electrons lies between zero and 1.68 atomic units. In spite of this fact, the extension of electrons past $r = 1.68$ makes a very important contribution to the diamagnetic susceptibility by virtue of the r^2 factor and the large number of 3d electrons. In order to show these effects, the definite integrals $\int_{1.6}^{\infty} 2(2l + 1)P_{nl}^2r^2\, dr$ must be evaluated. Calculations for $n = 3$ have been carried out; the values of P_{1l}^2 and P_{2l}^2 are so small for r greater than 1.68 that the corresponding integrals are almost zero. Table III shows the values obtained from the three schemes; in the last row, the per cent. contribution to the susceptibility of extension greater than $r = 1.6$ is presented. These considerations and results emphasize the fact that comparison of the Slater field and the Hartree–Fock field on the basis of corresponding diamagnetic susceptibilities is a stringent test of the exchange approximation. Gratifying agreement indicates the success of the Slater method.

Table III

Values of the Definite Integral

$$\int_{1.6}^{\infty} 2(2l + 1)P_{3l}^2r^2\, dr$$

l	Hartree	Hartree–Fock	Slater
s	0.05704	0.04799	0.04983
p	0.4004	0.3425	0.2861
d	10.89	6.053	4.408
% contr.	48.30	34.68	28.61

In addition to the diamagnetic susceptibility one can obtain from the quantity $\sum_i \overline{r_i^2}$ the values of the polarizability and ionic refractivity. Kirkwood has found[7] that the polarizability of a spherical atom or ion is given approximately by $\alpha = -(4a_0^3/9n_e)\left(\sum_i \overline{r_i^2}\right)^2$ where a_0 is the first Bohr radius and n_e is the number of electrons in the system. The radial distance is to be expressed in terms of atomic units, so that α has the units of a_0^3. The ionic refractivity is $(4\pi/3)N\alpha$ where N is Avogadro's number. The values of these properties appear in Table II for each of the three sets of wave functions. Squaring the sum which appears in the polarizability expression accentuates in α differences which come from differences in the sets of wave functions, but the Slater approximation still gives a satisfactory result.

Internal Diamagnetic Field.—In the determination of nuclear magnetic moments by the resonance method, correction for the shielding field at the nucleus is important. The magnitude of this diamagnetic field set up by moving electrons in the atom has been found by Lamb[8] to be $(eH/3mc^2)v(0)$ at the nucleus; e and m are charge and mass of the electron, c is the velocity of light, H is the external magnetic field with which the electrons interact, and $v(0)$ is given by

$$\int_0^{\infty} [\rho(r)/r]\mathrm{d}r$$

(0), which represents the electrostatic effects at the nucleus, is evaluated from the self-consistent field, since the radial wave functions and the density are simply related. The expression

$$\int_0^{\infty}\sum_{nl} 2(2l + 1)P_{nl}^2r^{-1}\mathrm{d}r$$

has been evaluated for Cu$^+$ by numerical integration with the Hartree–Fock–Slater wave functions. Multiplication of this integral by $eH/3mc^2$ gives $H'(0)$, the magnitude of the internal diamagnetic field at $r = 0$. For comparison, values of $-3mc^2H'(0)/eH$ obtained from the three sets of wave functions appear in Table II. The close agreement of Hartree–Fock and Slater results is again in evidence.

Scattering Factors.—Of the atomic properties which can be obtained from self-consistent field wave functions, one of the most important is the scattering power for X-rays. The coherent and incoherent scattering depend on the wave functions through the same fundamental quadratures but in different combinations. As showed by James and Brindley,[9] the contribution of ith electron to the X-ray scattering is connected with the quantity f_i given by

$$\int_0^{\infty} P_i^2(r)(\sin kr/kr)\, \mathrm{d}r$$

where P_i is the radial wave function for the electron and $k \equiv (4\pi/\lambda)\sin(\varphi/2)$. The atomic structure factor, F, is given by $\sum_i f_i$ for coherent scattering. The scattering power depends on F^2. In contrast, the incoherent scattering depends on $Z - \sum_i f_i^2$, that is, on the square of the individual f_i rather than on the square of their sum. In order to examine the applicability of the Slater functions in the calculation of structure factors, the f_i for the electrons in

---

(7) J. G. Kirkwood, *Physik. Z.*, **33**, 57 (1932).

(8) W. E. Lamb, Jr., *Phys. Rev.*, **60**, 817 (1941).

(9) R. W. James and G. W. Brindley, *Phil. Mag.*, **12**, 81 (1931).

TABLE IV

STRUCTURE FACTORS FOR Cu^+

$\lambda^{-1} \sin(\varphi/2)$	0	0.05	0.10	0.15	0.20	0.25	0.30	0.35	0.40
F (Hartree)[a]	28.00	26.58	23.35	19.80	16.49	13.80	11.75	10.20	9.02
F (H.-Fock)[a]	28.00	26.84	23.95	20.48	17.16	14.40	12.12	10.35	9.08
F (Slater)	28.00	26.89	24.31	20.98	17.69	14.67	12.45	10.42	9.08

[a] G. W. Brindley and P. Ridley, *Proc. Phys. Soc.* (*London*), **50**, 96 (1938).

Cu^+ have been calculated for values of $k/4\pi$ between 0 and 0.40 atomic unit in steps of 0.05. Table IV contains the atomic structure factors obtained from the three sets of wave functions.

For calculation of the atomic structure factors, the individual f_i were evaluated for each k by numerical integration and were summed. The nature of the function $\sin kr/kr$ made it desirable to obtain the quantity

$$\int_0^\infty P_i^2(1 - \sin kr/kr)\,dr$$

Since the radial wave functions are normalized, it is an easy matter to obtain the f_i once the above definite integrals are calculated. This procedure decreases the truncation error except for the case of 3d electrons at relatively large values of k.

Explicit calculation of each f_i followed by summation appears to be more accurate in practice than commuting the integration and sum operations, which is clearly equivalent in principle. Use of the total charge density functions and a single quadrature means that the integrands are large and that the corresponding truncation errors may be troublesome. The calculation of individual f_i is, of course, necessary for evaluation of the incoherent scattering function.

For scattering of fast electrons, differential elastic cross sections can be obtained[10] in terms of the atomic scattering factors by means of the Born approximation. The cross section depends on the quantity $(Z - F)^2$, which is easily obtained from the tabulated values of F.

Conclusion.—Examination of the preceding sections shows the excellence of the Slater wave equation solution for calculation of atomic properties. Its value for treatment of heavy systems has already been stressed. Interesting in this connection is the fact that the Thomas–Fermi field cannot always be relied upon even for heavy systems, for which it is known to be better than for light ones; straightforward use of the Thomas–Fermi field for calculation of $\sum_i f_i^2$ is not satisfactory. The utility and applicability of the Slater method thus recommends it as an important tool in the solution of problems in atomic and molecular structure.

(10) N. F. Mott and H. S. W. Massey, "The Theory of Atomic Collisions," Oxford University Press, London, 1933, p. 123.

THE INHIBITION OF FOAMING. VI. THE TRANSMISSION OF LIGHT BY UNSTABLE FOAMS[1]

By SYDNEY ROSS, BRUCE BARTH AND J. F. TERENZI

Department of Chemistry, Rensselaer Polytechnic Institute, Troy, N. Y.

Received September 23, 1953

The ratio of the incident to the emergent light (loss factor) passed through a foam is directly proportional to the specific surface between the phases, according to Clark and Blackman. This relation is used to obtain a measurement of the stability of the surface films for foams containing different compositions of two antifoaming agents. The results parallel those obtained by measuring the foam stability, L_f, from observations of the decrease in total volume of the foam. The increase of permeability of the liquid films to the passage of air is shown to be a concomitant effect with the decrease of cohesion and elasticity of the films, effected by the antifoaming agent. This work provides a simple method, using the Lumetron colorimeter, for the rapid evaluation of the effectiveness of different antifoams, their optimum concentrations, and the investigation of synergistic antifoaming mixtures.

It is a common observation that a coarse foam is less opaque than one composed of fine bubbles, which would provide greater opportunities for the scattering of incident light by multiple reflections and refractions. The opacity of a foam is also commonly observed to diminish as the foam ages, because of the increase in bubble size with time. This phenomenon can, under controlled conditions, be used to measure the relative stability of foams.

The loss of light on transmission through a layer of foam was first explored by Clark and Blackman[2] as a function of the degree of dispersion of air in the foam. The loss of light was defined as the "loss factor," the ratio of the incident to the emergent light, or I_0/I. These authors found experimentally that the loss factor varied linearly with the specific surface of the liquid/air interface. Consideration of a simplified theoretical model led them to a mathematical description that was in accord with the experimental observations. The present contribution uses this relation to measure the variation

---

(1) Presented before the Division of Colloid Chemistry of the American Chemical Society at the McBain Memorial Program, Chicago, Ill., Sept. 6–11, 1953. See Abstracts, p. 14-I.

(2) N. O. Clark and M. Blackman, *Trans. Faraday Soc.* **44**, 7 (1948).

of the specific surface as a foam ages, which is a significant process for the ultimate stability of the system. A convenient and rapid method for the evaluation of both foam-stabilizing and foam-inhibiting agents is a practical outcome of such a study.

Materials and Methods.—The solutions examined are similar to those described in the previous paper of this series,[3] where the trade-names, chemical descriptions and sources are already listed. A foaming solution containing 0.10% Aerosol OT was tested in the presence of mixtures of Ucon 50-HB-660 and 2-ethylhexanol. This differs slightly from the previous experiments by the substitution of a lower viscosity Ucon for the Ucon 50-HB-3520. A second foaming solution contained 0.50% Nacconol NRSF and was defoamed by mixtures of tributyl phosphate and methylisobutylcarbinol. This differs from the previous solution by the absence of 0.75% sodium silicate.

The transmission of light was measured with a Lumetron colorimeter (Model 402-E), manufactured by the Photovolt Corporation. The instrument was mounted on its side, with the collimated light beam vertical and the measuring photocell at the base, on an adjustable platform equipped with a spirit-level. In this way it is possible to introduce the foam-cell so that it sits directly above the measuring photocell. It was found to be greatly more convenient with these relatively unstable foams to operate the instrument as a direct-reading colorimeter. This is done by blocking out the light to the balance cell and taking direct readings on the galvanometer scale rather than using the slide-wire. The output of the lamp is stabilized with a constant voltage transformer.

With some mixtures the addition of the agent caused turbidity and it is necessary to correct for the absorbence of the liquid. The light intensity of the lamp is adjusted with a rheostat to give a full-scale deflection of the galvanometer when the foam-cell containing the appropriate volume of liquid is in place. Since the galvanometer has a linear response to the photocell, the ratio of the full-scale deflection (100) to the reading with the foam in position gives the loss factor directly.

The cell containing the foam must be air tight, so that the foam completely fills the volume of the container throughout the readings. A convenient container can be made by pouring the foam into a small cylinder and capping it with a second cylinder of slightly larger diameter and smaller length. On inverting the whole container, the liquid drained from the foam fills the space between the two cylinders, making the upper cylinder completely air tight.

The foam is produced from 100 ml. of foaming solution plus a measured volume of the antifoaming additive by the action of a Hamilton-Beach mixer for one minute. The timing begins when the mixer is turned off. The transfer of the foam to the foam-cell and the setting-up of the apparatus prevent any earlier reading than about one or two minutes after the foam is formed. Although unavoidable this is unfortunate as the rate of change of the loss factor is greatest during the early stages of the existence of the foam.

Results.—The 0.10% solution of Aerosol OT was tested with a series of mixtures of Ucon 50-HB-660 and 2-ethylhexanol in different proportions. The total concentration of each combination of the two agents was 0.50% by volume. The 0.50% solution of Nacconol NRSF was tested with a series of mixtures of tributyl phosphate and methylisobutylcarbinol in different proportions, at a total concentration of 0.10% by volume. The previous experiments had been performed with much higher concentrations of antifoam, namely, 2.0% for the first system and 0.50% for the second. It was found that such high concentrations made the foam too unstable for the present type of measurement, as was made evident by a rupture of the films and a diminution of the volume of the foam. The effect sought is the influence of the antifoams on the permeability of the films to the enclosed gas, as shown by the increase in bubble size with time, due to the decrease in size of the small bubbles. It is the higher gas pressure in the smaller bubbles that causes a more rapid diffusion of air from them through the bubble walls, and it is the rate of this diffusion, related to the permeability of the liquid film, that is investigated by this method. Any concomitant rupture of the films complicates the observations by increasing the light transmission for a second cause. It is reduced as much as possible by reducing the total concentration of antifoam.

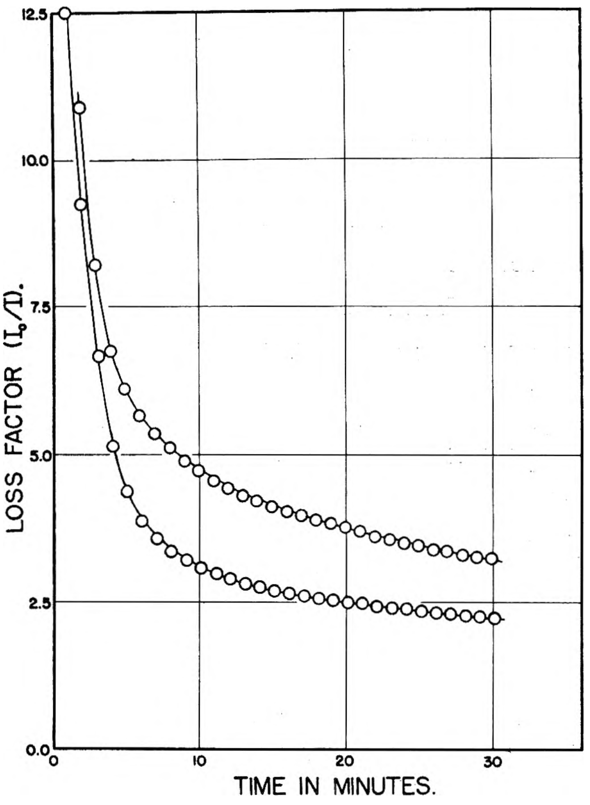

Fig. 1.—The variation with time of the loss factor, I_0/I, for foams produced from 0.10% Aerosol OT plus 0.50% by volume of synergistic antifoams: upper curve, antifoam 80% 2-ethylhexanol, 20% Ucon 50-HB-660; lower curve, antifoam 90% 2-ethylhexanol, 10% Ucon 50-HB-660.

Figure 1 illustrated the form of the loss-factor *vs.* time curves, for two antifoams differing only slightly in composition. The one that shows the more rapid reduction of the loss-factor represents the more effective antifoaming action. Since, for a non-absorbent solution, there is a proportionality between specific surface and (loss factor − 1)

$$S = k(I_0/I - 1) \qquad (1)$$

these curves represent the variation of the specific surface of the foam with time. Clark[4] has made direct measurements by photomicrography of the specific surface of stable foams as a function of time,

---

[3] S. Ross, A. F. Hughes, M. L. Kennedy and A. R. Mardoian, THIS JOURNAL, **57**, 684 (1953).

[4] N. O. Clark, "A Study of Mechanically Produced Foam for Combating Petrol Fires," D. S. I. R., Chemistry Research, Special Report No. 6, H. M. S. O., London, 1947, p. 106; N. O. Clark and M. Blackman, *Trans. Faraday Soc.*, **44**, 1 (1948).

and found that his results could be described by the equation

$$S = S_0 e^{-\alpha t} \quad (2)$$

where

S = specific surface at time t
S_0 = specific surface at time of preparation
α = a constant

The unstable foams of the present study are not described by this equation nor could a simple mathematical function be obtained for their description.

It is nevertheless desirable to characterize each of these curves by a number that gives a relative measurement of the stability of the interface. The most fundamental unit is the average time of existence of unit area of interface between two arbitrary limits that span most of the time during which measurements are taken. It is defined by the equation

$$t_{\text{av}} = \frac{1}{f(t_2) - f(t_1)} \int_{t_1}^{t_2} f(t)\, \mathrm{d}t \quad (3)$$

This unit can be evaluated by plotting $(I_0/I - 1)$ *vs.* t and integrating graphically[5] between arbitrary limits. Equally useful as a relative measure of stability, and more readily obtained, is the time elapsed between two arbitrary values of the specific surface, as measured by the function $(I_0/I - 1)$. Figure 2 shows values obtained in this way for Δt between values of $I_0/I = 10.0$ and 3.00, that is the time lapsed from 10% transmission of light by the foam until it reaches 33.3% transmission of light. Figure 3, for consistently less stable foams, has values of Δt between $I_0/I = 10.0$ and 2.00.

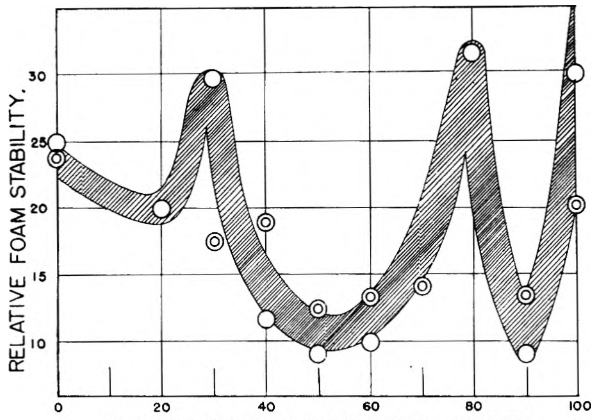

Fig. 2.—Comparison of relative foam stabilities, $0.028L_f$, ◎, and film stabilities, Δt from $I_0/I = 10.0$ to $I_0/I = 3.00$, ○, for various mixtures of 2-ethylhexanol and Ucon 50-HB-660 on a foam produced from 0.10% Aerosol OT solution.

In both Figs. 2 and 3 the values of Δt, which provide a relative measure of the stability of the interfacial film, are compared with relative foam stabilities, L_f multiplied by a factor to bring the two units on the same scale, obtained by direct measurement of the changing volume of foam with time. The values of L_f are derived from reference 3, where the method of measurement is described. Although the two units are derived from different sources and actually refer to different total concentrations of the antifoam, they agree in describing the behavior of varying compositions of the two synergistic mixtures that they were used to investigate. A major discrepancy occurs at only one point. The 100% methylisobutylcarbinol shows a high foam stability but a low film stability (Fig. 3). The absence of sodium silicate from the solution where the film stability was measured may account for the difference. Why the absence of sodium silicate should affect only this agent and not the other compositions, which differ from it by the inclusion of varying amounts of tributyl phosphate, is the subject of a future project.

Discussion.—Figures 2 and 3 illustrate one thesis of this paper, that antifoaming agents and synergistic mixtures of antifoams can be explored more rapidly, conveniently and equally effectively by means of light transmission than by the direct measurement of the collapse of foam. Extremely stable foams emphasize even more the convenience of the light transmission method, as direct observation of their collapse may require days or weeks, whereas changes in light transmission are observed immediately.

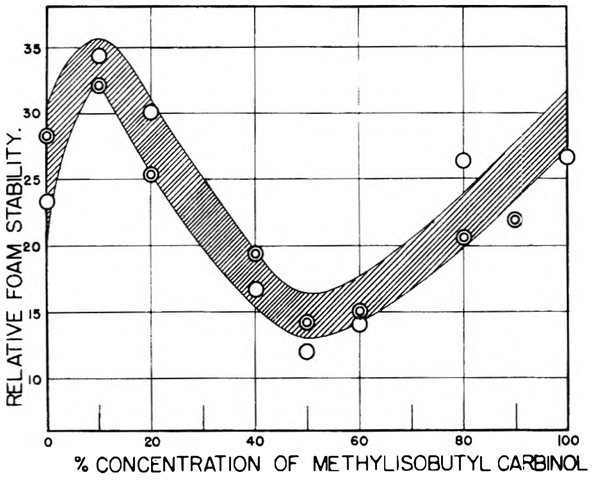

Fig. 3.—Comparison of relative foam stabilities, $0.067L_f$, ◎, and film stabilities, Δt from $I_0/I = 10.0$ to $I_0/I = 2.00$, ○, for various mixtures of methylisobutylcarbinol and tributyl phosphate on a foam produced from 0.50% Nacconol NRSF solution.

The general agreement between foam stability, which includes rupture of the films, and film stability as measured by light transmission, also is of interest in the consideration of mechanism of antifoaming action. The two synergistic systems investigated here have been shown previously[3] to act as antifoams by different mechanisms, one of them acting by virtue of the net hydrophilic–lipophilic balance of the mixture and the other by combining the two specific film-weakening effects of each of its components. The result achieved is the same. The foam is destabilized by a reduction in the cohesion and elasticity of the surface film, making it more likely to rupture under stress. The unit of foam stability, L_f, measures the last process of this chain of events.

---

[5] A rapid method of graphical integration is described by W. C. Johnson, "Mathematical and Physical Principles of Engineering Analysis," McGraw-Hill Book Co., New York., N. Y., 1944, pp. 80 82.

as it describes the variation of the total volume of foam with time. The present method of light transmission measures the stability of the liquid films under conditions where rupture is precluded. The change of film area is due to the diffusion of air from the smaller bubbles at higher pressures, and the measured effects of the antifoaming agents is caused by their alteration of the permeability of the films to the passage of gas. The general agreement between L_f and Δt means therefore that the increased permeability of the film is concomitant with and related to its reduction in cohesion and elasticity by the antifoaming agent.

A similar conclusion, though without reference to antifoaming agents, has already been stated by Brown, Thuman and McBain.[6] These authors measured the variation with time of the size of a single bubble on the surface of a solution, and compared the permeability coefficient thus obtained with the unit of foam stability, L_f. They write: "Foams of highest stability appear to be produced from solutions yielding lowest permeability values; solutions giving foams of very poor stability have the highest values for the permeability of the bubble film to air. Detailed correlation in the intermediate ranges is not, however, perfect."

The mechanism of antifoaming action is still obscure, but results such as those reported here focus attention on alterations of the adsorbed surface films as the origin of the effect.

[6] A. G. Brown, W. C. Thuman and J. W. McBain, "Transfer of Air through Adsorbed Surface Films as a Factor in Foam Stability," Contract No. N7-onr-321-T.O. II. Stanford Research Institute, 1949: A. G. Brown, W. C. Thuman and J. W. McBain, *J. Colloid Sci.*, **8**, 508 (1953).

METHODS FOR ESTIMATING THERMODYNAMIC QUANTITIES OF SPECIES IN LIQUID AMMONIA

By WILLIAM L. JOLLY

Radiation Laboratory, University of California, Berkeley, Calif.

Received October 12, 1953

Equations are given which permit estimation of heats, free energies and entropies for species in liquid ammonia. A method for estimating the differences in heats, free energies and entropies between ammonation processes and hydration processes for ions is discussed. It is shown that ions which are known to form stable ammonia complexes in aqueous solution, *e.g.*, H^+ and Ag^+, are "anomalously" very stable in liquid ammonia. The "anomalous" increased stability of hydroxide ion in water is explained by water complexing of the hydroxide ion.

It is possible to relate the usual relative entropies ($S° = 0$ for H^+) for ions in ammonia and water by the empirical expression

$$S^\circ_{NH_3} - S^\circ_{H_2O} = 23Z - 23 \quad (1)$$

where Z is the charge (taking account of sign) on the ion. For an ion X^z, the quantity $S^\circ_{NH_3} - S^\circ_{H_2O}$ is related to the solvation[1] entropies for X^z (ΔS^X_{am} and ΔS^X_{hyd}) and for H^+ (ΔS^H_{am} and ΔS^H_{hyd}) by the expression

$$S^\circ_{NH_3} - S^\circ_{H_2O} = (\Delta S^X_{am} - \Delta S^X_{hyd}) - Z(\Delta S^H_{am} - \Delta S^H_{hyd}) \quad (2)$$

Hence

$$\Delta S^X_{am} - \Delta S^X_{hyd} = (23 + \Delta S^H_{am} - \Delta S^H_{hyd})Z - 23 \quad (3)$$

In a recent paper[2] it was implied that the quantity $\Delta S^H_{am} - \Delta S^H_{hyd}$ is equal to -23 because when this value is used, a plot of "absolute" entropies in ammonia *versus* absolute entropies in water yields a straight line. This procedure simply eliminates the term involving Z in equation 3[3]:

$$\Delta S^X_{am} - \Delta S^X_{hyd} = -23 \quad (4)$$

It was therefore concluded that absolute entropies for ions are 23 e.u. higher in water than in liquid ammonia. This rule may not be valid for multiply-charged ions; insufficient experimental data exist for a test of the generalized rule.

Similar calculations may be made for heats of formation. Figure 1 is a plot of heats of formation for species in ammonia *versus* a simple function of heats of formation in water. The relation may be expressed by

$$\Delta H^\circ_{f\,NH_3} = \Delta H^\circ_{f\,H_2O} + 23Z - 5 \quad (5)$$

where $\Delta H^\circ_f = 0$ for H^+, Z refers to the actual charge on ions, and the units are kilocalories per mole. Figure 1 merely serves to show the agreement of equation 5 with the experimental data. By assuming that the ammonation energy of the hydrogen ion is 23 kcal./mole more negative than the hydration energy of the hydrogen ion,[4] we find that, in general, ammonation energies are 5 kcal./mole more negative than hydration energies.

From equations 1 and 5 one calculates

$$\Delta F^\circ_{f\,NH_3} = \Delta F^\circ_{f\,H_2O} + 16Z + 2 \quad (6)$$

---

[1] "Solvation" here refers to the transfer of an ion from a fixed standard state (*e.g.*, the gaseous phase) to the solvent. Hence ammonation entropies and hydration entropies are comparable because the same initial states are involved.

[2] W. M. Latimer and W. L. Jolly, *J. Am. Chem. Soc.*, **75**, 4147 1953).

[3] The coefficient of Z in equation 3 might be expected to have a small finite value. In the Powell–Latimer equation for the entropies of aqueous ions (*cf.* R. E. Powell and W. M. Latimer, *J. Chem. Phys.*, **19**, 1139 (1951)), the "effective radius" of the ion appears as an important term. The effective radii for positive ions are larger than the crystal radii by a constant different from that used for negative ions. The difference is ascribed to the opposite orientation of water molecules around positive and negative ions. This orientation effect might be expected to be entirely different from ammonia; hence equation 3 might retain the term involving Z, which differentiates between positive and negative ions.

[4] A value of 26 kcal./mole has been calculated by an entirely different means, *i.e.*, by assuming that the rubidium ion and bromide ion have identical ammonation energies. (*Cf.* W. L. Jolly *Chem Revs.*, **50**, 351 (1952).) The good agreement is taken as further justification of the present method.

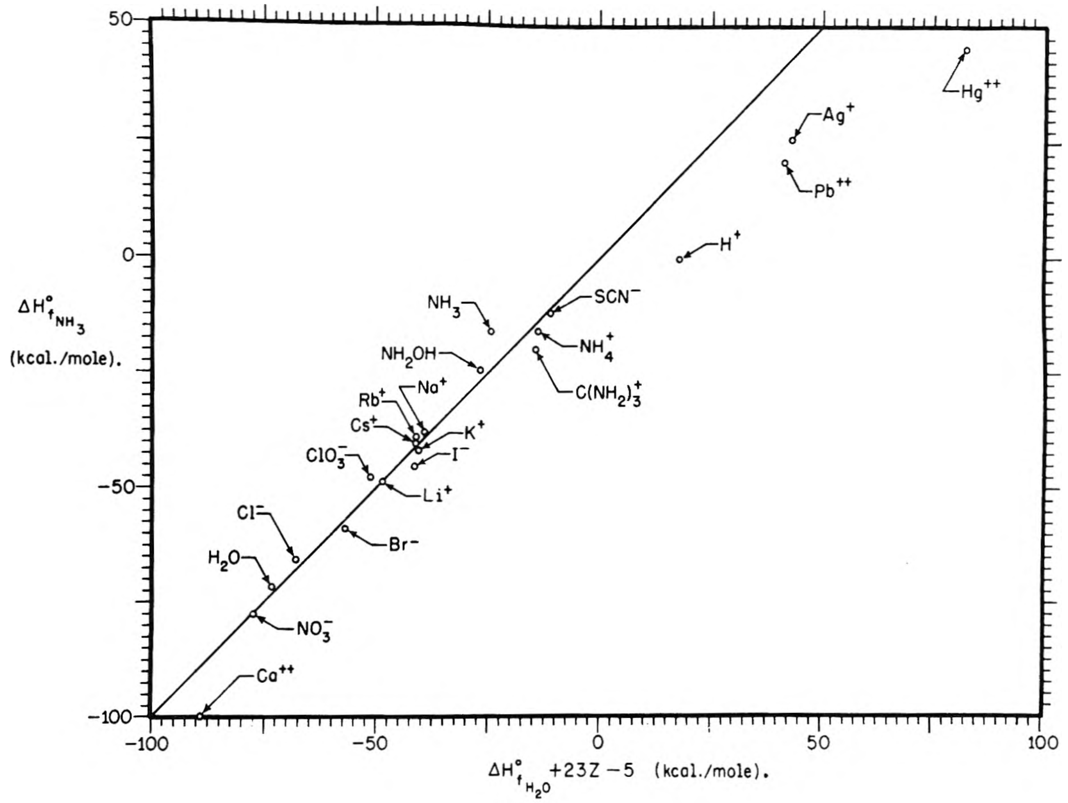

Fig. 1.

for 298°K. Figure 2 is a plot of the left side of equation 6 *versus* the right side of equation 6. By making an assumption similar to those already made for entropies and heats, we find that free energies of ammonation are 2 kcal./mole more positive than free energies of hydration.

It will be noted that heats and free energies for certain non-electrolytes have been included in the

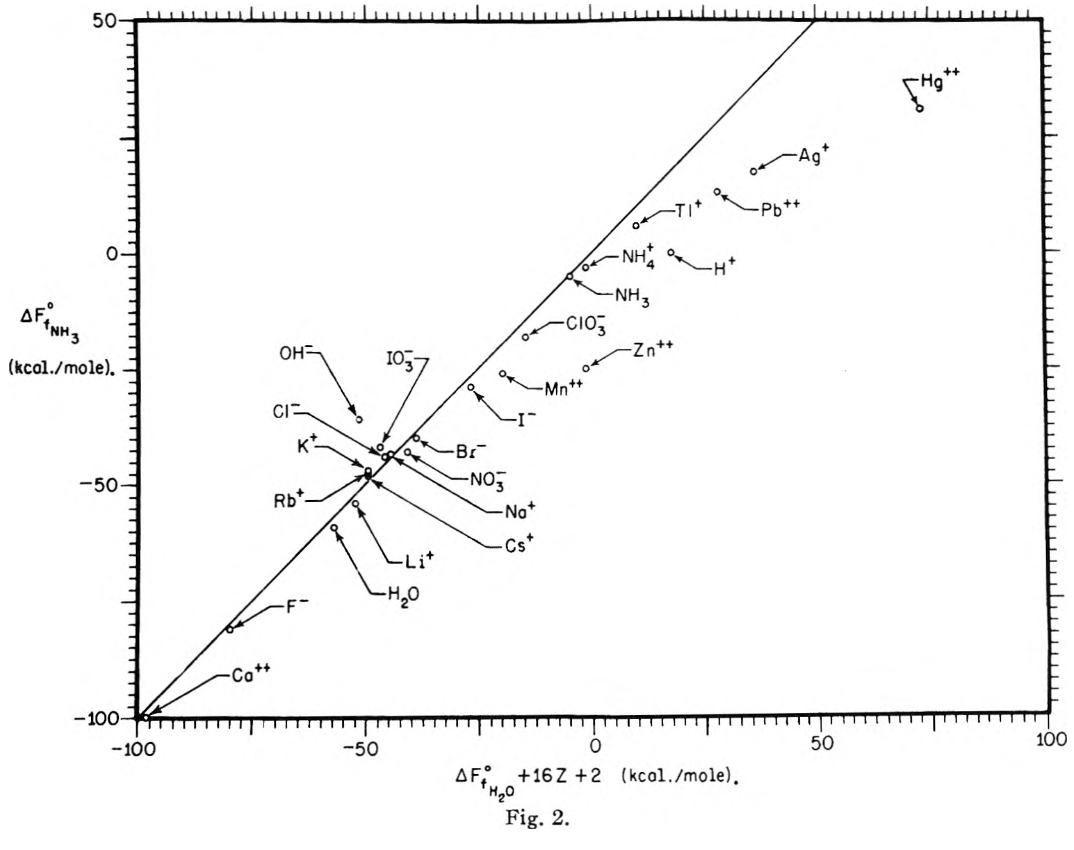

Fig. 2.

plots. Generally, these species fall on the straight lines.[5] By using these empirical relationships, one can roughly estimate the thermodynamic function for a species in ammonia when the same function is known for the species in water. Certain "irregularities," however, should be pointed out.

It will be noted that the hydrogen ion is abnormally stable in ammonia and the hydroxide ion is abnormally stable in water. The hydrogen ion undoubtedly obtains its stability through reaction to form the ammonium ion. The NH_4^+ configuration is much more stable than the H_3O^+ or $\left[\begin{array}{ccc} H & & H \\ & OHO & \\ H & & H \end{array}\right]^+$ configuration. (The free energies of NH_4^+ in water and in ammonia are in close agreement with the empirical rule.) Conversely, the hydroxide ion may exist as a stable hydrogen-bonded species of the type $HOHOH^-$ in water. No such stabilization is possible in anhydrous liquid ammonia, but it is possible in liquid ammonia containing water. It has been found that the presence of water in ammonia profoundly increases the solubility of sodium hydroxide.[6] Of course, the above phenomena may be explained by the acid–base character of the solvents. One would expect the H^+ ion, an acidic species, to be much more stable in a basic solvent like ammonia than in water, and *vice versa* for the OH^- ion. Certain other ions, *e.g.*, Ag^+, Pb^{++} and Hg^{++}, appear to be abnormally stable in ammonia. The data for the dipositive ions may be in error because of heat or free energy of dilution effects which are difficult to detect experimentally. In view of the strong tendency of Ag^+ to coordinate ammonia in aqueous solution, it might have been anticipated that the silver ion would be exceptionally stable in ammonia. By comparing the free energy of aqueous $Ag(NH_3)_2^+$ with $(Ag^+ + 2NH_3)$ in ammonia, one finds good agreement with equation 6. Apparently when an ion forms a stable ammonia complex in water, the free energy of this complex must be used in estimating the free energy of the corresponding ion in ammonia. On the other hand, when an ion forms a stable water complex in ammonia, it is this hydrated species that must be compared in the two solvents.

Equation 6 may be used to predict ionization constants for weak acids in ammonia. For an acid ionizing thus

$$HA = H^+ + A^- \qquad (7)$$

we write[7]

$$\begin{aligned}\Delta F^\circ_{NH_3} &= \Delta F^\circ_{H_2O} + (\Delta F^\circ_{fNH_3} - \Delta F^\circ_{fH_2O})_{A^-} - \\ &\qquad (\Delta F^\circ_{fNH_3} - \Delta F^\circ_{fH_2O})_{HA} \\ &= \Delta F^\circ_{H_2O} - 16\end{aligned}$$

Hence

$$pK_{NH_3} = pK_{H_2O} - 12 \qquad (8)$$

Equation 8 is a quantitative expression of the acid-levelling effect of ammonia. If we define a strong acid as one with $pK < 0$, then acids with ionization constants larger than 10^{-12} in water are predicted to be strong acids in ammonia.

Calculations.—The thermodynamic functions for species in water were taken from the Bureau of Standards compilation[8] and from Latimer.[9] Most of the thermodynamic functions for species in liquid ammonia have been tabulated elsewhere,[2] but the free energies for water and hydroxide ion have not previously been tabulated, and the calculations are presented here.

The vapor pressure of water over a 1 molal solution in ammonia at 25° is 0.4 mm.,[10] whereas the vapor pressure of pure water is 23.7 mm. at the same temperature. By neglecting gas imperfections and by using $\Delta F^\circ_f = -56.7$ kcal./mole for pure water,[8] we calculate $\Delta F^\circ_f = -59.1$ kcal./mole for water in liquid ammonia.

It is difficult to interpret many of the data in the literature on the solubility of hydroxides in ammonia. One of the more careful studies is that of Skossareswky and Tchitchinadzé.[6] These investigators found the solubility of NaOH to be *ca.* 6×10^{-5} molal at −40 to −45°. By estimating the entropy of solution as −46 e.u.,[8,11] we calculate $\Delta F^\circ = 12$ kcal./mole for the solution of NaOH at 25°. Using the known free energies for NaOH and Na^+, we calculate $\Delta F^\circ_f = -34.5$ for OH^- in ammonia. The solubility of RbOH in ammonia has been reported[12] as 0.09 molar at −40°. By estimating a mean activity coefficient of 0.2 for the saturated solution at −40° and by estimating[11] the entropy of solution as −37 e.u., we calculate $\Delta F^\circ = 6.1$ kcal./mole for the solution of RbOH at 25°. We then obtain $\Delta F^\circ_f = -32.5$ kcal./mole for OH^- in ammonia. We shall use an average value, $\Delta F^\circ_f = -34$ kcal./mole.

Acknowledgment.—The author wishes to thank Professors W. M. Latimer and R. E. Connick for their careful reading of the manuscript.

---

(5) The free energies for NH_3 in ammonia and for H_2O in water have been corrected to those for hypothetical 1 molal solutions.

(6) M. Skossareswky and N. Tchitchinadzé, *J. chim. phys.*, **14**, 153 (1916).

(7) Remembering that, by definition, $\Delta F^\circ_f = 0$ for H^+ in both solvents, we consider only the free energy changes for HA and A^-.

(8) National Bureau of Standards Circular 500, "Selected Values of Chemical Thermodynamic Properties," Washington, D. C., 1952.

(9) W. M. Latimer, "Oxidation Potentials," Prentice–Hall, Inc., New York, N. Y., 1952.

(10) J. H. Perry, editor, "Chemical Engineer's Handbook," McGraw–Hill Book Co., Inc., New York, N. Y., 1950, p. 171.

(11) Through use of equation 1.

(12) G. P. Nikol'skii, Z. A. Bagdassar'yan and I. A. Kazarnovskii, *Doklady Akad. Nauk S.S.S.R.*, **77**, 69 (1951); *C.A*, **46**, 5554*g* (1951).

EQUILIBRIA IN THE AQUEOUS SYSTEMS CONTAINING Ca^{2+}, Sr^{2+}, K^+, Na^+ AND Cl^- BETWEEN 18 AND 114°

By GUNNAR O. ASSARSSON AND AINO BALDER

Chemical Laboratory of the Geological Survey of Sweden, Stockholm 50, Sweden

Received October 2, 1953

The equilibria of the quaternary system $CaCl_2$–$SrCl_2$–KCl–H_2O between 18 and 114° have been examined. The system has the same general character as the ternary system $CaCl_2$–$SrCl_2$–H_2O. The temperature area, at which the existence region of the strontium chloride dihydrate overlaps that of the solid solution of the calcium and strontium chloride hexahydrates, has been investigated systematically. The solid solution of the hexahydrates, the α-calcium chloride tetrahydrate and the strontium chloride dihydrate can co-exist at 27.8 ± 0.2°, but the boundary surface between the existence region of the strontium chloride dihydrate and that of the solid solution of the hexahydrates has a temperature minimum at 26.6 ± 0.2°. The presence of strontium chloride influences only slightly the lowest formation temperature of the double salt $CaCl_2\cdot KCl$ (36.5°). The presence of potassium chloride has a similar effect on the lowest formation temperature of strontium chloride monohydrate (75.5°). In the quinary system the presence of sodium chloride lowers the invariant temperatures only some tenths of a degree. New compounds do not occur within the temperature range investigated.

In some earlier papers[1,2] the authors have shown the conditions for equilibria in the binary and ternary systems containing the chlorides of calcium, strontium, sodium and potassium. To complete these investigations further determinations were required on the connected quaternary and quinary systems. Equilibria in these systems will be briefly treated here.

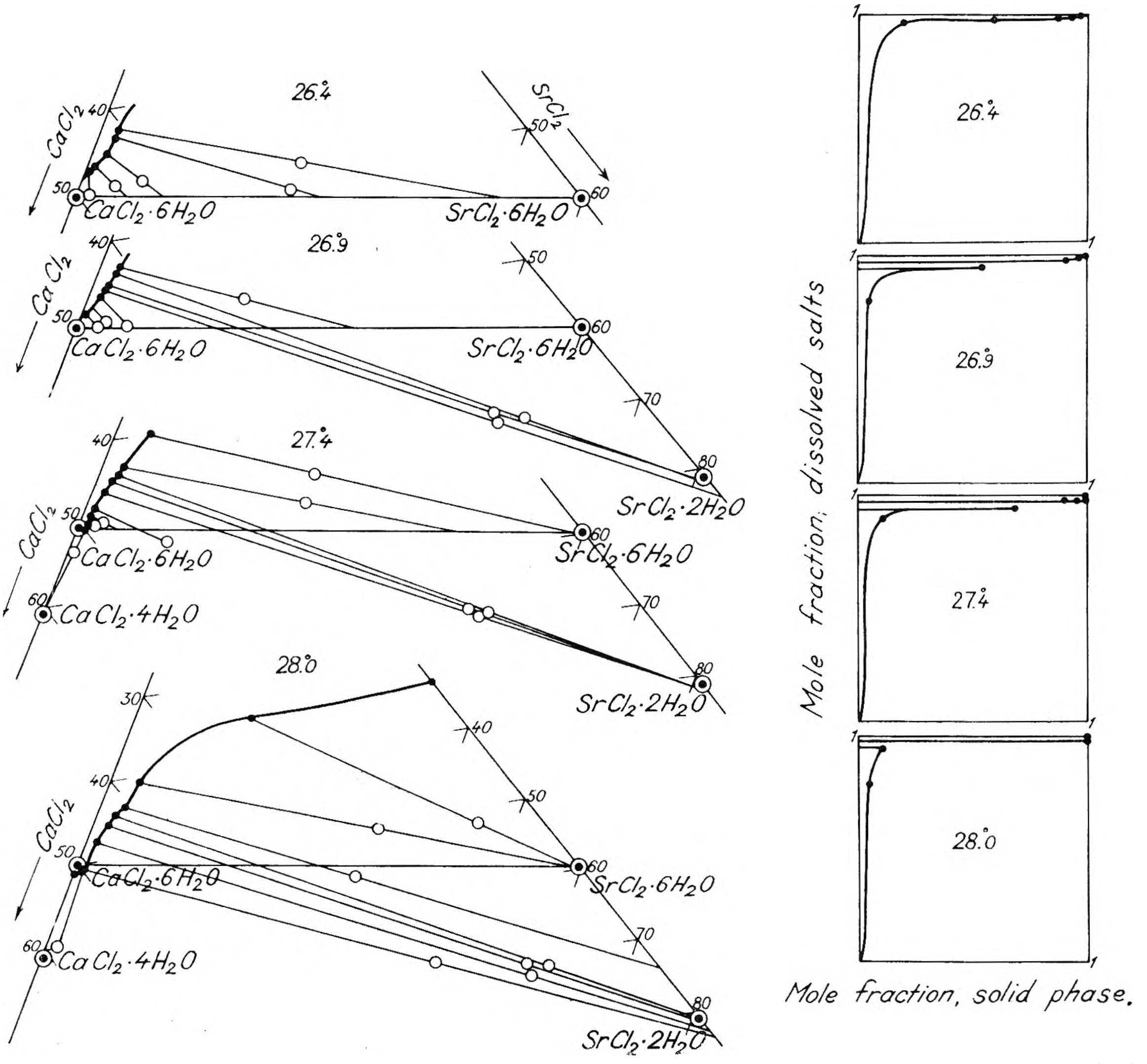

Fig. 1.—The system $SrCl_2$–$CaCl_2$–KCl–H_2O. The isotherms are projected on the $SrCl_2$–$CaCl_2$–H_2O plane; in the distribution diagrams the mole fraction 1 = 100% $CaCl_2$.

---

(1) G. C. Assarsson, *J. Am. Chem. Soc.*, **72**, 1433 (1950), and THIS JOURNAL, **57**, 207 (1953).

(2) G. O. Assarsson and A. Balder, *ibid.*, **57**, 717 (1953).

TABLE I

THE QUATERNARY SYSTEM $SrCl_2$–$CaCl_2$–KCl–H_2O ISOTHERMS BETWEEN 18 and 100°

Solid phases: b, $SrCl_2·2H_2O$; d, α-$CaCl_2·4H_2O$; e, $CaCl_2·2H_2O$; f, solid solution $(CaSr)Cl_2·6H_2O$; g, $SrCl_2·H_2O$; h, KCl; i, $KCl·CaCl_2$; k, NaCl.

Solution			Wet residue			Solid
$SrCl_2$	$CaCl_2$	KCl	$SrCl_2$	$CaCl_2$	KCl	phase
			18°			
0.8	39.6	2.6	3.8	42.7	0.8	f + h
1.2	38.4	2.6	10.8	36.7	1.2	f + h
6.7	25.4	4.2	40.4	9.9	2.0	f + h
23.4	7.2	6.3	49.0	2.1	1.6	f + h
			26.4°			
0.3	45.8	4.0	1.3	48.4	1.0	f + h
0.8	44.4	3.6	4.1	45.0	1.0	f + h
1.6	42.7	3.5	6.9	41.7	1.3	f + h
1.6	41.2	3.5	24.5	27.6	1.1	f + h
2.0	40.5	3.5	24.8	24.8	1.1	f + h
			26.9°			
0.3	46.2	3.8	2.4	47.0	1.0	f + h
0.9	45.0	3.7	3.4	46.2	1.5	f + h
1.2	43.9	3.2	5.9	45.0	1.0	f + h
1.6	42.9	3.4	53.6	15.5	1.2	b + h
1.5	42.4	3.3	52.7	15.3	1.2	b + h
2.1	40.6	3.3	56.6	12.8	1.0	b + h
2.0	40.2	3.4	18.2	31.3	1.0	f + h
			27.4°			
0.9	48.0	4.4	0.5	51.8	1.6	d + h
0.9	47.1	4.2	1.9	47.7	1.3	f + h
0.8	46.2	4.2	2.5	46.9	2.1	f + h
1.3	45.3	4.2	10.5	41.4	1.6	b + f + h
1.2	43.9	3.6	50.9	17.4	1.3	b + h
1.7	41.9	3.6	48.7	17.7	1.3	b + h
2.0	41.1	3.6	51.8	16.2	1.3	b + h
2.2	40.5	3.6	25.0	25.0	1.3	f + h
4.0	36.0	3.6	24.4	22.5	1.2	f + h
			28.0°			
1.1	47.4	4.7	1.3	57.7	1.7	b + d + h
1.1	47.1	4.7	46.2	21.7	2.0	b + h
1.1	44.6	2.7	58.2	13.1	0.8	b + h
1.7	42.2	3.0	57.2	13.0	0.9	b + h
1.9	41.1	3.0	59.9	11.5	0.8	b + h
2.9	39.1	3.0	33.1	22.9	1.2	b + f + h
3.3	35.7	3.3	35.7	16.7	1.3	f + h
13.0	20.0	5.2	44.2	6.4	1.4	f + h
			37.0°			
1.4	50.4	7.0	1.5	55.2	6.3	b + d
1.8	50.0	7.3	0.5	18.4	66.0	b + h
			37.5°			
1.4	50.7	7.0	1.3	56.9	31.2	b + i
1.3	50.4	7.4	0.5	22.9	65.4	b + h
			42.6°			
1.7	53.5	4.3	1.2	55.0	2.3	b + d
1.4	52.5	6.5	1.3	54.8	33.6	b + i
			42.8°			
1.2	53.2	4.2	1.3	62.8	2.1	b + e
1.2	52.5	5.2	0.6	52.9	33.4	b + i
			74.0°			
2.2	55.8	3.6	1.4	64.7	3.0	e + i
1.9	56.0	3.6	37.9	31.8	1.9	b + i
			75.0°			
2.0	56.0	3.8	26.5	41.0	2.5	g + i
3.1	54.5	4.6	50.7	22.4	1.6	b + i
			100°			
3.0	58.3	3.1	1.5	63.6	2.6	e + i
3.2	57.5	3.1	33.7	38.3	2.1	g + i
			The invariant points			
			26.6°			
1.8	41.8	3.5				b + f + h
			27.8°			
1.0	48.0	4.7				b + d + f + h
			37.2°			
1.5	50.4	7.2				b + d + h + i
			42.7°			
1.4	53.0	5.2				b + d + e + i
			74.5°			
2.0	56.0	3.5				b + e + g + i

All the figures in the tables are given as weight per cent.

The Quaternary Aqueous System Ca^{2+}, Sr^{2+}, K^+, Cl^-.—In this system are retained the main features of the ternary systems embraced by it. As it is a quaternary system of rather simple character, the composition of the solutions at the equilibria can best be represented by using a tetrahedral diagram with the composition of the equilibria solutions projected on one side.

The hexahydrates of strontium and calcium chloride crystallize at lower temperature (18, 26.4°, Table I, Fig. 1) as solid solution, in a similar manner to that earlier described,[2] but there are some features of special interest concerning the crystallization of the solid phases between the temperatures 26.9–28.0°. The isotherm at 26.9° shows a gap in the crystallization curve of the hexahydrates, the solutions corresponding to this gap being in equilibrium with strontium chloride dihydrate. At 27.4°, however, the equilibrium solutions very rich in calcium chloride, deposit crystals of α-calcium chloride tetrahydrate as first phase and when the concentration of calcium chloride is slightly lowered the solid phase is composed of crystals of the solid solution rich in calcium chloride. On further lowering the calcium chloride concentration the gap corresponding to the formation of strontium chloride dihydrate follows, and thereafter the solid solution of the hexahydrates rich in strontium chloride. At 28.0°, on the other hand, the strontium chloride dihydrate and α-calcium chloride tetrahydrate co-exist in equilibrium with saturated solutions. The distribution diagram (Fig. 1), according to Roozeboom, shows that the crystallization at 26.4° yields crystals of solid solution with complete miscibility of the hexahydrates, and that the gap in the 26.9° isotherm is bounded on both sides by areas corresponding to the solid solution of the hexahydrates. The 27.4° isotherm, however, has a part corresponding to crystallization of pure calcium chloride tetrahydrate and connected with the part of the curve corresponding to the solid solution crystallization.

The lowest formation temperatures in the quaternary system are found by interpolation to be at 26.6 ± 0.2° for the strontium chloride dihydrate and 27.8 ± 0.2° for the calcium chloride tetrahydrate. Thus the boundary surface between the existence area of the α-calcium chloride tetrahydrate and that of the solid solutions of the hexahydrates has a temperature minimum at 26.6°.

Other transformation temperatures of the system are given in Table I. They are slightly lower than those of the integrant ternary systems.

No new compound occurs in the quaternary system.

A correction of the lowest formation temperature of the α-calcium chloride tetrahydrate in the ternary system potassium chloride–calcium chloride–water must be made! In the ternary system mentioned the new determinations gave 43.0°.

The Quinary Aqueous System Ca^{2+}, Sr^{2+}, K^+, Na^+, Cl^-.—This system shows no features worthy of special note. The general observation can be made that sodium chloride is only very slightly soluble in solutions saturated with respect of the other three chlorides within the temperature area in question. Results from three determinations in saturated solutions are given in Table II.

TABLE II

THE QUINARY SYSTEM $SrCl_2$–$CaCl_2$–KCl–NaCl–H_2O SOLUTIONS SATURATED AT THE TEMPERATURES

Temp., °C.	Solution				Solid phase
	$SrCl_2$	$CaCl_2$	KCl	NaCl	
18.0	0.5	39.6	2.7	0.3	f + h + k
36.5	1.0	50.2	6.7	0.3	b + d + h + k
100.0	2.5	57.2	3.0	1.0	e + g + h + k

No new compound occurs in the quinary system mentioned.

VAPOR PRESSURES OF AQUEOUS POTASSIUM CHLORIDE SOLUTIONS AT 25° BY MEANS OF A NEW TYPE OF DIFFERENTIAL MANOMETER

BY OLIVER L. I. BROWN[1] AND C. MACGREGOR DELANEY[2]

Department of Chemistry, Syracuse University, Syracuse, N. Y.

Received October 7, 1953

A new type of differential manometer is described, which utilizes a flexible brass bellows and a Statham Strain Gage. The manometer may be made sensitive to a differential pressure of 10^{-6} mm. of mercury. This instrument was used as a null point indicator in comparing the temperatures of equal vapor pressure of potassium chloride solutions and pure water. The results indicate that high precision is possible, with temperature measurement and control the limiting factors.

Introduction

The investigation reported here was concerned with developing an extremely sensitive method for determining when the pressures on opposite sides of a barrier are equal, so that the lowering of the vapor pressure of a solvent by the addition of a nonvolatile solute may be determined by measuring the difference in temperature required to establish equal vapor pressures over the solution and the pure solvent. It was felt that such a method might be useful in dealing with solutes whose high molecular weights limit the applicability of other vapor pressure methods. For this purpose, a differential manometer was constructed in which a pressure difference of 10^{-6} mm. of mercury would cause a deflection of about 0.5 mm. on the galvanometer scale. This sensitivity was far greater than could be used for our purposes in view of the limitations in temperature measurement. The sensitivity was therefore reduced by the substitution of a Statham model G-1-4.5-225 Strain Gage for the more sensitive model G-1-1.5-315, and by shunting the galvanometer.

The development of the Isopiestic Method[3,4] has made the vapor pressures of potassium chloride solutions at 25° of particular importance as a standard of reference for other solutions. Since the various indirect means of determining the vapor pressure lowering as a function of concentration lead to important differences in the result, it was felt that a direct determination would be of value in itself, as well as providing information as to the precision of the apparatus.

Experimental

Materials.—The potassium chloride was of the highest commercially obtainable purity, and before use was recrystallized three times from conductance water and dried at 500° for 48 hours. The water used for recrystallization as well as in making up the solutions for study had a specific conductance of not more than 1.05×10^{-6} ohm^{-1} cm.$^{-1}$

Apparatus.—The null point manometer consisted of a very flexible brass bellows about four inches deep and two inches in diameter, to the closed end of which was attached the feeler arm of a Statham Strain Gage, model G-1-4.5-225. The strain gage is a Wheatstone bridge in which the resistance wires making up the arms of the bridge undergo changes in tension with motion of the feeler arm. This unit was soldered inside a heavy brass can in such a way that two chambers were formed, one on either side of the bellows. These chambers were connected through Pyrex tubes to a system of stopcocks, and through these to a vacuum pump and to two specially designed Pyrex vessels, one of which held a sample of pure water and the other the potassium chloride solution under investigation. The vessels were two inches in diameter and one inch deep and were each equipped with a Pyrex-sealed bar magnet and a ground glass ball joint for attachment to the manometer system.

Two small water-baths were insulated with glass wool and placed inside a larger copper container, which in turn was placed in a larger constant temperature water-bath, whose temperature was controlled with a cooling coil and an on-off Thyratron heating circuit. One of the small baths contained the vessel with the potassium chloride solution. A stirrer with a bar magnet at the lower end of the shaft was mounted over the vessel, and coupled with the magnet inside the vessel to stir the solution. A thermistor was mounted as close as possible to the outside wall of the vessel. This bath was allowed to reach a steady state at or close to 25°. The second small bath contained the vessel with the pure water, and was nearly the same as the solution bath, except that it had a small cooling coil and a phase-shifting Thyratron circuit for temperature control. The phase-shifting Thyratron operated from the unbalance of the

---

[1] Department of Chemistry, Connecticut College, New London, Conn.

[2] Based on the Dissertation submitted to the Graduate School of Syracuse University in partial fulfillment of the requirements for the degree of Doctor of Philosophy by C. MacGregor Delaney, Research Department, Shell Oil Co., Houston Refinery, Houston, Texas.

[3] D. A. Sinclair, THIS JOURNAL, **37**, 495 (1933).

[4] R. A. Robinson and D. A. Sinclair, *J. Am. Chem. Soc.*, **56**, 1830 (1934).

strain gage bridge through a galvanometer and photocell. The manometer was housed in an air-bath which was insulated and immersed in the large water-bath. An insulated protective cover was built over the large water-bath, and the air space above the water was kept warmer than the water, to prevent condensation in the glass lines and stopcocks which were located in this air space. The manometer had a small steady heat supplied to it for the same reason.

The temperature of the solution was determined with a platinum resistance thermometer of the calorimetric type which had been calibrated in terms of a National Bureau of Standards certified platinum resistance thermometer. The temperature difference between the solution and the pure water for the condition of equal vapor pressures was measured by a Wheatstone bridge consisting of two thermistors, a fixed resistance and an approximately equal fixed resistance with a higher resistance variable shunt which was adjusted to balance the bridge. The thermistors were Western Electric model 14-B which had been aged for 30 days at 150°. The thermistors were calibrated separately against the platinum resistance thermometer, about 25 points being taken for each in the range from 23 to 26°. The ratio of the resistances of the two thermistors when at the same temperature was determined as a function of temperature. The results of these three series of calibrations were combined in an equation relating the reading of the variable shunt to the temperature difference measured by the thermistors. The fixed resistances of the Wheatstone bridge were calibrated in terms of National Bureau of Standards certified standard resistors. Great care was taken to eliminate thermals in the bridge circuit.

Procedure.—Prior to making an observation of the vapor pressure lowering, a solution of potassium chloride and a sample of conductance water were placed in the two vessels, leaving an air space above the liquids. The vessels were then placed in their respective thermostats, connected to the stopcock system, and degassed. The degassing was a time-consuming operation since it had to be accomplished stepwise to avoid bumping or undue loss of solvent from the solution.

The manometer was evacuated, flushed out with vapor from one vessel, and this process repeated several times. The ultimate test for complete degassing lay in the instantaneous response of the manometer to very small temperature differences between solvent and solution. The temperature of the solvent was then adjusted so that its vapor pressure was less than that of the solution, which was kept as close as possible to 25°. The solvent vapor was allowed to enter both chambers of the manometer to establish the zero point of the instrument, then the two chambers were isolated and the solution vapor was allowed to enter one while the solvent vapor remained in the other. Both vapors, of course, were in contact with their respective liquids. The inequality of the two vapor pressures caused a motion of the bellows which was picked up by the strain gage, whose degree of unbalance was indicated by the galvanometer. The galvanometer mirror reflected a beam of light to the phototube of the phase-shifting Thyratron heater, which allowed ever decreasing amounts of heat to flow into the solvent-bath until the vapor pressure of the solvent just equalled that of the solution. At this point the temperature of the solution was measured, and also the temperature difference between solvent and solution. The average of five observations was taken as a run. The zero point of the manometer was then rechecked, and the connections of solvent and solution to the manometer were reversed for the next run. From six to eight runs were taken for each concentration of solution. The temperature of the solvent-bath was constant within 0.0005° during each run.

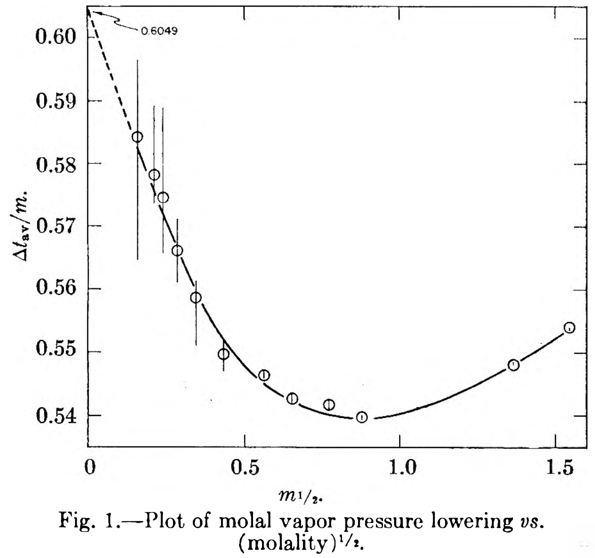

Fig. 1.—Plot of molal vapor pressure lowering *vs.* (molality)$^{1/2}$.

Analysis of Solutions.—The potassium chloride solution was removed from its vessel with a special transfer tube designed to prevent change in concentration by solvent loss. The solution was first analyzed by titration with silver nitrate solution using dichlorofluorescein as the indicator. The final analysis was made with a Rayleigh Interferometer, using as a comparison standard a solution made up by direct weighing to correspond as closely as possible to the approximate concentration as determined by the titration. All weighings were made with weights recently calibrated against National Bureau of Standards certified weights, and were corrected to vacuum. The accuracy of the interferometric method is about ±4 parts per million.

Results and Discussion

The experimental results are given in Table I, and in more detail in Table II. The temperature of the solution bath is t_1, and that of the solvent bath is $t_1 - \Delta t$. The osmotic coefficient ϕ, which is defined by equation 2 below, has been calculated from the observations by methods I and II, as described in the next paragraph, and is tabulated as ϕ, method I and method II. Figure 1 is a plot of $\Delta t/m$ *versus* $m^{1/2}$, with vertical lines used to mark the limits for extreme values of Δt as listed for each point in Table II. The point for zero concentration was obtained from equation 3 below and the relation

$$(\Delta t/m)_{m=0} = (2/55.5062)(\mathrm{d}T/\mathrm{d}\ln P)_{25°} = 0.6049 \quad (1)$$

Table I

Series	t_1 (av.)	Δt (av.)	m^a	$m^{1/2}$	ϕ Method I	ϕ Method II
1	25.042	0.0147	0.02515	0.1586	0.9588	0.9659
2	25.001	.0257	.04445	.2108	.9472	.9558
3	25.003	.0323	.05621	.2371	.9402	.9500
4	25.000	.0454	.08020	.2832	.9280	.9359
5	25.000	.0676	.1210	.3479	.9150	.9237
6	25.000	.1045	.1901	.4360	.9015	.9091
7	25.005	.1738	.3180	.5639	.8978	.9040
8	25.011	.2309	.4254	.6522	.8924	.8980
9	25.001	.3265	.6025	.7762	.8924	.8969
10	25.001	.4179	.7741	.8798	.8903	.8938
11	25.001	1.0211	1.8631	1.3650	.9096	.9095
12	25.001	1.3176	2.3783	1.5422	.9205	.9204

[a] m is the number of moles of KCl/kg. H_2O.

The conformity to a smooth curve extrapolating to the theoretical limit indicates a precision of better than 0.0005° for all points. Table II shows no systematic trend in Δt for runs taken with pure solvent vapor inside or outside the bellows. This indicates a precision of about 0.0001 mm. of mercury in reaching zero pressure differential.

The reduction of the measured temperature differences to the corresponding lowering of the vapor pressure of water required a precise vapor pressure–temperature relationship for water in the

TABLE II

DEVIATIONS OF INDIVIDUAL RUNS FROM AVERAGES IN TABLE I

(The numbers 3 and −68 for series 1, run A, for example, mean that for this particular observation the value of Δt was 3×10^{-4} degrees greater, and the value of t_1 was 68×10^{-3} degrees less than the averages for Series 1 listed in Table I. Other entries have corresponding meanings.)

Series Runs	1	2	3	4	5	6	7	8	9	10	11	12
A	3	0	−1	0	2	3	2	−1	1	0	1	1
	−68	0	−1	0	−2	0	−5	−11	−1	0	0	−1
B	0	5	−1	0	3	1	1	−3	−4	4	−2	−4
	−25	1	0	0	−1	0	−5	15	1	0	0	1
C	−3	−2	−4	3	−9	−3	−2	1	−3	6	−5	−9
	22	3	1	0	1	2	−5	20	2	1	−1	−1
D	−5	1	2	−3	0	−2	−2	1	4	−1	7	5
	100	6	2	1	1	0	14	23	−2	2	0	0
E	−1	−1	−5	−4	−2	5	−1	−1	2	−4	7	3
	112	−7	4	0	1	0	7	−11	0	−1	0	−1
F	2	1	8	0	3	−5	−1	−1	−3	−3	−1	5
	−72	−3	10	2	0	−1	−5	−9	0	−1	−1	0
G	2	−2	−1	3				2			−4	−3
	−70	0	−9	−1				−11			0	1
H			1	4				3				
			−7	−1				−12				

neighborhood of 25°. In method I, the values for the vapor pressure of water were taken from the "International Critical Tables."[5] To aid in smooth interpolation, an equation was derived which reproduced exactly the thirteen table entries from 24 to 25.2°. P^0 was interpolated to the value of t_1 for each run, and P to the value of $t_1 - \Delta t$. The osmotic coefficient was then calculated from the relation

$$\phi = -(55.5062/2m) \ln P/P^0 \qquad (2)$$

No correction was made for the very small change in P/P^0 with temperature over the 0.04° range by which t_1 departed from 25°. In method II it was assumed that the vapor pressure of water in the range from 15 to 25° could be expressed by the following equation[6]

$$P_{\text{mm}} = e^{[a - b/T + c/T^{3/4}]} \qquad (3)$$

Differentiating and using the Clapeyron equation, we obtain

$$\mathrm{d}P/\mathrm{d}T = \frac{[b - (3/4)cT^{1/4}]}{T^2} e^{[a - b/T + c/T^{3/4}]}$$

$$= \Delta H_v/T(V_g - V_l) \qquad (4)$$

Using the precisely known values of ΔH_v and $(V_g - V_l)$ from the tabulation of Osborne, Stimson and Ginnings[7] it was found that equation 4 reproduced exactly the five values of $\Delta H_v/T(V_g - V_l)$ for temperatures of 15, 20, 25, 30 and 35° when $a = 14.779367$, $b = 10{,}794.0544$, $c = 1764.4607$ and $T = t + 273.1600$. Therefore equation 3 with these same constants should reproduce the vapor pressure of water from 15 to 25°. It was found that the vapor pressures calculated from equation 3 for temperatures of 15, 20, 25, 30 and 35° were higher than the corresponding values for reference 7 by 0.013, 0.013, 0.012, 0.012 and 0.011 mm., respectively, and were higher than those of reference 5 by 0.007, 0.006, 0.005, 0.004 and 0.003 mm., respectively. Substituting values of T_1 and $T_1 - \Delta t$ into equation 3 gave values of $\ln P/P^0$ from which the ϕ values listed in Table I under method II were obtained. An Antoine equation was assumed using method II and while it fitted the five values of $\Delta H_v/T(V_g - V_l)$ exactly, it produced calculated pressures less than reference 5 by 0.025,

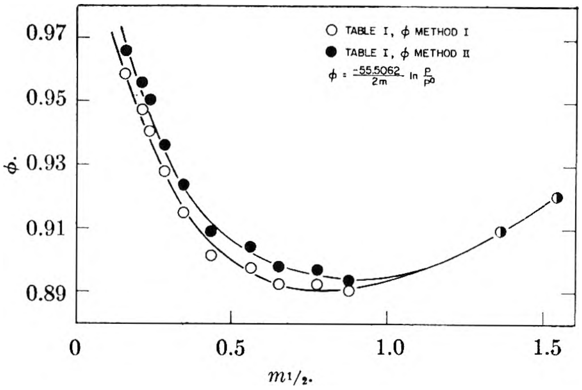

Fig. 2.—Osmotic coefficient vs. (molality)$^{1/2}$.

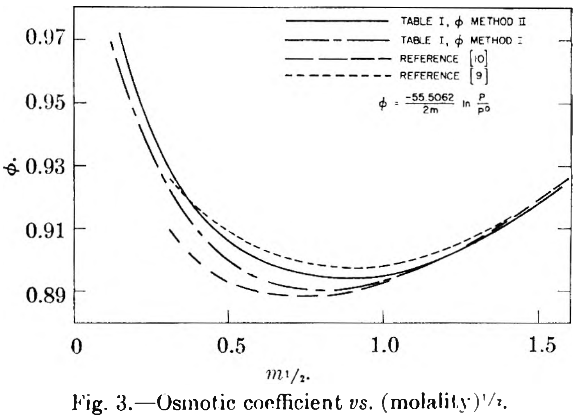

Fig. 3.—Osmotic coefficient vs. (molality)$^{1/2}$.

---

[5] "International Critical Tables," Vol. III, McGraw-Hill Book Co., Inc., New York, N. Y., 1928, pp. 211–212.

[6] A paper in preparation by O. L. I. Brown will present the evidence supporting this new type of equation.

[7] N. S. Osborne, H. F. Stimson and D. C. Ginnings, *J. Research Natl. Bur. Standards*, **23**, 261 (1939).

0.026, 0.026, 0.038 and 0.029 mm., respectively, and was therefore considered less accurate than equation 3.

Figure 2 presents our calculated values of ϕ from the above two methods, and Fig. 3 shows a comparison of these with the "best values" of Robinson, quoted by Harned and Owen[8] and with direct measurements by Lovelace, Frazer and Sease as recalculated to 25° from 20° by Robinson and Sinclair.[9] The present authors calculated the values of ϕ from the smoothed values of $\Delta P/P^0m$, the molal vapor pressure lowering, tabulated by Robinson and Sinclair.

Acknowledgment.—The authors wish to express their appreciation to Mr. C. L. Wilder of the Taylor Instrument Companies, Rochester, N. Y., for the gift of the bellows used in the manometer and to Mr. A. C. Hogge of the Shell Oil Company for the loan of the Rayleigh Interferometer.

---

(8) H. S. Harned and B. B. Owen, "The Physical Chemistry of Electrolytic Solutions," 2nd Edition, Reinhold Publ. Corp., New York, N. Y., 1950.

(9) R. A. Robinson and D. A. Sinclair, *J. Am. Chem. Soc.*, **56**, 1830 (1934).

BINDING ENERGIES OF GASEOUS DIATOMIC HYDRIDES AND HALIDES OF GROUP II AND GROUP III METALS[1]

By John L. Margrave

Department of Chemistry, University of Wisconsin, Madison, Wisconsin

Received October 13, 1953

The available data relating to binding energies of gaseous diatomic hydrides and halides of Group II (Be, Mg, Ca, Sr and Ba) and Group III (B, Al ,Ga, In and Tl) metals have been correlated on the basis of an ionic model similar to that used previously for the alkali halides and hydrides. Experimental values for the binding energies are calculated through thermochemical cycles. In the cases studied the binding energies calculated on the basis of pure ionic attraction (e^2/r) and neglecting repulsion and polarization effects compared well with the experimental values with an average deviation of ±12 kcal./mole. The use of estimated polarizabilities in a series of refined calculations gave values for the binding energies about the same as those given by e^2/r. This correlation has been used for critically evaluating the experimental data on molecules and for determining a series of gaseous cationic radii.

There are available in the literature spectroscopic data for nearly all of the diatomic gaseous hydrides and halides of the Group II (Be, Mg, Ca, Sr and Ba) and Group III (B, Al, Ga, In and Tl) metals. In addition a number of the halides have been studied by electron diffraction and microwave spectroscopy. In this work an attempt is made to correlate the experimental observations with a satisfactory model for these gaseous molecules.

The gaseous alkali metal halides and hydrides have been treated successfully on the basis of an ionic model by Brewer and Mastick,[2] Rittner,[3] and Klemperer and Margrave.[4] These compounds are definitely ionic and consist of metals and non-metals having electronegativity differences ranging from about 3.2 for CsF to about 1.3 for LiH. Binding in the alkali halides may be fairly well described by using only e^2/r for the ionic binding energy since detailed calculations taking into account polarization and repulsion effects show that they almost exactly counterbalance each other. In the alkali hydrides, however, these two effects make quite different contributions and must be considered separately to get proper values for ionic binding energies. The success of the ionic model in these cases indicates its possible application to Group II and III metal halides and hydrides.

The idea lying behind use of the ionic model for molecules of this type may be most easily understood by considering that in a molecule for which the difference between the ionization potential of the metal and the electron affinity of the non-metal is small, the ground state potential energy curve will be primarily determined by coulombic attraction of the ions. Herzberg[5] and others have considered this problem in detail and suggested rules for deciding when ionic character will be most important and when atomic character will predominate. One such rule is

$$R = r_s/r_e = [14.43/(I - E)]/r_e \geq 1.5$$

where r_s is the internuclear distance at which electrostatic attraction between ions has just compensated for the energy $(I - E)$, r_e is the observed internuclear equilibrium distance, $(I - E)$ is the difference in ionization potential and electron affinity as previously defined, and 14.43 is the constant necessary when $(I - E)$ is expressed in electron volts and r_e is expressed in Å. Herzberg states that in the range R = 1.5–2 the decision between ionic and atomic molecules is often difficult, but for $R >$ 2, a molecule usually shows ionic character in its ground state.

Values of R have been calculated for all the molecules involved and range from near 1.0 for some of the alkaline earth hydrides to nearly 4.0 for some Group III halides. Thus, a relatively wide range of R values is being considered, some actually outside the range suggested by Herzberg for ionic molecules.

In order to make a comparison of experimental and calculated ionic binding energies, one may use

---

(1) Presented before the Physical and Inorganic Division of the American Chemical Society in Chicago, September, 1953.

(2) L. Brewer and D. F. Mastick, *J. Am. Chem. Soc.*, **73**, 2045 (1951).

(3) E. S. Rittner, *J. Chem. Phys.*, **19**, 1030 (1951).

(4) W. A. Klemperer and J. L. Margrave, *ibid.*, **20**, 527 (1952).

(5) G. Herzberg, "Spectra of Diatomic Molecules," D. Van Nostrand Co., Inc., New York, N. Y., 1950.

the quantity U_{ionic} defined through the thermochemical cycle shown

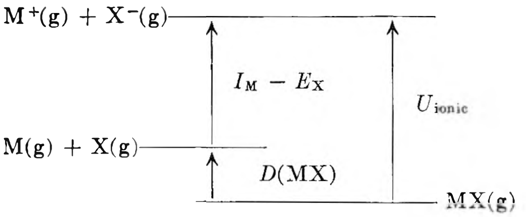

From this cycle $U_{\text{ionic}} = I_M - E_X + D(MX)$. One needs thermal or spectroscopic data to complete the thermochemical cycle except for U_{ionic} or else sufficient information about the molecule to allow direct calculation of U_{ionic} by use of the methods previously mentioned.

Data and Results

There are data available from the compilations of Herzberg[5] and Gaydon[6] for forty-three of the fifty possible halides and hydrides of Group II and III metals, and in forty-two cases dissociation energies have been estimated, usually from Birge–Sponer extrapolations. Unfortunately, in only twenty-two cases are the data complete enough to give values for internuclear distances; some other internuclear distances have been determined in electron diffraction and microwave studies.

Since any theoretical approach to the calculation of binding energies requires knowledge of the internuclear distances, it is first necessary to have a method for calculation of these values for all the molecules of interest. Rittner[3] has evaluated a series of gaseous ionic radii for the alkali metal ions and the halide ions. From his values one may evaluate a radius for H^- of 1.05 ± 0.03 Å. from the available spectroscopic data, and also radii for the Group II and Group III ions as shown in Table I.

TABLE I

Gaseous ion	r, Å.	Gaseous ion	r, Å.
Be^+	0.31 ± 0.02	B^+	0.17 ± 0.04
Mg^+	.70 ± .02	Al^+	.57 ± .03
Ca^+	.96 ± .02	Ga^+	.61 ± .10[a]
Sr^+	1.09 ± .10[a]	In^+	.80 ± .04
Ba^+	1.18 ± .10[a]	Tl^+	.89 ± .04

[a] Experimental data available for only one gaseous molecule.

In Tables II and III are summarized the results of the calculations performed. Values for internuclear distances obtained by addition of gaseous ionic radii were checked in many cases by calculation using the formulas of Guggenheimer[7] and found to be generally consistent. Agreement between r_{obsd} and r_{add} values is good in most cases where experimental data are available. From the binding energy viewpoint, the quantities to be compared are the last columns, $U_{\text{ionic}}^{\text{exp}}$ and $U_{\text{ionic}}^{\text{calcd}}$.

Conclusions

It is evident from a consideration of values for $U_{\text{ionic}}^{\text{exp}}$ that many of these molecules deserve further study. Generally speaking when a range of values is given the lower limit is set by the dissociation energy proposed by Gaydon[6] who pointed

TABLE II

Gaseous molecule	r_{exp},[a] Å.	r_{add}, Å.	$U_{\text{ionic}}^{\text{exp}}$, kcal./mole	$U_{\text{ionic}}^{\text{calcd}} = e^2/r$, kcal./mole
BeH	1.343	1.36	250	247
MgH	1.7306	1.75	205–216	191
CaH	2.002	2.01	163	166
SrH	2.145	2.14	158	155
BaH	2.232	2.23	144	149
BeF	1.3614	1.35	224–256	244
MgF	(1.752)	1.74	167–190	189
CaF	(2.02)	2.00	141	164
SrF		2.13	110–128	155[b]
BaF		2.22	106–124	149
BeCl	(1.7)	1.90	197–227	195
MgCl		2.29	151–163	144[b]
CaCl	(1.86)	2.55	118	178
SrCl		2.68	102–113	123[b]
BaCl		2.77	79– 95	120[b]
BeBr		2.05		161[b]
MgBr		2.44	153–172	135[b]
CaBr		2.70	127	122[b]
SrBr		2.83	114	117[b]
BaBr		2.92	103	113[b]
BeI		2.33		142[b]
MgI		2.72		122[b]
CaI		2.98	126–132	111[b]
SrI		3.11	104–108	106[b]
BaI		3.20		103

[a] ( ) enclose values for r_{exp} which are uncertain. [b] Values of $U_{\text{ionic}}^{\text{calcd}}$ computed using r_{add}; all other values were computed using r_{exp}.

TABLE III

Gaseous molecule	r_{exp},[a] Å.	r_{add}, Å.	$U_{\text{ionic}}^{\text{exp}}$, kcal./mole	$U_{\text{ionic}}^{\text{calcd}} = e^2/r$, kcal./mole
BH	1.233	1.22	243–254	269
AlH	1.646	1.62	188	201
GaH		1.66		199[b]
InH	1.838	1.85	175	180
TlH	1.870	1.94	170–174	177
BF	1.262	1.21	304	263
AlF		1.61	203	205[b]
GaF		1.65	201	200[b]
InF		1.84	182	180[b]
TlF		1.93	167	171[b]
BCl	1.7157	1.76	185–229	193
AlCl	2.138	2.16	161	155
GaCl	2.20	2.20	167	150
InCl	2.318	2.39	154	142
TlCl	2.541	2.48	142	130
BBr	1.887	1.91	214	175
AlBr	2.295	2.31	147	144
GaBr		2.35	120–138	140[b]
InBr	2.57(e)	2.54	127	129
TlBr	2.68(e)	2.63	134	123
BI		2.17		152[b]
AlI		2.59	132	128[b]
GaI		2.63	132	126[b]
InI	2.86(e)	2.82	123	116
TlI	2.87(e)	2.91	128	115

[a] (e) internuclear distance from electron diffraction studies. [b] Values of $U_{\text{ionic}}^{\text{calcd}}$ computed using r_{add}; all other values were computed using r_{exp}.

---

(6) A. G. Gaydon, "Dissociation Energies," John Wiley and Sons, Inc., New York, N. Y., 1947.

(7) K. Guggenheimer, *Proc. Phys. Soc.*, **58**, 456 (1946).

out that the linear Birge–Sponer extrapolations for molecules containing alkaline earth atoms (using data on the hydrides) are often much too high; Herzberg[5] has usually listed dissociation energies obtained by linear extrapolations.

In certain cases more recent data have been used for obtaining $U_{\text{ionic}}^{\text{exp}}$. Most important is that of the aluminum halides which have recently been studied extensively.[8] The new data agree very nicely with the calculated binding energies while older data are completely unacceptable. Chretien[9] has presented new work on gaseous boron halides; Levin and Winans[10] have studied gallium chloride; and Welti and Barrow[11] have studied GaF and InF.

Values of e^2/r correlate fairly well with $U_{\text{ionic}}^{\text{exp}}$ and it appears that, with a probable error of less than ±12 kcal./mole, one may approximate the binding energy of any of the molecules of these groups. In view of the generally good correlation, it is interesting to examine the situation where maximum deviation between $U_{\text{ionic}}^{\text{exp}}$ and $U_{\text{ionic}}^{\text{calcd}}$ occurs, namely, CaCl. The value for the internuclear distance estimated by Herzberg is 1.86 Å. but this distance is inconsistent with that calculated by additivity from ionic radii. The additivity value is 2.55 Å. and this gives an e^2/r value of 130 kcal./mole, about 12 kcal./mole higher than $U_{\text{ionic}}^{\text{exp}}$ but quite reasonable. Other large deviations, as yet unexplained, are observed for SrF, BaF, BaCl, MgBr, BF, BCl and BBr although polarization effects and uncertainties in D(MX) values are large in these cases. The internuclear distance suggested for BeCl from spectroscopic data is also lower than that calculated from addition of ionic radii.

An attempt was made to refine the calculation of $U_{\text{ionic}}^{\text{calcd}}$ by consideration of polarization and repulsion effects as was done for the alkali halides and hydrides but the large uncertainties in calculated values for the polarizabilities of the plus-one Group II and Group III ions made such a refinement of little value.

One important use of this correlation, besides its application in critical evaluation of available experimental data, is to allow prediction of ionic binding energies and dissociation energies for molecules which are incompletely characterized or as yet unobserved. In Table IV are presented estimates for internuclear distances, ionic binding energies, (e^2/r), and dissociation energies into atoms for BeBr, BeI, MgI, BaI, BI and GaH. It is apparent that certain of these molecules should be easily obtained in high concentration by use of well known experimental techniques.

Table IV

Molecule	r_{add}, Å.	$U_{\text{ionic}}^{\text{calcd}}$, kcal./mole	$D(\text{MX}) \rightarrow$ atoms, kcal./mole
BeBr	2.05	161	27
BeI	2.33	142	0
MgI	2.72	122	19
BaI	3.20	103	56
BI	2.19	151	34
GaH	1.66	199	78

---

(8) (a) P. Gross, C. Campbell, P. Kent and D. Levi, *Disc. Faraday Soc.*, (No. 4) 206 (1948); (b) L. M. Foster, A. S. Russel and C. N. Cochran, *J. Am. Chem. Soc.*, **72**, 2850 (1950); (c) F. Irmann, *Helv. Chim. Acta*, **33**, 1449 (1950); (d) M. Heise and K. Wieland, *ibid.*, **34**, 2182 (1951).

(9) M. Chretien, *Helv. Phys. Acta*, **23**, 259 (1950).

(10) F. Levin and J. G. Winans, *Phys. Rev.*, **77**, 741 (1949); *ibid.*, **84**, 431 (1951).

(11) D. Welti and R. F. Barrow, *Nature*, **168**, 161 (1951); *Proc. Phys. Soc.*, **65A**, 629 (1952).

WETTABILITY OF HALOGENATED ORGANIC SOLID SURFACES

By A. H. Ellison and W. A. Zisman

Surface Chemistry Branch, Chemistry Division, Naval Research Laboratory, Washington, D. C.

Received October 15, 1953

Wettability of solid surfaces containing covalent chlorine increases greatly with the chlorine content. There is no indication of hydrogen-bonding at the solid/liquid interface for surfaces containing carbon, hydrogen and chlorine. A close-packed monolayer of perchloro-2,4-pentadienoic acid adsorbed on a polished metal is shown to behave with respect to wetting like an organic surface comprising 100 atom per cent. of chlorine substitution. Increased wettability of fluorine-containing surfaces by hydrogen-bonding liquids is reported for a number of new, partially fluorinated plastic surfaces. The wettability of fluorinated surfaces varies with the type of spreading liquid. For non-polar liquids the wettability decreases with increasing fluorine substitution. For hydrogen-bonding liquids, the wettability increases in the order: polytetrafluoroethylene, polytrifluoroethylene, polyethylene, polyvinylidene fluoride and polyvinyl fluoride. The corresponding order for the halogenated liquids is polytetrafluoroethylene, polytrifluoroethylene, polyvinylidene fluoride, polyethylene and polyvinyl fluoride. Explanations are offered for the relation between wettability and the atom per cent. fluorine substitution in the surface based on the electronegativity of the fluorine atoms in the surface and the molecular structure of the spreading liquid.

Introduction

It has been shown in previous studies[1–6] that the wettability of a smooth solid surface is determined by the atomic composition of the surface and that the equilibrium contact angle (θ_E) for a given liquid is a reproducible and valuable measure of the wettability of a wide variety of surfaces. It has also been shown that the cosine of θ_E for a homologous series of liquids on a given surface increases linearly with decreasing liquid surface tension (γ_{LV°), while a linear relation holds approximately for most non-homologous liquids. But marked deviations from linearity have been observed with fluorinated sur-

---

(1) H. W. Fox and W. A. Zisman, *J. Colloid Sci.*, **5**, 514 (1950).

(2) *Ibid.*, **7**, 109 (1952).

(3) *Ibid.*, **7**, 428 (1952).

(4) E. G. Shafrin and W. A. Zisman, *ibid.*, **7**, 166 (1952).

(5) F. Schulman and W. A. Zisman, *ibid.*, **7**, 465 (1952).

(6) H. W. Fox, E. F. Hare and W. A. Zisman, *ibid.*, **8**, 194 (1953).

TABLE I

WETTABILITY VALUES FOR CHLORINATED SURFACES (20°)

Liquids		Surfaces							
		Perchloropentadienoic acid monolayer		Polyvinylidene chloride		Polyvinyl chloride		Polyethylene[a]	
	$\gamma_{LV°}$, dynes/cm.	θ_E, degrees	$\gamma_{LV°}(1 + \cos\theta_E)$, ergs/cm.^{2}	θ_E, degrees	$\gamma_{LV°}(1 + \cos\theta_E)$, ergs/cm.^{2}	θ_E, degrees	$\gamma_{LV°}(1 + \cos\theta_E)$, ergs/cm.^{2}	θ_E, degrees	$\gamma_{LV°}(1 + \cos\theta_E)$, ergs/cm.^{2}
Water	72.8	66	103.0	80	85.4	87	76.6	94	67.7
Glycerol	63.4	56	98.8	61	94.2	67	88.2	79	75.5
Formamide	58.2	32[b]	...	61	86.4	66	81.8	77	71.3
Methylene iodide	50.8	34	92.9	29	95.2	36	91.9	52	82.1
α-Bromonaphthalene	44.6	<5	>89.0	9	88.6	11	88.4	35	81.1
Tricresyl phosphate	40.9	<5	>81.6	10	81.2	14	80.6	34	74.8

[a] Data from reference 3. [b] Attacks layer.

faces when the conditions for hydrogen-bonding existed at the solid/liquid interface.[7] In the investigation reported here, these conditions have been studied further. Also of interest in their own right are the data presented on: (a) the wettability of surfaces containing chlorine and hydrogen atoms in which the atom per cent. of chlorine substitution is systematically varied from 0 to 100%, and (b) the wettability of some new plastic surfaces containing only fluorine and hydrogen in which the atom per cent. of fluorine substitution is systematically varied.

Materials and Procedures.—Plane surfaces of solid polyethylene, unplasticized polyvinyl chloride and polyvinylidene chloride contain 0, 25 and 50 atom per cent. of chlorine. A 100% chlorinated surface would be that of polytetrachloroethylene, but that polymer has never been prepared (presumably because of steric hindrances). However, we were successful in preparing on platinum foil a close-packed monolayer of perchloro-2,4-pentadienoic acid (subsequently referred to as perchloropentadienoic acid) with each molecule adsorbed *via* the carboxylic acid group. Evidently, the $-CCl_2$ terminal groups of the molecules in this film form a surface comprising only chlorine atoms. Since our previous work had shown repeatedly that the wetting properties were not significantly affected by atoms beneath the surface layer, it was inferred that this monolayer would act like an organic solid containing 100 atom per cent. of covalent substituted chlorine. The series of fluorinated surfaces studied comprised the following unplasticized polymers: polyethylene, polyvinyl fluoride, polyvinylidene fluoride, polytrifluoroethylene and polytetrafluoroethylene.

Polyvinyl chloride, polyvinylidene chloride, polyvinylidene fluoride and polytrifluoroethylene in the powdered form were molded into discs approximately 1" in diameter and $^1/_4$" thick using minimum molding temperatures to prevent charring. Smooth, grease-free surfaces of these plastics were obtained as previously described[8] by abrasion under water followed by heat-polishing against the smooth, clean surface of a $^3/_4$" thick acid-cleaned glass block. Polyvinyl fluoride, which was obtainable only as a thin translucent sheet (0.0025" thick), could not be abraded satisfactorily. Therefore, it was heat-polished and cleaned with a concentrated solution of the detergent "Tide." This procedure had been shown to give clean surfaces in boundary-friction studies[8,9]; in the present study this method resulted in surfaces which were identical in wettability with those prepared by abrasion and casting. The perchloropentadienoic acid used was recrystallized as a white flaky solid having a melting point of 123.5–124.0° which is in good agreement with a previously reported value.[10] Close-packed monolayers of this strong acid were formed (using previously described methods) on a freshly flamed platinum foil by adsorption from a saturated aqueous solution.[11]

The spreading liquids used and the methods of measuring θ_E have been described earlier.[1] The contact angle reported in each case is the average of at least four independent measurements made on two separately prepared surfaces; the average deviation from the mean was ±2°.

Results for Chlorinated Surfaces.—From earlier studies of the boundary frictional properties of these plastic surfaces,[8,9] it was concluded that the chlorinated surfaces had much higher adhesional energies than analogous hydrocarbon surfaces. Also, the surface energies of the chlorinated surfaces reported would be much higher than those of the hydrocarbon surfaces reported earlier.[3] Most liquids would be expected to spread readily on these chlorinated surfaces because one would expect that $W_A > W_C$. These conjectures were found correct, for only liquids having surface tensions greater than 40 dynes/cm. exhibited non-zero contact angles on these surfaces.

The results for the chlorinated surfaces are given in Table I. Some of the data for polyethylene surfaces reported earlier[3] are included for reference and comparison. The liquids are arranged in order of decreasing surface tension; for each liquid the value of $\gamma_{LV°}$ is tabulated as well as the experimental value of θ_E and the approximate work of adhesion calculated from the Young–Dupre equation, $W_A = f_{SV°} + \gamma_{LV°}\ (1 + \cos\theta_E)$, assuming that $f_{SV°}$ is negligible[1, 2] for each surface. Only six liquids were used due to the scarcity of pure stable liquids in the required high surface tension range. For a given liquid on the various chlorinated surfaces, θ_E increases as the atom per cent. chlorine substitution in the surface decreases, showing the increased affinity of the solid for the liquid as the chlorine content of the surface increases. Consistent with the findings reported in prior studies,[1–7] θ_E decreases with decreasing liquid surface tension for each solid surface.

Figure 1 shows the relationship between $\gamma_{LV°}$ and $\cos\theta_E$ for the several liquids on the three chlorinated surfaces. The relationship is best represented by a narrow rectilinear band. In Fig. 2 the relation between $\cos\theta_E$ and the atom per cent. chlorine substitution in the surface is shown for each of the liquids. The fact that smooth curves fit all the graphical points including the 100% point obtained from contact angle measurements on the perchloropentadienoic acid monolayer, justified our inclusion of the latter surface in the series

---

[7] A. H. Ellison, H. W. Fox, and W. A. Zisman, THIS JOURNAL, **57**, 622 (1953).

[8] R. C. Bowers, W. C. Clinton and W. A. Zisman, *J. Appl. Phys.*, **24**, 1066 (1953).

[9] R. C. Bowers, W. C. Clinton and W. A. Zisman, *Lubrication Engineering*, **9**, 204 (1953).

[10] J. S. Newcomer and E. T. McBee, *J. Am. Chem. Soc.*, **71**, 946 (1949).

[11] H. R. Baker, E. G. Shafrin and W. A. Zisman, THIS JOURNAL, **56**, 405 (1952).

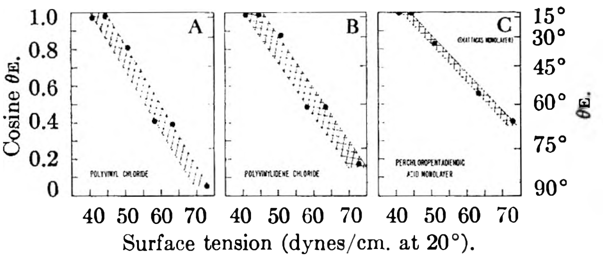

Fig. 1.—Cos θ_E *vs.* γ_{LV}° for various liquids on surfaces of: A, polyvinyl chloride; B, polyvinylidene chloride; C, a close-packed monolayer of perchloropentadienoic acid.

of chlorinated surfaces. In general, the initial slope of each curve in Fig. 2 decreases with increasing surface tension.

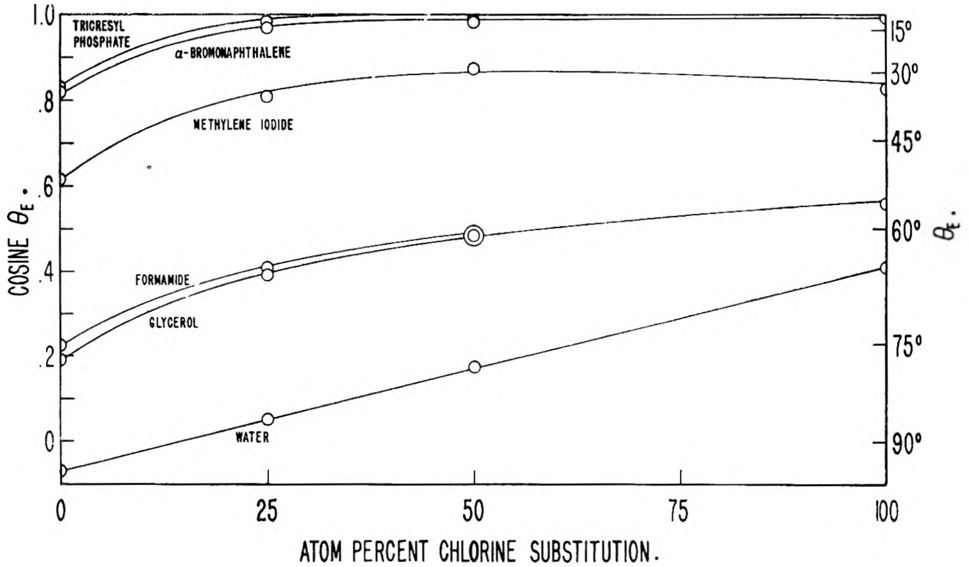

Fig. 2.—Cos θ_E for various liquids *vs.* atom per cent. chlorine substitution in the solid surface.

Results for Fluorinated Surfaces.—Although the replacement of covalent hydrogen atoms by chlorine atoms in the surface leads to increased friction[8,9] and greater wettability, the reverse is true for fluorinated surfaces not only for the friction,[8,9] but also for the wettability. Thus the number of non-spreading liquids should be greater for these surfaces than for the chlorinated surfaces.

In Table II the results for the fluorinated surfaces have been summarized in the same manner as in Table I for the chlorinated surfaces. With few exceptions, the contact angle on a given surface increases with increasing surface tension of the liquid. Several features of Table II are noteworthy. In going from 0 to 25 atom per cent. fluorine substitution, the contact angle for a given hydrocarbon liquid always increases. This is exemplified by the results obtained with benzene and *t*-butylnaphthalene. In the same region the contact angle for a given polar liquid decreases as the per cent. fluorination increases as shown by water, formamide and glycerol. But in going from 25 to 100 atom per cent. fluorine substitution, the contact angles increase for all liquids studied. Finally, it should be noted that the contact angles for the two diesters, bis-(2-ethylhexyl) phthalate and bis-(2-ethylhexyl) sebacate, are considerably greater on polytetrafluoroethylene than on polytrifluoroethylene. .

The relation between cosine θ_E and γ_{LV}° is graphed in Fig. 3 for the three fluorinated surfaces not previously investigated. Again, the relationships are best represented by narrow rectilinear bands. The width of each band is believed related to the variation of the solid/liquid interfacial tensions of the several liquids plotted in the band.

When the cosine of the contact angle for each liquid is plotted against the atom per cent. fluorine substitution in the surface, several distinct types of curves result (Figs. 4 and 5). The position of the curve with respect to the axis of ordinates is determined by the surface tension of the liquid and follows the general rule shown in Fig. 3 that high surface tension liquids display the highest contact angles. Figure 4A is typical of such strongly hydrogen-bonding liquids as water, formamide and glycerol. The curve in Fig. 4B for α-bromonaphthalene is similar to that for methylene iodide and presumably is typical of non-hydrogen-bonding polar liquids. The curve for benzyl phenylundecanoate in Fig. 5A is similar to that for tricresyl phosphate. These liquids are alike in that each has only one oxygen atom sterically available for hydrogen-bonding with a suitable surface. Bis-(2-ethylhexyl) sebacate exhibits a curve almost identical with the one shown for bis-(2-ethylhexyl) phthalate in Fig. 5B. These liquids have in com-

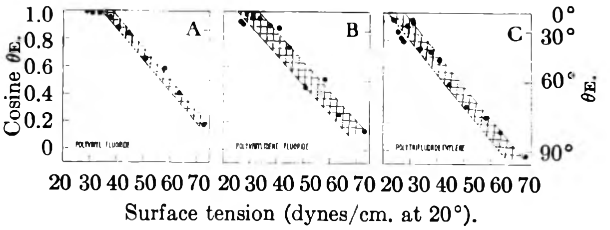

Fig. 3.—Cos θ_E *vs.* γ_{LV}° for various liquids on surfaces of: A, polyvinyl fluoride; B, polyvinylidene fluoride; C, polytrifluoroethylene.

TABLE II

WETTABILITY VALUES FOR FLUORINATED SURFACES (20°)

Liquids		Surfaces: Polytetrafluoroethylene[a]		Polytrifluoroethylene		Polyvinylidene fluoride		Polyvinyl fluoride		Polyethylene[b]	
	γ_{LV°, dynes/cm.	θ_E, degrees	$\gamma_{LV^\circ}(1 + \cos\theta_E)$, ergs/cm.^{2}	θ_E, degrees	$\gamma_{LV^\circ}(1 + \cos\theta_E)$, ergs/cm.^{2}	θ_E, degrees	$\gamma_{LV^\circ}(1 + \cos\theta_E)$, ergs/cm.^{2}	θ_E, degrees	$\gamma_{LV^\circ}(1 + \cos\theta_E)$, ergs/cm.^{2}	θ_E, degrees	$\gamma_{LV^\circ}(1 + \cos\theta_E)$, ergs/cm.^{2}
Water	72.8	108	50.3	92	70.3	82	82.9	80	85.4	94	67.7
Glycerol	63.4	100	52.4	82	72.2	75	79.8	66	89.2	79	75.5
Formamide	58.2	92	56.2	76	72.2	59	88.2	54	92.4	77	71.3
Methylene iodide	50.8	88	51.6	71	67.4	63	73.9	49	84.2	52	82.1
α-Bromonaphthalene	44.6	73	57.6	61	66.2	42	77.7	33	82.0	35	81.1
Tricresyl phosphate	40.9	75	51.5	49	67.7	28	77.0	28	77.0	34	74.8
Benzyl phenylundecanoate	37.7	67	52.6	44	64.8	26	71.6	17	73.8	28	71.0
t-Butylnaphthalene	33.7	65	48.0	42	58.7	18	65.8	10	66.9	7	67.2
Bis-(2-ethylhexyl) phthalate	31.2	63	45.4	22	60.1	17	61.0	9	62.0	5	62.3
Bis-(2-ethylhexyl) sebacate	31.1	62	45.7	18	60.7	13	61.4	10	61.7		
Benzene	28.9	46	49.0	25	55.1	11	57.3	7	57.6	<5	
n-Hexadecane	27.6	46	46.8	37	49.7	24	52.8	Spr[c]		Spr	
n-Tetradecane	26.7	44	45.9	35	48.6	22	51.5	Spr		Spr	
n-Dodecane	25.4	42	44.3	30	47.4			Spr		Spr	
n-Decane	23.9	35	43.5	18	46.6			Spr		Spr	

[a] Data from reference 1. [b] Data from reference 3. [c] Spr = liquid spreads ($\theta = 0°$).

mon two oxygen atoms accessible for hydrogen-bonding with a suitable surface. The curve for *t*-butylnaphthalene in Fig. 5C is much like that for benzene, and presumably this is characteristic of aromatic hydrocarbon liquids. The behavior of non-polar liquids like the *n*-alkanes is exemplified by the straight line graph for *n*-hexadecane of Fig. 5(D).

It is interesting to compare the wettability data given here for the surface of polyvinylidene fluoride with corresponding data given earlier[2] for a 50–50 copolymer of ethylene and tetrafluoroethylene. For polar liquids the contact angles are higher on the 50–50 copolymer, while the reverse is true for the non-polar *n*-alkanes. Unpublished friction data for polyvinylidene fluoride also differ from those reported for the 50–50 copolymer.[8,9]

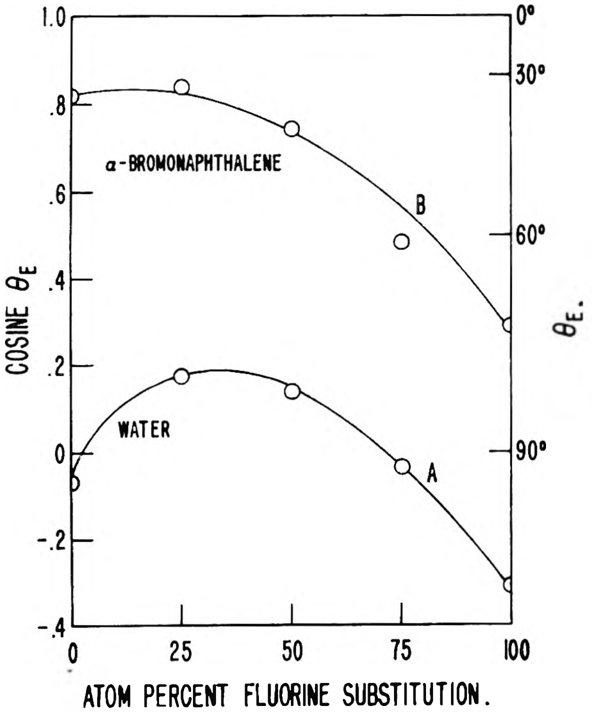

Fig. 4.—Cos θ_E of water and α-bromonaphthalene *vs.* atom per cent. fluorine substitution in the solid surface.

Discussion

It has been demonstrated that the wettability of a smooth solid surface containing covalent hydrogen and chlorine atoms is increased as the atom per cent. of chlorine substitution is increased.

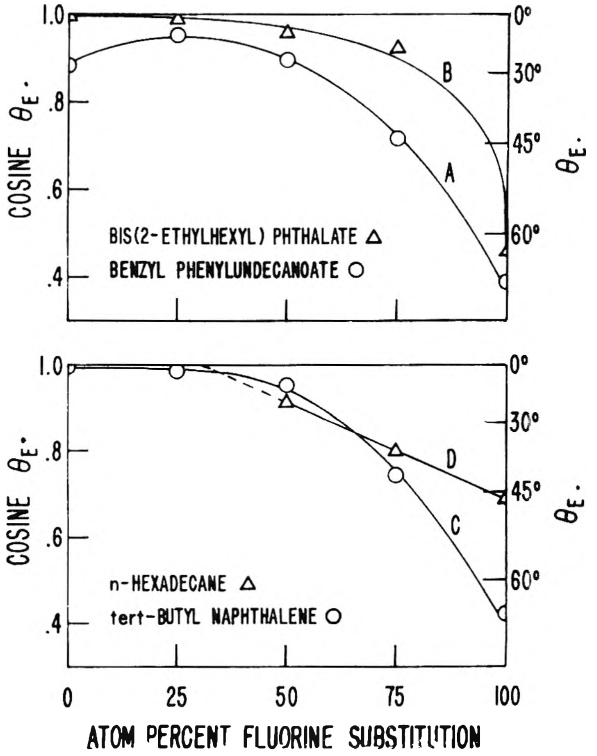

Fig. 5.—Cos θ_E of various liquids *vs.* atom per cent. fluorine substitution in the solid surface.

Ample evidence has been given for treating the surface of a perchloropentadienoic acid monolayer on platinum as a 100% chlorinated organic solid which behaves with respect to wetting properties entirely analogously to the series polyethylene, polyvinyl chloride and polyvinylidene chloride.

No marked difference was observed in the behavior of hydrogen-bonding liquids and non-hydrogen-bonding liquids on the chlorinated surfaces. This is shown clearly in Fig. 2 where the shapes of the curves for glycerol and methylene iodide are very similar. Also, the graphs in Fig. 1 do not curve in the high surface tension region as has been observed[7] when hydrogen-bonding occurs. According to Pauling,[12] the hydrogen-bonding ability of chlorine is weak, probably because the chlorine atom is significantly larger than the other atoms having equal or larger electronegativity values. It is concluded that hydrogen-bonding is not significant at the solid/liquid interface when the solid surface contains only covalent chlorine and hydrogen atoms.

The wettability data for the fluorinated plastics not previously reported are consistent with earlier data relating to other homologous fluorinated surfaces. The measurements recorded in Table II fill in gaps in our knowledge so that it is now possible to study the effect of varying the atom per cent. fluorine substitution for values of 0, 25, 50, 75 and 100%.

The first striking feature evident in Table II is that the contact angle for a polar liquid is less on polyvinyl fluoride than it is on polyethylene while the reverse is true for the non-polar liquids. This may be caused by an abnormally low solid/liquid interfacial tension (γ_{SL}) in the case of the polar liquids on polyvinyl fluoride. Table II shows that the replacement of hydrogen atoms by fluorine atoms renders the surfaces more non-wettable by non-polar liquids. As in the previous paper,[7] the contact angle differences which are to be explained are far greater than the experimental error.

Although γ_{SL} cannot be measured at present, we know from a consideration of liquid/liquid interfacial tensions that it decreases as the solubility or attraction of the two phases increases. This attraction varies considerably from one type of liquid to another. For example, γ_{SL} decreases when the two phases are of like molecular species[3] or when hydrogen-bonding exists between the two phases.[7] Reasons are given below for concluding that the latter mechanism is involved in the case of the hydrogen-bonding liquids on the fluorinated surfaces.

In the special case of the *n*-alkanes the relation between cos θ_E and F, the atom per cent. fluorine substitution, is linear (Fig. 5D). The Young equation for the liquid L, forming equilibrium contact angle θ_E, with the solid S, all in equilibrium with the saturated vapor of the liquid V°, is

$$\gamma_{SV^\circ} - \gamma_{SL} = \gamma_{LV^\circ} \cos \theta_E \qquad (1)$$

where γ is the surface free energy of the interface indicated by the subscripts. Now γ_{LV° = constant = K for the systems to be compared. Assuming that γ_{SV° for a non-spreading liquid is nearly the same as γ_{S° (the surface free energy of the solid in a vacuum) and rearranging equation 1, there results

$$\gamma_{S^\circ} = K \cos \theta + \gamma_{SL} \qquad (2)$$

If we make the reasonable assumptions that γ_{S° and γ_{SL} are each linear functions of the atom per cent. of fluorine in the surface, *i.e.*, $\gamma_{S^\circ} = a + bF$ and $\gamma_{SL} = \alpha + \beta F$ where b is negative and β is small and positive, equation 2 reduces to

$$F = K'' \cos \theta + A \qquad (3)$$

where K'' and A are constants. Equation 3 predicts the experimentally observed straight line (see Fig. 5D).

The linear relationship for water on the chlorinated surfaces (see Fig. 2) may be treated in the same fashion. The experimentally observed positive slope can be rationalized in this case on the basis of the reasonable assumption that γ_{S° is a linear *increasing* function of the atom per cent. of chlorine in the surface. In the case of the liquids which do not give linear relationships in Figs. 2, 4 and 5, one or more of the above assumptions are not valid. It is believed that the third assumption ($\gamma_{SL} = \alpha + \beta F$), contains the greatest error and the second (γ_{S° is a linear function of the atom per cent. halogen in the surface) contains the smallest error.

The other extreme of behavior is that of the highly polar hydrogen-bonding liquids and it is exemplified by the results for water in Fig. 4A. In the range $F = 0$ to $F = 25$ there is an increase in wettability with increased substitution of F atoms for H atoms. Here the conditions are suitable for hydrogen-bonding to occur at the solid/liquid interface for the appropriate liquids as we have pointed out earlier.[7] Briefly, for the hydrogen bond, A–H. . . .B, to form, A and B must be electronegative atoms one of which is more electronegative and the other less electronegative than their normal values. In the studies reported here B is a fluorine atom in the plastic surface and A-H is the hydrogen-donating group of the spreading liquid.

However, the relative electronegative character of a fluorine atom attached to a carbon atom depends upon the other substitutions made on the same carbon atom. It is reasonable from qualitative consideration of the electron displacements to conclude that the relative electronegativity of a fluorine atom attached to a carbon atom should decrease with increasing fluorine substitution even though the electronegativity of the entire group increases. Since the strength of a hydrogen bond depends on the relative electronegativity of each fluorine atom, a decrease in wettability by the hydrogen-bonding liquids is to be expected with further fluorine substitution. It should be noted that the decrease in wettability above 50 atom per cent. fluorine substitution is at a different rate for the hydrogen-bonding liquids than for the *n*-alkanes.

As for the esters, B of the above scheme would be an oxygen atom of the ester linkage and A a carbon atom attached to a hydrogen atom in the surface of the polymer. Such a carbon atom would be less electronegative than normally as a result of the

---

[12] L. Pauling, "The Nature of the Chemical Bond," Cornell University Press, Ithaca, New York, 1945.

very electronegative fluorine atoms attached to it or to the adjacent carbon atom and the hydrogen atom somewhat acidic.

We are concerned here with the inductive effect of the fluorine atoms on the appropriate carbon atom of the plastic. Henne has proposed a working hypothesis to explain the directing effect of the CF_3 and CF_2 groups in the vapor chlorination of polyfluorides.[13] He postulated that the CF_3 group and to a lesser extent the CF_2 group cause the hydrogen atoms on a carbon atom alpha to the CF_3 or CF_2 group to be acidic. It is not unreasonable, therefore, that the esters behave nearly like non-hydrogen-bonding liquids on the 0 to 25% fluorinated surfaces and like hydrogen-bonding liquids on the 75% fluorinated surface. The curves for the esters containing only one sterically available oxygen atom (Fig. 5A) resemble the curve for water in the region of $F = 75\%$. The difference in Fig. 5B for diesters and Fig. 5A for the monoesters is presumably caused by the existence of two hydrogen bonds per molecule of diester. An aromatic group in the molecule of ester has minor effect on the wettability here, for the results for the aliphatic diester bis-(2-ethylhexyl) sebacate are nearly identical with those of Fig. 5B for the phthalate diester.

The curves typified by α-bromonaphthalene (Fig. 4B) and *t*-butylnaphthalene (Fig. 5C) represent intermediate strengths of interaction between fluorinated solids and the spreading liquids. For the former we suggest a dipole–dipole interaction and for the latter the proton-donating ability of the aromatic nucleus.[14] An interesting result is obtained by drawing a straight line between the 0% point and the 100% point of the curves in Figs. 4B, 5A, 5B and 5C. The resulting straight line has nearly the same slope as the experimental straight line for the *n*-alkanes shown in Fig. 5D and would, therefore, appear to indicate what the relationship would be for these liquids in the absence of the interactions at the solid/liquid interface. The curve for the strong hydrogen-bonding liquids does not give the same result since these liquids interact with the fully fluorinated surface as well as the partially fluorinated surfaces.

It is clear from the data that the polyvinylidene fluoride and the 50–50 copolymer of ethylene and tetrafluoroethylene behave very differently. The average structure of the copolymer is an aliphatic chain of alternating C_2F_4 and C_2H_4 groups. Vinylidene fluoride may polymerize head-to-head, tail-to-tail, head-to-tail, or randomly. The first leads to the same structure as the average structure for the copolymer, the second results in an aliphatic chain of alternating CF_2 and CH_2 groups, and the last a mixture of the first two. The difference between the average structure of the copolymer and either the head to tail or random structure of vinylidene fluoride do not seem sufficient to account for the rather large differences in behavior that have been observed. However, without knowledge of the precise structure of these polymers further discussion is unwarranted.

The marked dependence of the wetting and frictional properties upon the halogen content of the surface[8,9] is good evidence that the halogen atoms of these polymers are exposed at the surface, for if they were buried these surfaces would have frictional and wetting properties closely approximating those of polyethylene.

In the fluorinated polymers the fluorine atoms must be located as much as possible in the surface because thereby the surface energy is reduced to a minimum. Earlier studies[2,5] have demonstrated that a surface containing covalent fluorine atoms has a lower surface energy than the corresponding hydrocarbon surfaces. The results presented here agree fully with these conclusions. But this reasoning does not hold for the chlorinated polymers because the substitution of covalent chlorine atoms for hydrogen atoms would increase the surface energy. However, chlorine atoms are much larger than hydrogen atoms, and they will be squeezed into positions in the surface whenever the cohesive forces between the polymer chains can thereby reduce the volume density and so make the *total energy* of the plastic a minimum.

Acknowledgments.—We are indebted to The B. F. Goodrich Chemical Company for the polyvinyl chloride, The Dow Chemical Company for the polyvinylidene chloride, Dr. Gouchenour of the Hooker Electrochemicals Company for the perchloropentadienoic acid, and the M. W. Kellog Company for the polyvinylidene fluoride and the polytrifluoroethylene; their coöperation is sincerely appreciated. Suggestions of H. W. Fox in the preparation of the plastic surfaces, and in discussions of the data are also appreciated.

---

[13] A. L. Henne, J. B. Hinkamp and W. J. Zimmerschied, *J. Am. Chem. Soc.*, **67**, 1906 (1945).

[14] M. Tamres, *ibid.*, **74**, 3375 (1952).

VARIATION OF THE MICHAELIS CONSTANT WITH THE CONCENTRATIONS OF THE REACTANTS IN AN ENZYME-CATALYZED SYSTEM[1]

By LLOYD L. INGRAHAM AND BENJAMIN MAKOWER
Western Regional Research Laboratory,[2] Albany, Calif.

Received October 17, 1953

An analysis has been made of the kinetics of an enzymatic system of two reactants to determine the dependence of the Michaelis constant on the concentrations of the reactants. Two previously suggested types of mechanism were examined. One type involves the familiar binary complex of the enzyme with one of the reactants; the other involves a ternary complex with both reactants. For the ternary complex type of mechanism consideration was given to four cases: (a) two mechanisms of formation of the ternary complex wherein the reactants combine with the enzyme in an ordered or in a random sequence; and to (b) two reaction conditions, equilibrium or steady-state. It was shown that for each of the above four cases there are four distinct experimental conditions under which the reaction kinetics can be studied according to the Michaelis–Menten analysis for maximal rates and that these four conditions give rise to three different expressions for maximal velocities and four different expressions for Michaelis constants. The four experimental conditions arise from the variation of the concentration of either reactant, while the other reactant's concentration is kept constant and is either at, or below, the concentration required for maximal rate. From the derived rate laws for the different experimental conditions, it was found that in only two out of the four conditions (one of the reactants present in large excess) is the expression for the Michaelis constant analogous in form and meaning to that for the binary enzyme–substrate complex, frequently described. Under the other two conditions (both reactants at limited concentrations), both the maximal velocity and the Michaelis constant for one reactant, vary with the concentration of the other reactant. This kind of variation (with the other reactant) is also expected for reactant concentrations required to give any fraction of the maximal velocity. This means that, in practice, such a variation may also be found in the experimental concentration of a given reactant required to produce a rate approximately independent of that reactant. Recently published data on the kinetics of lipoxidase and glucose oxidase are offered as examples of some of these predicted variations. Furthermore, the previously proposed binary-complex type of mechanism for glucose oxidase is ruled out and a ternary-complex type is offered as a reasonable possibility. It is also shown that the concept of a ternary complex is not essential for the explanation of the kinetics of two reactants. A more generalized formulation involving a modified form of the enzyme might be applicable instead.

Our recently published[3] and continuing investigations on the enzymatic browning of fruits have led us to a consideration of the significance of the experimentally determined Michaelis constants in enzyme systems which involve two reactants (substrates) at limited concentrations. As already pointed out by LuValle and Goddard[4] most enzyme systems involve at least two reactants, but one of them frequently is present in large excess (as might be the case when water is one of the reactants in a hydrolytic reaction) and the systems can then be analyzed by the familiar Briggs and Haldane[5] treatment in terms of a binary enzyme–substrate complex.

When both reactants are present at relatively low concentration, the above treatment has been reported to give anomalous variations, as large as seven to tenfold, in the measured Michaelis constant, with the concentration of one of the reactants.[6]

No satisfactory explanation has yet been offered to account for these variations in terms of the kinetics that might hold for such systems.

It is the purpose of this paper to present such an explanation. The variations noted above will be accounted for in terms of a reaction mechanism which involves the formation of a ternary complex of the enzyme with the two reactants. It will also be shown that the meaning of the measured Michaelis constant is analogous to that for a binary enzyme–substrate complex only under certain limited experimental conditions.

Rate Laws and Their Significance, for a Two Reactant System Involving a Ternary Complex.—Several investigators previously have postulated the existence of ternary complexes of enzymes with two reactants,[4,7,8] with one reactant and an activator or coenzyme,[9,10,11] and with one reactant and an inhibitor.[12]

The kinetics for two reactants have been deduced for the equilibrium condition by Laidler and Socquet,[13] and were extended to the steady-state conditions by Segal, Kachmar and Boyer.[14]

Some of the rate laws derived by these authors will serve as a basis for the discussions which are to follow. These laws were therefore collected, together with some new derivations, in Table I. The previously derived expressions, have been appropriately revised so as to present all the results in terms of uniform symbols and definitions. Two mechanisms of formation of a ternary complex of reactants A and B with enzyme E have been considered. Mechanism I requires that reactant A combines with the enzyme before reactant B. Mechanism II is a generalized form of I to include

---

(1) Presented at A.C.S. meeting, Chicago, Sept. 6–11, 1953.

(2) Bureau of Agricultural and Industrial Chemistry, Agricultural Research Administration, U. S. Department of Agriculture.

(3) L. L. Ingraham, J. Corse and B. Makower, *J. Am. Chem. Soc.*, **74**, 2623 (1952).

(4) J. E. LuValle and D. R. Goddard, *Quart. Rev. Biol.*, **23**, 197 (1948).

(5) G. E. Briggs and J. B. S. Haldane, *Biochem. J.*, **19**, 338 (1925).

(6) (a) H. Laser, *Proc. Roy. Soc. (London)*, **140B**, 230 (1952); (b) A. L. Tappel, P. D. Boyer and W. O. Lundberg, *J. Biol. Chem.*, **199**, 267 (1952).

(7) L. Michaelis, "Currents in Biochemical Research," (D. E. Green ed.), Interscience Publishers, Inc., New York, N. Y., 1946, p. 225.

(8) R. A. Alberty, *J. Am. Chem. Soc.*, **75**, 1928 (1953).

(9) J. F. Kachmar and P. D. Boyer, *J. Biol. Chem.*, **200**, 669 (1953).

(10) G. W. Schwert and M. T. Hakala, *Arch. Biochem. Biophys.*, **38**, 55 (1952).

(11) J. Botts and M. Morales, *Trans. Faraday Soc.*, **49**, 696 (1953).

(12) H. T. Huang and C. Niemann, *J. Am. Chem. Soc.*, **75**, 1395 (1953).

(13) K. J. Laidler and I. M. Socquet, THIS JOURNAL, **54**, 530 (1950).

(14) H. L. Segal, J. F. Kachmar and P. D. Boyer, *Enzymologia*, **15**, 187 (1952).

TABLE I

CALCULATED RATE LAWS FOR SEVERAL MECHANISMS

Mechanism	Rate of formation of product P[a]	
	Steady-state conditions	Equilibrium conditions
I. Two substrates, ternary complex, ordered sequence		
$E_1 + A \underset{k_2}{\overset{k_1}{\rightleftarrows}} E_2$	$V = k_5E_0\,f_I(A, B)^{b,f}$	$V = k_5E_0\,f_{II}(A, B)^{c,f}$
$E_2 + B \underset{k_4}{\overset{k_3}{\rightleftarrows}} E_3$	$V_{\max_A} = k_5E_0 \frac{k_3B}{k_3B + k_4 + k_5}$	$V_{\max_A} = \frac{k_5E_0K_2B}{1 + K_2B}$
$E_3 \xrightarrow{k_5} P + E_1$	$V_{\max_B} = \frac{k_5E_0\,k_1A}{k_1A + k_5}$	$V_{\max_B} = k_5E_0$
$K_1 = k_1/k_2,\ K_2 = k_3/k_4$	$V_{\max_{AB}} = k_5E_0$	$V_{\max_{AB}} = k_5E_0$
II. Two substrates, ternary complex, random sequence		
$E_1 + A \underset{k_2}{\overset{k_1}{\rightleftarrows}} E_2;\ E_1 + B \underset{k_7}{\overset{k_6}{\rightleftarrows}} E_4$	$V = k_5E_0\,f_{III}(A, B)^{d}$	$V = k_5E_0\,f_{IV}(A, B)^{e,f}$
$E_2 + B \underset{k_4}{\overset{k_3}{\rightleftarrows}} E_3;\ E_4 + A \underset{k_9}{\overset{k_8}{\rightleftarrows}} E_3$	$V_{\max_A} = k_5E_0 \frac{k_3B}{k_3B + k_4 + k_5}$	$V_{\max_A} = \frac{k_5E_0K_2B}{1 + K_2B}$
$E_3 \xrightarrow{k_5} P + E_1$	$V_{\max_B} = k_5E_0 \frac{k_8A}{k_8A + k_5 + k_9}$	$V_{\max_B} = \frac{k_5E_0K_4A}{1 + K_4A}$
$K_1 = k_1/k_2,\ K_2 = k_3/k_4,\ K_3 = k_6/k_7$	$V_{\max_{AB}} = k_5E_0$	$V_{\max_{AB}} = k_5E_0$
$K_4 = k_8/k_9$		$K_1K_2 = K_3K_4$
III. Two substrates, binary complex		
$E_1 + A \underset{k_2}{\overset{k_1}{\rightleftarrows}} E_2$	$V = \frac{k_5E_0\,k_1AB}{k_1A + k_2 + k_5B}$	$V = k_5E_0 \frac{ABK}{1 + KA}$
$E_2 + B \xrightarrow{k_5} P + E_2$	$V_{\max_A} = k_5E_0B$	$V_{\max_A} = k_5E_0B$
$K = k_1/k_2$	$V_{\max_B} = k_1E_0A$	$V_{\max_B} = \infty$
	$V_{\max_{AB}} = \infty$	$V_{\max_{AB}} = \infty$
IV. One substrate, binary complex		
$E_1 + A \underset{k_2}{\overset{k_1}{\rightleftarrows}} E_2$	$V = k_5E_0 \frac{k_1A}{k_1A + k_2 + k_5}$	$V = \frac{k_5E_0K_1A}{1 + K_1A}$
$E_2 \xrightarrow{k_5} P + E_1$	$V_{\max} = k_5E_0$	$V_{\max} = k_5E_0$
$K_1 = k_1/k_2$		

[a] $V_{\max_A}$ and $V_{\max_B}$ are the maximum rates reached as a limit upon increasing the concentration of substrates A and B, respectively. $V_{\max_{AB}} = k_5E_0$ is the maximum limiting rate for both substrates, A and B. E_0 is the total enzyme concentration, complexed or uncomplexed.

[b] $f_I(A, B) = E_3/E_0 = \frac{k_1k_3AB}{k_1k_3AB + (k_4 + k_5)k_1A + k_3k_5B + k_2(k_4 + k_5)}$.

[c] $f_{II}(A, B) = E_3/E_0 = \frac{K_1K_2AB}{1 + K_1A + K_1K_2AB}$. This was the expression previously derived by K. J. Laidler and I. M. Socquet.[13]

[d] $f_{III}(A, B) = E_3/E_0 = AB(k_1k_3k_7 + k_1k_3k_8A + k_2k_6k_8 + k_3k_6k_8B)/A^2(k_1k_4k_8 + k_1k_5k_8) + A^2B(k_1k_3k_8) + B^2(k_3k_3k_6 + k_3k_6k_9) + AB^2(k_3k_6k_8) + AB(k_2k_5k_8 + k_1k_3k_9 + k_1k_3k_7 + k_4k_6k_8 + k_3k_5k_8) + A(k_2k_4k_8 + k_2k_5k_8 + k_1k_4k_7 + k_1k_5k_7 + k_1k_1k_9) + B(k_3k_5k_7 + k_3k_7k_9 + k_2k_4k_6 + k_2k_5k_6 + k_2k_6k_9) + k_2k_4k_7 + k_8k_5k_7 + k_8k_7k_9$.

[e] $f_{IV}(A, B) = E_3/E_0 = \frac{K_1K_2K_4AB}{K_4 + K_1K_4A + K_1K_2B + K_1K_2K_4AB}$.

[f] These rate laws were previously derived by H. J. Segal, J. F. Kachmar and P. D. Boyer.[14]

cases where enzyme E combines with substrates A and B in a stepwise manner but in a random sequence to yield the complex E_3. Mechanism III involves the two reactants A and B again but they do not form a ternary complex.[15]

Mechanism IV, the familar one[5] for a single substrate system, has been included for comparison and to aid in the later discussion. For each mechanism, the results are given for both steady-state and equilibrium treatments.

The rate V, of the formation of product P, was calculated in a conventional manner by setting up steady-state or equilibrium equations for all the enzyme forms (E_1 to E_4), calculating the concentration of E_3 in terms of the concentrations of the substrates A and B and of total enzyme, E_0, and finally, evaluating the function $V = k_5E_3$.

The calculated expressions for V are shown in Table I as the first equations for each of the four mechanisms. It is seen that a very complicated expression, containing 24 terms in the denominator, is obtained for the general steady-state case of two substrates. The other three general equations for V, for mechanisms I and II, are essentially those of Segal, Kachmar and Boyer.[14]

---

[15] The transition state in the second step could be called the ternary complex but it differs from the ternary complexes in mechanisms I and II in that the potential energy of the system in III is a maximum whereas in the former cases (I and II) it is a minimum.

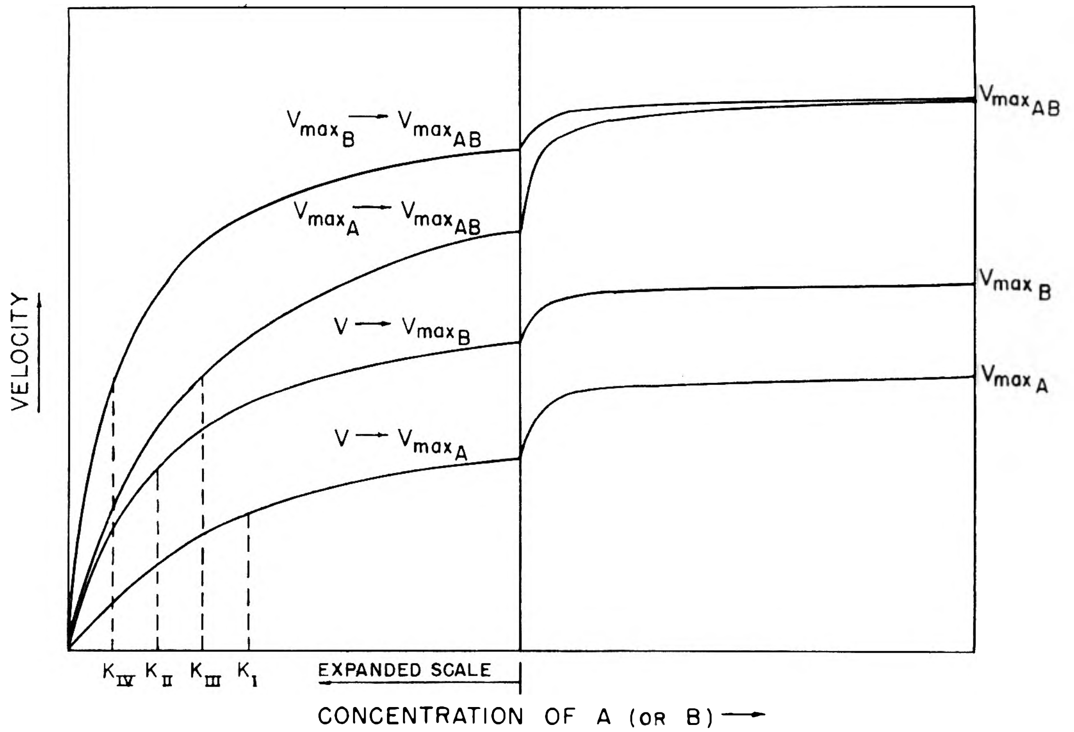

Fig. 1.—Curves of the velocity *versus* the concentration of the reactant A (or B), showing the three maximum velocities $V_{\max_A}$, $V_{\max_B}$ and $V_{\max_{AB}}$ and the four Michaelis constants, K_I, K_{II}, K_{III} and K_{IV} corresponding to the four experimental conditions, $V \rightarrow V_{\max_A}$, $V \rightarrow V_{\max_B}$, $V_{\max_A} \rightarrow V_{\max_{AB}}$ and $V_{\max_B} \rightarrow V_{\max_{AB}}$, respectively. The left-hand half of the graph has been expanded greatly to show the initial part of the concentration range in greater detail.

The equations for steady state conditions are expressed in terms of rate constants; equations for equilibrium conditions, in terms of equilibrium constants.

When these equations are analyzed according to the Michaelis–Menten[16] method for the evaluation of maximum rates it becomes apparent at once that the two substrate systems have three possible maximum rates as compared with one for the single substrate. Thus, by increasing the concentrations of A, or of B, or of both A and B, different limiting maximum rates will be obtained which will be designated here by the symbols $V_{\max_A}$, $V_{\max_B}$ and $V_{\max_{AB}}$, respectively. The equations for each of these, for the different mechanisms, are also shown in Table I. They were calculated from the general equations (for V) by dropping out those terms which approach zero with increasing concentration of the substrate involved. Some of these terms were of the type, const./AB, so that at low concentrations of A (or B) it may require a high concentration of B (or A) to allow this term to be neglected.

The consequence of this relationship is that the maximum rate, $V_{\max_A}$, for example, will be attained only at very high concentrations of reactant A, when the concentration of reactant B is held very low (and *vice versa*).

A further important consequence relates to experiments where it is desired to study the rate as a function of the concentration of one reactant while the concentration of the other reactant is high enough to yield a maximum rate. An example of such a study would be the dependence on oxygen pressure of the rate of enzymatic oxidation of a reducing substrate. In that case it is necessary to assure oneself that the maximum rate with respect to the reducing substrate is actually being maintained over the whole range of oxygen pressures under investigation. Obviously, concentration of the reducing substrate satisfactory for the lowest oxygen pressure studied, will also be satisfactory for the highest pressures (but not *vice versa*).

It is of interest to note that the equations for $V_{\max_A}$ and $V_{\max_B}$ are, in general, analogous in form to the general equation for V in the single substrate system (mechanism IV). This is to be expected inasmuch as $V_{\max_{A\ (\text{or}\ B)}}$ rate is only a function of the other substrate B (or A). The dependence on the other substrate leads in turn to an important observation that $V_{\max_{A\ (\text{or}\ B)}}$ is not a unique value but represents a series of values, depending on the concentration of substrate B (or A). For example, a plot of V *vs.* A could be shown as a family of curves, each curve representing a different concentration of B, and each curve levelling off at a different value of $V_{\max_A}$.

The last equations for each mechanism in Table I represent a condition where all of the enzyme exists essentially in the form of the complex E_3. The corresponding rate, $V_{\max_{AB}}$, is therefore a unique, single valued quantity.

Derivation of the Michaelis Constant.—The Michaelis constant is obtained experimentally from a study of the variation of the rate (toward a

---

(16) L. Michaelis and M. L. Menten, *Biochem. Z.*, **49**, 333 (1913).

TABLE II

MICHAELIS CONSTANTS[a] FOR VARIOUS MECHANISMS AND FOR DIFFERENT EXPERIMENTAL CONDITIONS[b]

Mechanism[c]	Experimental conditions $V \rightarrow V_{\max_A}$	$V \rightarrow V_{\max_B}$	$V_{\max_A} \rightarrow V_{\max_{AB}}$	$V_{\max_B} \rightarrow V_{\max_{AB}}$
		Steady state		
I. Two substrates, ternary complex, ordered sequence	$\frac{k_2k_4 + k_2k_5 + k_3k_5B}{k_1(k_4 + k_5 + k_3B)}$	$\frac{k_2k_4 + k_1k_4A + k_2k_5 + k_1k_5A}{k_3k_5 + k_1k_3A}$	$\frac{k_4 + k_5}{k_3}$	$\frac{k_5}{k_1}$
		Equilibrium		
	$\frac{1}{K_1 + K_1K_2B}$	$\frac{1 + K_1A}{K_1K_2A}$	$\frac{1}{K_2}$	Zero
		Steady state		
II. Two substrates, ternary complex, random sequence	$f_{(B)}$[d]	$f_{(A)}$[d]	$\frac{k_4 + k_5}{k_3}$	$\frac{k_5 + k_9}{k_8}$
		Equilibrium		
	$\frac{1 + K_3B}{K_1K_2B + K_1}$	$\frac{1 + K_1A}{K_3 + K_1K_2A}$	$\frac{1}{K_2}$	$\frac{1}{K_4}$
		Steady state		
III. Two substrates, binary complex	$\frac{k_2 + k_5B}{k_1}$	$\frac{k_1A + k_2}{k_6}$	∞	∞
		Equilibrium		
	$1/K_1 = k_2/k_1$	∞	∞	∞
		Steady state		
IV. One substrate, binary complex	$\frac{k_2 + k_5}{k_1}$	...	...	...
		Equilibrium		
	$1/K_1 = k_2/k_1$	...	...	...

[a] The first constant listed is that calculated from steady state conditions and the second is calculated from equilibrium conditions. [b] The experimental conditions designated as $V \rightarrow V_{\max_A}$, means that in these experiments concentration of B is constant and that of A is varied so that the velocity V approaches $V_{\max_A}$ as a limit; $V_{\max_A} \rightarrow V_{\max_{AB}}$ means that concentration of A is constant and high enough to yield maximum rate ($V_{\max_A}$) and concentration of B is varied to $V_{\max_{AB}}$. The other two conditions are similar to above with A and B interchanged. [c] Mechanisms are the same as in Table I. [d] $f_{(B)}$ and $f_{(A)}$ are functions of B and A, respectively, which could not be reduced to simple expressions and are therefore not presented here. In these cases, the Lineweaver–Burk[17] method does not give the same constants as those obtained from the substrate concentrations at half maximal velocity.

maximum) with increasing concentration of the substrate.

With a single-substrate enzyme system only one set of such experiments is possible (all other factors being constant), whereas with the two-substrate systems, four different sets of experimental conditions can exist. Thus, the concentration of each substrate, A (or B), can be varied while the concentration of the other substrate B (or A) is held constant, to obtain $V_{\max_A}$ (or $V_{\max_B}$). Once these maxima have been reached, the other corresponding substrates can be varied in each case to determine $V_{\max_{AB}}$ (see Fig. 1).

For each type of experiment it is possible to calculate a Michaelis "constant." Table II shows the results of such calculations for the four sets of conditions. In analogy with the single substrate system, the Michaelis "constant" calculated here is the value that would be found by treating the data by the Lineweaver–Burk[17] method, that is, from a plot of $1/V$ *vs.* $1/S$, of the expression $V/V_{\max} = S/(S + K_m)$ where S is the varying reactant, and K_m is the Michaelis constant. The results shown in Table II have been calculated from the ratios of $V/V_{\max_A}$ and $V_{\max B}/V_{\max_{AB}}$, etc., using the equations from Table I. If the "constants" in Table II were calculated as equal to the concentration of the varying substrate when the rate is one-half of the maximum rate, the same results would have been obtained in most cases. An exception is found for the two instances $V \rightarrow V_{\max_{A\ (\text{or}\ B)}}$, for the general case (mechanism II) of the two substrate systems. In these two instances linear Lineweaver–Burk plots are not obtained (as noted previously[8,14]) and the expressions evaluated from half maximal rates are too complicated and are not cited.

Significance of the Derived Expressions for Michaelis Constant.—It is to be noted from Table II that only under conditions $V_{\max_{A\ (\text{or}\ B)}} \rightarrow V_{\max_{AB}}$ are the constants generally analogous to those usually evaluated for a one-reactant system (mechanism IV). Under all other conditions there is no such similarity.

A corollary is that a linear Lineweaver–Burk plot is no assurance that a one-substrate system is being dealt with or that the evaluated Michaelis constant is analogous to the usual Michaelis constant for a one-substrate system.

It is to be noted also that in all three of the two reactant cases (mechanisms I, II and III) under experimental conditions where $V \rightarrow V_{\max_{A\ (\text{or}\ B)}}$ (see Table II) the experimental Michaelis constant is not a single valued quantity but its magnitude is a function of the concentration of that substrate

---

(17) H. Lineweaver and D. Burk, *J. Am. Chem. Soc.*, **56**, 658 (1934).

which is being held constant in the given series of experiments.

The results found for mechanism III are of special interest, since this mechanism has been postulated in order to explain the anomalous variation of Michaelis constant with substrate in the glucose oxidase–glucose–oxygen system.[6a] Although this mechanism accounts for the observed 7-fold variation in the Michaelis constant with 20-fold variation in oxygen pressure, it also predicts that $V_{\max_{A\ (\text{or } B)}}$ is linear with the substrate concentration B (or A), which is contrary to experimental facts. Experiments show[6a] that both $V_{\max_{\text{glucose}}}$ dependence on oxygen pressure and $V_{\max_{\text{oxygen}}}$ dependence on glucose concentration are not linear relationships but appear to obey the usual Michaelis–Menten law.

An explanation for, both, the variations of the Michaelis constant and of $V_{\max_{A\ (\text{or } B)}}$, can be offered in terms of mechanism I or II involving ternary complexes. Under the conditions, $V \rightarrow V_{\max_{A\ (\text{or } B)}}$, which prevailed during the experiments, the Michaelis constants would be expected to vary with concentrations of the reactants as shown in Table II and the maximum velocities, $V_{\max_{A\ (\text{or } B)}}$, would also vary as shown in Table I.

A similar explanation may be offered for the results of Tappel, Boyer and Lundberg,[6b] who found a 10-fold increase in the Michaelis constant for oxygen as the reducing substrate (linoleate) was increased 20-fold in a study of the reaction kinetics of soybean lipoxidase.

We see now that a variation in the Michaelis constant is to be expected if it is measured under conditions $V \rightarrow V_{\max_{A\ (\text{or } B)}}$ instead of the conditions $V_{\max_{A\ (\text{or } B)}} \rightarrow V_{\max_{AB}}$. Perhaps the term Michaelis constant should be reserved for the latter conditions, which yield a constant analogous to that derived for the classical one-reactant system.[5]

There are certainly many other mechanisms or variations of these mechanisms that could be discussed. We have pointed out one commonly postulated mechanism III that can usually be eliminated by the above analysis and have discussed two mechanisms (I and II) that demonstrate the pitfalls involved in measuring Michaelis constants.

It is important to note at this time that mechanisms I and II are special and simpler cases of a more general formulation which yields essentially the same kinetics. This formulation, previously mentioned by Laidler and Socquet,[13] is

$$
\begin{aligned}
E_1 + A &\rightleftharpoons E_2 + W \\
E_2 + B &\rightleftharpoons E_3 + X \\
E_3 &\longrightarrow P + E
\end{aligned}
$$

where E_2 and E_3 are modified forms of the enzyme, and W, X and P are products of the reactions. If W and X are non-existent, the above mechanism reduces to mechanism I or II and E_3 becomes a ternary enzyme–substrate complex. Thus, the concept of a ternary complex is not essential for the conclusions drawn concerning mechanisms I and II. However, the more general formulation above would require that the rate of the reaction would also be a function of the concentrations of the products W and X.

Acknowledgment.—We greatly appreciate the helpful discussions with Dr. Hans Lineweaver during the preparation of this paper.

PURIFICATION AND PROPERTIES OF TEN ORGANIC SULFUR COMPOUNDS[1]

BY WILLIAM E. HAINES, R. VERNON HELM, C. W. BAILEY AND JOHN S. BALL

Contribution from the Petroleum and Oil-Shale Experiment Station, Bureau of Mines, Laramie, Wyoming

Received October 26, 1953

Ten organic sulfur compounds, ethanethiol, 2-methyl-2-propanethiol, 1-pentanethiol, 2-thiabutane, 3-thiapentane, thiacyclobutane, thiacyclopentane, 2,3-dithiabutane, 3,4-dithiahexane and thiophene, were purified to at least 99.9 mole % purity. The stability of the compounds under storage and distillation conditions was investigated. In addition to the boiling point and freezing point, the following properties were measured at 20, 25 and 30°: density, viscosity, surface tension and refractive index for the r, C, D, e, v, F and g lines. Derived functions including refractivity intercept, specific dispersion, molecular refraction, parachor and molar volume were calculated and are discussed briefly. Mass, infrared and ultraviolet spectra were determined permitting some correlation of the effect of sulfur groupings on spectra.

Literature surveys[2] have shown that data on the physical properties of thiols, sulfides, disulfides and thiophenes are meager. Many of the data available are unreliable because they were determined on compounds of doubtful purity. Because these types of compounds occur in petroleum products, the Bureau of Mines and the American Petroleum Institute have coöperatively sponsored Research Project 48. This Project has among its purposes the production of sulfur compounds in high purity and the accurate determination of their physical properties. The attainment and measurement of the high purities are facilitated by the purification of a large quantity of each compound from which samples are available for sale by the American Petroleum Institute as calibration standards. Because of this latter activity, the stability of the compounds has been investigated.

---

(1) This investigation was performed as part of the work of American Petroleum Institute Research Project 48A on "The Production, Isolation, and Purification of Sulfur Compounds and Measurement of their Properties," which the Bureau of Mines conducts at Bartlesville, Okla., and Laramie, Wyo.

(2) W. E. Haines, W. J. Wenger, R. V. Helm and J. S. Ball, *U. S. Bur. Mines, Rept. Invest.*, 4060 (1946); R. V. Helm, W. E. Haines and J. S. Ball, *ibid.*, 4566 (1949).

Three groups of physical properties are determined: (1) common physical properties such as refractive index, density, viscosity, surface tension, melting point and boiling point; (2) thermodynamic properties; and (3) spectroscopic patterns. This paper reports properties in the first and third groups for ten sulfur compounds. The thermodynamic properties are reported in separate papers.[3]

The first ten sulfur compounds selected for purification were representative of the four types expected in petroleum: Three thiols (ethanethiol, 2-methyl-2-propanethiol and 1-pentanethiol); four sulfides (2-thiabutane, 3-thiapentane, thiacyclobutane and thiacyclopentane); two disulfides (2,3-dithiabutane and 3,4-dithiahexane); and thiophene.

Purification

To meet the needs of the program, a minimum of 1.5 liters of material with a purity of at least 99.9 mole % was required. Whenever possible, the compounds for purification were obtained from commercial sources; however, it was necessary to synthesize two of the compounds. The purification procedure was similar to that used for hydrocarbons by the National Bureau of Standards.[4] After preliminary purification by chemical procedures, a distillation was made, taking 30-ml. fractions. From density or refractive index determinations, certain fractions were selected for determination of purity by the freezing point method.[5] High purity fractions were combined, and the composite was tested for impurity by determining freezing point and mass spectra before it was sealed "in vacuum."[6] Variations in the procedure were made for individual compounds as described below. All distillations were made at atmospheric pressure (585 mm.) unless otherwise noted.

Ethanethiol.—A distillation of 2.5 l. of Eastman Kodak Co. "blue label" ethanethiol yielded insufficient material (0.6 l.). Therefore, 3 l. of "white-label" ethanethiol was added and was passed through silica gel to remove the water. Distillation was through a column 1 inch in diameter, having a 9-foot section packed with stainless-steel helices (hereafter designated as column 1). Yield of high-purity (99.95 mole %) material was 1.95 l.

2-Methyl-2-propanethiol.—Approximately 7 l. of 2-methyl-2-propanethiol donated by Phillips Petroleum Co. was distilled through a 1-inch by 8-foot glass Oldershaw column having 80 perforated plates (column 2). Yield of high-purity (99.92 mole %) material was 2.1 l.

1-Pentanethiol.—This compound was prepared by treating *n*-pentyl bromide with sodium hydrosulfide in alcoholic solution according to the general procedure of Ellis and Reid.[7] Several batches were prepared, the largest of which was 7 moles. Yields were 85–90% of theoretical. Oil-soluble impurities were removed from the crude thiol by ether extraction of the water-soluble sodium mercaptide. The thiol was regenerated, dried and 2.6 l. was distilled through column 1. Yield of high-purity (99.92 mole %) material was 2.4 liters.

2-Thiabutane.—Approximately 3 l. of 2-thiabutane (Eastman Kodak Co.) was distilled through a high-temperature Podbielniak heligrid column with a 5-foot packed section (column 3). Yield of high-purity (99.96 mole %) material was 1.53 l.

3-Thiapentane.—Approximately 3 l. of 3-thiapentane (Eastman Kodak Co.) was distilled through column 1. This distillation was made before freezing-point equipment was available, so that fractions were chosen on the basis of refractive index. Purity was measured on the composite at a later date. Yield of high-purity (99.94 mole %) material was 1.68 l.

Thiacyclobutane.—The method of synthesis was supplied by Bordwell and Pitt.[8] A mixture of 304 g. (4 moles) of thiourea, 819 g. of 1-bromo-3-chloropropane and 1.5 l. of ethanol was refluxed for 5 hours. The solvent was removed from the reaction mixture by distillation at atmospheric pressure up to a flask temperature of 90°. Excess halide was removed by heating the flask at 60–70°, for 2 hours under vacuum (20 mm.). The thiouronium salt was dissolved in 350 ml. of water and was added over a period of 2 hours to a solution of 513 g. of potassium hydroxide in 1.2 l. of water. The mixture was held at 60–80° during the addition and for 1 hour afterward. The reaction mixture was cooled by adding ice and the sulfide layer separated. The water layer was extracted with ether. Thirty-seven separate 4-mole batches were made, with an average yield of 53.5%.

The crude thiacyclobutane (5.8 l.) thus prepared was dried over anhydrous potassium carbonate and charged to column 3 for distillation. The composite was dried by low-temperature filtration and over anhydrous calcium sulfate before it was sealed "in vacuum." Yield of high-purity (99.95 mole %) material was 2.0 l.

Thiacyclopentane.—Nearly 10 l. of thiacyclopentane contributed by Oronite Chemical Co. was distilled through column 3. The high-purity composite was dried by a low-temperature filtration and then over anhydrous calcium sulfate and silica gel just before it was sealed "in vacuum." Yield of high-purity (99.95 mole %) material was 1.86 liters.

2,3-Dithiabutane.—Nearly 3 l. of 2,3-dithiabutane (Eastman Kodak Co.) was distilled through a column 1 inch in diameter having a 6-foot section packed with Stedman packing (column 4). Yield of high-purity (99.97 mole %) material was 1.6 l.

3,4-Dithiahexane.—Five liters of 3,4-dithiahexane (Eastman Kodak Co.) was distilled through column 4 at a pressure of 50 mm. Two separate distillations were made, and the high-purity fractions were combined. The yield of high-purity (99.90 mole %) material was 2.15 l.

Thiophene.—Nearly 4.5 l. of thiophene (Socony—Vacuum Oil Co.) was distilled through column 1. The high-purity (99.99 mole %) material (1.9 l.) was shown to be benzene free by means of the mass spectrometer. A benzene impurity would not be shown by the freezing-point method, because benzene and thiophene form a solid solution.[9]

Stability

Inasmuch as a portion of each of these compounds has been set aside as a standard sample, the storage stability was tested in the following manner. Samples of the purified compounds were sealed "in vacuum" in clear glass ampoules and exposed to sunlight for 1 year. Control samples were kept in the dark during the same period. Determinations of purity by the freezing-point method were then made on both the exposed and the control samples. The greatest variation in purity shown by the dark storage samples was 0.03 mole %, which is within experimental error.

Six of the compounds showed no decrease in purity after 1 year in strong sunlight. Of those affected by sunlight, two were easily separated from the impurity by a simple room-temperature vacuum transfer. Thiacyclobutane forms polymer upon exposure to light. Polymerization was evident after 2 weeks' exposure, and at the end of a year this sample was a thick white slurry. However, when the unpolymerized liquid was vacuum-transferred from the ampoule and analyzed by the mass spectrometer (there was insufficient volume for freezing-point determination) the pattern obtained was identical to that of the original sample. Polymerization may occur in 2-methyl-2-propanethiol to a very minor extent, as evidenced by a reduction in purity too small to be conclusive. Vacuum transfer again yielded material of the original purity.

Only the two disulfides showed significant deterioration, because some of the impurities formed are volatile so that they cannot be separated by a vacuum transfer. 2,3-Dithiabutane that had an original purity of 99.97 mole % was only 91.8 mole % after exposure to sunlight for a year.

---

(3) G. Waddington, H. M. Huffman and co-workers, *J. Am. Chem. Soc.*, **71**, 797 (1949); **72**, 2424 (1950); **73**, 261 (1951); **74**, 2801, 2804, 2478, 4656, 6025 (1952); **75**, 2795, 1818 (1953).

(4) A. J. Streiff, E. T. Murphy, V. A. Sedlak, C. B. Willingham and F. D. Rossini, *J. Research Natl. Bur. Standards*, **37**, 331 (1946).

(5) A. R. Glasgow, Jr., A. J. Streiff and F. D. Rossini, *ibid.*, **35**, 355 (1945).

(6) B. J. Mair, D. J. Termini, C. B. Willingham and F. D. Rossini, *ibid.*, **37** 229 (1946).

(7) L. M. Ellis, Jr., and E. E. Reid, *J. Am. Chem. Soc.*, **54**, 1674 (1932).

(8) F. G. Bordwell and B. M. Pitt, private communication from API Project 48B at Northwestern University.

(9) F. S. Fawcett and H. E. Rasmussen, *J. Am. Chem. Soc.*, **67**, 1705 (1945).

Table I

Properties of Ten Organic Sulfur Compounds

Cpd. no.	Compound	Impurity, mole %	F.p. for zero impurity, °C.	Cryoscopic constant A, deg.$^{-1}$	B.p. at 760 mm., °C.	Temp. of measurement, t, °C.	Density at t°, g./ml.	Viscosity at t° C., centipoises	Surface tension at t° C., dynes per cm.
1	Ethanethiol	0.05 ± 0.04	−147.89	0.036	35.0				
	(ethyl mercaptan)					20	0.83914	0.293	23.5
						25	.83316	.279	22.8
						30	[a]	[a]	[a]
2	2-Methyl-2-propanethiol	.08 ± .04	+ 1.11	.005	64.2				
	(t-butyl mercaptan)					20	.80020	.638	20.8
						25	.79472	.588	20.2
						30	.78929	.544	19.6
3	1-Pentanethiol	.08 ± .05	− 75.70	.048	126.5				
	(n-pentyl mercaptan)					20	.84209	.639	26.8
						25	.83763	.601	26.3
						30	.83317	.568	25.7
4	2-Thiabutane	.04 ± .04	−105.91	.04	66.7				
	(methyl ethyl sulfide)					20	.84221	.373	24.9
						25	.83679	.354	24.2
						30	.83145	.337	23.4
5	3-Thiapentane	.06 ± .04	−103.93	.04	92.1				
	(ethyl sulfide)					20	.83623	.440	25.2
						25	.83120	.417	24.5
						30	.82625	.396	23.9
6	Thiacyclobutane	.05 ± .05	− 73.25	.023	95.0				
	(trimethylene sulfide)					20	1.02000	.638	36.3
						25	1.01472	.607	35.6
						30	1.00957	.576	35.0
7	Thiacyclopentane	.05 ± .05	− 96.16	.028	120.9				
	(tetrahydrothiophene)					20	0.99869	1.042	35.8
						25	.99379	0.971	35.0
						30	.98928	.914	34.6
8	2,3-Dithiabutane	.03 ± .02	− 84.72	.030	109.6				
	(dimethyl disulfide)					20	1.06250	.619	33.6
						25	1.05690	.585	32.8
						30	1.05138	.555	32.2
9	3,4-Dithiahexane	.10 ± .08	−101.52	.038	152.6				
	(diethyl disulfide)					20	0.99311	.860	31.3
						25	.98818	.805	30.7
						30	.98332	.757	30.2
10	Thiophene	.013 ± .011	− 38.24	.0114	84.1				
						20	1.06485	.654	32.8
						25	1.05887	.613	32.0
						30	1.05309	.576	31.1

[a] This compound has a boiling point of 27.8° at 585 mm.

Vacuum transfer improved the purity to 96.3 mole %. 3,4-Dithiahexane deteriorated from 99.92 to 96.3 mole %. After vacuum transfer the purity was 98.1 mole %. Thus these two samples should be stored in the dark in order to maintain high purity.

A test of stability under distillation conditions was made by refluxing each of the pure sulfur compounds in an all-glass system at atmospheric pressure for 240 hours. The system was vented through a sodium hydroxide absorber and a Dry Ice trap to retain any decomposition products. After the reflux period, the sample was tested for purity, and the absorbers were examined for decomposition products.

The two disulfides were the only compounds that showed evidence of decomposition under these conditions. Both released traces of hydrogen sulfide and/or thiol and darkened. However, in contrast to the storage stability results, 3,4-dithiahexane showed the greater decomposition, its purity being reduced 0.6 mole % while the 2,3-dithiabutane showed a reduction of less than 0.1 mole %. This may be due to the higher reflux temperature of the 3,4-dithiahexane.

Physical Properties

Physical property data for the ten organic sulfur compounds are shown in Tables I and II. No comparison with literature values has been made in this paper, but excellent agreement may be noted for those values reported in recent papers on thiophene,[9] 2-thiabutane, 3-thiapentane, 2,3-dithiabutane, 3,4-dithiahexane[10] and thiacyclopentane.[11] Descriptions of apparatus, procedures and estimates of accuracy are included in the experimental section.

Experimental

Freezing Point, Purity and Cryoscopic Constants.—The freezing points were determined and the purities calculated from the time–temperature freezing and melting curves, according to the method of Glasgow, Streiff and Rossini.[5] Three different "impurities" were used in determining the cryoscopic constant, A. Accuracy of freezing points is estimated to be ±0.01°.

Boiling Point.—The boiling points were measured in a Cottrell ebulliometer, using a platinum resistance thermohm. The pressure was maintained by a Cartesian manostat (Emil Greiner), using an atmosphere of dry nitrogen. The pres-

---

(10) D. T. McAllan, T. V. Cullum, R. A. Dean and F. A. Fidler, *J. Am. Chem. Soc.*, **73**, 3627 (1951).

(11) E. V. Whitehead, R. A. Dean and F. A. Fidler, *ibid.*, **73**, 3632 (1951).

TABLE II

REFRACTIVE INDICES OF TEN ORGANIC SULFUR COMPOUNDS

Cpd. no.	Compound	Temp. of measurement, t, °C.	Refractive indices Helium r line n^t	Hydrogen C line n^t	Sodium D line n^t	Mercury e line n^t	Helium v line n^t	Hydrogen F line n^t	Mercury g line n^t
1	C_2H_5SH	20	1.42763	1.42810	1.43105	1.43356	1.43695	1.43836	1.44428
		25	1.42442	1.42486	1.42779	1.43027	1.43363	1.43505	1.44085
		30	[a]	[a]	[a]	[a]	[a]	[a]	[a]
2	t-C_4H_9SH	20	1.41992	1.42046	1.42320	1.42550	1.42852	1.42991	1.43534
		25	1.41699	1.41739	1.42007	1.42230	1.42545	1.42677	1.43214
		30	1.41392	1.41431	1.41697	1.41930	1.42231	1.42362	1.42894
3	$C_5H_{11}SH$	20	1.44374	1.44420	1.44692	1.44922	1.45224	1.45360	1.45902
		25	1.44121	1.44170	1.44439	1.44666	1.44974	1.45104	1.45639
		30	1.43872	1.43912	1.44180	1.44410	1.44707	1.44841	1.45371
4	$CH_3SC_2H_5$	20	1.43703	1.43747	1.44035	1.44278	1.44616	1.44759	1.45334
		25	1.43410	1.43450	1.43737	1.43984	1.44302	1.44455	1.45028
		30	1.43115	1.43153	1.43437	1.43678	1.44005	1.44146	1.44715
5	$(C_2H_5)_2S$	20	1.43971	1.44015	1.44298	1.44539	1.44858	1.44998	1.45568
		25	1.43695	1.43736	1.44017	1.44256	1.44577	1.44716	1.45280
		30	1.43408	1.43453	1.43734	1.43972	1.44290	1.44428	1.44988
6	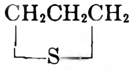 $CH_2CH_2CH_2$ (S)	20	1.50603	1.50660	1.51020	1.51330	1.51737	1.51922	1.52648
		25	1.50318	1.50379	1.50738	1.51050	1.51453	1.51635	1.52362
		30	1.50035	1.50093	1.50448	1.50755	1.51154	1.51337	1.52059
7	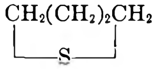 $CH_2(CH_2)_2CH_2$ (S)	20	1.50101	1.50154	1.50483	1.50764	1.51132	1.51295	1.51945
		25	1.49840	1.49891	1.50217	1.50495	1.50864	1.51021	1.51676
		30	1.49583	1.49634	1.49962	1.50237	1.50600	1.50761	1.51408
8	CH_3SSCH_3	20	1.52103	1.52163	1.52592	1.52970	1.53473	1.53683	1.54577
		25	1.51803	1.51871	1.52298	1.52669	1.53174	1.53387	1.54270
		30	1.51512	1.51575	1.51998	1.52366	1.52860	1.53075	1.53958
9	$C_2H_5SSC_2H_5$	20	1.50299	1.50354	1.50731	1.51055	1.51491	1.51680	1.52453
		25	1.50035	1.50097	1.50470	1.50793	1.51230	1.51411	1.52179
		30	1.49771	1.49826	1.50198	1.50524	1.50947	1.51140	1.51899
10	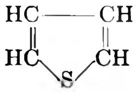	20	1.52339	1.52403	1.52890	1.53317	1.53888	1.54135	1.55174
		25	1.52019	1.52087	1.52572	1.52991	1.53566	1.53814	1.54838
		30	1.51708	1.51778	1.52257	1.52674	1.53245	1.53484	1.54507

[a] This compound has a boiling point of 27.8° at 585 mm.

sure was measured with a barometer, which had been calibrated using the vapor pressure of water as a standard. The accuracy of the boiling point data is estimated to be 0.1°.

Refractive Index.—Refractive indices were measured with a Bausch and Lomb Precision Oil Refractometer, Abbe type, enclosed in a specially built housing to eliminate convection currents. Data were obtained at 20, 25 and 30° for seven different wave lengths of light. The temperatures were maintained by circulating water, thermostated to a maximum variation of ± 0.005° as measured by a platinum resistance thermohm positioned in the refractometer. The room temperature was maintained within 1° of the temperature of measurement. The refractometer was calibrated with samples of toluene, 2,2,4-trimethylpentane and methylcyclohexane, which had been certified with respect to refractive index by the National Bureau of Standards. Duplicate determinations indicate a precision of ±0.00003. Accuracy of reported values is estimated at ±0.00006.

TABLE III

CORNING FILTERS USED FOR VARIOUS WAVE LENGTHS

Line		Wave length, Å.	Color	Corning filter no.
Helium	r	6678.1	Red	2424
Hydrogen	C	6562.8	Red	None required
Sodium	D	5892.6[a]	Yellow	None required
Mercury	e	5460.7	Green	3484, 5120, 4303
Helium	v	5015.7	Green	5031, 3387, 5120
Hydrogen	F	4861.3	Green	5031, 3387
Mercury	g	4358.3	Blue	3389, 5113

[a] Intensity weighted mean of the doublet, D_1, D_2.

The seven wave lengths of light were obtained from four different light sources: The standard "Sodium Lab Arc" furnished with the refractometer, the H-4 type capillary mercury arc available as an accessory to the instrument, a hydrogen-discharge lamp manufactured by Rankin Glass Blowing Co., and a helium spectrum tube with a narrow capillary for brilliant discharge. The Corning filters shown in Table III were used to isolate the specific wave lengths. These filters were checked for transmittancy over the visible range by means of a spectrophotometer and found satisfactory.

Density.—Densities were determined at 20, 25 and 30° with a Christian Becker chainomatic 5-place specific gravity balance with a 5-gram displacement plummet. The sample was placed in a vacuum-jacketed bath through which water, thermostated to ±0.005°, was passed during the determination. The balance was calibrated with a set of standard weights and with toluene, methylcyclohexane and 2,2,4-trimethylpentane as described by Forziati, *et al.*[12] Duplicate determinations show a precision of ±0.00003. The accuracy is estimated to be ±0.00005 g./ml.

Viscosity.—Viscosities were determined using two Geist–Cannon viscometers designed for non-viscous fluids.[13] A 4.0-ml. charge was pipetted at the temperature of measurement and the viscometer was made vertical in a bath thermostated to ±0.005°. At least two consecutive efflux times, agreeing within 0.1 second, were obtained. The viscometers were calibrated with conductance water and had efflux times of 315.0 and 415.4 seconds at 20°. Corrections were

---

(12) A. F. Forziati, B. J. Mair and F. D. Rossini, *J. Research Natl. Bur. Standards*, **35**, 513 (1945).

(13) J. M. Geist and M. R. Cannon, *Ind. Eng. Chem., Anal. Ed.*, **18**, 611 (1946).

Table IV

Derived Functions

Compound	Refractivity intercept $n^{20}{}_D - d^{20}{}_4$	Specific dispersion $\frac{(n^{20}{}_F - n^{20}{}_C)10^4}{d^{20}{}_4}$	Molecular refraction $M/d \frac{(n_D{}^2 - 1)}{(n_D{}^2 + 2)}$ Obsd.	Molecular refraction Calcd.	Parachor $M\gamma^{1/4}/(D - d)$ Obsd.	Parachor Calcd. Sugden	Parachor Calcd. M. & P.	Molar volume $M/d_{b.p.}$ Obsd.	Molar volume Calcd. Kopp	Molar volume Calcd. LeBas
Ethanethiol	1.01148	122.27	19.13	19.24	163.0	160.4	160.8	75.5	77.6	74.4
2-Methyl-2-propanethiol	1.02310	118.09	28.65	28.47	240.5	238.4	240.8	119.7	121.6	118.8
1-Pentanethiol	1.02588	111.63	32.99	33.09	281.0	277.4	280.8	139.2	143.6	141.0
2-Thiabutane	1.01925	120.16	23.80	24.05	201.7	199.4	200.8	96.0	99.6	96.6
3-Thiapentane	1.02487	117.55	28.53	28.67	241.3	238.4	240.8	117.8	121.6	118.8
Thiacyclobutane	1.00020	123.72	21.71	21.85	178.1	176.8	176.0	78.6	88.6	89.2
Thiacyclopentane	1.00549	114.25	26.13	26.47	215.6	212.7	213.0	97.4	110.6	111.4
2,3-Dithiabutane	0.99467	143.06	27.15	27.44	213.0	208.6	210.8	97.6	100.2	97.0
3,4-Dithiahexane	1.01076	133.52	36.58	36.67	290.6	286.6	290.8	141.3	144.2	141.4
Thiophene	0.99648	162.65	24.32	24.80	188.8	190.7	189.4	84.9	88.6	96.6

made for kinetic energy losses. A calibration value of 1.002 centipoise for water at 20° was used.[14] This value has recently been adopted by the National Bureau of Standards for use in certifying the viscosity of standard oils. The precision of the measurements was ±0.03%, and the accuracy is estimated to be ±0.001 centipoise.

Surface Tension.—Surface tensions were measured in Pyrex capillarimeters of U-tube design similar to those described in the literature.[15] One arm was constructed of precision-bore capillary tubing 0.05 cm. in diameter. The other arm was of large enough bore (4 cm.) to give a flat meniscus.[16] Surface tension was measured by adjusting the liquid level to a fine calibration mark on the capillary tube; the instrument was made vertical in a bath thermostated to ±0.005° and the capillary rise was measured by means of a cathetometer. Duplicate determinations were made for each compound, using two capillarimeters and making corrections as described in the literature.[17] Pure benzene, which was assumed to have a surface tension of 28.88 dynes/cm. at 20°,[18] was used for calibration. Precision of the method is ±0.05 dyne/cm. with an estimated accuracy of ±0.1 dyne/cm.

Derived Functions.—Two types of derived functions were calculated using the determined constants. Specific dispersion and refractivity intercept, used analytically to distinguish different classes of hydrocarbons, are functions of the non-additive type. The additive functions are molecular refraction, parachor and molar volume. All functions shown in Table IV were calculated at 20° except molar volume.

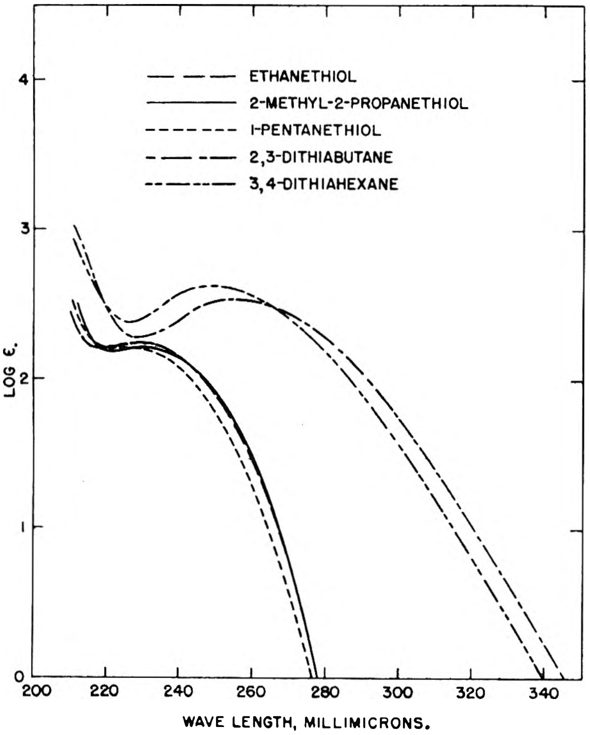

Fig. 1.—Ultraviolet spectra of thiols and disulfides.

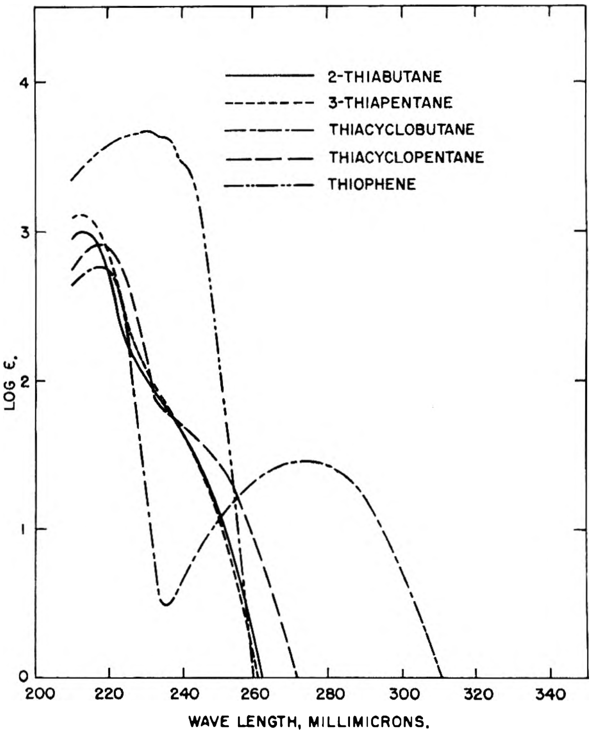

Fig. 2.—Ultraviolet spectra of sulfides and thiophene.

---

[14] J. F. Swindells, J. R. Coe, Jr., and T. B. Godfrey, *J. Research Natl. Bur. Standards*, **48**, 1 (1952).

[15] G. Jones and W. A. Ray, *J. Am. Chem. Soc.*, **59**, 187 (1937).

[16] T. W. Richards and L. B. Coombs, *ibid.*, **37**, 1657 (1915).

[17] A. Weissberger, "Technique of Organic Chemistry, Volume I, Physical Methods of Organic Chemistry," Interscience Publishers, Inc., New York, N. Y., 1949, p. 366.

[18] "International Critical Tables," Vol. IV, McGraw-Hill Book Co., Inc., New York, N. Y., 1928, p. 454.

TABLE V

MASS SPECTRA

Mass no. m/e	Relative intensity									
	Ethanethiol M.W. = 62	2-Methyl-2-propanethiol M.W. = 90	1-Pentanethiol M.W. = 104	2-Thiabutane M.W. = 76	3-Thiapentane M.W. = 90	Thiacyclobutane M.W. = 74	Thiacyclopentane M.W. = 88	2,3-Dithiabutane M.W. = 94	3,4-Dithiahexane M.W. = 122	Thiophene M.W. = 84
122									76.5	
104			32.4							
94								100.0	53.0	
90		43.8			70.4		2.33		0.10	
88		0.01	0.01				52.0			0.02
84		0.01					0.16			100.0
79								59.4	8.99	
76		0.84	0.40	64.0	3.85	1.86	0.03	0.47	0.15	
75		20.0	0.53	3.81	100.0	1.71	0.18		0.37	
74		0.70	0.48	0.09	0.02	42.0	0.16			
70		0.10	36.7		0.05	0.17	0.09		0.31	0.34
66			0.12					0.97	90.3	
65	0.11		0.22					0.46	4.00	
64	4.24		0.09	0.11	2.20		0.01	11.2	9.92	
62	96.5	0.06	1.50	3.09	50.8		4.46	0.68	3.73	
61	15.3	0.93	13.7	100.0	58.1	0.09	4.10	12.2	8.36	0.10
60	1.38	0.45	2.33	2.86	11.6	0.17	100.0	0.25	12.1	2.83
58	10.3	6.82	2.13	4.73	9.36	1.89	8.00	0.21	6.99	64.8
57	8.03	84.4	3.79	2.37	4.36	0.96	2.52	0.13	2.91	12.9
55		5.91	46.7		0.48		12.3		0.12	
48	2.13	0.39	4.07	56.0	2.69	4.57	2.18	14.3	0.37	0.67
47	80.4	10.4	27.8	43.3	93.4	7.23	28.1	26.4	4.89	2.55
46	15.2	1.07	5.66	13.7	17.7	100.0	33.1	37.6	5.72	1.41
45	24.4	6.43	10.6	27.9	23.2	24.6	38.1	62.6	17.7	57.8
42		4.21	100.0	0.44	0.24	0.42	4.21		0.07	4.43
41		100.0	41.1	4.83	6.38	8.35	10.4		0.42	2.10
39		30.5	18.7	0.75	0.75	9.59	13.3		0.24	28.6
35	15.3	0.91	4.31	21.9	19.4	0.79	0.94	0.92	9.92	
34	25.9	2.10	1.87	0.87	6.87	0.40	1.52	0.43	2.68	0.39
33	9.50	4.74	1.71	1.15	1.78	0.81	1.28	1.28	2.08	0.87
32	5.80	1.85	0.82	1.26	1.12	1.85	1.56	3.58	2.21	3.65
29	100.0	65.1	33.9	21.6	56.3	0.64	3.24	0.14	100.0	0.12
27	81.2	22.0	34.3	41.1	73.3	8.08	23.6	0.92	70.2	1.64

Refractivity-intercept values of all the compounds are low compared with corresponding values for hydrocarbons. The cyclic sulfur compounds and the disulfides show lower values than the rest of the compounds. On the basis of specific dispersion, the compounds are divided into three groups: the thiols and sulfides have values in the range 110–125; the disulfides, in the range 130–145; and thiophene, 162.6. These values correspond to those for olefins, diolefins and aromatics in the hydrocarbon series, as might be expected from the equivalence of the sulfur atom and the ethylenic group.[19]

The observed molecular refractions agree with the calculated values within 2%; but all are low, except for 2-methyl-2-propanethiol, the only compound studied with a tertiary linkage. Calculations are based on the increments of Eisenlohr[20] for carbon and hydrogen and Boudet and Rambaud[21] for sulfur. The latter workers suggest different increments for sulfur in different types of linkages. A value of 7.81 has been assigned to sulfur in aliphatic thiols; 8.00, in alkyl sulfides; and 7.26, in substituted thiophenes. If sulfur increments are calculated from the reported data, assuming the carbon and hydrogen increments to be correct, values of 7.8 ± 0.2 for sulfur in aliphatic thiols, 7.7 ± 0.1 in sulfides, 7.9 ± 0.1 in disulfides, and 6.8 in thiophene are obtained. Thus, except for thiophene, the values differ so much within the various types that assignment of different increments seems unwarranted.

Parachor values were calculated using increments from the work of Sugden[22] and also from Mumford and Phillips.[23] Although the agreement with the observed values is good using the increments of the latter workers, both calculations yield parachors that are lower than the observed, except for thiophene and 2-methyl-2-propanethiol. Mumford and Phillips use higher values for both CH_2 (40.0) and sulfur (50.0) than Sugden (39.0 and 48.2, respectively). Slightly higher values would bring the results into better agreement. Observed molar volumes were based on densities at the boiling point obtained by straight-line extrapolation of the reported data. Calculated values were obtained by using the increments of Kopp[24] and also by using the carbon and hydrogen increments

---

(19) F. C. Whitmore, "Organic Chemistry," D. Van Nostrand Co., Inc., New York, N. Y., 1937, p. 884.

(20) A. Weissberger, ref. 17, p. 1163.

(21) R. Boudet and R. Rambaud, *Bull. soc. chim. France*, 793 (1948); *C. A.*, **43**, 13 (1949).

(22) A. Weissberger, ref. 17, p. 418.

(23) *Ibid.*, p. 416.

(24) S. Glasstone, "Textbook of Physical Chemistry," D. Van Nostrand Co., Inc., New York, N. Y., 1946, p. 525.

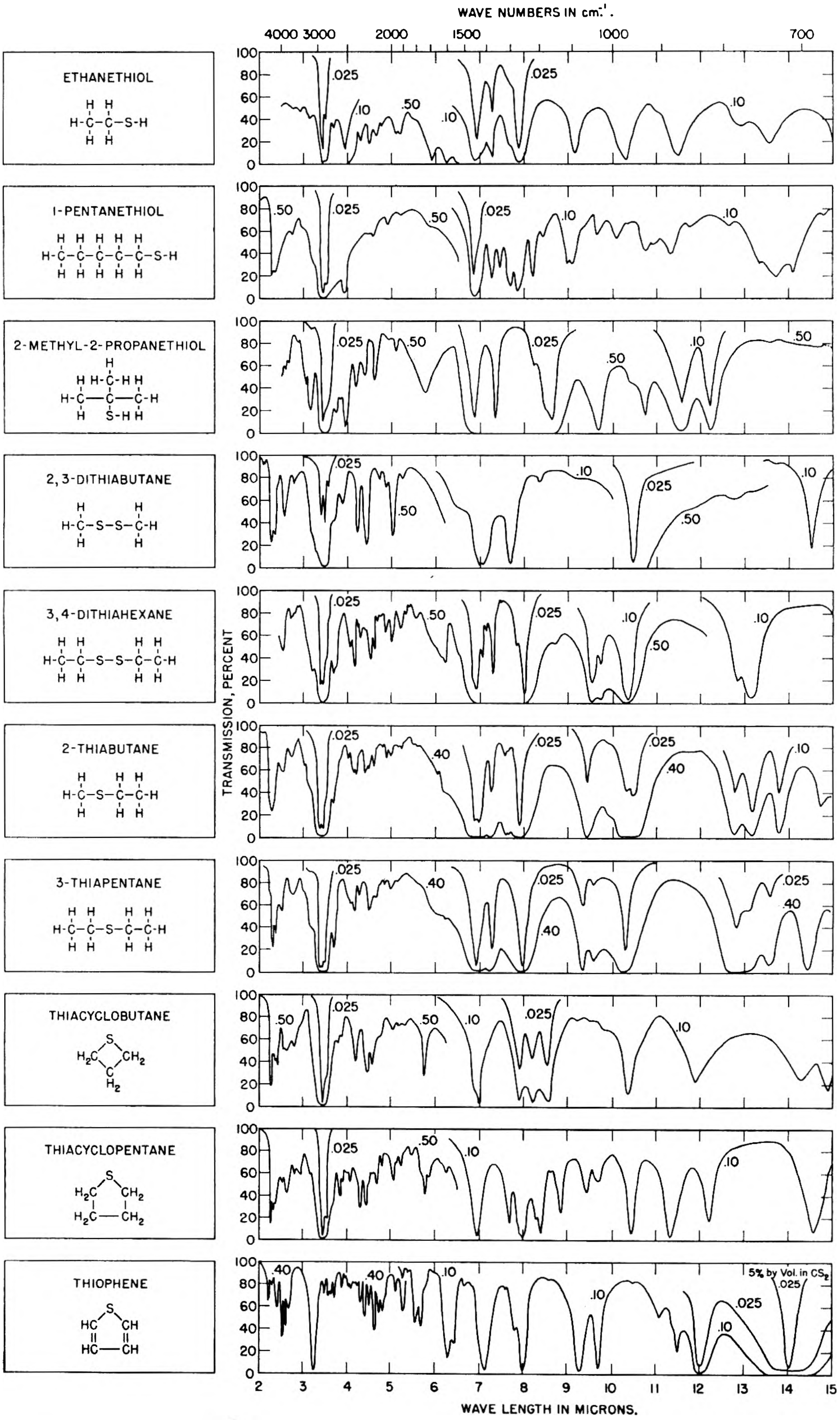

Fig. 3.—Infrared spectra (2–15 μ) of ten sulfur compounds.

of LeBas[24] together with the sulfur increment of Kopp. (LeBas does not report an increment for sulfur.) Values obtained from the latter calculation fit the data much better than those based on the Kopp increments. The three cyclic compounds show extreme deviations because no allowance has been made for the decrease in molar volume caused by cyclization.

Spectra.—Mass, ultraviolet and infrared spectra were determined on each of the ten compounds and complete spectra are included in the Catalogs of Spectral Data.[25] A thorough discussion of the spectra will have to await the determination of data on more members of the various homologous series, but some observations can be made especially with regard to the effect of the sulfur atom.

Mass Spectra.—Spectra were obtained with a Consolidated mass spectrometer, model 21–102.[26] Recommended procedures were followed in obtaining the spectra at an ionizing potential of 70 volts. Automatic controls maintained the catcher current (electron current to the collector) at 8.0 microamperes, and the temperature of the ionization chamber at 300°.

Ultraviolet Spectra.—The ultraviolet absorption spectra were determined with a Beckman quartz spectrophotometer, model DU, using matched silica sample cells 1.00 cm. in thickness. The solvent used for obtaining all of the spectra was 2,2,4-trimethylpentane, prepared by distilling "pure grade isoöctane" and then passing it through silica gel. The purified solvent was transparent down to 208 mμ. Data were taken at 1-mμ intervals except at inflection points, where readings were taken at 0.5-mμ intervals.

Infrared Spectra.—The infrared spectra were determined with a Perkin–Elmer spectrometer, model 12B. Spectra in the 2–15 μ region were obtained using a sodium chloride prism, and sample cells having sodium chloride windows. Spectra in the 14–25 μ region were obtained using a potassium bromide prism, and sample cells having potassium bromide windows. The spectra were calculated from point-by-point per cent. transmission measurements on the recorder tracing.

Discussion

Mass Spectra.—Abridged mass spectra of the compounds are presented in Table V. These spectra differ from those of hydrocarbons by the large number of peaks that cannot be explained by simple splitting of the molecule. One example of this is the mass 35 peak that was observed on several of the spectra and must result from a H_3S^+ particle. This suggests that, under the high-energy conditions in the mass spectrometer, the compounds rearrange so that three hydrogen atoms are associated with the sulfur atom at the time of splitting. Somewhat similar in showing the affinity of the sulfur atom for hydrogen are the rearrangement peaks of the disulfides. 3,4-Dithiahexane gives peaks corresponding to mass 66 ($HSSH^+$) and to mass 94 ($C_2H_5SSH^+$ or $CH_3SSCH_3^+$). 2,3-Dithiabutane has a peak at mass 48 (CH_3SH^+). Other rearrangement peaks include the mass 29 peak ($C_2H_5^+$) of 2-methyl-2-propanethiol; the mass 47 peaks (CH_2SH^+ or CH_3S^+) of 2-methyl-2-propanethiol, 3-thiapentane and thiacyclopentane; the mass 48 peak (CH_3SH^+) of 2-thiabutane; the mass 61 peak ($CH_3SCH_2^+$) of 2,3-dithiabutane; and the mass 62 peak ($C_2H_5SH^+$) of 3-thiapentane. All but one of these fragments include sulfur.

The most stable compounds to mass spectrometric breakdown are 2,3-dithiabutane and thiophene. Both compounds have, as their highest peak, the ion formed from the entire molecule. None of the other compounds have parent peaks of this magnitude. The sulfur–carbon bond appears to be particularly susceptible to cleavage, and large peaks often result from such splitting.

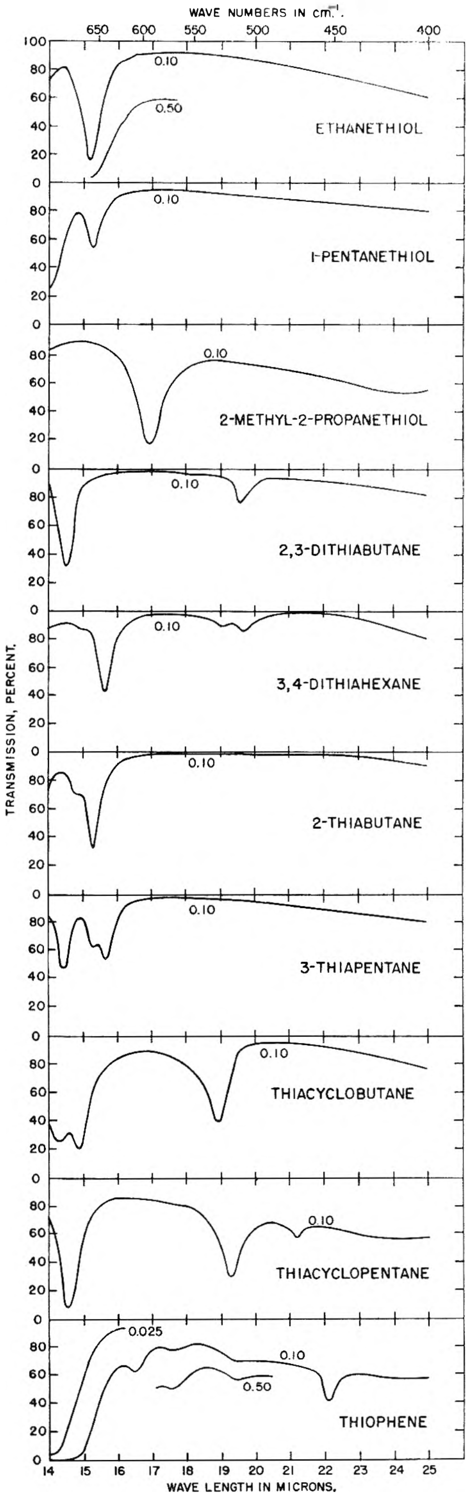

Fig. 4.—Infrared spectra (14–25 μ) of ten sulfur compounds.

Ultraviolet Spectra.—The ultraviolet absorption spectra of three thiols and two disulfides are shown in Fig. 1. The bands shown seem to be shoulders on more intense absorption maxima beyond the range of the instrument. The shoulder for ethanethiol and 2-methyl-2-propanethiol appears at 230 mμ, while for 1-pentanethiol it is displaced slightly toward shorter wave lengths (224 mμ). The two disulfides show similar bands but of

[25] American Petroleum Institute Research Project 44. Carnegie Institute of Technology. Catalog of Mass Spectral Data. Catalog of Ultraviolet Spectral Data. Catalog of Infrared Spectral Data.

[26] H. W. Washburn, H. F. Wiley, S. M. Rock and C. E. Berry, *Ind. Eng. Chem., Anal. Ed.*, **15**, 541 (1943).

greater intensity and at longer wave lengths (250–256 mμ).

The ultraviolet absorption spectra of four sulfides and thiophene are shown in Fig. 2. The sulfides have narrow absorption bands of rather high intensity at about 215 mμ. The bands for the cyclic sulfides are displaced about 5 mμ toward longer wave lengths, are broader and reduced in intensity compared to the straight-chain sulfides. Fehnel and Carmack[27] observed shoulders in the region of 225–235 mμ in the spectra of some aliphatic sulfides and thiacyclohexane and noted that, in the spectrum of thiacyclopentane, this shoulder was shifted 10 mμ toward longer wave lengths. The curves in Fig. 2 confirm these observations and show, in addition, that the shoulder for thiacyclobutane is resolved into a broad band whose maximum is shifted still farther toward longer wave lengths (275 mμ).

The effect of the double bonds in the five-membered ring may be seen by comparing the spectrum of thiophene with that of thiacyclopentane. For thiophene, the band has been broadened, greatly intensified, and shifted toward longer wave lengths. The maximum for thiophene occurs at 231 mμ, with slight shoulders at 240 and 235 mμ.

Infrared Spectra.—The infrared spectra of all of the compounds are shown in Figs. 3 and 4. The cell lengths used are noted on each of the curves.

The three thiols exhibit characteristic absorption bands at 3.90 μ. These bands, due to an S–H stretching vibration, should be useful for detecting the presence of thiols in mixtures of sulfur compounds. The thiols also exhibit absorption bands between 11.0–12.2 μ which are probably due to a C–S–H bending vibration.[3]

All of the compounds except thiophene have rather intense bands attributed to C–S stretching vibrations in the region 13.0–15.5 μ. Although thiophene exhibits an extremely intense absorption band in this region (14.03 μ) this has been attributed to a symmetrical hydrogen bending mode wherein the hydrogen atoms vibrate in unison out of the plane of the nucleus.[28]

The two disulfides have medium bands at 19.6 μ which are probably attributable to S–S stretching vibrations. These bands are not very useful for detecting the presence of disulfides in mixtures of sulfur compounds because the three cyclic sulfur compounds also exhibit bands in this region (19.0–22.0 μ). These vibrations are probably due to a ring deformation.

The remaining bands in the spectra are caused by vibrations involving the C–H and C–C linkages in the hydrocarbon part of the molecules. Bending and rocking vibrations due to CH_3 and twisting and wagging vibrations of CH_2 are found in their usual regions, 7.2–13.6 μ. The band at about 3.40 μ in all of the compounds except thiophene is attributed to C–H stretching vibrations. This band in thiophene falls at 3.23 μ which is similar in location to that of terminal olefin groups.

More complete vibrational assignments have been made on several of these compounds in a series of papers presenting thermodynamic properties of the sulfur compounds.[3]

Acknowledgments.—The authors wish to express their thanks to G. L. Cook for the mass-spectrometer analyses, to W. J. Wenger for the synthesis of 1-pentanethiol, to G. U. Dinneen for suggestion concerning the discussion of spectra, and to the students from the University of Wyoming, who were employed on a part-time basis, for assistance in operating the distillation columns and performing many other duties. This work was done under a coöperative agreement between the Bureau of Mines, United States Department of Interior, and the University of Wyoming.

---

(27) E. A. Fehnel and M. Carmack, *J. Am. Chem. Soc.*, **71**, 84 (1949).

(28) H. D. Hartough, "Thiophene and Its Derivatives," Interscience Publishers, Inc., New York, N. Y., 1952, p. 121.

THE HEATS OF HYDRATION OF TRICALCIUM SILICATE AND β-DICALCIUM SILICATE

BY STEPHEN BRUNAUER, J. C. HAYES AND W. E. HASS

Portland Cement Association Research and Development Laboratories, Chicago, Illinois

Received October 29, 1953

Tricalcium silicate, Ca_3SiO_5, hydrates at 23° by reacting with three moles of water per mole, and β-dicalcium silicate, β-Ca_2SiO_4, reacts with two moles of water per mole. When the hydration reactions take place in the form of hardened pastes at room temperature, with a water-to-solid ratio of 0.7 by weight, $\Delta H_{296} = -22{,}000 \pm 300$ cal. for the first reaction and $\Delta H_{296} = -4100 \pm 600$ cal. for the second reaction. Evidence is presented that in the hydration of the two substances the same calcium silicate hydrate is produced. For the reaction $Ca_3SiO_5(c, 23°) = \beta\text{-}Ca_2SiO_4(c, 23°) + CaO(c, 23°)$, $\Delta H_{296} = -2400 \pm 500$ cal.

Introduction

Tricalcium silicate, Ca_3SiO_5, and β-dicalcium silicate or calcium orthosilicate, β-Ca_2SiO_4, are the two most important components of portland cement; together they constitute at least 70% of portland cement by weight, and occasionally more than 85%. The hydration of the components of portland cement and of portland cement, itself, is exothermic. Values for the heats of hydration of tricalcium silicate and β-dicalcium silicate were first obtained by Woods, Steinour and Starke.[1] They determined the heat evolved in the hydration of portland cements of different chemical compositions, and calculated, by least squares analysis, the heats assignable to the individual components. For the two silicates the values thus determined were: tricalcium silicate, 136 cal./g.; dicalcium silicate, 62 cal./g. The cements were hydrated for one year.

Lerch and Bogue[2] determined the heats of hydration of tricalcium silicate and dicalcium silicate, hydrating the compounds themselves, and obtained the values 120 and 62 cal./g., respectively. Recently, Verbeck and Foster,[3] using the methods of Woods, Steinour and Starke, obtained 117 and 53 cal./g. for the heats of hydration of tricalcium and dicalcium silicate, respectively. Their data were obtained from 14 cements, hydrating for six and a half years. It will be noted that the three sets of results are in reasonably good agreement, suggesting that the heats of hydration of the two silicates in portland cement do not differ greatly from the heats of hydration of the pure compounds.

Powers and Brownyard[4] pointed out that the calorimetrically determined heat of hydration of a portland cement is a composite quantity. In the hydration process a finely divided substance forms, called the "cement gel," and this gel adsorbs large amounts of water. The over-all heat of hydration is the sum of the chemical heat of hydration and the heat of adsorption of water on the hydrated material. Powers and Brownyard determined the heat of adsorption of water on two hydrated portland cements, and came to the conclusion that the heat of adsorption was about 1/4 of the over-all heat of hydration.

The point raised by Powers and Brownyard is valid for all three sets of determinations of the heats of hydration of tricalcium silicate and dicalcium silicate cited above. The heat values obtained were composite quantities. Although for practical purposes these composite heats are of prime importance, from the point of view of basic information the breakdown of the over-all heats of hydration into their components is of considerable interest. The purpose of the present investigations was to determine the *chemical* heats of hydration of the two calcium silicates, *i.e.*, the changes in heat content (or enthalpy) occurring in the chemical reactions between the silicates and water. The experimental method used was that proposed by Woods and Steinour[5] and used by all of the investigators cited before. The heats of solution of the unhydrated and hydrated materials were determined calorimetrically and the heat of hydration was obtained as the difference. The chemical heat of hydration was obtained directly by removing the adsorbed water from the hydrated material prior to determining its heat of solution.

Experimental

Preparation of Ca_3SiO_5 and Ca_2SiO_4.—The tricalcium silicate used in these investigations was prepared by Dr. L. E. Copeland of this Laboratory, by burning a mixture of calcium carbonate and powdered quartz having a mole ratio of $CaCO_3$ to SiO_2 of 3.0. A two-burner gas-fired kiln with an approximately one cubic foot burning zone was used. Temperature readings were taken with an optical pyrometer through an opening in the kiln lining. Uniformity in burning was obtained by preparing the initial charge in the form of 1/2″ × 3/4″ × 10″ sticks that could be stacked (cross-hatch style) on the 12″ × 12″ hearth. The sticks were prepared by adding to the dry $CaCO_3$ and SiO_2 1% sugar and sufficient water to moisten the mix, troweling out the mixture on sheets of wax paper until the resulting slabs were about 1/2″ thick, drying, and cutting the slabs into the desired sticks.

Two burnings, with an intermediate cooling, grinding and second stick fabrication, were found to be necessary to obtain completeness of reaction. During each burn the charge was fired between 1500 and 1700° for about three hours. After the first burn the mixture dusted on cooling and was found, by microscopical examination, to contain about 70% γ-Ca_2SiO_4. In the second burn reasonably pure Ca_3SiO_5 was obtained. The sticks were ground in a laboratory ball mill to a Blaine surface (ASTM Designation C-204-51) of about 4500 cm.^{2}/g.

Two preparations of β-dicalcium silicate were used. These preparations, referred to as Ca_2SiO_4 (I) and (II), were made in 1938 at the Portland Cement Association Fellowship in

---

[1] H. Woods, H. H. Steinour and H. R. Starke, *Ind. Eng. Chem.*, **24**, 1207 (1932); *Eng. News-Record*, **110**, 431 (1933).

[2] W. Lerch and R. H. Bogue, *Bur. Standards J. Research*, **12**, 645 (1934).

[3] G. J. Verbeck and C. W. Foster, *Proc. Am. Soc. Testing Materials*, **50**, 1235 (1950).

[4] T. C. Powers and T. L. Brownyard, *J. Am. Concrete Inst.*, **18**, 549 (1947).

[5] H. Woods and H. H. Steinour, *ibid.*, **3**, 195 (1931).

Washington, D. C. The procedure was that described by Lerch and Bogue.[6]

Hydration Procedure.—The compounds were hydrated by Copeland. The original mixing with water was performed under reduced pressure (approx. 20 mm.) in order to obtain pastes free of air voids. The word "paste" as used by cement chemists, and as used here, means a mixture of a hydraulic material, such as portland cement, Ca_3SiO_5 or Ca_2SiO_4, with water. The proportion of water used is such as to make the mixture initially plastic, but after a few hours the mixture "sets" and then hardens. The dicalcium and tricalcium silicate pastes used in these experiments were hardened pastes.

The pastes were prepared with a water-to-solid ratio of 0.70 by weight. After mixing, they were poured into paraffin-lined molds, which were 1″ × 10″ soft glass tubes, closed at the bottom with a tight-fitting rubber stopper. The molds contained a $^1/_2$″ × 10″ rubber-tubing core in the center, which could later be extracted to produce tubular specimens with $^1/_2$″ inside diameter. Precooled mixing water was used to keep the paste temperature at the time of casting at 23 ± 3°. Immediately after casting, sufficient water was added to cover the paste surface completely. The opening of the glass tube at the top was then closed with a rubber stopper to prevent loss of water by evaporation. When the pastes were about 24 hr. old, the core was removed, and the hole was filled with water. The purpose of the water-filled hole was to maintain the paste in a saturated condition throughout the hydration process. The hydration was conducted in a room kept at 23 ± 0.5°.

The Ca_3SiO_5 paste was removed from the glass tube after approximately five months, during which time the hole was kept full of water. From this time on the specimen was stored in a humidifier where it was not in direct contact with water but was surrounded by a water-vapor-saturated atmosphere. At the time samples were taken for the present investigations the paste was approximately 21 months old, and crystals of $Ca(OH)_2$ lined the inside wall. In preparing samples for analysis care was taken to prevent loss of these crystals, inasmuch as they formed a part of the products of hydration.

The Ca_2SiO_4 paste sample was hydrated continuously under water in the stoppered tube from the time the central plug was removed at an age of 24 hr. until samples were taken for the present investigations at a paste age of approximately 21 months. Crystals of $Ca(OH)_2$ were likewise found lining the inside wall of this specimen.

Removal of Adsorbed Water.—The hydrated paste samples were ground to pass a U. S. Standard No. 100 sieve to hasten the establishment of the drying equilibrium and to aid the dissolution in the acids used in the calorimeter and in chemical analysis. The grinding, sieving and transfers of the materials were conducted in a controlled atmosphere manipulation cabinet equipped with Ascarite filters, to reduce contamination of the samples by carbon dioxide.

The adsorbed water was removed by reducing the partial pressure of water vapor in the system containing the hydrated sample to the vapor pressure of ice at Dry Ice-alcohol temperature, about −79°. (The vapor pressure was about 0.5 μ of Hg.) The samples were considered at equilibrium when the loss of water was less than 1 mg./g. of sample in two days. It usually took from one to two weeks to reach equilibrium. Details of the drying procedure will be published shortly by Copeland and Hayes.[7]

It is realized that the drying procedure adopted by us may not remove all of the adsorbed water, and it may remove some of the water of hydration. The calcium silicate hydrate formed is a colloidal substance, without any definite decomposition pressure at a given temperature. Because the gel particles are not all the same size, the amount of water of hydration given off varies continuously with pressure in the low pressure range; some of it may possibly come off even at a vapor pressure higher than 0.5 μ of Hg. Nevertheless, the uncertainty introduced by this factor is small. Copeland has obtained evidence (to be published later) that the uncertainty in the amount of the water of hydration under the drying conditions of the present experiments is less than 5%. Since the heat of hydration of the calcium silicate hydrate is not very different from the heat of adsorption of water, as will be seen later, the possible error due to this factor is less than 1 cal./g. of calcium silicate.

After establishment of the drying equilibrium, the pastes were kept in glass stoppered weighing bottles placed in desiccators containing a 1:1 mixture of Ascarite and Anhydrone. When the samples had to be kept in storage, the weighing bottles were sealed with paraffin. In all subsequent operations great care was taken to avoid contact of the hydrated samples with atmospheric carbon dioxide and water vapor. To the extent possible, operations were carried out in the controlled-atmosphere cabinet.

Loss on Ignition, Carbon Dioxide Content, Heat of Solution.—Because of possible inhomogeneity of the materials, and still more because of possible contamination by carbon dioxide and water vapor during handling, ignition loss, carbon dioxide and heat of solution determinations were made on 4 to 8 samples of each material. Determinations of each of the three quantities were made simultaneously, using samples taken from the same weighing bottles.

The ignition loss was determined on 0.5-g. samples, by heating them in a globar furnace kept at 1050°. An initial ignition period of 40 minutes was followed by successive reheat periods of 10 minutes each. The ignition was considered complete when the additional loss of weight was less than 0.2 mg. Usually only one reheat period was found necessary. At 1050° both the carbonates and the hydrates in the materials decompose completely. The carbon dioxide content was determined separately on samples of 0.5 to 1 g., using a modification of the ASTM procedure for the determination of the carbon dioxide content of limestone (Designation C-25-47). The water of hydration was taken as the difference between the ignition loss and the carbon dioxide content.

The heat of solution was determined on 1- to 2-g. samples of the materials, using the same calorimeter and essentially the same procedure that was described by Verbeck and Foster.[3] The solvent used was 8 ml. of 48% H_2F_2, with sufficient 2 N HNO_3 added to make the total weight 420 g. For about half of the samples we used a somewhat modified procedure. Samples were introduced after a 20–30 minute initial rating period, and temperature readings were recorded at the end of each successive 5-minute period during the following 80 minutes. Solution periods of 20, 25, 30, 35 and 40 minutes were assumed, with equally long final rating periods. This procedure made it possible to calculate five values of the calorimeter temperature rise for each sample. The average of the five values was taken as the temperature rise in these "long" runs. There was no systematic difference between the results obtained from the long and short runs.

Analysis and Composition of the Materials.—Since the materials used in these experiments contained some impurities, we attempted to make corrections for them. Careful and complete chemical analyses were performed on all of the substances by the Analytical Section of the Portland Cement Association Laboratories, and the composition of each substance was calculated on the basis of the analysis. The guiding principle in the calculation of the compounds present in the materials was the method developed by Bogue[8] for the calculation of the compounds present in portland cement. The heat of solution of each substance was corrected on the basis of the assumption that the heats of solution of the impurities were additive. The chemical analyses and the computed compositions of the substances are given in Table I.

Each analysis was performed on at least duplicate samples. ASTM procedures, described under ASTM Designations C-114-47 and C-228-49T, were used for all oxide analyses with the exception of B_2O_3, which was determined using a modification of the procedure recommended by Scott.[9]

Results

The experimental calorimetric results are listed in Table II.

The results are reported in calories per gram of material for the unhydrated substances and in calories per gram of ignited material for the hydrated

---

[6] W. Lerch and R. H. Bogue, THIS JOURNAL, **31**, 1627 (1927).

[7] L. E. Copeland and J. C. Hayes, to be published in ASTM Bull.

[8] R. H. Bogue, *Ind. Eng. Chem., Anal. Ed.*, **1**, 192 (1929).

[9] N. H. Furman, "Scott's Standard Methods of Chemical Analysis," 5th edition, Vol. I, D. Van Nostrand Co., Inc., New York, N. Y., 1939, p. 174.

TABLE I

CHEMICAL ANALYSIS AND COMPOSITION OF MATERIALS

Ca_3SiO_5			
Analysis		Composition	
Substance	%	Substance	%
Total CaO[1]	72.74	Ca_3SiO_5	95.12
Total SiO_2[2]	26.30	β-Ca_2SiO_4	1.92
Al_2O_3	0.02	$Ca_2SiO_4 \cdot 2H_2O$	1.79
MgO	0.10	$Ca(OH)_2$	0.55
SO_3	0.03	$CaCO_3$	0.25
H_2O	0.46	$Ca_3Al_2O_6 \cdot 6H_2O$	0.07
CO_2	0.11	$CaSO_4$	0.05
Na_2O	Nil	MgO	0.10
K_2O	Nil	SiO_2	0.15
Total[3]	99.76	Total	100.00

β-Ca_2SiO_4 (I)			
Analysis		Composition	
Substance	%	Substance	%
Total CaO[4]	64.57	Ca_3SiO_5	0.58
Total SiO_2[5]	34.32	β-Ca_2SiO_4	97.42
Al_2O_3	0.19	$Ca(OH)_2$	0.03
MgO	0.12	$CaCO_3$	0.66
SO_3	0.01	$Ca_3Al_2O_6$	0.50
H_2O	0.15	$CaSO_4$	0.02
CO_2	0.29	MgO	0.12
Na_2O	0.03	SiO_2	0.20
K_2O	Nil	B_2O_3	0.05
B_2O_3	0.30	H_3BO_3	0.32
Total[6]	99.98	$Na_2B_4O_7$	0.10
		Total	100.00

[1] Free CaO 0.42. [2] Free SiO_2 0.15. [3] Missing 0.24% was assumed to be Ca_3SiO_5. [4] Free CaO 0.02. [5] Free SiO_2 0.20. [6] Missing 0.02% was assumed to be Ca_2SiO_4.

β-Ca_2SiO_4 (II)			
Analysis		Composition	
Substance	%	Substance	%
Total CaO[7]	62.42	β-Ca_2SiO_4	88.83
Total SiO_2[8]	34.32	α-$CaSiO_3$	6.42
Al_2O_3	0.48	$CaCO_3$	1.91
MgO	0.12	$Ca_3Al_2O_6$	1.05
SO_3	0.01	$Ca_3Al_2O_6 \cdot 6H_2O$	0.31
H_2O	0.47	$CaSO_4$	0.02
CO_2	0.99	MgO	0.12
Na_2O	0.32	SiO_2	0.24
K_2O	Nil	$Na_2CO_3 \cdot H_2O$	0.42
B_2O_3	0.25	$Na_2B_4O_7 \cdot 10H_2O$	0.68
Total[9]	99.38	Total	100.00

Ca_3SiO_5 Paste (I)			
Analysis		Composition	
Substance	%	Substance	%
Ignited analysis		$Ca_3Al_2O_6 \cdot 6H_2O$	0.07
was the same		$CaSO_4$	0.05
as that of		$CaCO_3$	2.34
Ca_3SiO_5. It		$Mg(OH)_2$	0.14
was taken as	100.00	SiO_2	0.15
H_2O	19.44	Ca_3SiO_5	92.63
CO_2	1.03	Ca_2SiO_4 [10]	5.71
Total	120.47	H_2O	19.38
		Total	120.47

[7] Free CaO nil. [8] Free SiO_2 0.24. [9] Missing 0.62% was assumed to be Ca_2SiO_4. [10] The extent of hydration of Ca_3SiO_5 and Ca_2SiO_4 was calculated in different ways. See Discussion.

Ca_3SiO_5 Paste (II)			
Analysis		Composition	
Substance	%	Substance	%
Ignited analysis		$Ca_3Al_2O_6 \cdot 6H_2O$	0.07
was the same		$CaSO_4$	0.05
as that of		$CaCO_3$	0.77
Ca_3SiO_5. It		$Mg(OH)_2$	0.14
was taken as	100.00	SiO_2	0.15
H_2O	20.19	Ca_3SiO_5	96.22
CO_2	0.34	Ca_2SiO_4 [10]	3.00
Total	120.53	H_2O	20.13
		Total	120.53

Ca_2SiO_4 Paste			
Analysis		Composition	
Substance	%	Substance	%
Ignited analysis		$Ca_3Al_2O_6 \cdot 6H_2O$	1.78
was the same		$CaSO_4$	0.02
as that of		$CaCO_3$	1.32
β-Ca_2SiO_4(II).		$Mg(OH)_2$	0.17
It was taken		SiO_2	0.24
as	100.00	$Na_2CO_3 \cdot H_2O$	0.42
H_2O	7.91	$Na_2B_4O_7 \cdot 10H_2O$	0.68
CO_2	0.73	Ca_2SiO_4	90.74
Total	108.64	$CaSiO_3$ [11]	6.30
		H_2O	6.97
		Total	108.64

[11] The extent of hydration of Ca_2SiO_4 and $CaSiO_3$ was calculated in different ways. See Discussion.

TABLE II

HEATS OF SOLUTION OF UNHYDRATED AND HYDRATED MATERIALS (CAL./G.)

	Ca_3SiO_5	β-Ca_2SiO_4 (I)	β-Ca_2SiO_4 (II)	Ca_3SiO_5 Paste (I)	Ca_3SiO_5 Paste (II)	Ca_2SiO_4 Paste
	630.4	560.5	545.4	553.5	552.3	550.5
	629.9	562.7	549.6	550.5	550.9	547.1
	631.4	558.1	547.2	550.4	552.7	546.5
	632.9	561.8	[541.0]	553.0	553.3	[556.0]
	630.6(L)	561.4	547.5(L)		552.3(L)	548.8(L)
	630.7(L)	562.7	548.2(L)		554.2(L)	551.3(L)
		558.7(L)	548.3(L)			544.3(L)
		558.5(L)	547.8(L)			541.8(L)
Av.	631.0	560.6	547.7	551.9	552.6	547.2
Mean dev.	0.8	1.6	0.9	1.4	0.8	2.6
Std. dev.	1.1	1.9	1.3	1.6	1.1	3.3

substances. The two values in brackets were discarded. The letter (L) after the heat of solution value signifies a long run.

The scatter in the experimental results is attributed to lack of complete homogeneity of the substances, in addition to errors in the measurements. The standard deviation was between 1 and 2 cal. for five of the six materials; the large standard deviation obtained for hydrated dicalcium silicate was, doubtless, caused largely by inhomogeneity of the material.

The heat of solution values showed no trend with the weight of solute used, for any of the six materials. A twofold change in weight gave no detectable difference in the heat of solution, indicating that the concentration effects were negligible within our experimental error.

The experimental heats of solution were corrected for the heats of solution of the impurities, by using the values given in Table III.

TABLE III

HEATS OF SOLUTION OF IMPURITIES (CAL./G.)

Substance	Heat of soln.	Substance	Heat of soln.
SiO_2	570.8[a]	CaO	825.9[a]
MgO	562.0[b]	$Ca(OH)_2$	414.5[d]
$Mg(OH)_2$	455.5[b]	$CaCO_3$	86.0[c]
B_2O_3	642.1[c]	$CaSO_4$	31.2[a]
H_3BO_3	227.8[c]	$Ca_3Al_2O_6$	733.0[e]
$Na_2CO_3 \cdot H_2O$	73.2[a]	$Ca_3Al_2O_6 \cdot 6H_2O$	412.8[f]
$Na_2B_4O_7$	87.1[a]	α-$CaSiO_3$	525.1[g]
$Na_2B_4O_7 \cdot 10H_2O$	−50.0[a]	$CaSiO_3 \cdot H_2O$	435.5[h]

[a] Calculated from the National Bureau of Standards Thermodynamic Tables.[10] The value for SiO_2 was checked by us. [b] Roth and Chall.[11] [c] Determined experimentally by us. [d] Calculated from the heat of solution of CaO, and the heat of hydration of CaO, determined by Thorvaldson, Brown and Peaker.[12] [e] Lerch and Bogue.[2] [f] Calculated from Lerch and Bogue's heat of hydration of tricalcium aluminate, with the assumption that one-fourth of the heat of hydration is attributable to heat of adsorption. [g] Calculated from (1) the heats of solution of CaO and β-Ca_2SiO_4 (determined by us); (2) the heat of decomposition of β-Ca_2SiO_4 into β-$CaSiO_3$ and CaO (King[13]), and (3) the heat of transformation of wollastonite to pseudowollastonite (Wagner[14]). [h] Calculated from the data of Cirilli.[15]

Discussion

The Stoichiometry of the Hydration of Tricalcium and β-Dicalcium Silicate.—The stoichiometry of the hydration of the two calcium silicates is not fully settled. It is known that the products of the hydration are calcium hydroxide and a calcium silicate hydrate. The former appears as a crystalline substance, the latter as a finely divided "gel," which looks structureless in an ordinary microscope. The electron microscope, however, shows that the gel consists of roughly spherical particles, 50 to 200 Å. in diameter.[16] This is in good agreement with the results of Powers, Brownyard, Copeland, and Hayes, obtained in this Laboratory, who determined the specific surface areas of various hydrated portland cements and of hydrated tricalcium silicate by the BET method[17] and obtained an average particle diameter of 100 to 150 Å.

Investigators in the field have generally assumed, but there is no published proof in the literature, that in the hydration of Ca_3SiO_5 and Ca_2SiO_4 the same gel forms. It will be seen later that the present work furnishes strong evidence that the two calcium silicates, hydrating in the form of hardened pastes, actually form the same gel.

The assumption that the two gels are identical may be expressed in the form of the equations

$$Ca_2SiO_4 + mH_2O = \text{Gel} + nCa(OH)_2 + X \text{ cal.} \quad (1)$$

$$Ca_3SiO_5 + (m + 1)H_2O = \text{Gel} + (n + 1)Ca(OH)_2 + Y \text{ cal.} \quad (2)$$

X and Y are the heats of hydration of dicalcium and tricalcium silicate, respectively.

Grunwald, Copeland and Hayes hydrated the two calcium silicates in this Laboratory by grinding in a small steel ball mill, in excess water at 23°. The water-to-silicate ratio varied from 4 to 9. Complete hydration of Ca_3SiO_5 occurred in about a week, and the water of hydration corresponded almost exactly to three molecules per molecule of Ca_3SiO_5. The hydration of Ca_2SiO_4 progressed much more slowly; complete hydration did not occur even in six weeks of grinding in the ball mill. If it is assumed that complete hydration of Ca_2SiO_4 would correspond to an uptake of two molecules of water, the maximum hydration of Ca_2SiO_4 obtained was about 90%. Jacquemin,[18] hydrating Ca_3SiO_5 and Ca_2SiO_4 in a ball mill, also came to the conclusion that the water of complete hydration corresponded to three and two molecules, respectively.

Grunwald devised a method to find out whether ball-mill-hydrated Ca_3SiO_5 and Ca_2SiO_4 formed the same gel. He plotted the total water contents (water of hydration plus adsorbed water) of completely hydrated Ca_3SiO_5 and Ca_2SiO_4 samples at the same relative pressures against each other. If the two silicates produce the same gel and if calcium hydroxide has a negligible adsorbing surface compared to the gel, the adsorbed water held by 1 mole of completely hydrated Ca_3SiO_5 should be the same as that held by 1 mole of hydrated Ca_2SiO_4 at any relative pressure, but the water of hydration of the former should exceed that of the latter by 1 mole, as equations 1 and 2 show. Grunwald's plot, therefore, should give a straight line, the intercept of which on the Ca_3SiO_5 axis would correspond to the excess water held by Ca_3SiO_5 over Ca_2SiO_4 at zero adsorption. The plot did give a good straight line, and the value of the intercept was approximately 1 mole of water per mole of Ca_3SiO_5. Since the results of Powers and Brownyard[19] indicated earlier that the surface of calcium hydroxide was negligible compared to the surface of the gel, the results of Grunwald are consistent with

---

(10) Bur. Standards Circular 500 (1952).

(11) W. A. Roth and P. Chall, *Z. Elektrochem.*, **34**, 185 (1928).

(12) T. Thorvaldson, W. G. Brown and C. R. Peaker, *J. Am. Chem. Soc.*, **51**, 2678 (1929); **52**, 80, 910 (1930).

(13) E. G. King, *ibid.*, **73**, 656 (1951).

(14) H. Wagner, *Z. anorg. allgem. Chem.*, **208**, 1 (1932).

(15) V. Cirilli, *Ann. chim. appl.*, **28**, 151, 239 (1938).

(16) To be published in the Proceedings of the Third International Symposium on the Chemistry of Cement, as a discussion by R. H. Bogue of J. D. Bernal's paper.

(17) S. Brunauer, P. H. Emmett and E. Teller, *J. Am. Chem. Soc.*, **60**, 309 (1938).

(18) R. Jacquemin, "Recherches sur l'hydratation des liants hydrauliques," Dissertation, University of Liége, Desoer, Liége, 1944.

(19) T. C. Powers and T. L. Brownyard, *J. Am. Concrete Inst.*, **18**, 469 (1946).

the conclusions that (a) ball-mill-hydrated Ca_3SiO_5 takes up one more molecule of water than Ca_2SiO_4, and (b) both substances form the same gel.

Further evidence as to the identity of the two gels in hardened portland cement paste can be found in the work of Powers and Brownyard. They determined the surface area and the water of hydration for a large number of hydrated portland cements and evaluated the contributions of the individual components by least squares analysis. If in equations 1 and 2 $m = 2$, the surface area contribution per gram of water of hydration for Ca_2SiO_4 should be 1.5 times as great as for Ca_3SiO_5, provided (a) that the two substances form the same gel and (b) that calcium hydroxide does not contribute appreciably to the surface. The ratio was actually found to be close to 1.5. The same ratio was obtained later by Copeland and Hayes from another series of portland cements.

Although it appears quite certain that in equations 1 and 2 $m = 2$, nothing definite can be stated about the value of n and about the chemical composition of the gel. The reason for this is that there exists no completely reliable method for the determination of free lime in hydrated systems like these. The method of Lerch and Bogue[20] works very well for unhydrated cements, but the glycerol–alcohol solvent used by them, and other solvents proposed by others, dissolve not only the free $Ca(OH)_2$, but remove part of the lime from the calcium silicate hydrate as well. We are investigating the stoichiometry of the hydration of the two calcium silicates further. For the time being we can only say that the most probable value of n is either 0 or 0.5, which would make the composition of the gel either $2CaO \cdot SiO_2 \cdot 2H_2O$ or $1.5CaO \cdot SiO_2 \cdot 1.5H_2O$.

Relation between the Heats of Hydration of Ca_3SiO_5 and Ca_2SiO_4.—Consider the equations

$$\begin{aligned}
&Ca_3SiO_5 &&= Ca_2SiO_4 + CaO &&+ Z \text{ cal.} &&(3)\\
&Ca_2SiO_4 + mH_2O &&= \text{Gel} + nCa(OH)_2 &&+ X \text{ cal.} &&(1)\\
&CaO + H_2O &&= Ca(OH)_2 &&+ V \text{ cal.} &&(4)\\
\hline
&Ca_3SiO_5 + (m + 1)H_2O &&= \text{Gel} + (n + 1)Ca(OH)_2 &&+ Y \text{ cal.} &&(2)
\end{aligned}$$

It is evident that

$$Y = X + V + Z \qquad (5)$$

If Ca_3SiO_5 and Ca_2SiO_4 form the same gel, their heats of hydration can be obtained from each other, provided that V and Z are known. The heat of hydration of CaO was accurately determined by Thorvaldson, Brown and Peaker,[12] and it was found to be 15,600 cal./mole. However, for the heat of decomposition of Ca_3SiO_5 into Ca_2SiO_4 and CaO we found two widely differing values in the literature: Johansson and Thorvaldson[21] obtained the value 470 cal./mole, and King[13] obtained 3200 cal./mole. Because of this, we decided to redetermine the heat of decomposition of Ca_3SiO_5. It was obtained as the difference between the heat of solution of Ca_3SiO_5 and the sum of the heats of solution of Ca_2SiO_4 and CaO.

The estimated compositions of our substances, the experimental heats of solution and the heats of solution of the impurities have been given before. Aside from the experimental errors, the main uncertainty is introduced in the estimation of the compound composition of our materials. For example, in the calculation of the composition of Ca_3SiO_5 it was assumed that the 0.24% missing from the total chemical analysis was Ca_3SiO_5. This assumption introduces an uncertainty of about 1 cal./g. in the heat of solution. In some cases we have been forced to assume impurities which were not the most likely ones to occur in the system, because of lack of data. In such cases we selected compounds that were closest in composition to the most likely impurities. We believe that the errors introduced by uncertainties in the composition were no greater than the variation from sample to sample in the experimentally determined heats of solution. In addition, it should be noted that the heats of hydration of Ca_3SiO_5 and Ca_2SiO_4 were obtained as differences between the heats of solution of the same material in the hydrated and unhydrated state. Since in the calculation of their compositions similar assumptions were made, the uncertainties were reduced to a minimum.

The calculated heat of solution of Ca_3SiO_5 was found to be 639.0 ± 1.5 cal./g., and that of Ca_2SiO_4(I) was 564.0 ± 2 cal./g. The heat of decomposition of Ca_3SiO_5, Z in equation 3, is 2400 ± 500 cal./mole. The results were rounded off to the nearest 0.5 cal./g. and 100 cal./mole.

King attributed the difference between his value of 3200 cal./mole and Johansson and Thorvaldson's 470 cal./mole to the fact that the latter used silica gel in the preparation of the calcium silicates, whereas he used quartz. The calcium silicates we used were prepared from quartz and calcium carbonate; consequently, our value is comparable with King's.

King did not make corrections for the impurities in his Ca_3SiO_5 and Ca_2SiO_4. On the basis of his published chemical analyses one can estimate that his Ca_2SiO_4 was about 97% and his Ca_3SiO_5 perhaps better than 98% pure, but the analytical data are not sufficiently complete to enable one to correct for the impurities.

The experimental uncertainty in King's value is about 320 cal./mole. Thus, the difference of 800 cal./mole between King's value and ours is somewhat greater than the combined uncertainties of the two sets of experiments. We believe that our result is closer to the true value of the heat of decomposition of Ca_3SiO_5, partly because we have made an attempt to correct for the impurities in our silicates, and partly because we believe that King did not correct completely for the concentration effects in his solutions.

It follows from equation 5 that

$$Y = X + 18{,}000 \text{ cal./mole} \qquad (6)$$

The Heat of Hydration of β-Ca_2SiO_4.—The hydrated dicalcium silicate paste was prepared from the material designated Ca_2SiO_4(II), which, as the calculated composition shows, was considerably less pure than Ca_2SiO_4(I). The heat of solution of Ca_2SiO_4(II), corrected for impurities, was

---

[20] W. Lerch and R. Bogue, *Ind. Eng. Chem., Anal. Ed.*, **2**, 296 (1930).

[21] O. K. Johansson and T. Thorvaldson, *J. Am. Chem. Soc.*, **56**, 2327 (1934).

564.0 ± 2 cal./g. This material should have given a heat of solution about 0.5 cal./g. lower than Ca_2SiO_4(I), because it contained about 10% γ-Ca_2SiO_4, whereas Ca_2SiO_4(I) did not contain any. The agreement within 0.5 cal. is very gratifying in view of the experimental and theoretical uncertainties involved.

It was assumed that in the hardened Ca_2SiO_4 paste all of the hydratable compounds were fully hydrated except the two principal components, $CaSiO_3$ and Ca_2SiO_4. The heat of hydration of Ca_2SiO_4 was then calculated in two ways: (1) by assuming that $CaSiO_3$ was not hydrated at all, and (2) by assuming that $CaSiO_3$ was hydrated to the same extent as Ca_2SiO_4. If the first assumption is made, the extent of hydration of Ca_2SiO_4 was 36.5%, and the heat of hydration was 24.5 cal./g. of Ca_2SiO_4; if the second assumption is made, the extent of hydration of Ca_2SiO_4 was 35%, and the heat of hydration was 24.5 cal./g. of Ca_2SiO_4. The two values do not differ within our approximation of 0.5 cal./g., because the heats of hydration of the metasilicate and the orthosilicate of calcium per mole of water are close to each other.

The heat of hydration of β-Ca_2SiO_4 at 23°, X in equation 1, was

$$X = 4200 \pm 600 \text{ cal./mole}$$
$$\text{or } 24.5 \pm 3.5 \text{ cal./g. of } Ca_2SiO_4$$

The large uncertainty is probably attributable to lack of homogeneity of the material, as we stated before.

The Heat of Hydration of Ca_3SiO_5.—The heats of solution of hydrated Ca_3SiO_5 paste were determined on two sets of samples, designated (I) and (II). They differed primarily in the extent of the carbonation of the paste: (I) contained 1.03% CO_2, (II) only 0.34% CO_2. It was assumed in both cases that all hydratable compounds in the samples were fully hydrated, except the two calcium silicates, Ca_2SiO_4 and Ca_3SiO_5. The heat of hydration of Ca_3SiO_5 was then calculated in two ways: (1) by assuming that the two silicates were hydrated to the same extent, and (2) by assuming that Ca_2SiO_4 was hydrated to the extent it was hydrated in its own paste. Although Ca_2SiO_4 hydrates more slowly than Ca_3SiO_5, especially in the initial stages, there is some evidence to show that it hydrates faster in the presence of certain other substances than when it hydrates alone. Thus, assumptions (1) and (2) set an upper and a lower limit to the heat of hydration of Ca_3SiO_5.

If the first assumption is made, Ca_3SiO_5 Paste (I) was 84% hydrated, and the heat of hydration of Ca_3SiO_5 was 96.5 cal./g. If the second assumption is made, the Ca_2SiO_4 in Ca_3SiO_5 Paste (I) was 36% hydrated and the Ca_3SiO_5 was 86% hydrated. The calculated heat of hydration of Ca_3SiO_5 for this case is 94.5 cal./g. For Ca_3SiO_5 Paste (II) the extent of hydration on the basis of the first assumption was 86%, and the heat of hydration was 97.5 cal./g.; on the basis of the second assumption Ca_2SiO_4 was 36% and Ca_3SiO_5 was 87% hydrated, and the heat of hydration of Ca_3SiO_5 was 96.5 cal./g.

Taking the average of the four values as the heat of hydration of Ca_3SiO_5 at 23°, we find Y in equation 2 to be

$$Y = 22{,}000 \pm 300 \text{ cal./mole}$$
$$\text{or } 96.5 \pm 1.5 \text{ cal./g. of } Ca_3SiO_5$$

If in the hydration of Ca_3SiO_5 and Ca_2SiO_4 the same calcium silicate hydrate or "gel" is produced, equation 6 holds, and X can be obtained by subtracting 18,000 cal. from Y. The result is 4000 cal./mole, which is 200 cal./mole less than the heat of hydration obtained from the Ca_2SiO_4 paste. Actually, the value of X obtained from Ca_3SiO_5 Paste (II) is 4200 cal./mole; and we consider the results from this paste more reliable than that obtained from Ca_3SiO_4 Paste (I). The agreement indicates strongly that Ca_3SiO_5 and Ca_2SiO_4 hydrating in the form of hardened pastes (in the same form in which portland cement hydrates in concrete) produce identical gels.

Conclusions.—For the reaction Ca_3SiO_5 (c, 23°) = β-Ca_2SiO_4(c, 23°) + CaO(c, 23°), $\Delta H_{296} = -2400 \pm 500$ cal. For the reaction of Ca_3SiO_5(c, 23°) with $3H_2O$ (l, 23°), $\Delta H_{296} = -22{,}000 \pm 300$ cal. For the reaction of β-Ca_2SiO_4(c, 23°) with $2H_2O$ (l, 23°), $\Delta H_{296} = -4100 \pm 600$ cal. The stoichiometry of the products formed in the hydration reactions is not definitely known, but it appears safe to conclude that in the hydration of Ca_3SiO_5 and Ca_2SiO_4 the same calcium silicate hydrate is produced, when the hydration takes place in the form of hardened paste at room temperature, with a water-to-solid ratio of 0.7 by weight.

It is of interest to compare the chemical heats of hydration, obtained in the present experiments, with the over-all heats of hydration of Verbeck and Foster.[3] The value they obtained for Ca_3SiO_5, from portland cements hydrating for six and a half years, was 117 cal./g., which is 21 cal. higher than our value. The difference may be considered the heat of adsorption of water on the gel. Since one mole of Ca_3SiO_5 produces the same amount of gel as one mole of Ca_2SiO_4, the adsorbing surface produced by 1 g. of Ca_2SiO_4 after complete hydration should be 32.5% larger than that produced by Ca_3SiO_5. Thus, the heat of adsorption for 1 g. of hydrated Ca_2SiO_4 should be 28 cal., which, added to the chemical heat of hydration, 24 cal./g., should give an over-all heat of hydration of 52 cal./g. Verbeck and Foster obtained 53 cal./g., in good agreement with the calculated value.

The agreement between our results and those of Woods, Steinour and Starke[1] and Lerch and Bogue[2] is not quite so good. The first named investigators used cements hydrated only for one year, which doubtless accounts for the fact that the agreement is only qualitative. Lerch and Bogue used a different method of hydration, and their heats of solution were not corrected for the impurities present in their Ca_3SiO_5 and Ca_2SiO_4 samples.

The heat of hydration of Ca_3SiO_5, on equal weight basis, is about four times as large as that of Ca_2SiO_4. The heat of hydration of Ca_2SiO_4, indeed, is remarkably small; it is about 2000 cal./mole of water. Powers and Brownyard[4] found that the average net heat of adsorption of water on hydrated portland cement gel was about 2000 cal./mole of water, and that the heat of adsorption in the first adsorbed layer was more than twice as large. For comparison, we may also mention that the heat of hydration of anhydrite, $CaSO_4$, to gypsum, $CaSO_4 \cdot 2H_2O$ is 2000 cal./mole of water[10]; the heat of hydration of pseudowollastonite, α-$CaSiO_3$, to the monohydrate is 2600 cal./mole; and the heat of hydration of wollastonite, β-$CaSiO_3$, to the monohydrate is 1300 cal./mole.[15]

Acknowledgments.—We wish to acknowledge our great indebtedness to Dr. L. E. Copeland for generously supplying us with most of the materials used in these experiments; to Mr. C. L. Ford and his associates, Mr. E. E. Pressler, Mr. E. LaBonde, Mr. W. G. Hime, and Miss Helen E. McMillen for the very fine analytical work performed on the materials; and to Mr. T. C. Powers, Dr. L. E. Copeland, Dr. H. H. Steinour, Mr. G. J. Verbeck and Dr. D. L. Kantro for the helpful discussions and suggestions contributed to this work.

NOTES

THE APPROXIMATE SOLUBILITY OF DIBORANE IN PENTANE[1]

By L. V. McCarty and John Guyon

Research Laboratory, General Electric Company, Schenectady, N. Y.

Received October 19, 1953

The solubility of an impure sample of diborane gas is calculated from pressure measurements of the gas in equilibrium with normal pentane solutions at various temperatures. A number of assumptions have to be made for lack of a detailed knowledge of this system. Raoult's law is applied to the solutions, and all vapors are treated as ideal gases. The molar volume of diborane in solution is ignored in the calculations, but this should not cause an error of more than 3% in the concentration of diborane in the liquid phase at the highest concentrations. The coefficient of expansion of normal pentane[2] is used up to 55° even though it is given for the 0–30° temperature range only. The vapor pressure of *n*-pentane is taken from Stull's tables.[3] The data recorded in the table under "B_2H_6 pressure" are obtained by subtracting the vapor pressure of *n*-pentane from the "observed pressure."

The equilibrium constants for the system

$$B_2H_6(g) = B_2H_6 \text{ (in pentane solution)}, \; K = S/P$$

are recorded in Table I. S is the solubility expressed as mole per cent. diborane in solution, and P is the partial pressure of diborane in atmospheres.

The solubility of diborane in *n*-pentane is somewhat less than observed for ethyl ether.[4] Calculations based on the diborane vapor pressure equation of H. L. Johnston,[5] *et al.*, indicate that Raoult's law applies very well to the system diborane–*n*-pentane. The observed partial pressures of diborane in equilibrium with a *n*-pentane solution in the temperature range 0–55° are reproduced by the equation

$$\log_{10} P = -\frac{547}{T} + 1.46 + \log_{10} S$$

The heat of solution is −2500 cal./mole which is somewhat less than observed for ethyl ether as the solvent.[3]

Table I

Equilibrium Pressures for Diborane in Pentane

Mmoles B_2H_6		3.26	5.84	9.81	12.68	24.0
Mmoles C_5H_{12}		85.4	85.4	85.4	85.4	85.4
Cylinder vol., cc.		100.8	101.8	104.7	73.5	101.0
		Observed pressure, p.s.i. abs.				
T °C.						
0.0		10.4	...	23.7	34.2	50.2
10.2		13.2	18.4	27.8	39.5	56.5
19.6		15.8	22.0	32.2	45.2	63.7
30.7		20.5	27.1	38.2	53.2	72.2
39.0		24.6	32.1	43.9	60.2	80.2
54.8		35.6	44.7	57.0	75.4	98.2
		B_2H_6 pressure, atm.				
0.0		0.466	...	1.37	2.09	3.20
10.2		.507	0.862	1.51	2.31	3.45
19.6		.532	0.958	1.66	2.56	3.84
30.7		.588	1.041	1.81	2.85	4.17
39.0		.653	1.103	1.91	3.05	4.45
54.8		.693	1.245	2.09	3.42	5.03
		Mole % B_2H_6 in liquid				
0.0		1.59	...	4.50	7.32	11.25
10.2		1.49	2.83	4.12	6.96	11.04
19.6		1.47	2.53	3.74	6.56	9.95
30.7		1.31	2.37	3.42	6.07	9.65
39.0		1.15	2.28	3.27	5.85	9.24
54.8		1.15	1.98	2.98	5.32	8.10
		$K = S/P$ (mole % B_2H_6/atm. of B_2H_6)				
	(Av. K)					
0.0	(3.4)	3.4	...	3.3	3.5	3.5
10.2	(3.0)	2.9	3.3	2.7	3.0	3.2
19.6	(2.6)	2.8	2.6	2.3	2.6	2.6
30.7	(2.2)	2.2	2.3	1.9	2.1	2.3
39.0	(1.9)	1.8	2.1	1.7	1.9	2.1
54.8	(1.6)	1.7	1.6	1.4	1.6	1.6

---

(1) This work was done for Army Ordnance Contract TU1-2000A.

(2) M. P. Doss, "Physical Constants of the Principal Hydrocarbons," The Texas Company, 1943.

(3) D. R. Stull, *Ind. Eng. Chem*, **39**, 517 (1947).

(4) J. R. Elliott, W. L. Roth, G. F. Roedel and E. M. Boldebuck, *J. Am. Chem. Soc.*, **74**, 5211 (1952).

(5) "Condensed Gas Calorimetry," E. B. Rifkin, E. C. Kerr and H. L. Johnston, Tech. Report No. 5, Project RF-309, The Ohio State Univ. Research Foundation.

Experimental

Materials.—The n-pentane was Phillips Pure Grade 99+ per cent. pure. The diborane was analyzed by infrared absorption, and it contained 2.1 mole per cent. ether, 3.5 mole per cent. ethane and 94.4 mole per cent. diborane.

Procedure.—The stainless steel cylinders were attached to a vacuum system and 10.00 cc. of n-pentane was distilled into each one. The number of moles of diborane added to each cylinder was measured by filling a vacuum system of known volume to a given pressure and condensing the diborane in the cylinder with a liquid nitrogen bath. The cylinders were then warmed to 0.0° and thoroughly agitated to ensure equilibrium, and this process was repeated for each succeeding higher temperature. Pressures were read on ordinary gages as received with no special calibration.

SILVER ETHYLAMINE COMPLEXES IN ALCOHOLIC SOLUTIONS

By Hans B. Jonassen, Thomas F. Fagley, C. C. Rolland and P. C. Yates

Richardson Chemistry Laboratory of Tulane University, New Orleans, La.

Received October 23, 1953

Introduction.—Silver(I) occupies a relatively unique position among the transition elements. Although it is commonly supposed that it exhibits a stable coördination number of two in its complex ions, there are numerous cases[1] in which observed data can best be explained in terms of a coördination number of three or four or even six. Theoretically, there should be little difference in the relative stabilities of the two and four coördinated states.[2]

This investigation was undertaken in order to examine some of the factors which would influence the formation of silver(I) complexes with a coördination number higher than two. It has been noted elsewhere[3] that one of the principal contributions to the stability of complex ions lies in the dielectric constant of the solvent medium. Thus, on the basis of electrostatics, a lower dielectric constant of the solvent should serve to increase the effective polarizing power of the cation in question, and so enhance the stability of the higher coördinated state.

Theoretical.—The method employed to determine the dissociation constants of the complexes studied is a modification of the potentiometric method of Bodländer[4] and Koch.[5] In this, the Nernst expression for the cell

$$\mathrm{Ag,\ Ag^+ + ligand} \parallel \mathrm{Ag^+}$$

Ag is related to the mass action expression for the dissociation of the complex ion formed in the left hand half-cell. For a one-electron change at 30°, the resulting equation is

$$pK_\mathrm{i} = -\log K_\mathrm{i} = \frac{E}{0.06016} - \log \mathrm{Ag_r}^+ - N \log L_\mathrm{f} + \log \mathrm{AgL_N}^+ \quad (1)$$

where K_i is the dissociation constant of the complex, E is the potential difference between the electrodes, $\mathrm{Ag_r}^+$ is the concentration of the reference silver solution, N is the number of ligand molecules per silver ion in the complex, L_f is the concentration of free ligand, and $\mathrm{AgL_N}^+$ is the concentration of the complex ion formed. In the region of amine concentration where the maximal coördination number attains equation 1 can be recast in the form

$$pK_\mathrm{i} = \frac{E}{0.06016} - \log y\, \mathrm{Ag_r}^+ - N \log y'(L_\mathrm{t} - N\, \mathrm{Ag_t}^+) + \log y''\, \mathrm{Ag_t}^+ \quad (2)$$

where L_t is the total ligand concentration, $\mathrm{Ag_t}^+$ is the total silver ion concentration in the amine solution, and y, y' and y'' are the respective molar activity coefficients.

Values of N were assumed and constancy of pK_i as calculated from equation 2 noted. A plot of $-E/0.06016$ *versus* $-N \log y' (L_\mathrm{t} - N\,\mathrm{Ag_t}^+) + \log y''\, \mathrm{Ag_t}^+$ gave a straight line with a slope of 1.0 for $N = 2$.

In addition, conductance titrations run over the concentration range employed in the e.m.f. studies point to the validity of the choice of 2 for N.

After the method of Bjerrum,[6] silver nitrate and the complex compound in the alcoholic media were considered as weak electrolytes. Bjerrum's theory allows the calculation of the association constant of such ion-pairs, but the solution of the equations depends on the value assigned to the parameter "$\mathring{a}$," which in turn depends on the effective radii of the ions in solution. Crystallographic radii were used for the ions involved. In the case of the complex ion $\mathrm{Ag(C_2H_5NH_2)}_x{}^+$, where x is any integer, Fischer–Hirschfelder models were used to decide the statistically most probable shape of the ethylamine molecule and its effective length calculated from covalent radii. When added to the value for $\mathrm{Ag^+}$, this yielded 4.48 Å. for the effective radius of the complex ion. This value should be independent of the number of ethylamine molecules attached to the silver ion, since the ion formed could be viewed as spherical in any such case.

The values of the association constants K^{-1} calculated for isopropyl alcohol solutions at 30° were 489.3 for $\mathrm{AgNO_3}$ and 116.3 for the complex $\mathrm{Ag(C_2H_5NH_2)}_x\mathrm{NO_3}$. For ethanol solution at 30°, the values are 142.4 for $\mathrm{AgNO_3}$ and 39.73 for the complex.

The mean molar activity coefficient of the ion-pairs, $y_{\pm 1}$ was expressed as a function of α the degree of dissociation, by use of the "extended" Debye–Hückel equation and the resulting equation used to evaluate α by successive approximations. The molar activity coefficient for the uncharged ion-pair, y_{12}, was assumed to be unity. This is not without precedent.[7]

Furthermore, in the actual calculation of pK_i values, it was necessary to assign a value of unity for the activity coefficient of ethylamine in the alcohols. This procedure was primarily due to the

---

[1] $\mathrm{AgCl_4}^{-3}$, W. Erber and A. Schühly, *J. prakt. Chem.*, **158**, 176 (1941); $\mathrm{Ag_2Br_6}^{-4}$, W. Erber, *Z. anorg. Chem.*, **248**, 32, 36 (1941); $\mathrm{Ag(OAc)_3}^{-2}$, I. Leden, *Svensk. Kem. Tid.*, **58**, 129 (1946).

[2] L. Pauling, "The Nature of the Chemical Bond," 2nd Edition, Cornell University Press, Ithaca, N. Y., 1948, pp. 81–89.

[3] H. B. Jonassen, *Record of Chemical Progress*, **13**, 135 (1952).

[4] G. Bodlander, as cited in S. Glasstone, "Textbook of Physical Chemistry," 2nd Ed., D. Van Nostrand Co., Inc., New York, N. Y., 1946, pp. 972–974.

[5] F. K. V. Koch, *J. Chem. Soc.*, 2053 (1930).

[6] N. Bjerrum, as cited in H. S. Harned and B. B. Owen, "The Physical Chemistry of Electrolytic Solutions," 2nd Ed., Reinhold Publ. Corp., New York, N. Y., pp. 42–45.

[7] D. A. MacInnes, "The Principles of Electrochemistry," Reinhold Publ. Corp., New York, N. Y., 1939, p. 372.

lack of available data, and while not entirely justifiable, the error introduced should certainly lie within the limits of other necessary approximations.

Experimental.—All chemicals employed were of C.P. grade.

Ethanol was dried according to the method of Lund and Bjerrum[8] and suitable precautions were employed throughout the measurements to prevent its exposure to moisture. The isopropyl alcohol contained 0.50% water. The dielectric constant of the ethanol was taken as 24.2 at 30°, from the data of "International Critical Tables."[9] The dielectric constant of the isopropyl alcohol was determined by a resonance circuit method[10] and found to be 19.2 at 30°.

The alcoholic $AgNO_3$ solutions were standardized against NaCl. The ethylamine solutions were standardized potentiometrically against aqueous hydrochloric acid.

The silver electrodes were prepared after the method of MacDougall and Peterson.[11] The measurements were made using two half-cells containing silver nitrate solutions of the same concentration, connected through an agar salt bridge (saturated with KNO_3) to a standard potentiometer set-up.

The e.m.f. values were measured for concentration increments of amine reagent, and pK_i's were calculated for each as shown by a few representative calculations for the two solvents in the Table I (ethanol) and Table II (isopropyl alcohol). The average pK_i value for the complex in ethanol was 8.22 and in isopropyl alcohol as a solvent was 8.50.

TABLE I

ETHYL ALCOHOL

$\log y\ Ag_r^+ = -1.92$

Amine, ml.	7.00	8.02	8.98	10.00	12.00
$E/0.06016$	6.757	6.862	6.953	7.028	7.183
Ag_t^+	0.04599	0.04556	0.04515	0.04474	0.04394
L_t	0.3088	0.3363	0.3617	0.3882	0.4388
$2 \log L_f$	1.328	1.221	1.133	1.050	0.910
α-Complex	0.759	0.760	0.760	0.761	0.763
$-\log (c\alpha)$	1.457	1.461	1.465	1.468	1.475
$-\log y''_{\pm}$	0.320	0.319	0.318	0.317	0.316
pK_i	8.23	8.22	8.22	8.21	8.22

TABLE II

ISOPROPYL ALCOHOL

$\log y\ Ag_r^+ = -2.05$

Amine, ml.	20.00	22.00	24.00	26.02	28.02
$E/0.06016$	8.125	8.215	8.285	8.339	9.391
Ag_t^+	0.03616	0.03515	0.03420	0.03329	0.03243
L_t	0.7656	0.8187	0.8689	0.9170	0.9642
$-2 \log L_f$	0.3182	0.2517	0.1933	0.1408	0.0942
α-Complex	0.678	0.681	0.683	0.685	0.687
$-\log (c\alpha)$	1.611	1.622	1.632	1.642	1.652
$-\log y''_{\pm}$	0.389	0.386	0.384	0.381	0.378
pK_i	8.49	8.50	8.51	8.50	8.50

Discussion.—Even though in a strict sense direct comparison is invalidated by the fact that each complex ion is referred to a different solvated ion, one must note the increase in stability of the $Ag(EtNH_2)_2^+$ complex with a decrease of dielectric constant of the solvent. The inclusion of the value for the aqueous system as determined by Carlson, *et al.*,[12] yields the following table for this complex.

Solvent	Dielectric constant	pK_i
Water	76.7	7.14
Ethanol	24.2	8.22
Isopropyl alcohol	19.2	8.50

At high concentrations of amine, *i.e.*, at mole ratio of amine to Ag^+ of 30, the assumption of a coördination number of 3 gives a constant pK_i value of 8.42 for ethanol solution. This constancy may be illusory since at such high amine concentrations the quantity ($L_t - NAg^+$) is practically constant and relatively insensitive to the value of N chosen. Furthermore, the constancy of the pK_i values at these high concentrations may be a reflection of significant departures of the activity coefficient of the free amine from unity.

Acknowledgment.—The authors are indebted to the Office of Naval Research for the sponsorship of this and continuing investigations.

---

[8] H. Lund and J. Bjerrum, *Ber.*, **64B**, 210 (1931).

[9] "International Critical Tables," Vol. VI, McGraw-Hill Book Co., Inc., New York, N. Y., 1929, p. 85.

[10] The authors wish to thank Dr. F. Boylan (formerly of these laboratories) who determined this value for us.

[11] P. H. MacDougall and S. Peterson, THIS JOURNAL, **51**, 1346 (1947).

[12] C. A. Carlson, J. P. McReynolds and F. R. Verhoek, *J. Am. Chem. Soc.*, **67**, 1334 (1945).

COMMUNICATION TO THE EDITOR

HOMOTATTIC SURFACE—A SUGGESTED NEW WORD

Sir:

The purpose of this letter is to suggest precise terms for discussion of certain surface phenomena.

Taylor and others[1] have demonstrated that solid surfaces are irregular in construction. More recent work, notably on surface adsorption,[2,3,4,5,6] has indicated that a solid surface sometimes includes, or may consist of, submicroscopic patches or regions of regular and uniform construction.

These regular and uniform patches are generally described in the literature as together forming a *relatively homogeneous* surface: the *relatively* sometimes being used in the sense of "somewhat" or "rather," sometimes indicating a comparison with the non-homogeneous portions of the same surface.

The term relatively homogeneous is bad. Firstly, it may offend the precisian to whom the idea of *homogeneity* does not admit of qualification. Secondly, it conveys no notion of the scale of the phenomena to which it is applied: the surface of a sheet of paper, or of a macadam road, might in some contexts be reasonably described as "relatively homogeneous." Some more precise term is needed, specific to the aspects of surface homogeneity studied by the physical chemist.

We accordingly suggest the term *homotattic* (Gr. *tattein*, to draw up in orderly array). A *homotattic* surface is the surface of a sub-microscopic patch or region, part of a larger surface, which acts as if its structure were uniform and homogeneous.

A crystal surface of, say, sodium chloride may contain (or may perhaps consist of) a single homotattic surface, which would normally be the {100} surface planes. Another sample, prepared under special conditions, may contain two homotattic surfaces, the {100} surface planes and the {111} surface planes. We do not exclude by this term the interpretation that homotattic surfaces may be evident by virtue of regularities in the surface energies, as well as by crystallographic regularities. Two or more crystallographic homotattic surfaces may behave as one energetically homotattic surface toward certain adsorbates.[7] Alternatively, a single crystallographic homotattic surface may behave as two or more energetically homotattic surfaces toward certain adsorbates.[8]

The term *homotattic* has not hitherto been applied, as far as we know, in any other connection.

DEPARTMENTS OF ENGLISH AND OF CHEMISTRY
RENSSELAER POLYTECHNIC INSTITUTE
TROY, N. Y.
CHRIS SANFORD
SYDNEY ROSS

RECEIVED JANUARY 20, 1954

---

[1] H. S. Taylor and S. C. Liang, *J. Am. Chem. Soc.*, **69**, 1306, 2989 (1947).

[2] W. D. Harkins, G. Jura and E. H. Loeser, *ibid.*, **68**, 554 (1946).

[3] Sydney Ross and G. E. Boyd, "New Observations on Two-Dimensional Condensation Phenomena," MDDC Report No. 864, 1947.

[4] L. G. Joyner and P. H. Emmett, *J. Am. Chem. Soc.*, **70**, 2353 (1948).

[5] C. Pierce and R. N. Smith, THIS JOURNAL, **54**, 354 (1950).

[6] M. H. Polley, W. D. Schaeffer and W. R. Smith, *ibid.*, **57**, 469 (1953).

[7] For example, asbestos: see A. C. Zettlemoyer, G. J. Young, J. J. Chessick and F. H. Healey, *ibid.*, **57**, 649 (1953).

[8] For example, graphite: see G. Jura and D. Criddle, *ibid.*, **55**, 163 (1951).

New Schedule

BACK ISSUE PRICES

AMERICAN CHEMICAL SOCIETY JOURNALS

Effective January 1, 1953

Single copies or complete volumes of nearly all the ACS journals listed below may be purchased at these prices.

Journal	Current Year		Back Years			
	Member	Non-Member	Member	Non-Member	Foreign Postage	Canadian Postage
AGRICULTURAL AND FOOD CHEMISTRY	$0.40	$0.50	....	....	$0.15	$0.05
ANALYTICAL CHEMISTRY	.40	.50	$0.60	$0.75	.15	.05
Analytical Edition (I&EC)						
Volumes 1–4	....	....	1.60	2.00	.15	.05
Volumes 5–8	....	....	1.00	1.25	.15	.05
Volumes 9, et seq.	....	....	.60	.75	.15	.05
CHEMICAL ABSTRACTS, Volumes 11–44						
Numbers 1–22	....	....	1.00	1.25	.15	.05
Numbers 23 and 24	....	....	2.40	3.00*	.45	.15
CHEMICAL ABSTRACTS, Vol. 45, et seq.						
Numbers 1–22	1.00**	2.00	1.60**	2.00	.15	.05
Number 23 (Author Index)	6.00**	12.00	9.60**	12.00	free	free
Number 24 (Subject, Patent, Formula Indexes, complete)	12.00**	24.00	19.20**	24.00	free	free
CHEMICAL AND ENGINEERING NEWS	.15	.15	.15	.15	.05	free
INDUSTRIAL AND ENGINEERING CHEMISTRY	.60	.75	.80	1.00	.15	.05
Industrial Edition (I&EC)	....	....	.80	1.00	.15	.05
JOURNAL OF THE AMERICAN CHEMICAL SOCIETY, Vols. 32–73	....	....	1.00	1.25	.15	.05
JOURNAL OF THE AMERICAN CHEMICAL SOCIETY, Vol. 74, et seq.	.50	.75	.80	1.00	.15	.05
JOURNAL OF PHYSICAL CHEMISTRY	1.00	1.25	1.20	1.50	.15	.05

RATES FOR VOLUMES OF BACK NUMBERS

Journal	Member	Non-Member	Foreign Postage	Canadian Postage
ANALYTICAL CHEMISTRY (formerly Analytical Edition)	$6.00	$7.50	$0.75	$0.25
CHEMICAL ABSTRACTS				
Volumes 11–44	20.00	25.00	2.40	.80
Volume 45, et seq.	50.80**	63.50	2.40	.80
CHEMICAL AND ENGINEERING NEWS (Volumes 1–24)	2.80	3.50	2.25	.75
CHEMICAL AND ENGINEERING NEWS (Vol. 25, et seq.)	5.60	7.00	2.25	.75
INDUSTRIAL AND ENGINEERING CHEMISTRY	8.80	11.00	2.25	.75
JOURNAL OF THE AMERICAN CHEMICAL SOCIETY (Vol. 32, et seq.)	12.00	15.00	1.50	.50
JOURNAL OF PHYSICAL CHEMISTRY (Vol. 56, et seq.)	10.00	12.50	1.20	.40

(Prior Volumes—Order from Walter Johnson, 125 East 23rd Street, New York 10, N. Y.)

* Each part, when divided.

** The member discount for Volumes 45, et seq. applies only if purchase is for personal use and not for resale.

●

AMERICAN CHEMICAL SOCIETY

Back Issue Department

1155 Sixteenth St., N.W. • Washington 6, D. C.

AZEOTROPIC DATA

-- *Advances in Chemistry Series Volume No. 6*

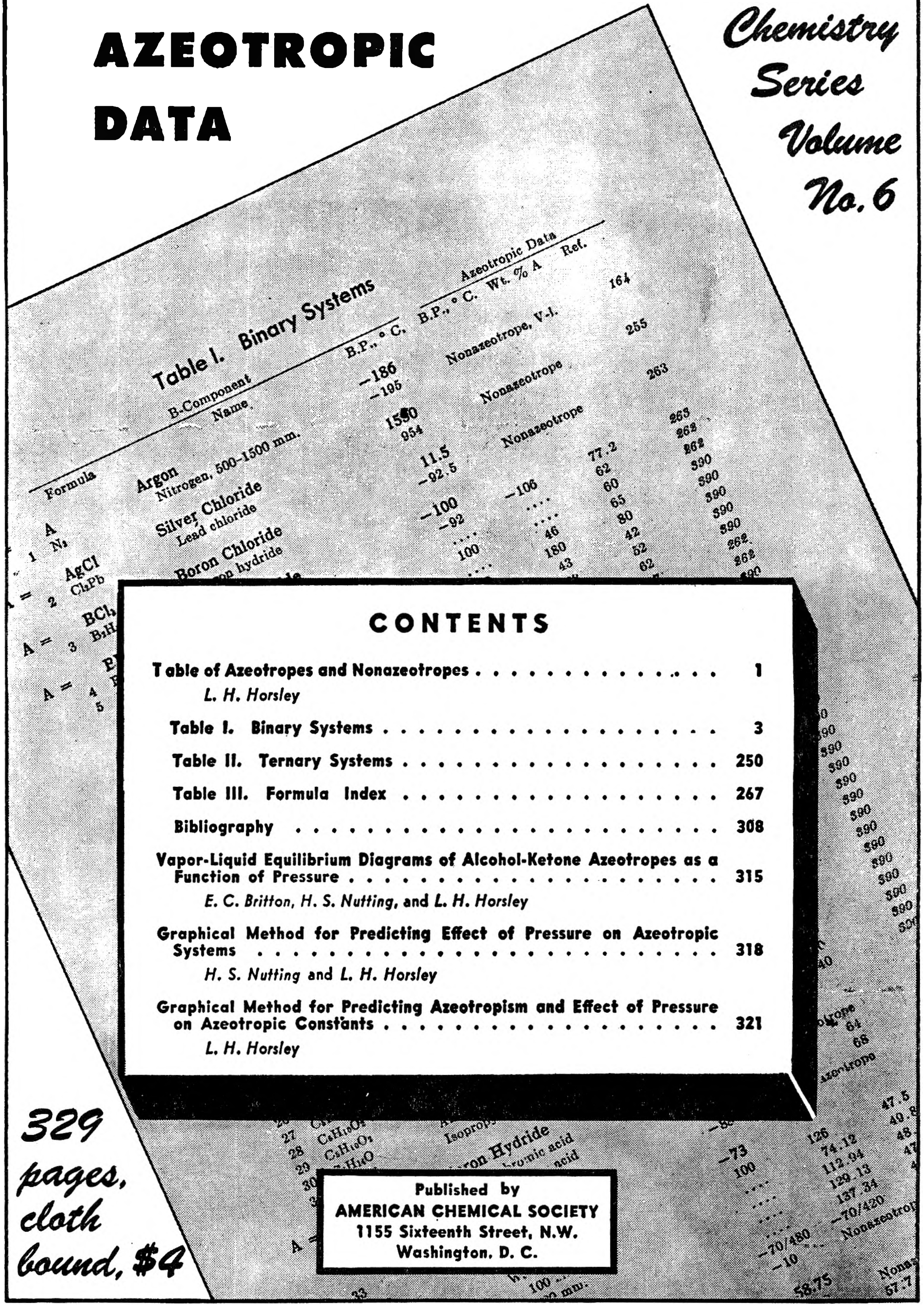
Table I. Binary Systems

Formula	B-Component Name	B.P., ° C.	Azeotropic Data B.P., ° C.	Wt. % A	Ref.
A	Argon	−186	Nonazeotrope, V.-l.		164
1 N_2	Nitrogen, 500-1500 mm.	−195			
AgCl	Silver Chloride	1550	Nonazeotrope		255
2 ClPb	Lead chloride	954			
BCl_3	Boron Chloride	11.5	Nonazeotrope		263

CONTENTS

329 pages, cloth bound, $4

Published by
AMERICAN CHEMICAL SOCIETY
1155 Sixteenth Street, N.W.
Washington, D. C.